Investigating the Role of APOE2 in Alzheimer's Disease

Using Human Induced Pluripotent Stem Cell Derived

Neurons and Astrocytes

by

Sreedevi Raman

A Dissertation Presented in Partial Fulfillment
of the Requirements for the Degree
Doctor of Philosophy

Approved March 2021 by the
Graduate Supervisory Committee:

David Brafman, Chair
Barbara Smith
Christopher Plaisier
Xiao Wang
Xiaojun Tian

ARIZONA STATE UNIVERSITY

May 2021

ABSTRACT

Genome wide association studies (GWAS) have identified polymorphism in the Apolipoprotein E (*APOE*) gene to be the most prominent risk factor for Alzheimer's disease (AD). Compared to individuals homozygous for the *APOE3* variant, individuals with the *APOE4* variant have a significantly elevated risk of AD. On the other hand, longitudinal studies have shown that the presence of the *APOE2* variant reduces lifetime risk of developing AD by 40 percent. While there has been significant research that has identified the risk-inducing effects of APOE4, the underlying mechanisms by which APOE2 influences AD onset and progression have not been extensively explored. The hallmarks of AD pathology manifest in human neurons in the form of extracellular amyloid deposits and intracellular neurofibrillary tangles, whereas astrocytes are the primary source of the APOE protein in the brain. In this study, an isogenic human induced pluripotent stem cell (hiPSC)-based system is utilized to demonstrate that conversion of *APOE3* to *APOE2* greatly reduced the production of amyloid-beta (Aβ) peptides in hiPSC-derived neural cultures. Mechanistically, analysis of pure populations of neurons and astrocytes derived from these neural cultures revealed that mitigating effects of *APOE2* is mediated by cell autonomous and non-autonomous effects. In particular, it was demonstrated the reduction in Aβ and pathogenic β-C-terminal fragments (APP-βCTF) is potentially driven by a mechanism related to non-amyloidogenic processing of amyloid precursor protein (APP), suggesting a gain of protective function of the *APOE2* variant. Together, this study provides insights into the risk-modifying effects associated with the *APOE2* allele and establishes a platform to probe the mechanisms by which APOE2 enhances neuroprotection against AD.

DEDICATION

To my first teachers, Subhadra and Raman.

To my rock, Srikumar.

ACKNOWLEDGMENTS

TABLE OF CONTENTS

LIST OF TABLES

LIST OF FIGURES

PREFACE

Chapters presented in this PhD dissertation document contain text and figures that are in part reproductions from previously published manuscripts as described below:

Chapter 1**: Raman S*,** Brookhouser N*, Brafman DA. 2020. Using human induced pluripotent stem cells (hiPSCs) to investigate the mechanisms by which Apolipoprotein E (APOE) contributes to Alzheimer's disease (AD) risk. Neurobiology of Disease. 138 (2020) 1047882.

Chapter 2: **Raman S*,** Srinivasan G*, Brookhouser N*, Nguyen T, Henson T, Morgan D, Cutts J, Brafman DA. 2020. A Defined and Scalable Peptide-Based Platform for the Generation of Human Pluripotent Stem Cell-Derived Astrocytes. ACS Biomater. Sci. Eng. 2020, 6, 6, 3477–3490.

Chapter 3: Brookhouser N*, **Raman S***, Frisch C, Srinivasan G, Brafman DA. 2021. APOE2 mitigates disease-related phenotypes in an isogenic hiPSC-derived model of Alzheimer's disease. *Accepted for publication.*

*=Equal Contribution. In all cases, the dissertation author was the primary author and researcher pertaining to the work.

CHAPTER 1

USING HUMAN INDUCED PLURIPOTENT STEM CELLS (HIPSCS) TO INVESTIGATE THE MECHANISMS BY WHICH APOLIPOPROTEIN E (APOE) CONTRIBUTES TO ALZHEIMER'S DISEASE (AD) RISK

1.1   Introduction

Alzheimer's disease (AD) is currently the 6th leading cause of death in the United States and affects an estimated 5.8 million Americans, with this figure expected to rise to nearly 14 million individuals by 2050 ("2019 Alzheimer's disease facts and figures," 2019). In 2018 alone, costs associated with the care of patients with Alzheimer's and other dementias totaled nearly $234 billion. Worldwide prevalence is estimated to be as high as 24 million, with AD accounting for more than 50% of all dementia cases (Bekris et al., 2010; Mayeux and Stern, 2012). Prevalence rates of AD increase with age, increasing dramatically after age 65, with a documented nearly 15-fold increase in the prevalence of predominantly Alzheimer's dementia in individuals between 60 and 85 years of age (Evans et al., 1989; Mayeux and Stern, 2012).

Animal models that overexpress Alzheimer's disease (AD)-related proteins or have familial AD (fAD)-related mutations introduced into the genome have provided important insights into AD (Bettens et al., 2010; Drummond and Wisniewski, 2017; Esquerda-Canals et al., 2017). Unfortunately, these models do not display important pathological hallmarks of the human disease and have not adequately modeled the complex genetics associated with sporadic AD (sAD) (Duff and Suleman, 2004; Seok et al., 2013; Warren et al., 2015). In addition, the complexity of in vivo experiments makes it difficult to eliminate confounding variables and directly investigate the manifestation of molecular, biochemical, and cellular phenotypes. Studies of human neuronal cells have been restricted to experiments with cadaveric tissue samples, which are limited in supply and rapidly lose disease phenotypes with extensive ex vivo culture. Because of the limitations of current animal and human models of AD, the mechanisms that cause AD onset and progression remain poorly understood, possibly explaining the failure of recent experimental therapies (Qosa and Volpe, 2018).

1

Moving forward, accessible and reproducible human in vitro models are needed to compliment these existing models. Advances in cellular reprogramming have enabled the generation of in vitro central nervous system (CNS) disease models that can be used to dissect disease mechanisms on a cellular level and evaluate potential therapeutics (Goldstein et al., 2015; Robbins and Price, 2017). In this review, we will summarize how human induced pluripotent stem cells (hiPSCs) have emerged as viable system to model various aspects of AD pathogenesis. In particular, we will discuss how emerging technologies in genome engineering and organoid culture in conjunction with hiPSC-based models could provide new opportunities to investigate the risk-modifying effects of Apolipoprotein E (ApoE).

1.2   Alzheimer's Disease: Pathophysiology, Molecular Mechanisms, and Genetics

Neuropathological hallmarks of AD include extracellular amyloid plaques, cerebral amyloid angiopathy, and neurofibrillary tangles in the form of intraneuronal aggregations of modified Tau proteins (Selkoe, 1991; Serrano-Pozo et al., 2011). In addition, cortical thinning can be observed early in the disease process by MRI, showing symmetrical atrophy of the cortex in the medial temporal lobes (Dickerson et al., 2011, 2009; Serrano-Pozo et al., 2011). Amyloid plaques seen in the brains of AD patients result from the extracellular accumulation of 40 or 42 amino acid amyloid-beta (Aβ) peptides, produced by proteolytic cleavage of amyloid precursor protein (APP) in neurons. Broadly speaking, amyloid plaques can be characterized as either diffuse or dense-core plaques. Although diffuse amyloid plaques can be detected in cognitively normal aging adults, dense-core plaques are commonly seen in the brains of individuals with AD, and are associated with damage to surrounding cellular architecture causing synapse loss, neuron death, and activation of astrocytes and microglial cells (Itagaki et al., 1989; Knowles et al., 1999; Vehmas et al., 2003). Neurofibrillary tangles are formed by aggregation of Tau, a microtubule-associated protein, leading to neuron death. Under physiological conditions, Tau regulates the stability of microtubule structure. However, in AD and other tauopathies, Tau is hyperphosphorylated causing microtubule disassembly and aggregation of phosphorylated Tau (p-Tau) filaments (Guo et al., 2017; Medeiros et al., 2011). Interestingly, although global amyloid

2

burden is associated with decreased cognitive function and may predict longitudinal cognitive

decline, recent neuroimaging studies suggest Tau positron emission tomography (PET) may be

more sensitive than Aβ PET and increasing levels of Tau may be a better predictor of early

decline in cognition than Aβ alone (Aschenbrenner et al., 2018; Farrell et al., 2017; Ossenkoppele

et al., 2019).

1.2.1   The amyloid hypothesis

The Aβ peptide observed in the cortex of AD patients was first isolated and sequenced in

1984 and found to be homologous to the amyloid peptide seen in the brains of individuals with

Down's syndrome (Glenner and Wong, 1984a, 1984b). This finding was the first to suggest the

genetic deficit in AD may be localized on chromosome 21. Subsequent cloning and

characterization of a cDNA that encoded the amyloid peptide revealed a highly conserved β-

amyloid precursor protein (APP) gene product that was mapped to human chromosome 21,

further suggesting a causal relationship between trisomy 21 in Down's syndrome and AD

pathology (Goldgaber et al., 1987; Robakis et al., 1987). These discoveries set the stage for

further investigation in the field built on the premise that Aβ accumulation is the primary

pathogenic event leading to Alzheimer's dementia.

Genetic investigations quickly linked mutations in the APP gene with early-onset AD,

providing evidence that polymorphisms in the APP gene can drive early-onset amyloid pathology

(Goate et al., 1991), although mutations across independent families were shown to be

heterologous. Further characterization of APP mutants revealed that mutations within APP were

generally localized in or flanking the region coding for the amyloid peptide that altered the

processing of the gene product by proteases α-, β-, and γ- secretase, leading to increased

production of Aβ peptide (Cai et al., 1993; Citron et al., 1992). Additionally, it was demonstrated

that polymorphisms in the Presenilin 1 and Presenilin 2 (PSEN1, PSEN2) genes led to increased

Aβ generation and altered APP processing through direct effect on γ-secretase (De Strooper et

al., 1998; Levy-Lahad et al., 1995; Scheuner et al., 1996; Sherrington et al., 1995). These

seminal studies pushed the field to focus research heavily on the proposed 'amyloid cascade

hypothesis' that postulated AD pathogenesis begins with missense mutations in APP, PSEN1, or PSEN2 genes leading to the downstream cascade of altered APP processing, increased Aβ production, and deposition in the form of diffuse plaques that represent the catalyst for widespread neuronal dysfunction and the clinical presentation of dementia (Hardy and Selkoe, 2002). Additionally, mutations defined within the gene encoding the tau protein leading to frontotemporal dementia and neurodegeneration do not induce amyloid pathology, which has strengthened the hypothesis that Aβ seeding precedes neurofibrillary tangle formation and is the initial event leading to downstream neurodegeneration in AD (Hardy et al., 1998).

1.2.2   Familial Alzheimer's disease (fAD)

Familial Alzheimer's disease (fAD) is characterized by early age of dementia onset, ranging from 30 to 65 years of age, and accounts for 1-6% of overall cases (Bekris et al., 2010). The accelerated onset in fAD is driven by highly penetrant autosomal mutations in the coding sequence of PSEN1, PSEN2, or APP (Bertram and Tanzi, 2005; Chartier-Harlin et al., 1991; Goate et al., 1991; Janssen et al., 2003; Levy-Lahad et al., 1995; Rovelet-Lecrux et al., 2006; Scheuner et al., 1996). The Presenilins encode major components responsible for γ-secretase cleavage, and therefore modulate Aβ levels by altering cleavage of APP. Mutations in the APP and PSEN1 genes are associated with complete penetrance, while mutations in the PSEN2 gene show 95% penetrance (Goldman et al., 2011; Sherrington et al., 1996). Nearly 300 autosomal dominant pathogenic mutations within these three genes have been identified thus far, however novel disease-causing mutations continue to be revealed (Giau et al., 2019; *Mutations | ALZFORUM*, 2019) along with numerous variants of unknown pathogenicity.

1.2.3   Sporadic Alzheimer's disease (sAD)

The late onset sporadic form of AD (sAD), associated with onset after the age of 65, accounts for more than 95% of all AD cases (Reitz et al., 2011; van der Flier and Scheltens, 2005) and is directed by genetic and environmental risk factors. A genome wide association meta-analysis study of 94,437 individuals diagnosed with late onset AD, identified 25 risk loci that

regulate pathways of immunity, lipid metabolism, tau binding proteins, and amyloid precursor protein (APP) metabolism (Kunkle et al., 2019). Although numerous common and rare variants continue to be identified that may contribute to disease risk, polymorphism in the Apolipoprotein E (APOE) gene has been identified as the strongest risk factor for sAD (Corder et al., 1993; Liu et al., 2013; Saunders et al., 1993; Strittmatter et al., 1993), and continues to be replicated by GWAS analyses (Jansen et al., 2019; Kunkle et al., 2019).

1.3   The Role of Apolipoprotein E (APOE) in Alzheimer's Disease

Apolipoprotein E (ApoE) is a cholesterol transport protein secreted primarily by astrocytes in the CNS, conferring its effect on neurons primarily through low-density lipoprotein (LDL) family of receptors (Grehan et al., 2001; Holtzman et al., 2012; R. E. Pitas et al., 1987; Robert E. Pitas et al., 1987). Human APOE is present as three main variants- ε2, ε3, and ε4- with typical allele frequencies of ~8%, ~75%, and ~15% respectively (Farrer et al., 1997; Raber et al., 2004). The ApoE isoforms differ by single amino acid substitutions at amino acid position 112 and 158: ε2 (Cys112, Cys158), ε3 (Cys112, Arg158), ε4 (Arg112, Arg158). Compared to individuals with an APOE3/3 genotype, the presence of the ε2 allele confers ~40% decrease in risk of developing AD, while one or two copies of the ε4 allele introduce a 3-fold and up to ~12- fold increase in risk, respectively (Corder et al., 1994; Holtzman et al., 2012). Despite the relatively low population frequency of the ε4 allele, frequency among individuals with AD increases significantly to ~40% (Liu et al., 2013; Raber et al., 2004). In addition to Alzheimer dementia, the frequency of the ε4 allele has been shown to be elevated in pure synucleinopathies without Alzheimer pathology such as pure dementia with Lewy bodies (pDLB) and Parkinson's disease dementia (PDD) (Tsuang et al., 2013). Interestingly, this suggests that ApoE may be capable of facilitating neurodegeneration through non-amyloidogenic mechanisms. Further, it has been shown in human and rodent models that the ε4 allele exacerbates tau-mediated neurodegeneration and decreases age of onset in patients with tauopathy, independent of amyloid pathology (Koriath et al., 2019; Shi et al., 2017). Recent evidence in a mouse model of tauopathy suggests a role of ApoE in

modulating activation of microglia leading to neurodegeneration and tau pathogenesis (Shi et al., 2019).

The 299 amino acid ApoE protein is composed of two distinct domains, the N-terminal domain contains the receptor binding region whereas the C-terminal domain is responsible for lipid binding (Weisgraber, 1994). The LDL receptor family including LDLR and LDL receptor protein 1 (LRP1), as well as heparan sulfate proteoglycans (HSPG) are responsible for a majority of the ApoE and Aβ endocytosis in the CNS (Kanekiyo and Bu, 2014; Liu et al., 2013). ApoE and Aβ bound lipoproteins can be endocytosed by (i) direct interaction with LDL receptors (ii) the LRP/HSPG complex or (iii) HSPG alone (Mahley et al., 1999). The presence of Cys158 in the ApoE2 isoform impairs its ability to bind to LDL receptors (Kowal et al., 1990), making individuals homozygous for the ε2 allele susceptible to type III hyperlipoproteinemia (Weisgraber et al., 1982). The conversion of ApoE2 cysteine residues at the 112 and 158 sites to a positively charged residue increases its receptor affinity. In contrast to the low binding affinity of ApoE2 to LDLR (~1-2% of ApoE3/4 binding), the binding affinity of ApoE2 to LRP1 is less affected (~40% of ApoE3/4 binding) (Kowal et al., 1990) and the binding affinity to HSPG is not isoform specific (Mahley and Rall, 2000).

Several amyloid-dependent and -independent mechanisms have been postulated to explain the risk-modulating effects of various ApoE isoforms (**Figure 1-1**). Here, we will summarize the current data from various in vitro and in vivo studies that support each of these proposed mechanisms prior to focusing on hiPSC based studies in section 4.

1.3.1   Lipidation status and Aβ binding

Conflicting in vitro results obscure the extent of Aβ and ApoE interaction due to variations in purification and detection methods, source of the complex, and the molar ratio of the components (Tai et al., 2014). While some in vitro studies have indicated that the ApoE2 and E3 isoforms are more lipidated than the pathogenic E4 isoform (Bell et al., 2007; Fu et al., 2016), others have found ApoE4 is more lipidated (DeMattos et al., 2001; Kara et al., 2017). Isoform specific differences in the lipidation of ApoE have shown to cause dramatic changes in its

structure, affecting its conformation and subsequent Aβ complex formation and receptor interaction (Saito et al., 2001). For instance, analysis of unpurified ApoE protein showed lipidated ApoE3 bound Aβ with higher avidity compared to ApoE4, but this isoform specific effect was abolished upon the purification of the protein, which involves its delipidation (LaDu et al., 1995). Although the isoform specific effect is lost, delipidated ApoE has been reported to bind to Aβ with ~5-10-fold higher affinity than the lipidated forms (Tokuda et al., 2000).

The glial ATP binding cassette proteins ABCA1 and ABCG1 are responsible for cholesterol and phospholipid transfer to ApoE in the CNS (Vance and Hayashi, 2010). It has been demonstrated that ABCA1 deficient astrocytes secrete smaller lipoprotein particles with significantly lower amounts of ApoE, effectively reducing cholesterol efflux (Hirsch-Reinshagen et al., 2004; Wahrle et al., 2004) that is crucial to neuronal health (Valenza et al., 2015, 2010; Zhang and Liu, 2015). In this vein, cholesterol efflux from ApoE3 astrocytes has been shown to be greater than that of ApoE4 astrocytes (Gong et al., 2002). Abca-/- FAD mice displayed lower ApoE levels but increased amyloid deposition, pointing to the importance of ApoE lipidation in Aβ clearance (Corona et al., 2016; Koldamova et al., 2005; Wahrle et al., 2005). Remarkably, the expression of ApoE4 but not ApoE3 reduced Aβ clearance in this Abca1-/+ FAD model (Fitz et al., 2012). These conflicting results of ApoE-Aβ binding experiments are likely due to the presence of Aβ in distinct pools in the monomeric, oligomeric and fibrillar forms both unassociated and complexed with ApoE (O'Brien and Wong, 2011; Steinerman et al., 2008). In addition, the size of these pools likely depends on Aβ levels and ApoE isoform specific binding affinity (Tai et al., 2013).

1.3.2   Aβ production, degradation, deposition and clearance

There are some data that has suggested that ApoE isoforms may differentially regulate Aβ production. For example, ApoE4 has been found to be associated with increased endocytosis of APP and production of Aβ relative to the E2 and E3 isoforms (He et al., 2007; Ye et al., 2005). Along similar lines, in several cell-based models ApoE has been found to increase APP transcription and subsequent Aβ production in the order E4>E3>E2 (Huang et al., 2017; C. Wang

et al., 2018). This role of ApoE in APP transcription has been supported by studies that have shown reduced levels of mature full-length APP in an ApoE deficient FAD mouse model relative to the wild type control (Dodart et al., 2002).

ApoE isoform-specific differences in Aβ binding may directly result in differential Aβ clearance and subsequent deposition in the brain (Bales et al., 2009; Buttini et al., 2002; Dodart et al., 2005; Dolev and Michaelson, 2004; Fagan et al., 2002; Holtzman et al., 2000). Two main mechanisms result in Aβ clearance from the brain to mitigate deposition—transport across the blood brain barrier and cellular uptake. It has been shown that the clearance of Aβ-ApoE2 and –ApoE3 complexes is more effective through the blood brain barrier (Deane et al., 2008). Specifically, these studies demonstrated that Aβ-ApoE2 and -ApoE3 complexes were cleared at a rapid rate by both LRP1 and VLDL receptor (VLDLR) but Aβ-ApoE4 was cleared only through the slow VLDLR. In terms of clearance of Aβ by cellular uptake, ApoE isoforms have been found to influence binding and endocytosis by cell surface receptors on astrocytes where Aβ is degraded in the lysosome (Li et al., 2018). For example, the pathological acidification of endosomes in astrocytes expressing ApoE4, but not ApoE3, lowered surface presentation of the LRP1 which impaired Aβ clearance in vivo (Prasad and Rao, 2018). Additionally, astrocytic LRP1 deficiency increased amyloid deposition in vivo (Liu et al., 2017a), while ApoE deficiency facilitated Aβ clearance (DeMattos et al., 2004). Thus, ApoE isoform specific differences in receptor affinity could affect Aβ clearance due to direct competition (Verghese et al., 2013) or ApoE-Aβ complex preference. The role of the ApoE2 isoform in these mechanisms is unclear and requires further investigation.

In addition to clearance across the blood brain barrier, the degradation of Aβ by proteolytic enzymes such as neprilysin and insulin-degrading enzyme (IDE) secreted by microglia and astrocytes, is essential to its clearance (Farris et al., 2003; Iwata et al., 2000). While neprilysin and IDE deficiency leads to increased Aβ peptide levels and amyloid deposition in vivo (Farris et al., 2007, 2003; Iwata et al., 2001; Miller et al., 2003), their overexpression leads to more efficient clearance of the peptide and reduced amyloid burden (Hemming et al., 2007; Iwata et al., 2004; Leissring et al., 2003; Spencer et al., 2008). Related to these processes, lipidated

human ApoE increased Aβ degradation in the order E2>E3>E4 in ApoE deficient microglia by enhancing neprilysin and IDE activity (Jiang et al., 2008).

1.3.3 Neurotoxicity

Although astrocytes are the primary source for ApoE in the CNS under physiological conditions (Boyles et al., 1985), neurons produce ApoE in response to excitotoxic injury (Xu et al., 2006) and astroglial factors (Harris et al., 2004; Xu et al., 2008). As such, neuronal, but not astrocytic, ApoE4 has been demonstrated to be more likely to undergo proteolysis compared to ApoE3 and produce truncated neurotoxic fragments in AD brains as well as cultured neurons (Brecht et al., 2004; Harris et al., 2003; Huang et al., 2001; Rohn, 2013). More specifically, a chymotrypsin-like serine protease secreted by neurons has been implicated in proteolytic activity that causes neurotoxic ApoE4 fragments to escape the secretory pathway and translocate to the cytosol where they lead to mitochondrial dysfunction and disrupted neurite outgrowth (Harris et al., 2003; Mahley and Huang, 2012; Tamboli et al., 2014). In addition, it has been established that ApoE4 displays a higher propensity to form neurotoxic fibrillar oligomers compared to the E2 and E3 isoforms, which might be responsible the isoform specific differences in amyloid plaque nucleation (Hatters et al., 2006). In a related study, astrocytic ApoE4, but not ApoE3 enhanced plaque seeding by increasing the half-life of Aβ, amyloid deposition and reducing amyloid induced gliosis in mouse brains (Liu et al., 2017).

1.3.4 Protection against oxidative stress

It is well established that Aβ induces astrocytic glutamate release and disrupts glutamate uptake by astrocytes and neurons (Li et al., 2009; Matos et al., 2008; Talantova et al., 2013). In vitro studies have suggested that ApoE protects against glutamate-induced toxicity by reducing oxidative stress (Lee et al., 2004; Zhou et al., 2013). Similarly, ApoE displayed an isoform-specific antioxidant activity (E2>E3>E4) in the presence of hydrogen peroxide (Miyata and Smith, 1996). Finally, ApoE deficient mice have elevated levels of oxidative stress and increased antioxidant production, suggestive of ApoE's protective role in the brain (Shea et al., 2002).

However, the isoform-specific effects of ApoE on oxidative stress observed with in vitro studies have not been recapitulated in vivo and have yielded conflicting results (Dose et al., 2016).

1.3.5 Modulation of neuroinflammation

Post-mortem analysis of brain tissue from AD patients has revealed chronic neuroinflammation (Gomez-Nicola and Boche, 2015). Mechanistically, it has been shown that Aβ induces an inflammatory response in the form of reactive gliosis (Canning et al., 1993; Heurtaux et al., 2010), which has been hypothesized to result in subsequent neurodegeneration (Lucin and Wyss-Coray, 2009). Several studies indicate that ApoE exhibits both anti- and pro- inflammatory activities. In one such study, exogenous ApoE in the presence of Aβ reduced the inflammatory response in glia cells (Guo et al., 2004). However, in the absence of Aβ, ApoE induced the secretion of pro-inflammatory cytokines, with ApoE4 eliciting a greater response than ApoE3. Additional research with in vitro models has shown that this ApoE isoform effect on neuroinflammation is cell-type dependent (Maezawa et al., 2006). Specifically, the inflammatory response in microglia derived from ApoE targeted replacement (TR) mice was greater in E4 microglia (E4>E3>E2) (Maezawa et al., 2006) but cytokine secretion by astrocytes followed the reverse order, with the highest response elicited in E2 astrocytes (E2>E3>E4) (Maezawa et al., 2006). By comparison, in vivo studies have not fully recapitulated these context-specific effects of various ApoE isoforms. Instead, in vivo studies have consistently showed that ApoE4 promotes higher levels of inflammation relative to ApoE2 and ApoE3 (Shi et al., 2017; Zhu et al., 2012). Consistent with these findings, compared with patients without any ApoE4 alleles, AD patients with at least one copy of ApoE4 displayed significantly higher levels of the pro-inflammatory cytokines IL-1β and IL-6 (Olgiati et al., 2010).

1.3.6 Synaptic plasticity and integrity

Soluble Aβ oligomers have been shown to cause synaptic dysfunction and impair long-term potentiation (LTP) prior to the amyloid deposition (Selkoe, 2002). In healthy brains, the extracellular matrix protein Reelin promotes LTP by binding to the Apoer2-VLDLR complex in

postsynaptic neurons and activating NMDA receptors to strengthen synaptic networks (Wasser and Herz, 2017). Moreover, Reelin antagonizes Aβ-mediated LTP suppression that occurs in AD (Durakoglugil et al., 2009). As it relates to the effects of ApoE on this process, in a study with primary cortical neurons ApoE4 reduced the recycling and cell surface expression of Apoer2, impairing Reelin-mediated LTP (Chen et al., 2010). These results were supported by in vivo work where ApoE genotype influenced Aβ-induced LTP suppression in the order E4 > E3 = apoE-KO > E2 (Trommer et al., 2005). Other studies have shown that ApoE can indirectly affect synaptic integrity through the action of astrocytes. For example, Chung and colleagues demonstrated that ApoE controlled the rate of synaptic pruning of astrocytes in an isoform- specific manner E2>E3>E4 (Chung et al., 2016). In turn, it is hypothesized that this defective phagocytic capacity of ApoE4 astrocytes may increase the rate of C1q-coated senescent synapses, thereby leading to increased synaptic vulnerability to complement-cascade mediated neurodegeneration (Chung et al., 2016).

1.4 Human Induced Pluripotent Stem Cells as a Tool to Model Alzheimer's Disease

In 2007, Yamanaka and colleagues first described the generation of human induced pluripotent stem cells (hiPSCs) from human somatic cells through retroviral overexpression of transcription factors KLF4, c-MYC, OCT4, and Sox2 (Takahashi et al., 2007). More recently, advances in reprogramming technologies have allowed for the generation of integration-free hiPSCs using sendai viruses (Fusaki et al., 2009), mRNA (Warren et al., 2010), and episomal vector expression (Junying et al., 2009; Okita et al., 2011). HiPSCs provide a nearly unlimited starting material from which specialized cell types that mimic those found in the adult human body can be generated. As such, directed differentiation protocols, largely based on the modulation of the chemical microenvironment, have been developed to generate the various neurons and supporting cell types of the central nervous system (CNS) from hiPSCs. Specifically, robust protocols have been developed for the differentiation of hiPSCs to neurons (Bardy et al., 2015; Begum et al., 2015; Zhang et al., 2013), astrocytes (Shaltouki et al., 2013; TCW et al., 2017; Zhao et al., 2017), microglia (Abud et al., 2017) and oligodendrocytes (Wang et al., 2013). More

recently, overexpression of specific transcription factors in the context of developmentally relevant signaling molecules has allowed for the differentiation of hiPSCs to relatively homogenous neural cell types (Nehme et al., 2018; Sun et al., 2016; Zhang et al., 2013). Numerous studies have shown that neural cells derived from both fAD and sAD hiPSCs display disease-relevant phenotypes such as elevated secreted Aβ42 levels, increased Aβ42/40 ratio, and hyperphosphorylation of tau at various epitopes (Arber et al., 2019; Israel et al., 2012; Muratore et al., 2014; Ochalek et al., 2017). Together, these pioneering studies laid the groundwork for hiPSC modeling of AD by validating that an accessible, human cell-based platform can be used to study potential mechanisms by which identified mutations modulate detectable disease-relevant phenotypes. Here, we will discuss how hiPSC-based models provide a valuable resource for studying AD-related mechanisms and elucidating the processes by which defined risk factors, such as ApoE, influence disease onset and progression (**Table A-1**).

1.4.1   Genetic modification of hiPSCs for disease modeling

To date, numerous hiPSC lines have been developed from patients with diverse genetic variants and repositories have been established to provide researchers access these cell lines for disease modeling (e.g. CIRM, WiCell, NYSCF, Coriell). However, genetic diversity among patient samples may make it difficult to tease apart observed phenotypic differences because of their inherent genetic and epigenetic diversity. To this end, the development of genome engineering tools has greatly increased the utility of hiPSCs by allowing targeted modifications without altering the genetic background (Brookhouser et al., 2017a). Specifically, the CRISPR/Cas9 system has provided major advances in efficient genome engineering of mammalian cells allowing for editing at single base pair resolution (Cong et al., 2013; Paquet et al., 2016). It is estimated that over 10,000 human diseases are caused by monogenic mutations (World Health Organization), allowing the possibility of inducing or correcting disease-relevant gene mutations and comparing to the parental, or isogenic, cell line. As we will discuss, the use of such isogenic cell lines with identical genetic background has become the gold standard in modeling and analyzing the effects of AD-related mutations and risk factors.

12

1.4.2 Modeling of fAD with hiPSC-based models

Numerous studies have employed hiPSCs derived from patients with fAD-related mutations in PSEN1/2 and APP to demonstrate the utility of such models in recapitulating disease-relevant phenotypes in vitro. As it relates to PSEN1/2, hiPSC-derived neurons from fAD patients harboring various mutations in PSEN1 (ΔE9 (Woodruff et al., 2013), V89L (Nemes et al., 2016), M146L (Liu et al., 2014), M146V (Paquet et al., 2016), L150P (Ochalek et al., 2017), H163R (Liu et al., 2014), L166P (Koch et al., 2012), ΔS169 (Yang et al., 2017), A246E (Armijo et al., 2017; Liu et al., 2014; Yagi et al., 2011), D385N (Koch et al., 2012)), and PSEN2 (N141I (Yagi et al., 2011; Yu et al., 2010)) have been analyzed for disease-relevant phenotypes. While analysis of cells from all PSEN1/2 mutations revealed an increased Aβ42/40 ratio compared to control lines, only the L166P and ΔE9 increased this ratio by decreasing Aβ40 whereas for all other mutations an increase in Aβ42 was responsible for an elevated ratio. As such, through the study of neurons from these various hiPSC lines it has been suggested that PSEN1/2 mutations might be context-specific with some mutations causing a toxic gain-of-function through elevated Aβ42 production and others inducing a loss-of-function through decreased Aβ40 generation. In addition, further phenotypic characterization of cells revealed other disease-specific phenotypes including higher levels of phosphorylated tau (Ochalek et al., 2017; Yang et al., 2017), sensitivity to neurotoxic stimuli (Armijo et al., 2017), and electrophysiological deficits (Ortiz-Virumbrales et al., 2017). Importantly, in some of these studies genetic engineering approaches were used to correct these disease-causing mutations to establish direct causal links between genotype and phenotype (Ortiz-Virumbrales et al., 2017; Woodruff et al., 2013).

With regards to familial mutations in APP, neurons generated from hiPSCs with various APP mutations including missense (V717I (Muratore et al., 2014), V717L (Shirotani et al., 2017)), truncation (E393Δ (Kondo et al., 2013)), duplication (DP ((Israel et al., 2012)), and triplication (TP (Ovchinnikov et al., 2018; Shi et al., 2012)) have been extensively phenotypically characterized. For example, Israel et al. (Israel et al., 2012) demonstrated that neurons generated from hiPSCs with a duplication in the APP gene (APPdp) exhibited higher levels of Aβ, hyperphosphorylated tau, and increased activity of the GSK3β kinase compared to healthy control lines. Critically, this

study validated the production of detectable disease phenotypes in hiPSC-derived neurons within weeks of culture, despite the relatively long time required for phenotypes to become evident in AD patients. Moreover, treatment of APPdp neurons with β- secretase (BACE) inhibitors reduced tau phenotypes and reduced GSK3β activity (Israel et al., 2012).

In a similar study, neurons generated from APPV717I hiPSCs displayed elevated Aβ42/40 levels with a corresponding increase in phosphorylated tau that was reduced through γ-secretase inhibition (Moore et al., 2015). Likewise, treatment of APPV717I hiPSC derived neurons with Aβ-specific antibodies ameliorated elevated tau levels (Muratore et al., 2014). Together, these studies establish a causal relationship between APP processing and tau-related phenotypes. Alternatively, a recent study highlighted that genome modification to restore a euploid karyotype in neurons generated from an individual with Down syndrome rescued Aβ phenotypes due to APP gene dose, however, was insufficient to reduce tau hyperphosphorylation (Ovchinnikov et al., 2018). These data challenge the proposed model that elevated Aβ is directly responsible for downstream tau pathology, suggesting that a more complex mechanism may govern disease progression.

HiPSC-based systems have also allowed for the investigation of the precise molecular mechanisms that lead to these mutation-specific phenotypes. For example, neurons derived from APPV717I mutant hiPSCs demonstrated abnormal subcellular localization of APP within acidic early endosomes containing active BACE, modulating APP processing by β- and γ- secretase and potentially driving increased levels of Aβ and phosphorylated tau (Muratore et al., 2014). In another study, it has been shown that APPdp hiPSC-derived neurons exhibit a similar early endosome accumulation phenotype that may be driven by increased β-CTF levels (Israel et al., 2012). Similarly, analysis of neurons from fAD-hiPSC with mutations such as PSEN1ΔE9, APPV717F, and APPswe revealed increased β-CTF generation and impairment of lipoprotein endocytosis and transcytosis to the axon, suggesting that fAD mutations may result in convergence on common molecular pathways (Woodruff et al., 2016). On the other hand, a recent phenotypic screen of seven diverse fAD hiPSC lines revealed that APP mutations altered γ-secretase cleavage site preference whereas PSEN1 mutations altered amyloid peptide profile

through several mechanisms including decreased γ-secretase activity, decreased protein stability, and reduced PSEN1 maturation (Arber et al., 2019).

Non-neuronal cells, specifically astrocytes and microglia, play an important role in maintaining brain homeostasis and aberrant function of these effector cells has been shown to be a major contributor to brain dysfunction in AD (Colombo and Farina, 2016; Dzamba et al., 2016; V. M. Sofroniew and Vinters, 2010). Because hiPSCs can be directed into precise cell types, hiPSC-based models have been employed to investigate cell type-specific effects in fAD. For example, Oksanen et al. demonstrated that hiPSC-derived astrocytes with a PSEN1ΔE9 point mutation exhibited AD-relevant phenotypes including increased levels of Aβ production and decreased Aβ clearance, as well as altered cytokine secretion, mitochondrial metabolism, and Ca2+ homeostasis (Oksanen et al., 2017). Importantly, these phenotypes were reversed upon isogenic correction of the PSEN1 mutation, demonstrating a direct genotype-to-phenotype relationship. In another study, astrocytes from several isogenic hiPSCs lines harboring mutations in APP were examined (Fong et al., 2018). Notably, astrocytes derived from hiPSCs homozygous for the APP Swedish (APPSwe/Swe) mutation displayed Aβ endocytosis defects due to increased β-secretase cleavage whereas astrocytes with other APP mutations, such as V717F, did not display these deficits.

The use of hiPSCs to study ApoE in the context of these fAD related mutations has been limited. To date, the majority of studies have primarily employed lines homozygous for the ε3 allele or of an unreported genotype. In the future, the use of genome editing technologies to generate fAD hiPSC lines with various ApoE isoforms will allow for the determination of the extent to which the introduction of various APOE alleles modulates disease-related phenotypes.

1.4.3   Investigating effects of APOE genotype in AD with hiPSC models

Broadly speaking, the presence of disease-related phenotypes in cells generated from sAD hiPSCs have been highly variable (Duan et al., 2014; Israel et al., 2012). For example, one of the earliest iPSC models of sAD compared neurons derived from two sAD patients with iPSC-derived neurons of two fAD and non-demented control individuals (Israel et al., 2012). Neurons

derived from one of the two sAD lines used in this study exhibited higher levels of Aβ40, p-Tau and active glycogen synthase kinase-3β (GSK3β), similar to the phenotype observed in fAD derived neuronal cultures. In a related study, analysis of neurons derived from several independent sAD hiPSC lines revealed elevated Aβ42/40 ratios only in a subset of the lines (Duan et al., 2014). Despite the variability in observed phenotypes in sAD hiPSC models, these studies provided proof-of-principle for using hiPSC-based models to investigate the role of various AD risk factors, such as ApoE, in a simplified and accessible system.

1.4.3.1 Phenotypic characterization of hiPSC lines with various APOE genotypes

Over the past several years, numerous hiPSC lines have been generated from individuals with various ApoE genotypes (Brookhouser et al., 2018, 2017b, 2017c; Peitz et al., 2018; C. Wang et al., 2018; Zhao et al., 2017; Zollo et al., 2017; Zulfiqar et al., 2016a, 2016b). Detailed biochemical analysis and phenotypic characterization of neural cells derived from these hiPSC lines have revealed several interesting ApoE isoform-specific effects. In one such study, neurons were derived from hiPSCs homozygous for APOE4 and APOE3 (C. Wang et al., 2018). This analysis revealed that Aβ secretion, p-Tau levels, and GABAergic neuron degeneration were elevated in APOE4/4 neurons when compared to APOE3/3 neurons. Moreover, treatment of these cells with β- or γ-secretase inhibitors decreased Aβ40 and Aβ42 levels in the culture medium while phosphorylated tau levels were unaffected, suggesting p-Tau accumulation occurs in an Aβ-independent manner. A related study attempted to use hiPSC-derived neurons to examine the mechanism behind this isoform- specific effect on Aβ levels (Huang et al., 2017). Specifically, Huang et al. demonstrated that ApoE binding to neuronal ApoE receptors activated a non-canonical MAPK pathway which led to cFos phosphorylation. In turn, the transcription factor activating protein-1 (AP-1) became activated, which increased expression of APP and, subsequently, Aβ levels in the rank order ApoE4>ApoE3>ApoE2. In a complementary study, Zollo et al. demonstrated that ApoE modulated sortilin-receptor (SORL1)-related APP trafficking and processing (Zollo et al., 2017). Specifically, the authors showed that in APOE4 neurons there was increased Aβ/SORL1 localization along the degenerated neurites when compared to

neurons without an APOE4 allele. Moreover, SORL1 binding to APP was compromised in these APOE4 neurons which contributed to elevation of secreted Aβ.

Additional studies have revealed other neuronal phenotypes associated with various ApoE isoforms. For example, when co-cultured with neurons, APOE3/3 hiPSC-derived astrocytes provided neuroprotective effects when compared to neurons cultured with APOE4/4 astrocytes (Zhao et al., 2017). In addition, APOE genotype influenced synaptic integrity as demonstrated by the increased expression of synaptic proteins in neurons co-cultured with APOE3/3 astrocytes relative to those cells co-cultured with APOE4/4 astrocytes (Zhao et al., 2017). Mechanistically, a parallel study of hiPSC-derived neurons treated with recombinant ApoE suggests that this altered synaptogenesis is mediated by CREB activation in the rank order ApoE4>ApoE3>ApoE2 (Huang et al., 2019).

HiPSC-based models have also been used to examine the effect of APOE genotype in other neural cell types. For example, Zhao et al. characterized the lipidation status of ApoE secreted from astrocytes differentiated from APOE3/3 and APOE4/4 hiPSCs (Zhao et al., 2017). This analysis revealed that ApoE produced by APOE3/3 astrocytes was more lipidated than that produced by APOE4/4 cells. The authors speculate that this reduced cholesterol transport from APOE4/4 astrocytes could be detrimental to neuronal health. In a separate study, microglia differentiated from a library of hiPSCs with various fAD mutations and APOE genotypes were examined. These experiments showed that microglia derived from APOE4 iPSCs demonstrated aberrant functional phenotypes including decreased chemokinesis, reduced phagocytosis and aggravated cytokine response to inflammatory stimuli compared to microglia derived from hiPSCs harboring fAD mutations (Konttinen et al., 2019).

1.4.3.2 Engineering hiPSCs to elucidate APOE genotype-to-phenotype relationships

Although the analysis of hiPSC lines derived from patients with various APOE genotypes has revealed some potential isoform-specific effects, the analysis of these phenotypic effects has been somewhat confounded by the genetic and epigenetic differences inherent in individual hiPSC lines derived from distinct patients. To that end, advances in genome editing technologies

has allowed for the generation of isogenic hiPSC lines from both NDC and AD patients that will only differ with respect to their APOE genotype and not their genetic background.

In a landmark study using CRISPR/Cas9-edited hiPSCs, Lin et al. examined the effect of APOE genotype in hiPSC-derived neurons, astrocytes, and microglia (Lin et al., 2018). Relative to the APOE3/3 counterparts, APOE4/4 neurons had a higher number of synapses, more early endosomes, and increased Aβ42 secretion. In addition, APOE4/4 astrocytes demonstrated less efficient Aβ clearance, lower ApoE levels, and accumulation of cholesterol. Likewise, APOE4/4 microglia had impaired Aβ42 uptake while also displaying an altered inflammatory profile. Moreover, transcriptome profiling of all three cell types was consistent with these phenotypes as the ApoE variant modulated the expression of several pathways associated with synaptic function, lipid metabolism, and immune response. Finally, isogenic conversion of sAD hiPSCs from APOE4/4 to APOE3/3 reversed these defects, as observed by the reduced number of synapses in neurons, as well as restored ApoE levels and Aβ uptake capacity in astrocytes and microglia. A separate study employing isogenic lines also confirmed many of these isoform-dependent effects (C. Wang et al., 2018). Specifically, conversion of APOE4 hiPSCs to an APOE3 genotype increased the levels of full-length ApoE in neuronal lysates and decreased Aβ42 secreted into the culture media. In addition to these effects, this analysis also revealed that this conversion resulted in fewer phosphorylated tau-positive GABAergic neurons. Finally, the introduction of the APOE3 alleles rescued the degeneration of GABAergic neurons observed in in APOE4/4 neuronal cultures, as measured by increased levels the synaptic marker GAD67.

The use of genetically modified hiPSCs lines have also allowed for the identification of novel target pathways that are influenced by APOE genotype. For example, Meyer et al. report that accelerated differentiation and reduced progenitor cell self-renewal was observed in neural cultures derived from APOE4/4 hiPSCs (Meyer et al., 2019). In addition, the authors demonstrated that the function of the transcriptional repressor REST was impaired in APOE4/4 cells. Moreover, the loss of REST function was attributed to reduced nuclear translocation and chromatin binding. Importantly, gene editing of these cells to an APOE3/3 genotype reversed these observed phenotypes. Because REST plays a role in the repression of neuronal genes

during early nervous system development, the authors speculated that ApoE4-depdent dysregulation of REST may reduce hippocampal adult neurogenesis through depletion of the endogenous neural progenitor pool. In turn, this effect may accelerate the onset of AD by reducing this regenerative capacity.

Existing in vitro models of AD are largely monotypic, with disease progression, phenotype and drug development in neuronal cultures. The complexity of modelling SAD in vitro however necessitates the addition of other cell types identified with risk variants like astrocytes (*APOE*) and microglia (*TREM2*). The completion of this study will advance our understanding of the molecular mechanisms that underlie astrocyte dysfunction in AD in addition to improving currently existing in vitro AD models for the high throughput screening of potential therapeutics.

1.5   Specific Aims

This study investigates the mechanism underlying the protective effect of *APOE2* in AD by addressing the following specific aims.

1.5.1 Specific Aim 1

Generate, characterize and evaluate the scalability and cryopreservation-potential of functional astrocytes derived from fAD-hiPSC lines so as to develop assays to measure AD phenotype across multiple cell lines.

1.5.2 Specific Aim 2

Develop and characterize a system to evaluate the cell- type specific contribution of both neurons and astrocytes to AD phenotype in *APOE2* and *APOE3* isogenic neural cultures derived from fAD and non-demented control patient iPSCs.

1.5.3 Specific Aim 3

Elucidate differences in APP processing between *APOE2* and *APOE3* isogenic neural cultures by investigating pathway intermediates that may confer a protective effect to APOE2.

Acknowledgments

Figure 1.1. APOE Isoform Specific Effects in AD.
Amyloid-β (Aβ) is produced primarily by neurons in the brain (①) where it interacts with lipidated ApoE secreted by microglia and astrocytes (②) in an isoform specific manner. ApoE4 promotes the oligomerization and aggregation of Aβ (③) and the subsequent deposition of plaques (④) in vivo. Cell surface low-density lipoprotein receptor (LDLR), LDLR-related protein 1 (LRP1) and heparan sulfate proteoglycan (HSPG) receptors mediate the endocytosis of Aβ by astrocytes and microglia. In addition to promoting the production and aggregation of Aβ, ApoE4 impairs Aβ clearance by reducing cellular uptake and transport across the blood brain barrier in vivo (⑤). ApoE2 overexpression enhances the proteolytic degradation of Aβ by insulin-degrading enzyme (IDE) and neprilysin produced by microglia and astrocytes (⑥). The enhanced proteolysis of neuronal ApoE4 by a chymotrypsin-like serine protease produces neurotoxic fragments (⑦). ApoE4-astrocytes exhibit reduced synaptic pruning capacity triggering the synaptic accumulation of the complement-component 1q (C1q) protein, possibly inducing complement pathway mediated neurodegeneration in vivo (⑧). ApoE4 expression also elicits a prolonged increase in pro-inflammatory cytokine secretion by astrocytes and microglia leading to chronic neuroinflammation and neurodegeneration (⑨). ApoE isoform specific roles in these processes are indicated. Figure was generated with the assistance of Biorender.

CHAPTER 2

GENERATION OF HUMAN INDUCED PLURIPOTENT STEM CELL (HIPSC) DERIVED

ASTROCYTES

2.1   Introduction

Astrocytes are an abundant, specialized non-neuronal cell type in the central nervous system

(CNS) that have numerous functions in maintaining healthy neural tissue including axonal

development and guidance, synapse formation and function, ion and neurotransmitter balance,

and energy metabolism (De Pittà et al., 2016; Khakh and Sofroniew, 2015; Oberheim et al., 2006;

M. V. Sofroniew and Vinters, 2010). In addition, astrocytes are important mediators in response to

traumatic injury and infectious agents (Khakh and Sofroniew, 2015; Zhang and Barres, 2010).

Moreover, death or dysregulation of astrocytes has been implicated in numerous CNS

pathologies and disorders such as multiple sclerosis, Alzheimer's disease (AD), amyotrophic

lateral sclerosis (ALS), and Parkinson's disease (M. V. Sofroniew and Vinters, 2010). Because of

the diverse roles that astrocytes play in CNS homeostasis and disease, there is a critical need for

models to study astrocyte biology in vitro and strategies to replace diseased astrocytes in vivo.

Advances in cellular reprogramming have allowed for the generation of human induced

pluripotent stem cells (hPSCs) that can be used to dissect disease mechanisms on a cellular

level, evaluate potential therapeutics on human cells with euploid karyotypes, and provide the

unlimited raw material for cell-based therapies. Specifically, hPSC-derived astrocytes have

allowed for the study of a variety of neurodegenerative diseases in a simplified and accessible

system (Gonzalez et al., 2017). In addition, astrocytes generated from hPSCs have enabled a

variety of novel neurotoxicity and drug screening paradigms (Oksanen et al., 2019; Pei et al.,

2016). Finally, astrocytic populations produced from hPSCs have shown promise in replacing the

diseased and damaged tissue in conditions such as ALS, stroke, and AD (Izrael et al., 2018;

Kokaia et al., 2018; S.-M. Wang et al., 2019).

Despite these advances, according to several technology roadmaps developed by the

regenerative medicine industry, scalable and adaptable culture methods that employ cost-

effective, chemically defined substrates are still needed to generate the large quantities of cells required for downstream applications in disease modeling, drug screening, and cell-based therapies (Aijaz et al., 2018; Hunsberger et al., 2019, 2018; Shariatzadeh et al., 2020). More specifically, current biomanufacturing techniques are limited by the following. First, current differentiation protocols employ undefined substrates such as MatrigelTM (Serio et al., 2013) or extracellular matrix proteins (ECMPs) isolated from animal sources (Haidet-Phillips et al., 2014; Krencik et al., 2011; Roybon et al., 2013; Shaltouki et al., 2013). In turn, such heterogeneous, xenogeneic components not only pose a risk of transmitting adventitious pathogens but also suffer from batch-to-batch variability which might limit their compatibility with downstream clinical applications (De Sousa et al., 2016; Stacey et al., 2019). Second, conventional astrocyte generation strategies employ traditional two-dimensional (2-D) culture techniques which do not allow for production of large cell quantities needed for drug screening and cell-based therapies. For example, it has been estimated that 109 to 1010 cells will be required to screen a 1 million-compound library or provide a single therapeutic dose (M. M. Silva et al., 2015; Simaria et al., 2014), which will not be achievable with typical 2-D differentiation methods. Lastly, existing schemes require the differentiation of astrocytes in real-time immediately prior to their application and do not allow for their long-term storage to enable point of use (Lin et al., 2017; M. Silva et al., 2015).

In previous work, we identified a completely synthetic substrate, termed vitronectin-derived peptide (VDP), that allowed for the long-term expansion and neuronal differentiation of multiple human neural progenitor cell (hNPC) lines (Varun et al., 2017). Here, we significantly expand upon this work to use this peptide as a fully defined surface for the differentiation of astrocytes from multiple independent hPSC lines. We demonstrate that these cell populations express high levels of canonical astrocytic markers and display a genome-wide transcriptional profile that is indistinguishable from cells generated on conventional animal-derived ECMP-based surfaces. Moreover, these populations displayed properties of functionally mature astrocytes including production of Apolipoprotein E (APOE), responsiveness to inflammatory stimuli, ability to uptake amyloid-β (Aβ), and presentation of robust calcium transients. In addition, we

demonstrate that this defined peptide substrate is compatible with scalable microcarrier (MC)-based techniques. Finally, we establish that these astrocytes can be cryopreserved without any loss of functionality. Overall, the strategies developed here will enable biomanufacturing processes for the large-scale production and long-term storage of hPSC-derived astrocytes needed for downstream application in disease modeling, drug screening, and regenerative medicine.

2.2   Experimental Methods

2.2.1   Synthesis of vitronectin derived peptide (VDP)

Peptide synthesis was performed as we previously described (Srinivasan et al., 2018).

2.2.2   Human neural progenitor cell (hNPC) generation and expansion

Human neural progenitor cells (hNPCs) were generated and culture similar to as previously described (Varun et al., 2017). Briefly, hNPCs were culture on laminin (LN) or VDP-coated tissue culture plates in the presence of neural expansion medium [NEM; 1X DMEM-F12 (ThermoFisher), 0.5% (v/v) N2 supplement (Thermo Fisher), 1% (v/v) B27 supplement (Thermo Fisher), 1% (v/v) GlutaMAX supplement (Thermo Fisher), 1% (v/v) Penicillin Streptomycin (Thermo Fisher), 30 ng/ml FGF2 (STEMCELL Technologies), and 30 ng/ml EGF (STEMCELL Technologies)]. Every 3-4 days hNPCs were enzymatically passaged with Accutase (ThermoFisher) onto freshly coated LN or VDP plates.

2.2.3   Differentiation of hNPCs to astrocytes on 2-D surfaces

HPSC-derived astrocytes were generated as previously described (Zhao et al., 2017). Briefly, astrocytes were differentiated for a minimum of 50 days (unless otherwise noted) on LN- or VDP-coated plates by culturing high passage (> passage 6) hNPCs cultured in astrocyte differentiation medium [ADM; 1X complete astrocyte medium (ScienCell), 10ng/ml human

recombinant BMP4 (STEMCELLTechnologies), 10ng/ml human recombinant Heregulin-β (STEMCELLTechnologies), and 10ng/ml human recombinant CNTF (STEMCELLTechnologies)].

2.2.4 VDP and LN coating of microcarriers (MCs)

MCs (Corning Enhanced Attachment Microcarriers) were coated with VDP or LN using methods similar to those as previously described (Srinivasan et al., 2018) .

2.2.5 Differentiation of hNPCs to astrocytes on MCs

HNPCs were seeded on VDP-coated MCs in 6-well ultra-low attachment plates (Corning) with 1.5×10^6 cells per well and 1 mg/mL MCs. The cells and MCs were suspended at half the final culture volume of 4mL in NEM supplemented with 5µM Rho kinase inhibitor (ROCKi Y-27632). The plates were then placed in the incubator for 12 hours to allow for cell attachment. The rest of the media and ROCKi were added to the cultures after 12 hours and the cells were placed on an orbital shaker at 95 rpm; the cultures were agitated for the rest of the culture period. After 24 hours of seeding the hNPCs on MCs, the media was switched to ADM to start hNPC differentiation to astrocytes. Cells were maintained in ADM for 50 days with half media changes every day until further analysis or replating. Cells were removed from the MCs by incubating in a papain solution containing Earle's balanced salt solution (Alfa Aesar), 20U/mL papain (Worthington), 1mM L-Cysteine, 22.5mM D-glucose, 26mM $NaHCO_3$ and 125U/mL DNase (Roche) for 20 minutes at 37°C and then triturated with an inhibitor solution containing 1mg/mL ovomucoid inhibitor (Roche) and 1mg/mL BSA (Sigma). A 40µm cell strainer was used to separate the cells from the MCs and the cells were seeded on freshly coated VDP MCs.

2.2.6 Differentiation of hNPCs to neurons on MCs

HNPCs were differentiated to neurons on MCs as previously described (Srinivasan et al., 2018). HNPCs were differentiated on MCs for a minimum of 30 days before further analysis or replating.

2.2.7   Flow cytometry analysis

Cells were processed for flow cytometry analysis using an ACCURI C6 (BD Biosciences) as previously described (Srinivasan et al., 2018). For viability assessment, cells were stained with 0.01mg/mL propidium iodide (Thermo Fisher) in PBS. **Supplementary Table B.1** lists antibodies and isotype negative controls used in this study.

2.2.8   Quantitative PCR (qPCR)

Gene expression was measured using qPCR and normalized to 18S rRNA levels as described previously (Srinivasan et al., 2018). The list of specific primer sequences that were employed in qPCR analysis is provided in **Supplementary Table B.2**.

2.2.9   Immunofluorescence

Immunofluorescence staining of cells on 2D and MC surfaces as well as subsequent image analysis was performed as previously described (Srinivasan et al., 2018). Primary and secondary antibodies that were used are listed in **Supplementary Table B.1**. All images were acquired on an automated confocal microscope (Leica TCS SP5) or EVOS microscope.

2.2.10   RNA-seq analysis

All sequencing was performed at BGI Americas Corporation using BGISEQ-500 for a single end 50 bp run as described previously (Srinivasan et al., 2018). Reads were subsequently mapped to the hg19 human reference genome using STAR 2.5.2b (Dobin et al., 2013). Differential analysis was performed using gene counts obtained from featureCounts (Liao et al., 2014) in EdgeR.(Robinson et al., 2010). Gene ontology analysis was performed using lists of differentially expressed genes in DAVID (Huang et al., 2009).

2.2.11 Cytokine bead array

Astrocytes were seeded in a 24 well plate at a density of 25×10^3 cells per well. Three days later, cells were treated with 25μg/mL lipopolysaccharide (ThermoFisher) for 24 hours as

previously described (TCW et al., 2017). The cell supernatant was collected after lipopolysaccharide treatment and stored at -20°C and thawed on ice before cytokine analysis using the LEGENDplex™ Human Inflammation Panel (Biolegend) as directed by the manufacturer. The samples were subsequently analyzed on an Attune NxT Flow Cytometer (ThermoFisher) and cytokine concentration was determined using the LEGENDplex™ data analysis software.

2.2.12 Apolipoprotein E (APOE) ELISA

Astrocytes were seeded in a 12 well plate at a density of 1×10^5 cells per well. Three days later, the cell supernatant was concentrated using Amicon Ultra filters (EMD Millipore) and stored at -80°C until analysis. APOE levels in the medium were measured with the Human APOE (AD2) ELISA Kit (Thermo Scientific).

2.2.13 Calcium imaging

For calcium imaging analysis, astrocytes were seeded at a density of 2×10^5 in a glass 40mm dish. Cells were incubated with $2\mu M$ Fluo-4 AM (ThermoFisher) and 0.02% Pluronic™ F-127 in DMEM for 15 min at 37°C. After one wash in HEPES-buffered Tyrode's solution (Alfa Aesar), they were allowed to de-esterify at room temperature for 20 minutes prior to imaging on a Zeiss AxioObserver Z1. Fluorescent time-lapse images were acquired (20x objective) at 1 s intervals for 360 s. Calcium spike traces were generated by quantifying the mean pixel intensity of manually identified regions of interest using the ImageJ software. For astrocytes cultured on microcarriers, cells differentiated for at least 45 days were replated at a density of 1.4×10^6 cells onto VDP-coated glass 40mm dishes and cultured for 2-4 days prior to staining and imaging.

2.2.14 β-amyloid and dextran uptake assay

FAM-labelled β-amyloid peptide (Aβ-FAM 1-42; Anaspec) was reconstituted using a minimal volume of 1%NH_4OH and immediately diluted to a 1mg/mL solution in PBS. Single-use

aliquots were stored at -20°C till use. For the uptake assay, astrocytes seeded in a 24 well plate were treated with 500 nM-1000nM Aβ-FAM and/or 50 µg/ml dextran-Alexa Fluor 647 (ThermoFisher) for 24 hours. For flow cytometry, cells were washed with cold PBS and dissociated using Trypsin (ThermoFisher) for 5 min at 37°C to remove any surface-bound peptide. Samples were placed on ice and 5,000-10,000 live cells were analyzed on a Accuri C6 flow cytometer (BD Biosciences) to quantify median fluorescence intensity. For fluorescent imaging, cells were imaged on a Nikon Ti2 Eclipse.

2.2.15 Cryopreservation of differentiated astrocytes

After a minimum of 45 days of differentiation, astrocytes that were 85% confluent were dissociated using Accutase and resuspended in cryopreservation medium. The cells were first gradually cooled to -80°C in a Mr. Frosty™ freezing container (ThermoFisher) for 24 hours, after which the vials were transferred to -150°C for long term storage. For the functional comparison experiments astrocytes were thawed 7 days after freezing.

2.2.16 Statistical analysis

Student's t-test and ANOVA were used to analyze the data, with a Bonferroni post hoc correction where appropriate. Significance represents a p-value < 0.05. Additionally, all data are displayed as mean ± standard error of the mean (S.E.M.) unless otherwise specified.

2.3 Results

2.3.1 Highly efficient generation of astrocytes from multiple independent hPSC lines on a defined substrate.

We previously described a protocol that employs a fully defined peptide-based substrate, referred to as vitronectin-derived peptide (VDP), that allows for the differentiation and long-term expansion of multipotent human neural progenitor cells (hNPCs) (Srinivasan et al., 2018). To that

end, we derived hNPCs from six independent hPSC lines (**Supplementary Table B.3**), two lines from healthy non-demented control patients (herein referred to as NDC-1 and NDC-2), two lines from familial Alzheimer's disease patients (herein referred to as FAD-1 and FAD-2), and two lines from sporadic Alzheimer's disease patients (herein referred to as SAD-1 and SAD-2). Similar to our other established hNPC lines, all six hNPC lines expressed high levels of the canonical hNPC markers SOX1, SOX2, and NESTIN (**Supplementary Figure B.1**). To determine if VDP could support the differentiation of hNPCs into functional astrocytes, hNPCs were seeded onto VDP or control animal-derived laminin (LN) (an extracellular matrix protein commonly used in astrocytic differentiation of hPSCs; (Haidet-Phillips et al., 2014; Krencik et al., 2011; Roybon et al., 2013; Shaltouki et al., 2013)) substrates and the medium was changed from neural expansion medium (NEM) to astrocyte differentiation medium (ADM). HNPCs differentiated on both VDP and LN substrates rapidly acquired a flat, star-shaped astrocytic morphology (**Figure 2.1A**). By day 30, the majority of the cells (>90%) on both substrates acquired the astrocyte progenitor marker CD44 (Liu et al., 2004) (**Figure 2.1B**). In addition, quantitative RT-PCR (qPCR) showed that expression of genes associated with an astrocytic phenotype such as *GFAP* (Ludwin et al., 1976) and *VIM* (Schnitzer et al., 1981) was similar in astrocytes generated on VDP- and LN-coated surfaces (**Figure 2.1C**). Similarly, immunofluorescence (**Figure 2.1D**, **Supplementary Figures B.2-3**) and flow cytometry (**Figure 2.1E**) demonstrated that a high percentage (>85%) of hNPCs cultured on VDP-coated surfaces expressed the astrocyte markers GFAP and S100β (Ludwin et al., 1976). In sum, this data demonstrates that VDP can support the differentiation of hNPCs into astrocytes at an efficiency similar to that on conventional LN substrates.

2.3.2   Astrocytes generated on LN and VDP share a similar transcriptional profile

To further characterize the extent to which astrocytes generated on VDP were similar to those differentiated on LN, we performed RNA-sequencing (RNA-seq) analysis on hNPCs, neurons, and astrocytes derived from NDC-1 hPSCs generated on VDP and LN substrates (**Supplementary Table B.4**). Clustering **(Figure 2.2A)**, correlation (**Figure 2.2B**), and multidimensional scaling (**Figure 2.2C**) analysis revealed that astrocytes generated on VDP and

LN showed a high degree of similarity and grouped distinctly from the hNPC and neuronal cell populations. A closer examination of the genes statistically significantly upregulated (log$_2$ FC >1.5, FDR < 0.05; **Supplementary Table B.5**) in the astrocytic populations revealed high levels of not only established astrocyte markers (e.g. *CD44*, *GFAP*, *NFIX*, *VIM*) but also processes associated with astrocytic function including growth factor production (e.g. *BDNF, CTGF, IGF2, TGFBI*), mediation of cell-adhesion (e.g. *ICAM1*, *ITGA1*, *ITGA5*, *ITGA6*, *ITGB1*, *ITGB3 ITGB5*), extracellular matrix secretion (e.g. *COLL11A1*, *FN1, LAMB2*, *TNC*), and inflammatory and immune response (e.g. *CCL2*, *IL1A*, *IL6*, *IL8*). In addition, astrocytes derived both on VDP and LN surfaces did not display significant levels of hNPC- (e.g. *SOX1*, *SOX2*) or neuronal-associated (e.g. *MAP2*, *RBFOX3*, *TUBB3*) markers. Gene ontology (GO) analysis further confirmed that genes up-regulated in both VDP- and LN-derived astrocytes were related to typical astrocytic biological processes (e.g. immune system processes, cytokine-mediated signaling (Colombo and Farina, 2016b; Dong and Benveniste, 2001; Guerriero et al., 2017; Sofroniew, 2014)), cellular components (e.g. cell substrate junction, focal adhesion (Cho et al., 2018; Moeton et al., 2016; Wiese et al., 2012)), and molecular functions (e.g. cadherin, cell adhesion molecule, and integrin binding (Hillen et al., 2018; Liddelow and Hoyer, 2016)) (**Figure 2.2D**). On the other hand, GO analysis revealed that gene sets concomitantly downregulated in the astrocyte cell populations but upregulated in the neuronal cells were typical of the biological processes, cellular components, and molecular functions of electrophysiologically active neurons. Overall, these results indicate that astrocytes generated on VDP substrates are not only transcriptionally indistinguishable from those derived on control LN substrates but have an expression profile that is characteristic of functional astrocytes.

2.3.3 VDP-derived astrocytes secrete robust amounts of ApoE

Although the astrocytes generated on VDP expressed the genes and proteins typically associated with astrocytes, we next wanted to measure their functional characteristics. Apolipoprotein E (ApoE) is a lipoprotein transporter involved in cholesterol transport that is generated and secreted by functionally mature astrocytes (Hauser and Ryan, 2013). In the brain,

ApoE also plays important roles as it relates to neuronal growth, synaptic plasticity, and membrane repair (Lane-Donovan and Herz, 2017; Suri et al., 2013). To determine whether astrocytes generated on VDP produced ApoE, we measured the amount of ApoE in the conditioned media by ELISA. Compared to hNPCs, which produced no detectable level of ApoE, astrocytes generated on both VDP and control LN substrates produced ApoE in the range of 50-150 ng/mg protein (**Figure 2.3A**), which is consistent with the levels of ApoE produced by hPSC-derived astrocytes in other studies.(Zhao et al., 2017) In addition, there was no consistent difference between astrocytes generated on VDP or LN surfaces in terms of levels of ApoE secretion. These results indicate that hPSC-derived astrocytes generated on VDP secrete robust and comparable amounts of ApoE to those astrocytes generated on LN control substrates.

2.3.4 Astrocytes derived on VDP are responsive to inflammatory stimuli

Astrocytes play a chief role in the inflammatory response in the central nervous system through secretion of cytokines and growth factors that mediate tissue damage, repair, and survival (Colombo and Farina, 2016a; Liddelow and Barres, 2017; Sofroniew, 2015). Given the importance of astrocytes regulating the neuroinflammatory processes in the central nervous system in response to neurodegenerative disease, ischemia, or acute brain injury, we wanted to determine if astrocytes differentiated on VDP substrates were responsive to inflammatory stimuli. To that end, we utilized a cytokine bead array to measure the amount of inflammation-related cytokines in the conditioned media of astrocytes derived on VDP and control LN surfaces. In the absence of any stimulation, we found that astrocytes on VDP and LN secreted modest or undetectable levels of numerous pro-inflammatory (IFN-α, IL-1β, TNF-α, MCP-1, IL-6, IL-8, IL-10, IL-18, IL-23, IL-33) and anti-inflammatory cytokines (IFN-ɣ, IL-12, IL-17α) (**Figure 2.3B**), consistent with previous reports in primary and hPSC-derived astrocytes which show low levels of such cytokines in unstimulated conditions (Choi et al., 2014; Lundin et al., 2018; Perriot et al., 2018; Santos et al., 2017; Sofroniew, 2014; TCW et al., 2017; van Neerven et al., 2010). In order to test if these astrocyte populations altered their cytokine secretion profile in response to inflammatory stimuli, we treated cell populations generated on both VDP and LN with

lipopolysaccharide (LPS), a bacterial cell wall endotoxin widely used to study cellular responses to inflammation (Hamby et al., 2012; Strokin et al., 2011; Zamanian et al., 2012). Across all astrocytic populations tested, we observed an increase of IL-6, IL-8, and MCP-1, which is consistent with previous studies in primary and hPSC-derived astrocytes showing that these cytokines are the prime mediators of the inflammatory response (Lundin et al., 2018; Martinez and Modric, 2010; Perriot et al., 2018; Santos et al., 2017; TCW et al., 2017) (**Figure 2.3C**). Moreover, there was no obvious difference in the responses of VDP- or LN-derived astrocytes. Together, these findings indicate that astrocytes generated on VDP are capable of responding to inflammatory stimuli through modulation of their secreted cytokine profile.

2.3.5 VDP-generated astrocytes have the ability to uptake amyloid (Aβ)

Amyloidogenic processing of the full-length transmembrane protein β-amyloid precursor protein (APP) is a multi-stage process that results in generation of Aβ peptides of various lengths, most commonly Aβ38, Aβ40, Aβ42 (Oksanen et al., 2017). Under healthy physiological conditions in the central nervous system, Aβ peptides play important roles as it relates to synapse function and neuronal activity (Palop and Mucke, 2010; Vallée and Lecarpentier, 2016). The levels of Aβ in the extracellular space are, in part, regulated by astrocytes and play a significant role in Aβ clearance (Ries and Sastre, 2016). To that end, to determine whether the astrocytes generated on VDP and LN surfaces were able to internalize Aβ, we treated astrocytes with FITC-conjugated Aβ(1-42) and measured uptake 24 hours later with flow cytometry (**Figure 2.4**). In addition, confocal analysis of astrocytes treated with FITC-Aβ and fluorescently-labeled dextran confirms cell internalization of Aβ via the endosomal pathway (**Supplementary Figure B.4**). This analysis revealed that astrocytes generated on both substrates were capable of significant uptake of Aβ (**Figure 2.4**).

2.3.6 VDP-generated astrocytes display spontaneous calcium activity

A hallmark property of mature astrocytes is the ability to exhibit spontaneous calcium transients (Levin et al., 1989; Shigetomi et al., 2016; Volterra et al., 2014). As such, we used Fluo-4AM to monitor calcium signaling in hPSC-derived astrocytes differentiated on VDP and control LN substrates in a subset of our lines—NDC-1, FAD-1, and SAD-1. We found that cells on both surfaces displayed spontaneous waves of calcium transients with characteristics similar to that of previous reports with primary or hPSC-derived astrocytes (Santos et al., 2017; TCW et al., 2017; Volterra et al., 2014), with no distinguishing features between those on VDP or LN (**Figure 2.5**). In addition, single cell quantification of the amplitudes of the calcium spikes revealed no obvious differences in the distribution of these responses among the cell populations on VDP and LN substrates (**Supplementary Figure B.5**). Finally, astrocyte populations on both surfaces displayed continuous propagation of waves of calcium transients among neighboring cells suggesting networks of connected astrocytes (**Supplementary Movies B.1-6**). Taken together, these results suggest that hPSC-derived astrocytes produced on VDP and LN substrates exhibit characteristic calcium responses typical of functionally mature cells.

2.3.7 Astrocytes can be generated on VDP using scalable culture methods

Although we were able to employ VDP as a fully defined culture substrate for the generation of astrocytes, the inadequate surface area-to-volume ratio provided by such traditional two-dimensional (2-D) methods is not sufficient to generate astrocytic cell populations in quantities sufficient for uses in disease modeling, drug discovery, and regenerative medicine. As an alternative, microcarrier (MC)-based technologies can facilitate the generation of large numbers of cells in reduced culture volumes (Badenes et al., 2016). More specifically, in microcarrier culture cells are grown as monolayers on the on the surface of small polystyrene spheres of approximately 200 μm while suspended in culture with mild stirring. Importantly, the flexibility of MCs allows them to be easily employed in a variety of bioreactor systems including stirred-tank, rotating wall vessel, and vertical wheel (Abraham et al., 2017; Maartens et al., 2017). To that end, we developed a strategy to coat polystyrene MCs with VDP. As proof-of-principle,

hNPCs derived from our two NDC hPSC lines were seeded onto the VDP-coated MCs in 6-well ultra-low attachment plates. After seeding, the medium was changed to astrocyte differentiation medium. We optimized the initial seeding and MC density to allow for continuous attachment of cells and even distribution on the MCs through the differentiation period (**Figure 2.6A**). Differentiation on MCs allowed for a 10-15 fold increase in astrocyte cell number per culture volume when compared to conventional 2-D culture methods (**Figure 2.6B**). In addition, immunofluorescent (**Figure 2.6C**) and flow cytometry (**Figure 2.6D**) analysis demonstrated that astrocytes generated on MCs expressed similar levels of the established astrocyte markers S100β and GFAP to those cells generated on typical 2-D surfaces. Finally, calcium imaging was performed on astrocytes that were generated on VDP-coated MCs and then subsequently replated onto VDP-coated 2-D surfaces. This analysis revealed that cells generated with the MC-based system displayed calcium transients with the same properties as those generated on 2-D surfaces (**Figure 2.6E; Supplementary Movie B.7-8**). Therefore, astrocytes generated with these scalable methods can be dissociated and replated onto VDP-coated 2-D surfaces without loss of functionality. In sum, these experiments establish proof-of-principle that VDP is compatible with scalable culture methods to generate functionally mature astrocytes in quantities required for downstream applications.

2.3.8   Astrocytes generated on VDP can be cryopreserved without loss of functionality

Now that we established that VDP could be used to support the scalable generation of hPSC-derived astrocytes, we wanted to investigate if these cell populations could be cryopreserved while maintaining their functional phenotypes. As proof-of-principle, astrocytes were generated from NDC-1 hNPCs on VDP-coated surfaces, dissociated to single cell suspensions, and placed in a DMSO-based cryoprotectant. Cells were then cooled from room temperature at a rate of $1^{O}C/min$ until $-80^{O}C$ and then placed in long-term storage at $-150^{O}C$. After a minimum of 7 days in storage, cells were thawed onto VDP-coated surfaces. Thawed astrocytes displayed a typical flat, star-shaped morphology that was similar to cells prior to cryopreservation (**Figure 2.7A**). In addition, cells that were cryopreserved continued to express

high levels of the astrocytic markers S100β and GFAP as determined by immunofluorescence (**Figure 2.7B**, **Supplementary Figure B.6**) and flow cytometry (**Figure 2.7C**). In addition, there was no significant difference in the levels of ApoE secreted between pre- and post-cryopreserved astrocytes (**Figure 2.7D**). Along similar lines, thawed astrocytes retained their characteristic secretory profile and retained the ability to respond to inflammatory stimuli such as LPS through upregulation of expression of cytokines IL-6, IL-8, and MCP-1 (**Figure 2.7E**). Finally, cryopreserved astrocytes continued to display spontaneous calcium transients with profiles similar to those of cells prior to cryopreservation (**Figure 2.7G; Supplementary B.Movie 9 and 10**). As a whole, these results demonstrate that not only can VDP provide for the scalable generation of hPSC-derived astrocytes but also the resultant populations can be cryopreserved without any adverse effects on their functionality.

2.5   Discussion

In the central nervous system (CNS), astrocytes play numerous roles to maintain the homeostasis of neural microenvironment such as regulating neurotransmitter levels in the interstitial tissue, supporting synaptic health and function, and modulating energy and lipid metabolism. More broadly, not only are astrocytes mediators of the systemic inflammatory and injury response in healthy tissue (Khakh and Sofroniew, 2015; Zhang and Barres, 2010) but have also have been implicated as central players in numerous neurodegenerative diseases (M. V. Sofroniew and Vinters, 2010). As such, hPSC-derived astrocytes provide a unique opportunity to generate accessible models to understand the molecular underpinnings of neurodegenerative disease as well as serve as the raw material to replace diseased or damaged tissue. In this vein, reproducible and defined methods for the generation of astrocytes from hPSCs will significantly advance their use in these various downstream applications (Gonzalez et al., 2017). To that end, in this study we employed a completely defined peptide-based substrate, vitronectin-derived peptide (VDP), for the efficient generation of astrocytes from hPSCs. Overall, the cells generated on these substrates not only expressed high levels of conventional astrocytic markers but also displayed transcriptional and functional characteristics that consistent with hPSC-derived

astrocytes generated by other groups on undefined, xenogeneic substrates (Lundin et al., 2018; Santos et al., 2017; TCW et al., 2017; Zhao et al., 2017) (**Supplementary Table B.6**) as well as astrocytes fetal and primary human astrocytes. Specifically, hPSC-derived astrocytes were generated from six independent hPSC lines and subject to a series of primary characterization assays that are broadly accepted in the field (Lundin et al., 2018; Santos et al., 2017; TCW et al., 2017) as demonstration of bona fide astrocytes including morphological assessment, expression of high levels of astrocytic markers, ability to produce and secrete APOE, and ability to uptake soluble Aβ. In addition, we performed more in-depth characterization on a select number of lines of these hPSC-derived astrocytes using RNA-seq and calcium imaging. In the future, direct comparative investigations will be necessary to compare hPSC-derived astrocytes generated using the defined approaches described in this study with those isolated from fetal and primary sources. In addition, these astrocytes can also be evaluated in the context of other hiPSC-derived neural populations such as neurons (D'Souza et al., 2020) and microglia (Hirbec et al., 2020) to understand and model the complex interactions between these cell types. Furthermore, we demonstrated that VDP was compatible with microcarrier (MC)-based cell culture technologies to facilitate the large-scale generation of astrocytes from hPSCs. Finally, astrocytes generated on these defined substrates could be cryopreserved without adverse effects on functionality. Notably, VDP can be coated onto tissue-culture treated polystyrene plates or MCs and does not require complex chemical conjugation or fabrication that is typical of other peptide-based culture systems for growth or differentiation of hPSCs (Deng et al., 2014; Melkoumian et al., 2010). Because of this ease of use, we contend that VDP can be widely adopted by researchers as a defined substrate for the generation of hPSC-derived astrocytes for disease modeling and regenerative medicine applications.

Loss or dysfunction of astrocytes contributes to a wide variety of neurological disorders, including Huntington's disease, amyotrophic lateral sclerosis (ALS), epilepsy, and Alzheimer's disease (AD) (Molofsky et al., 2012; Scuderi et al., 2013). Recent pre-clinical studies have provided great enthusiasm for the potential of using hPSC-derived astrocytes in the treatment of numerous CNS diseases and disorders. For example, astrocytes generated from hPSCs have

been shown to functionally replace astrocytes in adult mice (Chen et al., 2015). More recently, intrathecal delivery of similar astrocyte populations into mouse models of ALS were able to mitigate disease onset and progression (Y. Wang et al., 2018). In this vein, the results presented here will enable the development of biomanufacturing processes with the following features that will be critical for the translation of hPSC-derived astrocytes from bench-to-bedside: (i) Fully defined conditions. Current astrocytic differentiation protocols exclusively employ substrates from xenogeneic origins (Chen et al., 2015; Haidet-Phillips et al., 2014; Krencik et al., 2011; Roybon et al., 2013; Serio et al., 2013; Shaltouki et al., 2013) which are subject to batch-to-batch variation and pose risk for transmission of adventitious agents in clinical situations (De Sousa et al., 2016; Stacey et al., 2018, 2019). As described in this study, the use of VDP provides a completely synthetic and off-the-shelf substrate to generate human induced pluripotent stem cell (hiPSC)-derived astrocytes in reproducible, animal-free conditions. In fact, we demonstrate that VDP allows for the generation of astrocytes that are transcriptionally and functionally indistinguishable from cells derived on conventional animal-derived substrates such as laminin (LN) (ii) Robust. It has been widely established that variability between individual hPSC lines can lead to directed differentiation protocols that work well in a subset of cell lines and, alternatively, lead to the generation of heterogeneous cell populations in other lines (Nishizawa et al., 2016; Ortmann and Vallier, 2017). Here, we show that VDP provides for the highly efficient differentiation of six independent hiPSC lines into relatively pure, homogenous astrocyte populations. In addition, we do not observe any significant differences in cell phenotype with independent VDP batches or independent differentiations. As such, we anticipate that VDP can serve as the universal substrate enabling the development of biomanufacturing processes and personalized therapies. (iii) Scalable. Current astrocyte differentiation strategies utilize planar culture surfaces that will not be able to facilitate the anticipated large-scale clinical demands of up to 10^9-10^{10} cells per dose. Alternatively, microcarrier (MC)-based systems have the ability to enhance production capacity, improve culture robustness, facilitate scale-up, and reduce costs associated with cell manufacturing (Badenes et al., 2016). Here, we use VDP in conjunction with a MC-based culture system to allow for the scalable generation of functionally mature hPSC-derived astrocytes.

Although we only demonstrate the utility of this MC-based system in a subset of our hPSC lines, our proof-of-principle studies demonstrate the broad utility of VDP to be employed in such scalable formats with minimal optimization. In the future, we anticipate that such MC-based systems used in conjunction with established bioreactor systems (Abraham et al., 2017; Maartens et al., 2017) will allow for the production of astrocytes in quantities sufficient for cell-based therapy applications. More precisely, in the proof-of-principle experiments we performed, VDP-coated MCs were cultured in 6-well ultra-low attachment plates placed on placed on an orbital shaker in a tissue culture incubator. From this culture system, each well yielded on average 6 x 10^6 astrocytes compared to 0.5 x 10^6 astrocytes obtained from a single well when cultured using 2-D. As such, we estimate that a single 500 ml vessel of a rotating wall vessel (RWV) bioreactor could be used to generate 10^9 astrocytes using VDP-coated MCs (Srinivasan et al., 2018) (iv) Point-of-use. Future clinical applications of astrocytes created from hPSCs will require processes that are compatible with cryopreservation techniques that allow for the generation of master banks which can be deployed directly at the point-of-use (De Sousa et al., 2016; Stacey et al., 2018, 2019). Towards this goal, we provide proof-of-concept in a subset of our hPSC lines that the astrocyte populations generated on VDP can be dissociated into single cells and cryopreserved without any loss of phenotypical integrity and functionality for long-term study.

Recently, suspension or 'organoid'-based methods have emerged as a strategy to generate neural cell populations, including astrocytes, in a format that might preclude an adhesive matrix (Di Lullo and Kriegstein, 2017; Huch and Koo, 2015; Kelava and Lancaster, 2016; Krencik and Zhang, 2011; Lancaster et al., 2013; Paşca et al., 2015). It should be noted that while these organoid-based systems are impressive in their ability to recapitulate aspects of human neural development, in practical terms these protocols result in a heterogenous mixture of neurons, astrocytes, and other neural progenitor cell types which might limit downstream applications where pure cell populations are required. Specifically, oragnoid-based systems suffer from limitations such as batch-to-batch variability in size and cellular composition, as well as potential issues that arise from necrotic cores that develop during prolonged culture. By comparison, the methods described in this study, which employ a fully defined substrate that is

compatible with both conventional 2-D and scalable MC-based culture systems, results in highly pure populations of astrocytes free from any contaminating (i.e. neuronal, progenitor) cell populations. In the future, such astrocytic populations could be combined at precise ratios with other hPSC-derived neural populations such as neurons (D'Souza et al., 2020) and microglia (Hirbec et al., 2020) to generate highly reproducible, complex culture systems. In addition, these organoid suspension culture systems rely on the aggregation of cells into large spheroids which might result in cell necrosis in the center of the organoid due to limitations in oxygen diffusion and nutrient mass transfer (Kinney et al., 2011). In this study, the MC-based cultures form small aggregates with a non-cellular MC core that does not exhibit necrosis. In fact, analysis of astrocytes generated on MCs revealed no observable necrosis as measured by propidium iodide staining (Crowley et al., 2016). As such, the MC-based methods described in this study offer the scalability advantages afforded by suspension-based systems without these aforementioned caveats.

The work that we performed in this study also has important practical implications for the use of hPSC-derived astrocytes in disease modeling and drug screening applications. In particular, cellular models for phenotypic drug screens need to be reproducible and homogenous (Lundin et al., 2018; Thorne et al., 2016). In addition, such cell types will need to be generated at large scale given the estimates that it would take approximately 10^{10} cells to screen a 1 million compound library. The use of VDP as fully defined, synthetic substrate to generate relatively pure and homogenous astrocytes from hPSCs will eliminate the batch-to-batch variability that could arise from the use of animal-derived substrates. Moreover, VDP does not pose the same potential complications as undefined matrices such as Matrigel™ which might contain biologically active components that could potentially interfere with the interpretation of phenotypic results (Astashkina et al., 2012; Hughes et al., 2010). In addition, we demonstrate that the use of scalable MC-based technologies and conventional cryopreservation techniques will enable the generation of large stocks of consistent cellular identity. In turn, we show that cryopreserved cells can be thawed directly onto VDP-coated 2-D surfaces which will enable future downstream high-throughput phenotypic drug screening assays.

Classically, the roles of astrocytes in CNS function and neurodegenerative disease have been studied in a variety of animal models. While these model systems have provided many insights, the complexity of *in vivo* experiments make it difficult to eliminate confounding variables and directly investigate the specific role of astrocytes in neural tissue health, damage, and disease. In addition, given the differences between human and rodent astrocytes including their morphology, transcriptional profiles, and functionality (Oberheim et al., 2009; Tarassishin et al., 2014; Zhang et al., 2016), there is significant concern that these models do not fully recapitulate human disease. As such, considerable effort has been devoted to developing representative human *in vitro* astrocytic models including those from immortalized (Fan et al., 2016; Finan et al., 2016) and primary sources (Malik et al., 2014; Zhang et al., 2016). However, immortalized cell lines can be aneuploid with unknown dosage at key-disease relevant genes while primary cell systems are difficult to isolate and rapidly lose phenotypes during prolonged *in vitro* culture. In this vein, the hPSC-astrocytes generated in this study have many functional features that would make them attractive for AD-related disease modeling and drug screening. In the classic form of the amyloid cascade hypothesis of AD, generation and subsequent accumulation of Aβ peptides is the key step that leads to neuronal loss and subsequent cognitive decline associated with AD (Chow et al., 2010; Oksanen et al., 2017; Zhang et al., 2011

). Related to this process, astrocytes have been shown to play an important role in Aβ clearance (Ries and Sastre, 2016). In this study, we demonstrated that astrocytes generated on VDP had the ability to uptake Aβ from the surrounding media. Moving forward, the cells generated as part of this study will provide for the investigation into the mechanistic connections between astrocytic amyloid processing and AD-related phenotypes. Another characteristic of the astrocytes generated as part of this study that makes them attractive drug screening models is their ability to secrete ApoE. Given the broad functions of ApoE in maintaining health in the CNS (Liu et al., 2013), augmenting the functions of ApoE has been explored as a potential therapeutic strategy in treating AD (Fan et al., 2016; Finan et al., 2016). As such, several screens utilizing immortalized and primary cell sources have identified small molecule enhancers of ApoE production (Fan et

al., 2016; Finan et al., 2016). Moving forward, the astrocytes generated in this work could serve as a more robust human cellular model for such high-throughput screens. Finally, although the work presented in this manuscript only focused on the generation of astrocytes from non-demented control (NDC) or AD hiPSCs, we envision that the robustness of the VDP-based culture methods will allow for the generation of astrocytes from other hiPSC lines derived from patients of other diseases in which astrocytic dysfunction has been implicated (Molofsky et al., 2012; Scuderi et al., 2013).

2.6 Conclusion

In summary, we developed a completely defined peptide-based substrate that allows for the generation of highly pure populations of astrocytes from several independent hPSCs lines. Moreover, this peptide is compatible with conventional planar culture formats as well as scalable MC-based technologies. Importantly, astrocytes generated on these peptide-based surfaces not only displayed typical astrocytic morphology and high expression of canonical astrocyte markers but also demonstrated properties characteristic of functionally mature cells including secretion of ApoE, responsiveness to inflammatory stimuli, and presentation of spontaneous calcium transients. In the future, the use of this peptide-based system as a scalable and defined culture system will enable the application of hPSC-derived astrocytes in a variety of downstream applications in drug screening, disease modeling, and regenerative medicine.
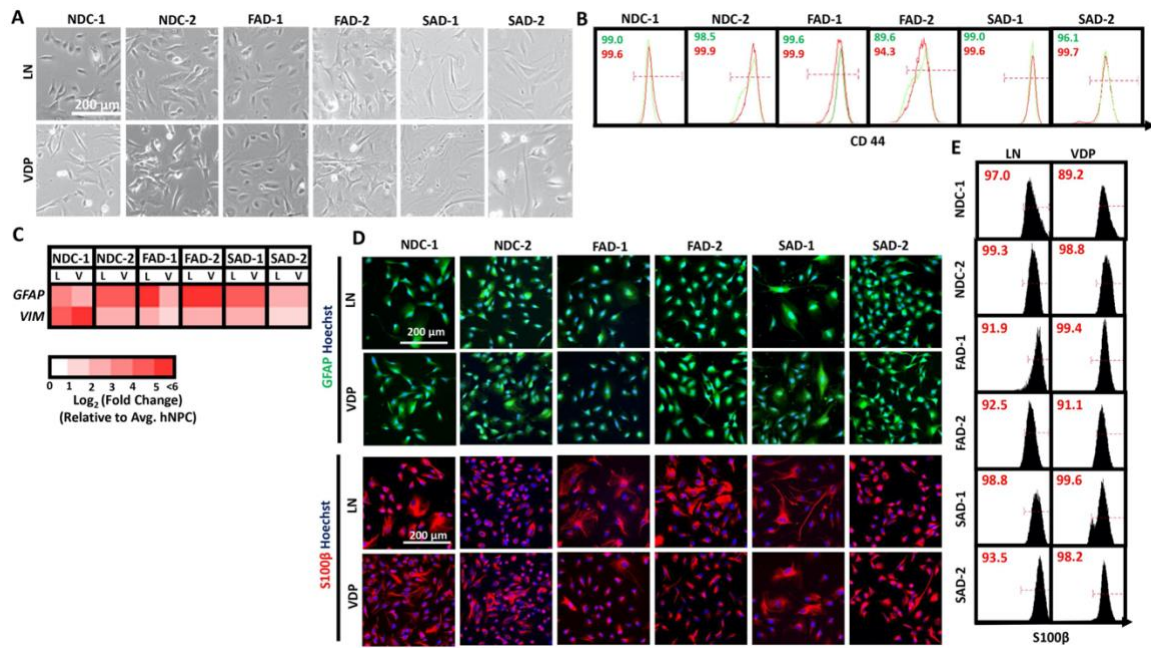
Figure 2.1. Generation of hPSC-derived astrocytes on a completely synthetic peptide substrate.

(A) Representative phase contrast images of D50+ hPSC-derived astrocytes generated (scale bar = 200 µm). **(B)** Representative flow cytometry plots of CD44 expression of D30+ astrocytes on VDP (green traces) and LN (red traces) substrates. Gates were determined using isotype antibody only controls listed in Supplementary Table B.1. **(C)** Quantitative PCR (qPCR) analysis for expression of astrocyte markers GFAP and VIM in D50+ cultures. Gene expression fold changes were calculated relative to expression levels in undifferentiated hNPCs. **(D)** Immunofluorescence analysis for expression of GFAP and S100β in D50+ cultures. **(E)** Representative flow cytometry plots of S100β expression of D50+ astrocytes. Gates were determined using isotype or secondary antibody only controls listed in Supplementary Table B.1.
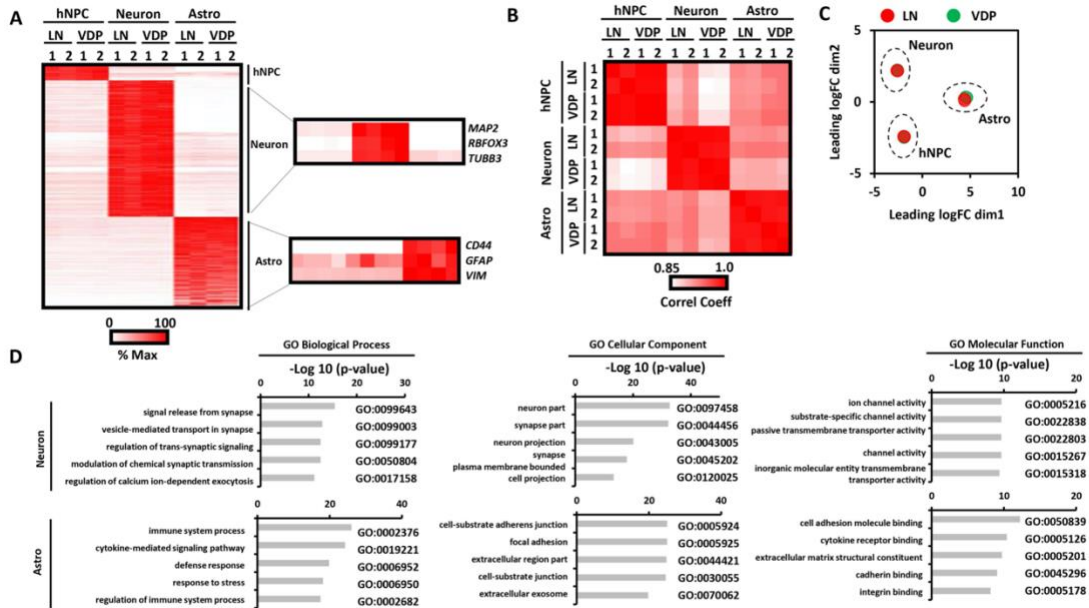
Figure 2.2. Transcriptional profiling of astrocytes generated on VDP and control LN surfaces.

(A) Heatmap for differentially expressed genes (FDR < 0.05; |log2 (fold change)| > 1.5) identified between NDC-1 derived hNPCs, astrocytes, and neurons cultured on VDP and LN surfaces. Genes related to post-mitotic neurons and astrocytic phenotype are highlighted. The entire RNA-seq data set can be found in Supplementary Table B.4 and the differentially expressed genes can be found in Supplementary Table B.5 **(B)** Pearson's correlation between RNA-sequencing data of hNPCs, astrocytes, and neurons generated on VDP and LN substrates. **(C)** Multidimensional scaling (MDS) plot measuring differences in the transcriptional profiles of hNPCs, astrocytes, and neurons differentiated on VDP- and LN-coated surfaces. **(D)** Gene ontology (GO) analysis identified biological processes (left panels), cellular components (middle panels), and molecular function (right panels) related to astrocytic functions were upregulated in neuronal (top panels) and astrocyte (bottom panel) populations derived on both VDP- and LN-coated surfaces.

43
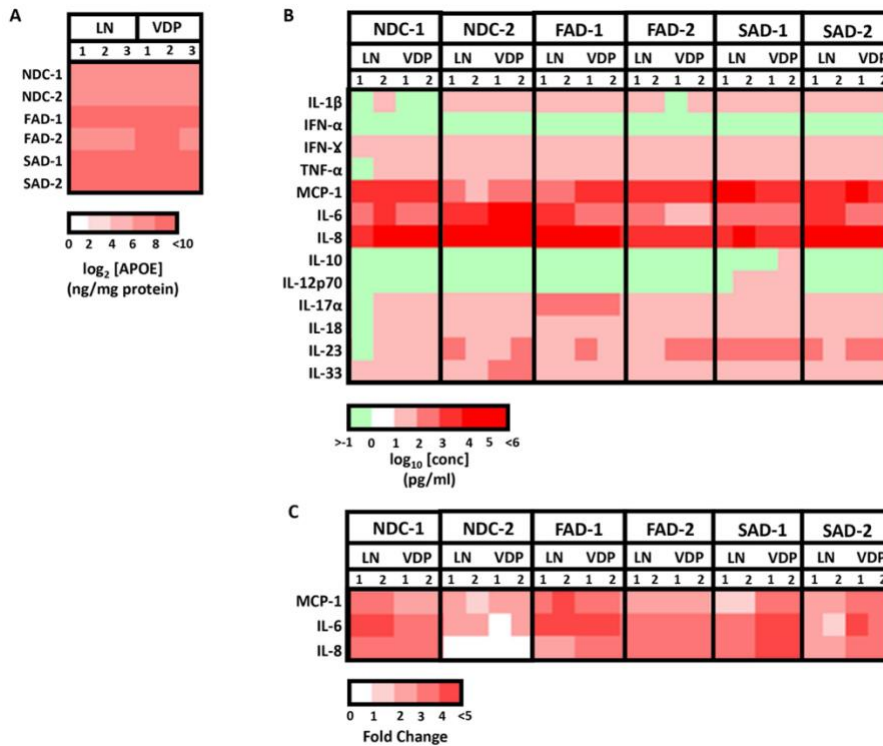
Figure 2.3. Secretory profiling of VDP- and LN-derived astrocytes.

(A) ApoE secretion was measured in the conditioned medium of D50+ astrocytes. **(B)** Secretory profile of pro- and anti-inflammatory cytokines in D50+ astrocytes cultured under basal conditions. **(C)** D50+ astrocytes were treated with LPS for 24 hrs and the secretion of MCP-1, IL-6, and IL-8 was measured. Data is shown as fold-change increase in cytokine secretion when compared to untreated conditions.

Figure 2.4. Analysis of β-amyloid (Aβ) uptake in astrocytes.

Flow cytometry analysis of Aβ internalization in un- (black traces) and Aβ-FITC-treated (green traces) astrocytes.
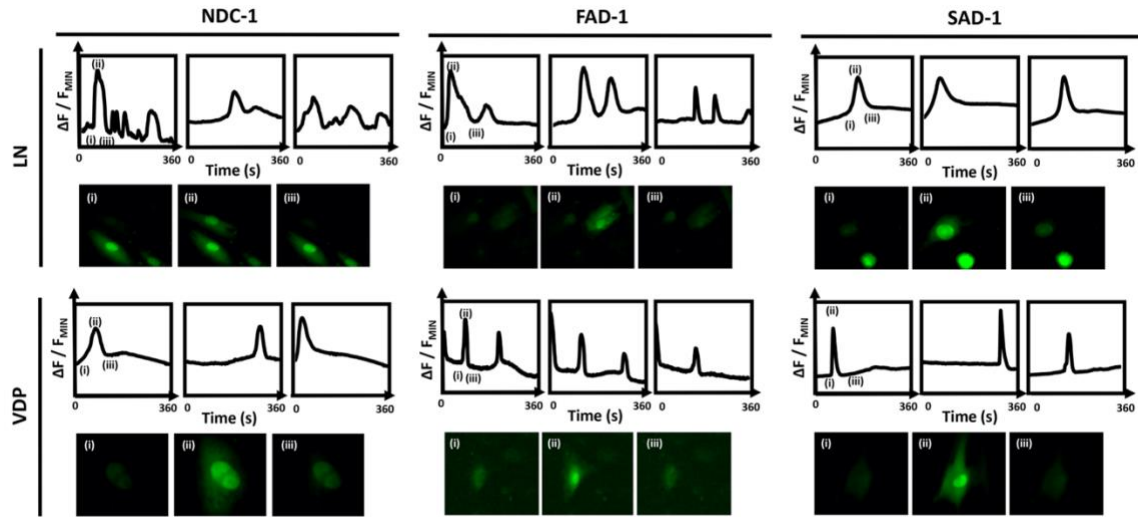
Figure 2.5. Measurement of spontaneous calcium activity in astrocytes differentiated on VDP- and LN-coated plates.

Plots of changes (ΔF/F) in fluorescence of calcium indicator (Fluo-4) in single astrocytic cells. Representative images of Fluo-4 stained astrocytes at the indicated time points.
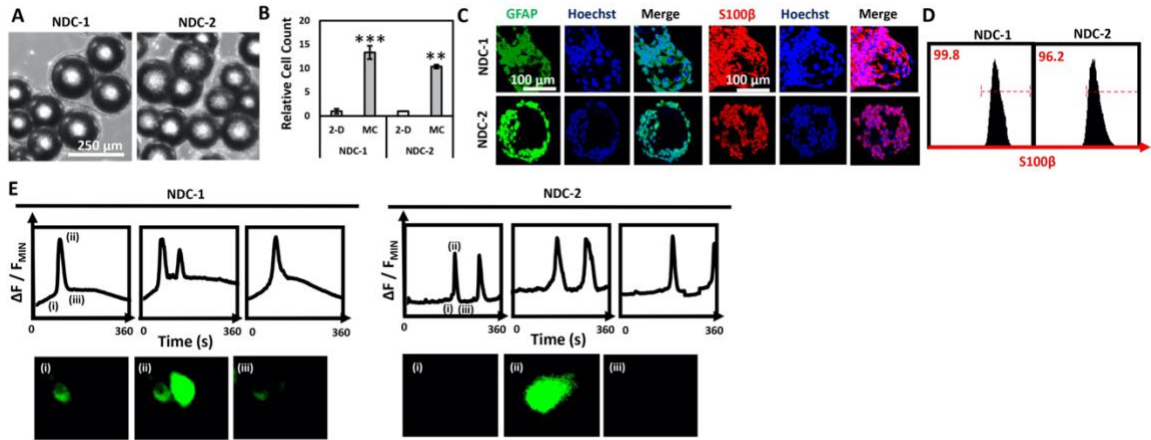
Figure 2.6. Scalable generation of hPSC-derived astrocytes on VDP-coated microcarriers (MCs).

(A) Representative phase contrast images of astrocytes cultured on VDP-coated MCs (scale bar = 250 µm). **(B)** Cell counts of astrocytes generated on VDP-coated two-dimensional (2-D) and MCs. Student's t-test, ** = p< 0.01, *** = p<0.001 **(C)** Representative fluorescent images of GFAP (left panels) and S100β (right panels) in astrocyte cultures derived on VDP-coated MCs (scale bar = 100 µm). **(D)** Representative flow cytometry plots of S100β expression of astrocytes derived on MCs. Gates were determined using isotype or secondary antibo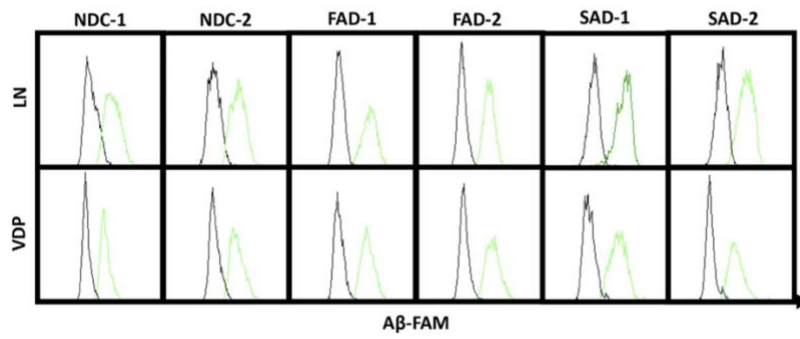dy only controls listed in Supplementary Table B.1. **(E)** Plots of changes (ΔF/F) in fluorescence of calcium indicator (Fluo-4) in single astrocytic cells grown on MCs. Inset images of Fluo-4 stained astrocytes are shown at the indicated time points.
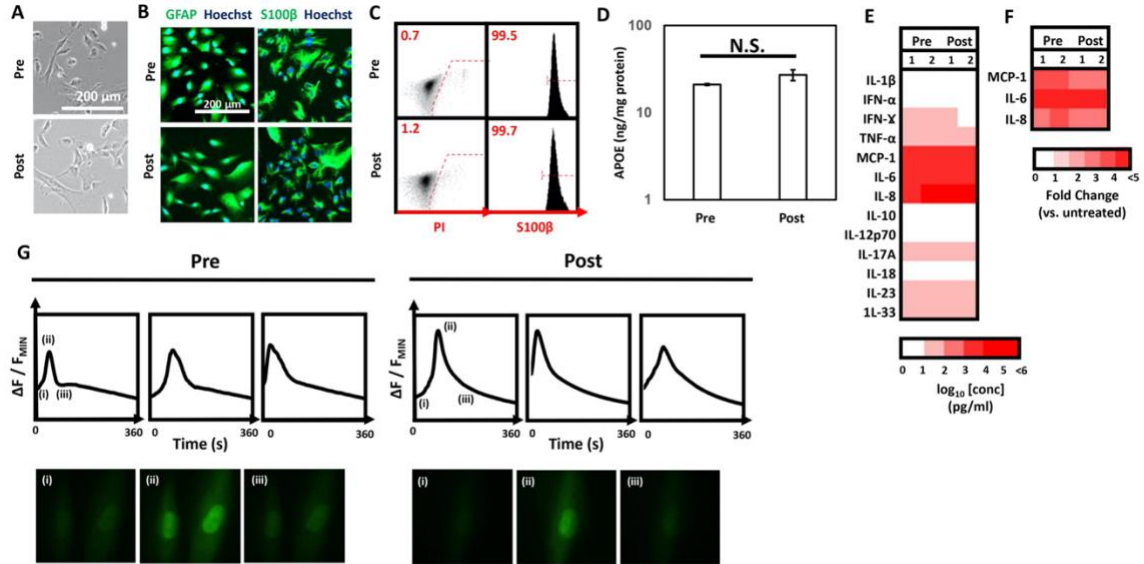
Figure 2.7. Characterization of cryopreserved astrocytes generated on VDP.

(A) Representative phase contrast images of pre- and post-cryopreserved astrocytes generated on VDP-coated surfaces. **(B)** Representative immunofluorescent images of GFAP (left panels) and S100β (right panels) in pre- and post-cryopreserved astrocytes. **(C)** Representative flow cytometry plots of S100β expression in pre- and post-cryopreserved astrocytes. Gates were determined using isotype or secondary antibody only controls listed in Supplementary Table B.1. **(D)** Measurement of secreted ApoE in pre- and post-cryopreserved astrocytes cultured on VDP surfaces. N.S. = not statistically significant, Student's t-test. **(E)** Profile of pro- and anti-inflammatory cytokines in pre- and post-cryopreserved astrocytes cultured under basal conditions. **(F)** Measurement of upregulated cytokines in pre- and post-cryopreserved astrocytes after treatment with LPS. Data is shown as fold-change increase in cytokine release compared to untreated astrocytes. **(G)** Measurement of changes (ΔF/F) in fluorescence of calcium indicator (Fluo-4) in single pre- and post-cryopreserved astrocytes. Inset images of Fluo-4 stained astrocytes are shown at the indicated time points.

CHAPTER 3

APOE2 MITIGATES DISEASE-RELATED PHENOTYPES IN AN ISOGENIC HIPSC-BASED MODEL OF ALZHEIMER'S DISEASE

3.1 Introduction

Although a vast majority of AD cases are sporadic, numerous genetic risk factors have been identified that contribute to lifetime risk of developing the disease (Bertram and Tanzi, 2009). While not deterministic, the polymorphisms in the *APOE* gene have been established to be the most potent modulator of late onset, sporadic, AD. In the central nervous system, ApoE is generated and secreted principally by astrocytes and microglia, and, to a lesser degree, neurons. In the brain, ApoE functions to transport cholesterol and other lipids to neurons and plays important roles as it relates to neuronal growth, synaptic plasticity, and membrane repair (Mahley, 1988; Suri et al., 2013). Human APOE has three major isoforms, APOE2, APOE3, and APOE4, which differ by two amino acid substitutions at residues 112 and 158 in exon 4—APOE2 (Cys112, Cys158), APOE3 (Cys112, Arg158), APOE4 (Arg112, Arg158). With respect to AD, compared to individuals homozygous for the *APOE3* allele (referred to as the 'risk neutral' allele), heterozygosity for the ε4 allele increases AD risk by 3-fold, and homozygosity for the ε4 allele increases risk over 10-fold (Corder et al., 1994; Raman et al., 2020). Conversely, individuals with the ε2 allele (referred to as the 'protective' allele) are 40 percent less likely to develop AD (Corder et al., 1994; Raman et al., 2020). In fact, recent epidemiological studies have revealed that *APOE2* homozygotes have an exceptionally low likelihood of AD (Reiman et al., 2020). As such, understanding the mechanisms that underlie the association between *APOE2* and protection against neurodegeneration may provide new therapeutic targets.

Extensive work has examined the role of *APOE4* in contributing to AD onset and age-related progression. Previous studies have established that the *APOE4* variant increases likelihood of developing AD in a dose dependent manner as the number of *APOE4* alleles increases, while greatly reducing the mean age of onset (Corder et al., 1993). In addition, it has been demonstrated that APOE4 modulates the formation of amyloid plaques and neurofibrillary

tangles (Raman et al., 2020), two pathological hallmarks of AD. Moreover, numerous studies have identified several amyloid-dependent and -independent mechanisms to explain the risk-inducing effects of *APOE*4 (Liu et al., 2013; Michaelson, 2014). By comparison, there is significantly less research that has examined the protective effects of *APOE2*. In general, the presence of an *APOE2* allele has been associated with decreased AD-related neuropathology, age-associated cognitive decline, and greater cortical thickness (Farfel et al., 2016; Nagy et al., 1995). Along similar lines, several studies have suggested that *APOE2* modulates Aβ deposition, clearance and degradation, antioxidant and anti-inflammatory activity, and neuronal glucose metabolism (Deane et al., 2008; Drouet et al., 2001; Suri et al., 2013). Finally, while the risk modifying effects of APOE have been largely studied in the context of late-onset AD (LOAD) patient populations, there are some studies that have examined the effect of *APOE* genotype in the context of familial AD (fAD)-related mutations. Consistent with what is observed in LOAD subjects, the presence of *APOE4* significantly reduces the age of disease onset whereas carriers of *APOE2* have delayed age of onset (Olarte et al., 2006; Pastor et al., 2003; Sorbi et al., 1995; Vélez et al., 2016; Wijsman et al., 2005).

Animal models have provided important insights to explain the risk-modulating effects of various *APOE* isoforms (Belloy et al., 2019; Liu et al., 2013; Michaelson, 2014). However, the inherent complexities of such model systems made it difficult to make definite mechanistic links between *APOE* genotype and AD-related phenotypes. In addition, the multi-cellular composition of the *in vivo* environment does not allow for the identification of cell-autonomous versus cell-non autonomous aspects of such relationships. Due to the limitations of current animal-based models, complimentary human cell-based models are needed study the biochemical, molecular, and cellular mechanisms that underlie risk-modifying effects of various *APOE* isoforms. To date, most studies have been limited to immortalized cell lines, which are karyotypically abnormal with non-physiological dosage at disease-relevant genes (Goldstein et al., 2015). Conversely, studies of normal human cells from cadaveric tissue samples with respect to *APOE2* are often limited to small sample sizes (given the low allele frequency), making it challenging to assign observed

phenotypes to a specific *APOE* genotype or as a by-product of the genomic diversity present across individuals.

Over the past several years, hiPSC-based models have been used extensively by numerous groups to study AD (Israel et al., 2012; Kondo et al., 2013) and, to a lesser extent, the influence of *APOE* on disease-relevant phenotypes (Huang et al., 2017; Konttinen et al., 2019) in a simplified and accessible system. However, the analysis of the phenotypic effects of specific risk factors, such as those in the *APOE* locus, has been confounded by the genetic and epigenetic differences inherent in the individual hiPSC lines derived from distinct patient genomes. As such, the use of isogenic cell lines with identical genetic backgrounds that only differ with respect to individual variants has become essential making definitive genotype-to-phenotype relationships as it relates to the modeling of AD-related mutations and risk factors. To this end, we recently reported the development of a series of methods that employ a transient reporter for editing enrichment (TREE) which allows for the generation of isogenic hiPSC lines with clonal homozygous editing efficiencies approaching 90% (Brookhouser et al., 2020; Standage-Beier et al., 2019). In this study, we leverage this technology to characterize AD-related phenotypes in neural cultures derived from hiPSC lines harboring early onset, familial AD (fAD), mutations with an *APOE3* genotype and gene edited isogenic *APOE2* matched pairs. Detailed phenotypic analysis of these cultures revealed that conversion of *APOE3* to *APOE2* significantly reduced Aβ secretion. In addition, we found that *APOE2* significantly decreased levels of phosphorylated tau in isogenic cultures that showed a concomitant decrease in the Aβ42/40 ratio. Furthermore, we developed a cell separation protocol to study AD phenotypes in pure populations of neurons and astrocytes. This analysis revealed that the protective effect conferred by *APOE2* had cell autonomous and non-autonomous contributions as cultures consisting exclusively of neurons displayed a reduction, but not complete abrogation of the *APOE2* protective effect. Mechanistically, we demonstrate that *APOE2* contributes, in part, to the mitigation of these AD-related phenotypes through changes in amyloid precursor protein (APP) processing. Overall, a more thorough understanding of the mechanisms by which *APOE2*

enhances neuroprotection against AD will have a significant translational impact on the design of therapeutic interventions.

3.2   Experimental Methods

3.2.1   Human iPSC culture.

HPSCs were maintained in mTeSR1 medium (Stemcell Technologies) on feeder-free Matrigel (Corning)-coated plates. Subculture was performed every 3 days using Accutase (Life Technologies) in mTeSR1 medium supplemented with 5μM Rho kinase inhibitor (ROCKi; Y-27632 [Tocris Bioscience]). Control and AD-patient hPSCs were generated from dermal fibroblasts as previously described (Park et al., 2008). HPSC lines described in the manuscript are as below.

Cell Line	Disease Status	MMSE	Mutation	Citation
hPSC Line 1 *APOE3/3*	Familial AD	n/a	APP V717I	Muratore et al. 2014
hPSC Line 1 Isogenic *APOE2/2*	Familial AD	n/a	APP V717I	Brookhouser et al. 2020
hPSC Line 2 *APOE3/3*	Familial AD	n/a	APPdp	Israel et al. 2012
hPSC Line 2 Isogenic *APOE2/2*	Familial AD	n/a	APPdp	This paper
hPSC Line 3 *APOE3/3*	Familial AD	n/a	PSEN1 A246E	https://biomanufacturing.cedars-sinai.org/product/cs40ifad-nxx/
hPSC Line 3 Isogenic *APOE2/2*	Familial AD	n/a	PSEN1 A246E	Brookhouser et al. 2020
hPSC Line 4 *APOE3/3*	Non-demented control	30	n/a	Hjelm et al. 2011
hPSC Line 4 Isogenic *APOE2/2*	Non-demented control	n/a	n/a	Brookhouser et al. 2020

Table 3.1. Isogenic hiPSC lines used in this study.

3.2.2 Neuronal differentiation of hiPSCs.

HiPSCs were differentiated to hNPCs as previously described with some modifications (Cutts et al., 2016). Briefly, to initiate neural differentiation hiPSCs were cultured in feeder-free conditions (Matrigel^{TM} [BD Biosciences]; mTeSR1™ Medium [Stemcell Technologies]) for a minimum of 2 passages. Cells were then detached with Accutase (ThermoFisher) and resuspended in mTeSR1 media supplemented with 5 µM Y-27632. Next, 1-2 x 10^6 cells were pipetted to each well of a 6-well ultra-low attachment plate (Corning). The plates were then placed on an orbital shaker set at 95 rpm in a 37°C/5% CO_2 tissue culture incubator. The next day, the cells formed spherical cultures (embryoid bodies [EBs]) and the media was changed to neural induction media (NIM) [1X DMEM-F12 (ThermoFisher), 0.5% (v/v) N2 supplement (ThermoFisher), 1% (v/v) B27 supplement (ThermoFisher), 1% (v/v) GlutaMAX supplement (ThermoFisher), 1% (v/v) Penicillin Streptomycin, 50 ng/ml recombinant human Noggin (R&D Systems), 0.5 µM Dorsomorphin (Tocris Bioscience)]. Half of the media was subsequently changed every day. After 6 days in suspension culture, the EBs were then transferred to a 10 cm dish (1-2 6 wells per 10 cm dish) coated with Matrigel™. The plated EBs were cultured in NIM for an additional 5-7 days. Cells were then plated on surfaces that had to be coated first with poly-L-ornithine (PLO; Sigma) and then with mouse laminin (LN; 4µg/mL; ThermoFisher). For routine maintenance, hNPCs were passaged onto LN-coated plates at a density of 1-5 x 10^4 cells/cm^2 in neural expansion media (NEM; [1X DMEM-F12, 0.5% (v/v) N2 supplement, 1% (v/v) B27supplement, 1% (v/v) GlutaMAX supplement, 1% (v/v) Penicillin Streptomycin, 30 ng/ml FGF2, and 30 ng/ml EGF]). hNPCs were expanded and seeded on Ln-coated microcarriers (MCs) in ultra-low attachment 6-well plates (Corning) at a density of 3 x 10^6 cell per well and 1mg/mL MCs. The plates were placed under static conditions with 2 mL of NEM in each well to allow for cell attachment on MCs for 12 hours after which an additional 2 mL of NEM was added to the wells. The plates were placed on an orbital shaker (Dura-Shaker, VWR) at 95 RPM. Three-fourths of the media (~3 mL) was changed after 24 hours of culture to remove the ROCKi and half of the media (~2mL) was changed every day thereafter. HNPCs were expanded on LN-coated MCs for 4-5 days until 80-90% confluent after which the media was switched to neuronal

differentiation media (NDM; [1X DMEMF12, 0.5% (v/v) N2 supplement, 1% (v/v) B27 supplement, 1% (v/v) GlutaMAX, 1% (v/v) Penicillin Streptomycin, 20 ng/ml BDNF (STEMCELL Technologies), 20 ng/ml GDNF (STEMCELL Technologies)]. Cells were differentiated for a minimum of 30 days prior to replating for analysis.

3.2.3   Coating of microcarriers (MCs) with laminin.

To coat MCs (Corning Enhanced Attachment Microcarriers) with LN, MCs were suspended in 4µg/mL PLO solution and incubated overnight at 37°C, after which the MCs were washed twice with PBS. The MCs were then coated with 4µg/mL LN solution at 37°C overnight. Coated MCs were washed once with PBS and once with culture media prior to use.

3.2.4   Dissociation of neurons from microcarriers.

Cells were incubated in Accutase for 5 minutes and the aggregates were pipetted up and down gently using a P1000 to break apart large aggregates. Next, cells were detached from the MCs by incubating in a papain solution containing Earle's balanced salt solution (Alfa Aesar), 30U/mL papain (Worthington), 1mM L-Cysteine, 22.5mM D-glucose, 26mM $NaHCO_3$ and 125U/mL DNase (Roche) for 70 minutes at 37°C and then triturated with an inhibitor solution containing 1mg/mL ovomucoid inhibitor (Roche) and 1mg/mL BSA (Sigma) after which the cell-suspension was passed through a 40µm cell strainer to remove the MCs and obtain a single cell suspension (Paşca et al., 2015).

3.2.5   Isolation of pure neuronal and astrocytic populations using MACS.

Following dissociation from MCs, cells were placed at 37°C for 1 hr to allow recovery of cell surface proteins. Cells were washed with MACS buffer and resuspended at a concentration of 1×10^8 cells/mL in MACS buffer in a 5mL round bottom tube. Biotinylated human anti-CD44 antibody (BD Biosciences, Cat # 550989) was added according to manufacturer recommendations and incubated on ice for 15 min. Next, streptavidin conjugated magnetic beads were added following manufacturer protocol, and allowed to incubate on ice for 15 min. The tube

was then placed in the magnet (BioLegend) and incubated for 5 min at room temperature (RT).

Following the incubation, CD44 negative (CD44-) cells were transferred to a new tube while

CD44 positive (CD44+) cells remained in the tube bound to the magnet. The tube was then

removed from the magnet, and cells were resuspended in astrocyte media (ScienCell) and plated

in Matrigel coated wells and expanded for downstream assays. CD44- neurons were plated in a

Matrigel coated 24-well plate at 1×10^6 cells per well for downstream assays.

3.2.6   Immunofluorescence.

Cultures were gently washed twice with PBS prior to fixation for 15 min at RT with BD

Cytofix Fixation Buffer (BD Biosciences). The cultures were then washed twice with PBS and

permeabilized with BD Phosflow Perm Buffer III (BD Biosciences) for 30 min at 4°C. Cultures

were then washed twice with PBS. Primary antibodies were incubated overnight at 4°C and then

washed twice with PBS at room temperature. Secondary antibodies were incubated at RT for 1

hr. Nucleic acids were stained for DNA with Hoechst 33342 (2 µg/mL; Life Technologies) for 10

min at RT and then washed twice with PBS. Antibodies were used at the following

concentrations: TUJ1 (1:1000; Fitzgerald Industries International, Cat# 10R-T136A), MAP2

(1:500; Millipore, Cat# AB5622), NEUN (1:500; Millipore, Cat# MAB377), GFAP (1:500; Abcam,

Cat# AB7260), S100B (1:500; Sigma, Cat# S2532), AFP (1:50; Santa Cruz Biotechnology, Cat#

sc-8399), SMA (1:50; Santa Cruz Biotechnology, Cat# sc-53015), Alexa 488 donkey anti-mouse

(1:500; ThermoFisher, Cat# A-21202), and Alexa 488 donkey anti-rabbit (1:500; ThermoFisher,

Cat# A-21206), Alexa 647 donkey anti-mouse (1:500; ThermoFisher, Cat# A-31571), and Alexa

647 donkey anti-rabbit (1:500; ThermoFisher, Cat# A-31573).

3.2.7   Tri-lineage differentiation of edited hiPSCs.

HiPSCs were harvested using Accutase and plated on ultra-low attachment plates in

mTeSR1 medium. The following day, media was changed to differentiation medium (DM;

DMEM/F12, 20% FBS(ThermoFisher), 1% Pen/Strep). After 5 days, EBs were plated on Matrigel-

coated plates and cultured with DM. After 21 days in DM, cells were fixed, permeabilized, and stained for germ layer markers.

3.2.8   Flow cytometry analysis of CD44 expression.

Cells were dissociated with Accutase for 10 min at 37°C, triturated, and passed through a 40 μm cell strainer. Cells were then washed twice with flow cytometry buffer (BD Biosciences) and resuspended at a maximum concentration of 1×10^6 cells per 100 μL. Cells were stained with PE-Mouse anti-human CD44 or isotype control (PE-Mouse IgG1,κ, BD Biosciences, Cat# 555749) antibodies for 1 hr on ice. Cells were washed twice with flow cytometry buffer prior to analysis. Flow cytometry analysis was performed on an Accuri C6 flow cytometer (BD Biosciences). Flow cytometry files were analyzed using FlowJo (FlowJo LLC, Ashland, OR, USA).

3.2.9   Fluorescence microscopy.

All imaging was performed on a Nikon Ti2-Eclipse inverted microscope with an LED-based Lumencor SOLA SE Light Engine using a Semrock band pass filter.

3.2.10   Measurement of Aβ40, Aβ42, sAPPα and sAPPβ.

Neurons were seeded in a 24-well plate at a density of 1×10^6 cells per well. Six-day conditioned media was collected and Aβ levels were measured using the R&D Systems Human Amyloid Beta 40 and 42 ELISA Kits. Six-day conditioned media was used to quantify sAPPα and sAPPβ using highly sensitive ELISA kits (IBL). Cell lysate was collected for normalization to cellular protein amounts.

3.2.11 Measurement of total APP and APP-βCTF in cell lysates.

Neurons were seeded in a 24-well plate at a density of $1\text{-}2 \times 10^6$ cells per well for six days and subsequently lysed in RIPA buffer containing protease inhibitors (ThermoFisher). Total APP and APP-βCTF levels in the cell lysates were measured using commercially available ELISA kits from ThermoFisher and IBL respectively.

3.2.12 Measurement of pTau and Total Tau in cell lysates.

Cell lysates were analyzed using the ThermoFisher Human Tau ELISA kits (ThermoFisher) to determine pTau and total tau levels.

3.2.13 Measurement of APOE protein

Six-day conditioned media was collected from neurons and astrocytes seeded in a 24-well plate. APOE levels were measured using a human APOE ELISA kit (ThermoFisher) and were normalized to total cellular protein level.

3.2.14 Calcium transient imaging

Calcium imaging was performed on cells seeded on a 30mm glass bottom dish (TED PELLA) coated with Matrigel. Neurons were incubated with 1μM Fluo-4-AM (Invitrogen) and 0.02% Pluronic™ F-127 in DMEM for 30 min at 37°C. To reduce dye associated cytotoxicity, astrocytes were incubated with 0.5 μM Fluo-4-AM (Invitrogen) and 0.02% Pluronic™ F-127 in DMEM for 15 min at 37°C. Cells were then washed once with HEPES-buffered Tyrode's solution (Alfa Aesar), and allowed to de-esterify at RT in the dark for 20 minutes prior to imaging on a Nikon Ti2-Eclipse inverted microscope. Fluorescent time-lapse images for both neurons and astrocytes were acquired (20x objective) using an 80 ms exposure time at one frame per second for 300 s. Calcium spike traces were generated by quantifying the mean pixel intensity of manually identified regions of interest using Fiji (Schindelin et al., 2012).

3.2.15 β-amyloid uptake assay.

FAM-labelled β-amyloid peptide (Aβ-FAM 1-42; Anaspec) was reconstituted as per manufacturer's instructions. Briefly, a minimal volume of 1%NH$_4$OH was added to the peptide and immediately diluted to a 1mg/mL solution in PBS prior to storage as single-use aliquots at -80°C. To measure Aβ uptake, astrocytes and neurons seeded in a 24-well plate were treated with 500

nM Aβ-FAM for 24 hours. For flow cytometry analysis, cells were washed with cold PBS and dissociated using 0.25% Trypsin-EDTA (ThermoFisher) for 5 min at 37°C to remove any surface-bound peptide. Samples were filtered using a 40 μm cell strainer and placed on ice till analysis. An Accuri C6 flow cytometer (BD Biosciences) was to quantify the median fluorescence intensity (MFI). Following background correction using untreated cell MFI, signal was normalized to bulk endocytosis MFI from cells treated with 50ug/mL Dextran, Alexa Fluor™ 647 (10,000 MW; Invitrogen) for 1 hour at RT.

3.2.16 Surface receptor expression measurement.

Astrocytes seeded on a 6-well plate were dissociated non-enzymatically by gentle scraping following incubation with Versene (Gibco) for 15 min at 37°C. Subsequently, cells were washed twice in stain buffer (BD Biosciences). Cells were then incubated with primary antibodies (and appropriate isotype controls) specific to the cell surface epitope of the LRP-1 (Biotechne) or LDLR (BD Biosciences) for 30 min on ice. Following two washes in stain buffer, 5,000-10,000 live cells were acquired on an Accuri C6 flow cytometer (BD Biosciences).

3.2.17 RNA-seq Analysis.

Single end sequencing was performed at BGI Americas Corporation using BGISEQ-500 for a 50 bp run as described previously (Srinivasan et al., 2018). Reads were subsequently mapped to the hg19 human reference genome using HISAT2 (Kim et al., 2015, p. 2). Differential analysis was performed using DEseq2 algorithms (Love et al., 2014). Gene ontology analysis was performed using lists of differentially expressed genes using PANTHER v16 (Mi et al., 2021).

3.2.18 Statistical analysis.

Differences between groups was determined using unpaired two-sided t-test (Welch's t-test for comparison of unequal sample sizes) with $P < 0.05$ considered to be significant using GraphPad Prism version 9.0.0 for macOS. Unless otherwise noted, all data are displayed as mean ± s.e.m.

3.3   Results

3.3.1   Generation of an isogenic hiPSC-derived cell culture model of AD to study effects of *APOE2*

We have previously described a highly efficient method for the generation of isogenic hiPSCs (Brookhouser et al., 2020). To that end, we applied these strategies in hiPSC lines homozygous for the *APOE3* allele to generate isogenic pairs with an *APOE2* genotype. For this study, we focused on the analysis of three isogenic pairs with mutations in APP (APP^{V717I}, APP^{dp}) and PSEN1 (PSEN1^{A246E}). hiPSC lines harboring these mutations have been previously published and shown to produce robust phenotypes *in vitro* when differentiated to neural cultures (Israel et al., 2012; Kondo et al., 2013; Konttinen et al., 2019), making them advantageous for detecting phenotypic differences that may arise as a result of genome modification. In addition, we analyzed one isogenic pair derived from a non-demented control (NDC) individual identified by clinical studies and post-mortem histopathological examination negative for major neurological and neuropathological conditions (Hjelm et al., 2011). Characterization of isogenic APP^{V717I}, PSEN1^{A246E}, and NDC lines has been described previously (Brookhouser et al., 2020), and full characterization of the APP^{dp} *APOE2* line was performed prior to phenotypic analysis in this study (**Supplemental Figure C1**). Specifically, all clonal isogenic hiPSC lines displayed a characteristic hiPSC morphology, high expression of pluripotency markers OCT4, NANOG, and SOX2, ability to differentiate *in vitro* into cell types representative of three primitive germ layers, and a normal euploid karyotype. We then used scalable, microcarrier (MC)-based differentiation strategies developed in our laboratory (Srinivasan et al., 2018) to generate neural cultures from each isogenic pair. Briefly, multipotent human neural cells (hNPCs) were established using our previously described methods (Varun et al., 2017). HNPCs were then seeded on laminin (LN)-coated microcarriers in 6-well ultra-low attachment plates and the medium was changed to a neural differentiation medium. After a minimum of 30 days of differentiation, cultures were dissociated into single cells and replated onto Matrigel-coated tissue culture plates. Analysis of these cultures revealed a large percentage of cells that expressed the mature neuronal markers

TUJ1, MAP2, and NEUN (**Figure 3.1A**). In addition, these differentiation conditions also resulted in the generation of numerous supporting GFAP+ astrocytes (**Figure 3.1A**), which is important because many AD-related neuronal phenotypes modulated by *APOE* are mediated by their interactions and signals from astrocytes (Rodríguez-Arellano et al., 2016; Verkhratsky et al., 2010). Overall, neural differentiations as measured by TUJ1, MAP2, and NEUN expression were consistent across lines, isogenic pairs, and independent differentiations, suggesting no change in differentiation potential as a result of genome modification (**Supplemental Figure C2**).

3.3.2 *APOE2* modulates AD-related phenotypes in hiPSC-derived neural cultures

In the strictest form of the amyloid cascade hypothesis, generation and subsequent oligomerization of Aβ is the primary step that leads to elevated phosphorylated tau (p-tau) and subsequent synaptic and neuronal loss. To that end, several studies have suggested that the AD-risk modulating effects of *APOE* occur at multiple levels in the amyloid cascade (Liu et al., 2013; Michaelson, 2014). To investigate the extent to which Aβ secretion is influenced by *APOE2*, we measured the neural cultures for levels of Aβ40, and Aβ42 released into the extracellular medium by ELISA. This analysis revealed that conversion of *APOE3* to *APOE2* significantly reduced levels of secreted aggregation-prone Aβ42 in cell supernatant (**Figure 3.1B**). Additionally, *APOE2* neurons secreted less Aβ40 peptide compared with *APOE3* matched pairs (**Figure 3.1B**), suggesting *APOE2* plays a critical role in the regulation of Aβ peptide generation and, consequently, in lowering total amyloid burden. Finally, we assessed the Aβ42/40 ratio in the neural cultures and found the reduction in amyloid significantly reduced the ratio in *APOE2* neurons harboring the PSEN1[A246E] mutation, however had no effect on the ratio in neural cultures derived from APP mutants (**Figure 3.1B**). As it has been reported that the APP mutations can specifically increases Aβ42 generation, we speculate that the conversion to *APOE2* may not be sufficient to alter the ratio in these mutants due to production of such high levels of Aβ42 (Konttinen et al., 2019). Finally, the introduction of *APOE2* into non-demented control (NDC) hiPSCs did not reduce Aβ levels or the Aβ42/40 ratio in the neural cultures (**Supplemental Figure C3.A**). Taken together, these data suggest that conversion of *APOE3* to *APOE2*

significantly moderated levels of Aβ that were elevated by fAD-related mutations (**Supplemental Figure C4**).

Next, we investigated the effect of *APOE2* on levels of p-tau in isogenic fAD and NDC neural cultures. As such, we measured tau phosphorylation at Thr231, a tau phosphoepitope, (**Figure 3.2A; Supplemental Figure C.3B, left panel**) as well as total tau in neural cell lysates (**Figure 3.2B; Supplemental Figure C.3B, center panel**). Interestingly, we found that relative levels of phosphorylated tau to total tau were significantly reduced only in *APOE2* isogenic cultures that showed a decrease in Aβ42/40 ratio (i.e. PSEN1^{A246E}; **Figure 3.2C; Supplemental Figure C.3B, right panel**). Overall, our results are consistent with emerging evidence that tau pathology is largely driven by the Aβ42/40 ratio and not total amyloid levels (Kwak et al., 2020).

3.3.3 Astrocytes mediate the mitigating effects of APOE2 on amyloid levels in hiPSC-derived neurons

To dissect if the observed *APOE2* phenotypes were mediated through neurons, astrocytes, or both, we sought to generate cultures that consist exclusively of neurons or astrocytes. In this vein, we employed a magnetic activated cell sorting (MACS) protocol targeting an established astrocyte-restricted cell surface marker, CD44, to deplete neural cultures of astrocytes (Liu et al., 2004; Santos et al., 2017) (**Figure 3.3A**). Briefly, hiPSC-derived hNPCs were differentiated to mixed neural cultures, dissociated, and MACS-separated into CD44-positive and –negative populations. Upon separation, we analyzed both populations for levels of CD44 expression using flow cytometry. As expected, the presumptive neuron population was negative for the CD44 surface maker while the isolated astrocyte population was 92-99% CD44-positive (**Figure 3.3B**). Importantly, the relative CD44 levels were consistent between independent differentiations and MACS isolations (**Supplemental Figure C5**). Further analysis of the isolated cell populations demonstrated the CD44-negative neuronal population expressed robust levels of neuronal marker TUJ1 and mature neuron markers MAP2 and NEUN (**Figure 3.3C; Supplemental Figure C.6A**). On the other hand, CD44-positive astrocytes lacked

expression of neuronal markers and displayed immunoreactivity for the astrocytic maker S100β (**Figure 3.3C; Supplemental Figure C.6B**).

To characterize the transcriptional profile of these isolated neuron and astrocyte populations we performed RNA-sequencing (RNA-seq) analysis (**Supplemental Figure C7**). Analysis of the genes upregulated in the CD44-positive astrocytic population revealed high expression of astrocyte-specific markers (e.g. *CD44*, *VIM*, *S100A16*, *TIMP1*, *LIF*, *OSMR*, *PLD1*, *FKBP5*, *SDC4*) that regulate processes related to astrocyte function including extracellular matrix secretion and remodeling, cytokine release, and inflammatory response (**Supplemental Figure C.7A**) (Clarke et al., 2018; Holmberg and Patterson, 2006; Ito et al., 2016; Jin et al., 2002; Yu et al., 1998; Zhang et al., 2014). By comparison, expression of these markers was largely absent in the CD44-negative neuronal population which expressed high levels of neuronal specific-makers (e.g. *MAP2, RBFOX3, SYP, DLG4, SLC17A6, GRIN1, GRIN2B, GRIN2D*) associated with neuronal function including cytoskeletal protein regulation, synapse formation, and neurotransmitter release (**Supplemental Figure C.7A** (Garcia-Marin et al., 2013; Kalsi et al., 1998; Monyer et al., 1992; Mullen et al., 1992). In addition, gene ontology (GO) analysis further confirmed the identity of these cell populations (**Supplemental Figure C.7B**). Specifically, the CD44-negative neuronal population was enriched for genes related to neuronal biological processes (e.g. synaptic signaling, neurotransmitter exocytosis), cellular components (e.g. axon, dendrite), and molecular functions (e.g. ion channel activity, neurotransmitter binding) (**Supplemental Figure C.7B, left panel**). Likewise, GO-analysis confirmed that the CD44-positive astrocyte population contained gene sets related to canonical astrocytic biological processes (e.g. cytokine response, immune system processes), cellular components (e.g. focal adhesion, extracellular matrix), and molecular functions (e.g. extracellular matrix adhesion, cytokine binding) (**Supplemental Figure C.7B, right panel**). Importantly, correlation analysis revealed a high degree of transcriptional similarity between cells isolated from independent differentiations and MACS separations (**Supplemental Figure C.7C**).

Although the CD44-positive and –negative cell populations expressed the genes and proteins typical of astrocytic and neuronal populations, respectively, we next wanted to confirm

the functional identity of these cell types. As it relates to APOE, astrocytes are the primary

producers of APOE in the central nervous system (CNS), although it has been shown that

neurons also produce APOE to a lesser degree (Raman et al., 2020; C. Wang et al., 2018).

Therefore, we measured the amount of secreted APOE in the medium in the astrocytic and

neuronal cultures. Indeed, we confirmed that levels of APOE levels secreted by the astrocyte

cultures was significantly higher compared to purified neuronal populations (**Figure 3.3D**). Finally,

to evaluate functional differences between the neuron and astrocyte populations, we assessed

spontaneous calcium transients in pure cultures. Consistent with functional characteristics of

neurons and astrocytes, we found that astrocytes exhibited slow calcium transients with longer

periods compared to the rapid, frequent firing of neurons, further confirming cellular identity

(Ikegaya et al., 2005) (**Figure 3.3E**). Collectively, these data demonstrate that our MACS-based

protocol allows for the efficient separation of functionally mature astrocytic and neuronal sub-

populations.

Next, we wanted to assess the contribution of the astrocyte populations on the AD-

related phenotypes observed in the isogenic pairs. Thus, we measured the levels of secreted Aβ

in the mixed neuron-astrocyte cultures and cultures that consisted exclusively of neurons. Across

all three isogenic pairs, we found that levels of secreted Aβ42 were significantly higher in the

neuron only cultures compared to the mixed cultures, underscoring the role of astrocytes in

amyloid clearance via uptake and degradation (**Figure 3.4A, upper panels**). This result is

consistent with previous studies employing mouse cell lines in the context of co-culture systems

that have demonstrated the importance of astrocytes regulating neuronal APP expression levels

(Vincent and Smith, 2001). Moreover, we found that removal of astrocytes led to elevated levels

of secreted Aβ40 in the APP^{dp} and PSEN1^{A246E} neuron cultures but not in the APP^{V717I} cultures

(**Figure 3.4A, middle panels**). Likewise, the relative Aβ42/40 ratio was only increased in the

pure neuronal cultures derived from the APP^{dp} and PSEN1^{A246E} (**Figure 3.4A, lower panels**).

Notably, the levels of phosphorylated tau were unaffected by removal of astrocytes from the

mixed cultures (**Figure 3.4B**), providing further evidence that pathological phosphorylation of tau

is governed by a mechanism independent to increased amyloid. Together, these findings suggest

that APOE2 modulates the secreted amyloid profile of neurons, in part, through interactions with the astrocytes.

3.3.4   Differences in AD phenotypes cannot be explained by differences in astrocyte Aβ uptake or receptor expression profile

We next wanted to explore the possible mechanisms by which astrocytes could reduce Aβ levels in *APOE2* mixed cultures. It has been well documented that astrocytes play a critical role in regulating the extracellular levels of Aβ through multiple clearance mechanisms (Ries and Sastre, 2016). Moreover, numerous studies have shown that APOE influences AD pathology by regulating Aβ uptake by astrocytes (Fu et al., 2016; Verghese et al., 2013). In fact, recently it was shown that *APOE4* hiPSC-derived astrocytes exhibit compromised Aβ uptake when compared to *APOE3* astrocytes (Lin et al., 2018). Therefore, we speculated that *APOE2* astrocytes uptake Aβ more efficiently than *APOE3* astrocytes, which could potentially account for the reduction in Aβ levels seen in our *APOE2* isogenic mixed cultures. To test this hypothesis, we treated purified astrocytes from isogenic pairs with FAM-labelled Aβ42 for 24 hrs. After 24hrs, cells were washed and treated with trypsin to remove surface-bound Aβ. The levels of internalized FAM-Aβ were then measured by flow cytometry. As expected, astrocytes internalized a significantly greater amount of Aβ (**Supplemental Figure C.8A**) compared to neurons across all cell lines. In addition, our analysis revealed that compared to neurons, astrocytes did not secrete significant levels of Aβ42 or Aβ40, consistent with previous studies with primary astrocytes (LeBlanc et al., 1997, 1996) (**Supplemental Figure C.8B**). However, of all the cell lines analyzed, only *APOE2* astrocytes harboring the APP^{V717I} mutation showed a significant increase in Aβ uptake compared to *APOE3* astrocytes (**Figure 3.5A, Supplemental Figure C.3C**).

Previous work has shown that Aβ can be cleared by astrocytes through indirect or direct association with APOE in the context of several receptors mainly LDL receptor-related protein 1 (LRP1) and LDL receptor (LDLR) (Basak et al., 2012; Kanekiyo and Bu, 2014; Kim et al., 2009; Liu et al., 2017a). In particular, work has shown that suppression of LRP1 reducing amyloid uptake, suggesting uptake may be dependent on LRP1 (Kanekiyo et al., 2011; Verghese et al.,

2013). To assess differences in surface expression of LRP1 and LDLR between isogenic pairs, we compared fluorescence intensity of isogenic astrocytes stained with fluorescently labeled antibodies for LDLR and LRP1 (**Figure 3.5B-C, Supplemental Figure C.3C**). This analysis revealed that in three of four lines examined a statistically significant decrease in LDLR expression in *APOE*2 astrocytes (**Figure 3.5B, Supplemental Figure C.3C**) and no significant difference in LRP1 expression between any of the isogenic pairs (**Figure 3.5C, Supplemental Figure C.3C**). We next examine if there was a correlation between the levels of Aβ uptake and the expression levels of LDLR and LRP1 (**Supplementary Figure C.9**). When examining all cell lines, regardless of *APOE* genotype, mutation type, and disease status, we observed a slight negative correlation between Aβ uptake and LDLR expression and a modest positive correlation between Aβ uptake and LRP1 expression (**Supplementary Figure C.9A**). Further probing these relationships revealed that these correlations only reached levels of significance when considering mutation type or disease status (**Supplementary Figure C.9B**) and not *APOE* genotype (**Supplementary Figure C.9C**). In sum, this data indicates that the reduction of Aβ levels observed in the *APOE*2 cultures compared to *APOE3* cultures cannot be attributed solely to differences in astrocytic uptake of secreted Aβ or related receptors.

3.3.5   *APOE2* alters Aβ profile through changes in APP processing

Because we did not observe any *APOE* genotype-dependent effects on Aβ uptake or clearance from cell culture media, we wanted to examine potential mechanisms by which *APOE2* might modulate production of Aβ. In particular, we hypothesized that the reduction of Aβ levels observed in the *APOE2* cultures could be attributed to differences in amyloidogenic versus non-amyloidogenic processing of APP. In the amyloidogenic processing of APP, β-secretase cleavage of full-length APP results in the generation of the membrane-bound C-terminal fragment (CTF-β) and extracellular release of soluble APPβ (sAPPβ). Subsequent processing of CTF-β by γ-secretase results in the generation of amino-terminal APP intracellular domain (AICD) as well as Aβ species. Conversely, α-secretase cleavage of full length APP via the non-amyloidogenic pathway results in the release of soluble APPα (sAPPα) and CTF-α which precludes Aβ

production (Zhang et al., 2011). Therefore, to investigate how *APOE2* may affect these processes in our isogenic cell culture system, we compared the levels of soluble APP (sAPP) fragments secreted into culture medium generated by APP cleavage due to the pathogenic β-secretase (sAPPβ) or non-pathogenic α-secretase (sAPPα) pathway. Comparing the ratio of sAPPβ/sAPPα in isogenic mixed cultures, we observed that the ratio was reduced in APP[dp] and PSEN1[A246E] *APOE2* cultures relative to *APOE3* cultures (**Figure 3.6A**). However, the effect was more modest in APP[V717I] cells (**Figure 3.6A**), perhaps due to strong mutation-specific effect on amyloidogenic processing of APP (Konttinen et al., 2019) that cannot be entirely mitigated by *APOE2*. In agreement with these findings, we also found that the levels of CTF-β relative to total APP were also reduced in APP[dp] and PSEN1[A246E] *APOE2* cultures relative to *APOE3* cultures (**Figure 3.6B**). In addition, there was no significant difference in total APP levels between isogenic pairs suggesting that the increased sAPPβ/sAPPα ratio and CTF-β levels were likely attributed to a shift from amyloidogenic to non-amyloidogenic processing and simply not reduction in total APP (**Figure 3.6C**). To further investigate if this effect was mediated by the presence of astrocytes in cultures, we measured sAPPβ/sAPPα ratios in purified neuronal cultures. This analysis revealed an increase in the levels of sAPPβ relative to sAPPα across lines, consistent with the increase in Aβ peptides observed upon astrocyte removal in neuronal cultures (**Figure 3.6D**). Overall, a reduction in the ratio of sAPPβ/sAPPα suggests a shift from amyloidogenic to non-amyloidogenic processing when *APOE3* is converted to *APOE2*. Given that astrocyte populations did not display significant Aβ production relative to neurons (**Supplemental Figure C.8B**) (Laird et al., 2005; Zhao et al., 1996), this consistent trend suggests a protective function of APOE2 involving the modulation of APP processing in neurons that might drive the isoform-specific reduction in Aβ in *APOE2* cultures.

3.4   Conclusion

It has been well-established that polymorphism in the *APOE* gene is one the strongest genetic predictors of sporadic Alzheimer's disease (AD) risk (Holtzman et al., 2012). In particular, the *APOE2* is linked to significantly reduced likelihood of AD onset and progression as well as

increased life span (Drenos and Kirkwood, 2010; Suri et al., 2013). As such, it has been

suggested that mimicking the protective effects of *APOE2* is a viable therapeutic intervention

(Chiang et al., 2010). Nonetheless, with much of the field focused on the risk-inducing effects of

APOE4, the mechanisms of the protective effect of *APOE2* have not been extensively studied

(Chiang et al., 2010; Suri et al., 2013). In particular, studies using isogenic hiPSC lines to study

APOE function have all focused on elucidating toxic functions of *APOE4*, leaving mechanisms

governing *APOE2* protective function largely unexplored (Lin et al., 2018; Rieker et al., 2019; C.

Wang et al., 2018). In this study, we utilized three hiPSC lines derived from patients with early

onset familial AD (fAD) caused by three independent autosomal mutations, including one of the

most common point mutations in APP (APP^{V717I}), a point mutation in PSEN1 (PSEN1^{A246E}), and a

duplication in APP (APP^{dp}). Previous studies have demonstrated that relative to neural cultures

derived from non-demented control hiPSC lines that neural cells generated from these lines

display robust AD-related phenotypes including elevated levels of Aβ and phosphorylated tau

(Israel et al., 2012; Kondo et al., 2013; Konttinen et al., 2019). To allow for the identification of

phenotypic differences attributed solely to *APOE* genotype, we used genome editing to generate

matched *APOE2* lines from each *APOE3* parental line. To our knowledge, this is the first isogenic

hiPSC-derived culture system that allows for to study the effects of *APOE2* on disease-related

phenotypes.

Analysis of mixed neuronal-astrocytic cultures derived from *APOE* isogenic pairs,

revealed that conversion of *APOE3* to *APOE2* dramatically reduced secreted Aβ levels. These

data are consistent with evidence seen clinically where *APOE2* is associated with milder AD

pathology including significantly reduced amyloid deposited in the neocortex, as well as animal

studies that suggest the *APOE2* allele markedly reduces brain amyloid pathology in Alzheimer's

disease mouse models (Nagy et al., 1995; Serrano-Pozo et al., 2015; Zhao et al., 2016). Further,

these data suggest that conversion of *APOE3* to *APOE2* was sufficient, at least in part, to reduce

levels of Aβ to those observed in cells derived from non-demented control (NDC) hiPSCs.

Interestingly, we did not observe a difference in Aβ levels in isogenic cultures derived from NDC

hiPSCs. This suggests that the protective effects of *APOE2* are only observed in the context of

fAD cultures with elevated Aβ species and cannot be readily observed in context of NDC cultures that do not have significantly elevated Aβ levels. Moreover, analysis of the Aβ42/40 ratio in neural cultures revealed a reduced ratio in the *APOE2* cells harboring the APP[dp] and PSEN1[A246E] mutations but no difference between isogenic pairs with the APP[V717I]. Although it has been postulated that elevated ratios of Aβ42:Aβ40 directly result in the pathological amyloid plaques found in AD patients (Chow et al., 2010; Zhang et al., 2011) we speculate that differences in this ratio observed across cell lines may be a result of fAD mutation-specific differences in amyloid species generation. In particular, previous studies with the APP[V717I] line have demonstrated that this mutation leads elevated levels of Aβ42, but not Aβ40, compared to cells derived from non-demented controls (Konttinen et al., 2019). Therefore, the modulating effect of *APOE2* on Aβ42 and Aβ40 observed in this line may not be sufficient to lower the Aβ42:Aβ40 ratio. Overall, the reduction in total amyloid mediated by the *APOE2* genotype seen across all three isogenic pairs, coupled with other studies that have shown that *APOE* mediates Aβ aggregation in an isoform-specific manner (APOE2<APOE3<APOE4) (Hashimoto et al., 2012), suggests a potential mechanism by which *APOE2*-dependent modulation of amyloid production coupled with *APOE2* isoform reducing aggregation of amyloid, may work in concert to prevent severe neuron dysfunction (Lanz et al., 2003).

Broadly speaking, it has been reproducibly shown that AD patients that are carriers of *APOE2* have significantly reduced cortical Aβ deposition(Nagy et al., 1995), while the effect of *APOE2* on tau pathology has not been as conclusive (Berlau et al., 2009; Farfel et al., 2016; Morris et al., 1995). In our analysis, we show that only cultures with altered Aβ42/40 ratio also showed alterations in levels of pathogenic tau in response to conversion of *APOE3* to *APOE2*. Our results linking these changes in Aβ and p-tau closely parallel new evidence from Kim and colleagues that provide strong evidence that tau pathology is tightly correlated with Aβ42/40 ratio alone, and not total Aβ levels as previously thought (Kwak et al., 2020). Further, in an independent study using hiPSC-derived neurons, it was demonstrated that abrogating amyloid production using small molecules had no effect on levels of tau phosphorylation in cultured neurons (C. Wang et al., 2018). Taken together, this suggests that the modulation of tau

pathology by *APOE2* might be driven solely by the effects on Aβ42/40 ratio and not increased amyloid generation.

In the central nervous system, neurons act as the primary producers of Aβ whereas non-neuronal cells, such as astrocytes, facilitate its clearance (Liu et al., 2013). The imbalance in these processes is thought to be a primary driver of Aβ oligomerization and subsequent formation of amyloid plaques found in AD patients (Chow et al., 2010; Zhang et al., 2011). However, the role of *APOE2* in Aβ generation and extracellular removal is not well known (Raman et al., 2020). As it relates to ApoE and Aβ clearance by astrocytes, previous studies with immortalized (Prasad and Rao, 2018; Verghese et al., 2013) and hiPSC-derived (Lin et al., 2018) astrocytes have shown that *APOE4* astrocytes display reduced Aβ clearance when compared to *APOE3* astrocytes. Therefore, we speculated that *APOE2* astrocytes might exhibit a gain-of-protective function by enhancing Aβ clearance in our mixed cultures. However, we only observed higher levels of Aβ uptake in purified *APOE2* astrocytes with the APP^{V717I} mutation. Interestingly, when we examined the relationship between levels of Aβ uptake and LDLR/LRP1 receptor expression we observed only mutation- and not *APOE*-genotype specific correlations. This is consistent with other studies that have shown LRP1 expression can have fAD mutation-dependent expression patterns (Fong et al., 2018; Shinohara et al., 2017). Likewise, other groups have reported that although LDLR is responsible for Aβ-uptake in astrocytes, this occurs independent of APOE (Basak et al., 2012). Alternatively, other studies have shown compared to *APOE3* that *APOE4* astrocytes have reduced surface expression of LRP1 leading to impaired Aβ clearance (Prasad and Rao, 2018). Therefore, we speculate that effect of APOE isoform on Aβ clearance in astrocytes is driven primarily by mutation-specific effects on receptor expression. Future studies in which expression of these receptors are experimentally modulated (i.e. knockdown, overexpression) in the context of *APOE* isogenic lines with various fAD-related mutations will need to be performed to further probe these relationships. With respect to neurons, recent work has shown that LDLR and LRP1 facilitate the endocytosis of tau and its subsequent spread (Cooper et al., 2020; Rauch et al., 2020). In this regard, future studies that examine the ApoE isoform-dependent relationship between neuronal expression of LDLR/LRP1 and tau uptake

would be of interest in elucidating the effects of *APOE2* on the mitigation of AD-related

phenotypes.

 With regards to the effects of ApoE and Aβ production by neurons, ApoE has been found

to elevate APP transcription and resultant Aβ generation in cultured neurons in the order

E4>E3>E2 (Huang et al., 2017). However, the isoform-specific effects of ApoE on amyloidogenic

processing of APP have not been extensively studied. To that end, we investigated if altered

amyloidogenic processing could be implicated in the reduction of Aβ species observed in the

APOE2 mixed cultures. Soluble APP fragments are an indirect measurement of pathogenic

processing and sAPPβ and CTF-β peptides have been shown to increase in fAD neurons (Kwart

et al., 2019; Muratore et al., 2017, 2014) . Our analysis of secreted amyloidogenic sAPPβ relative

to non-amyloidogenic sAPPα as well as CTF-β revealed a significant reduction in pathogenic

processing in APP[dp] and PSEN1[A246E] *APOE2* cultures compared to *APOE3* cultures. While this

trend was also seen in APP[V717I] cells, it was much less pronounced related to the other two cells

lines. It was been documented that the APP[V717I] mutation is located within the transmembrane

region of APP which preferentially increases amyloidogenic β-secretase cleavage at levels that

exceed other fAD-related mutations (Konttinen et al., 2019). Therefore, we contend that the

significantly elevated mutation-specific levels of sAPPβ reduced the protective *APOE2* effect size

in APP[V717I] cultures relative to the other two cell lines. In addition, we observed that although the

removal of the astrocyte subpopulation led to increased levels of pathogenic sAPPβ, congruent

with our observation of increased Aβ, this did not diminish the effect of *APOE2* on APP

processing. This suggests that both cell autonomous and cell non-autonomous aspects contribute

the effect of *APOE2* on APP processing by neurons. Currently, the specific mechanisms by which

APOE2 alters APP processing are unclear. A variety of mechanisms regulate amyloidogenic

versus non-amyloidogenic processing of APP, including but not limited to the following: (i)

cytoplasmic phosphorylation of APP, (ii) levels of activity of kinases implicated in APP

phosphorylation, (iii) expression and activity levels of enzymes (i.e. α-, β, and γ-secretase)

involved in APP cleavage, and (iv) intracellular APP trafficking (Campion et al., 2016; Haass et

al., 2012; Yuksel and Tacal, 2019). In particular, ApoE has been shown to form a physical

association with APP, casually altering Aβ output by potentially acting as a molecular chaperone for APP processing (Sawmiller et al., 2019; Verghese et al., 2013). In addition, blocking this interaction could abrogate the isoform specific effects of *APOE4* on Aβ levels (Hass et al., 1998; Sawmiller et al., 2019). Therefore, we speculate that *APOE2* might directly affect how APP is presented to APP cleavage enzymes, resulting in alterations in APP processing and Aβ profiles. However, future studies will be required to resolve the particular mechanisms that enable this potential gain-of-protective effect of *APOE2*.

In conclusion, our findings using isogenic hiPSC-derived neurons provide some of the first characterization of *APOE2*-dependent changes in a hiPSC cell culture model. In particular, we choose to examine these *APOE2* effects in the context of fAD lines that have consistently displayed robust AD-related phenotypes (Israel et al., 2012; Kondo et al., 2013; Konttinen et al., 2019). Remarkably, introduction of *APOE2* into hiPSCs with fAD-related mutations significantly mitigated the strong disease-related phenotypes typically observed in the neural cultures derived from these cell lines. Even though disease-relevant phenotypes in neural cells generated from sporadic AD (sAD) hiPSCs have been highly variable or largely absent (Raman et al., 2020), future studies that employ *APOE* isogenic sAD hiPSCs will be necessary to increase the translation of these findings to LOAD. Finally, although we did not interrogate all the potential hypothesized mechanisms by which *APOE2* modulates AD-risk, we uncovered clues that will set the stage for more detailed studies. In particular, *APOE2* had a strong mitigating effect on Aβ production likely through a mechanism related to modulation of amyloidogenic processing APP. Collectively, these results open up potential new targets to mimic the protective effects of *APOE2* to alleviating AD onset and disease-related progression.
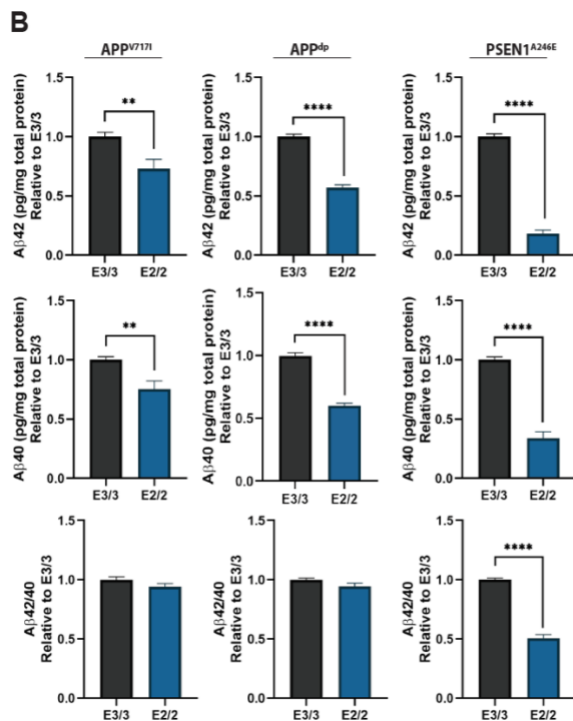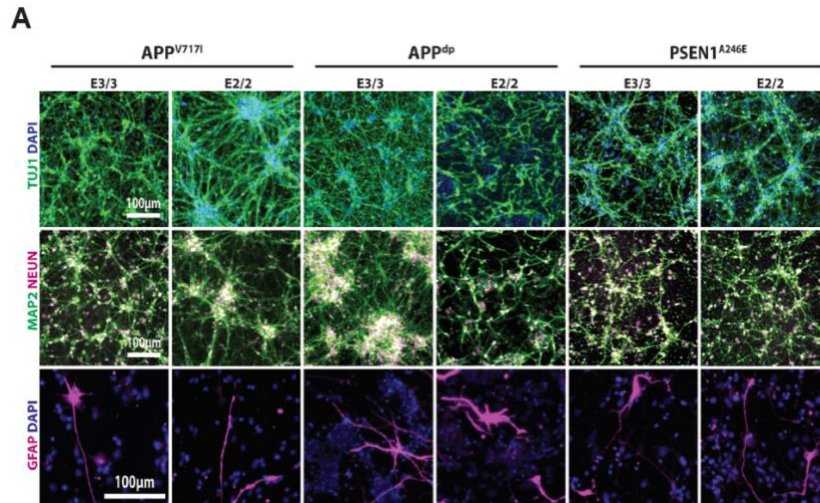
Figure 3.1. Isogenic hiPSC-derived model of AD reveals isoform-specific effects of *APOE2*.
(**A**) Characterization of hiPSC-derived neural cultures by immunofluorescence for neuronal marker TUJ1, mature neuron markers MAP2 and NEUN, and astrocyte marker GFAP. (**B**) Quantification of secreted soluble Aβ levels in cell supernatant normalized to cellular protein amounts, relative to corresponding E3/3 cultures. n=15~16 from 3 independent differentiations; * = p<0.05, ** = p<0.01, *** = p<0.001, **** = p<0.0001.
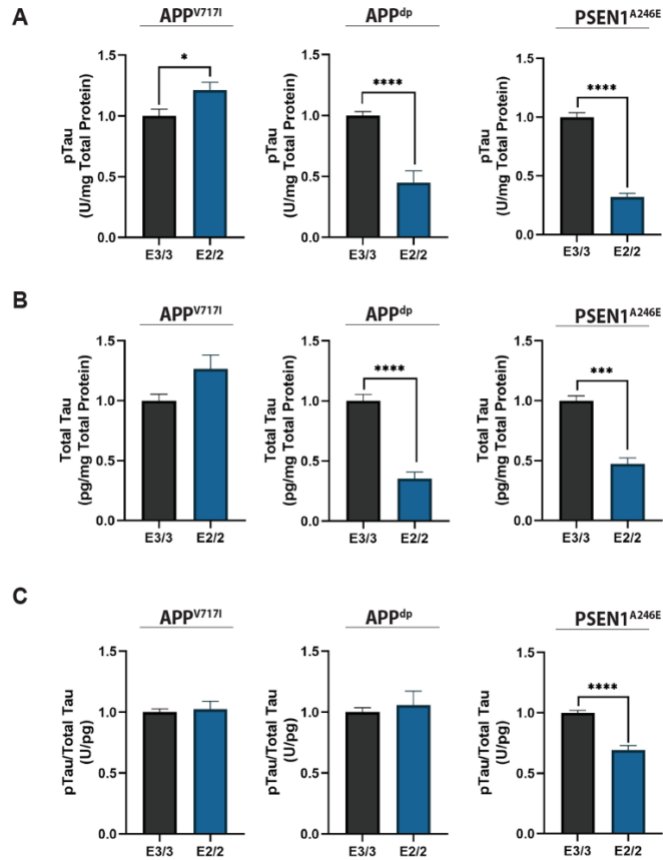
Figure 3.2. Isoform-specific effect of *APOE2* on tau protein.
(A) Quantification of phosphorylated-tau in cell lysates normalized to total protein. **(B)** Quantification of total tau normalized to total protein in lysate **(c)** Corresponding ratio of phosphorylated-tau protein to total tau. n=14~15 from 3 independent differentiations; * = p<0.05, ** = p<0.01, *** = p<0.001, **** = p<0.0001.
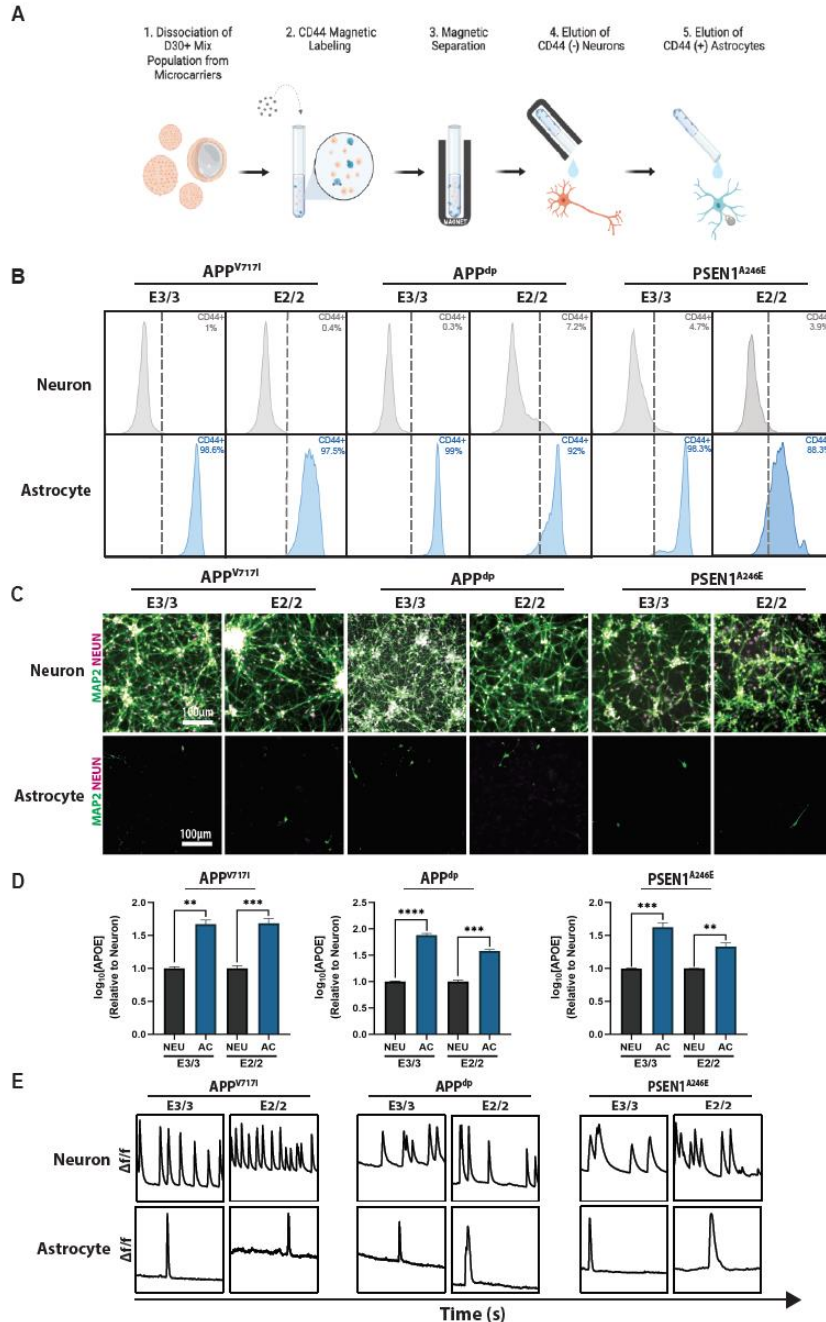
Figure 3.3. Isolation of pure populations of neurons and astrocytes from mixed cultures.
(**A**) Schematic of magnetic activated cell separation (MACS) used to isolate pure neuronal and astrocytic cell populations. (**B**) Representative flow cytometry analysis of CD44 expression in separated CD44- neurons and CD44+ astrocytes. (**C**) Immunofluorescence showing expression of mature neuron markers MAP2 and NEUN in neuron, but not astrocyte populations. (**D**) Quantification of APOE secretion by astrocyte and neuron populations. (**E**) Analysis of calcium transients show slow calcium transients in the separated astrocytes compared to neuron populations. n=3~5; * = p<0.05, ** = p<0.01, *** = p<0.001, **** = p<0.0001.

Figure 3.4. Amyloid and phosphorylated-tau (p-tau) levels in astrocyte-depleted cultures.
(**A**) Quantification of secreted Aβ in mixed and pure neuronal cultures. (**B**) Quantification of tau levels in mixed and pure neuronal cultures. n=6; * = $p<0.05$, ** = $p<0.01$, *** = $p<0.001$, **** = $p<0.0001$.
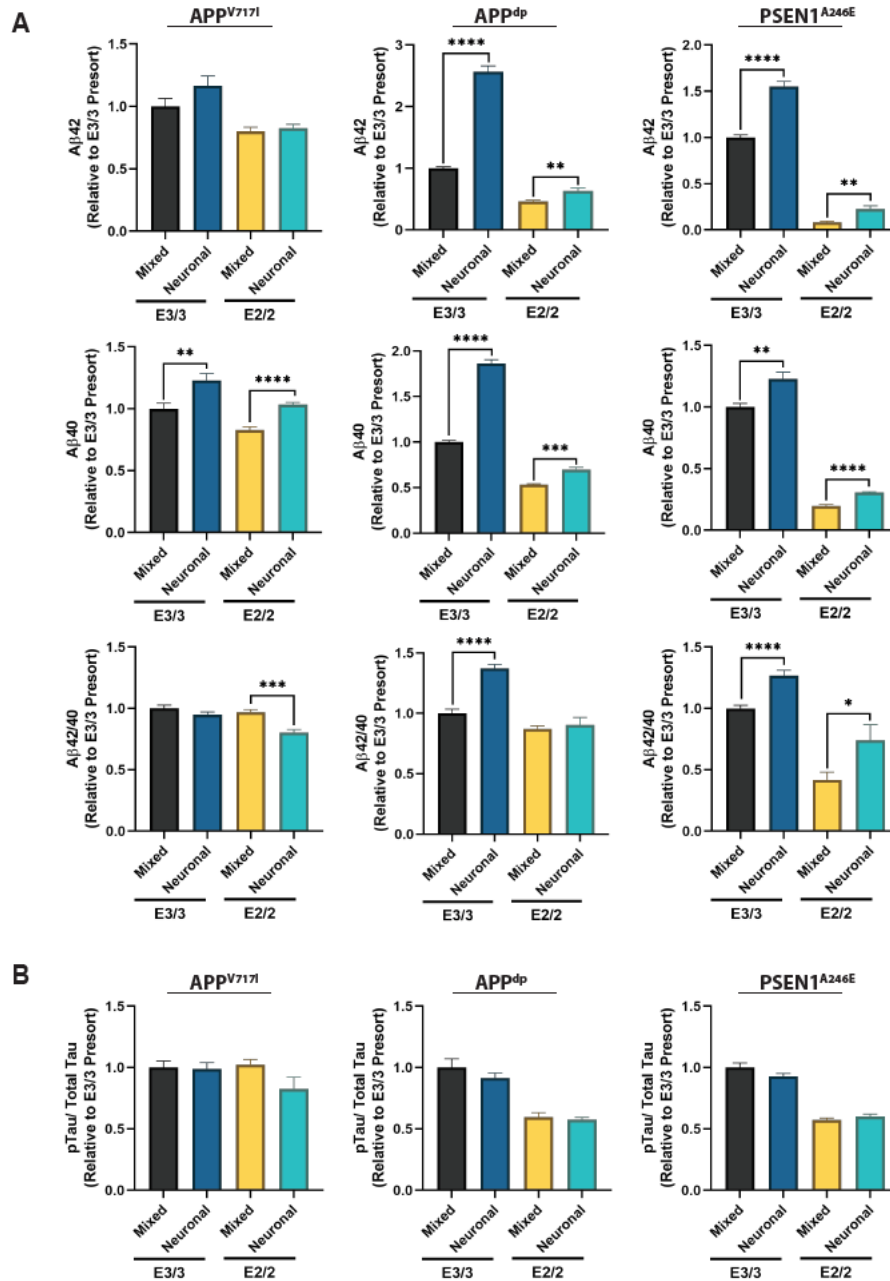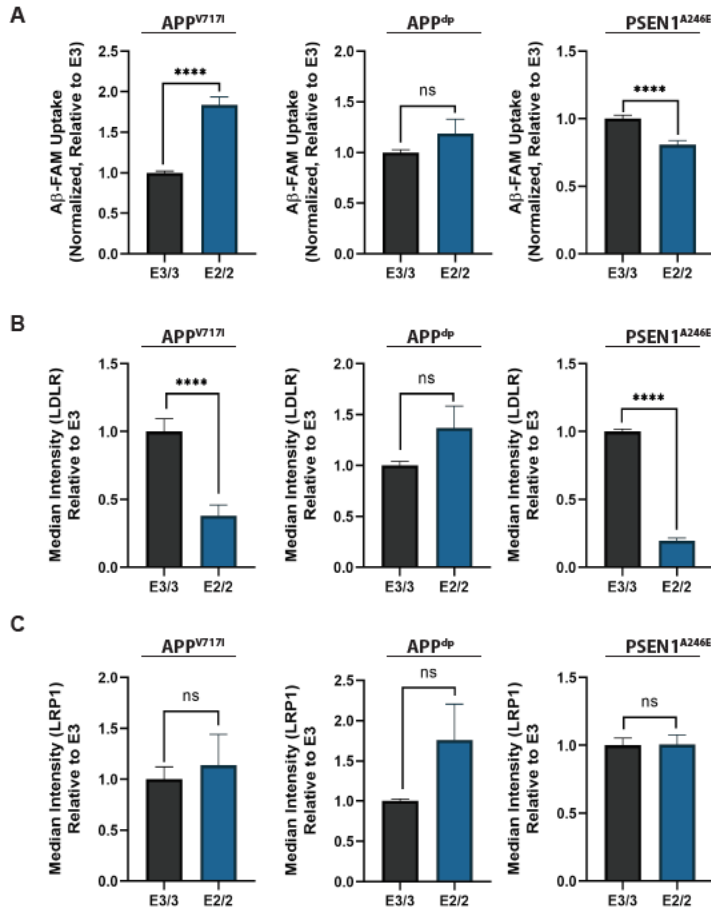
Figure 3.5. Characterization of Aβ uptake and receptor expression in pure astrocytic populations.
Quantification of internalized FAM labelled Aβ42 (n=14~20 from 2-3 independent differentiations) (**A**), LDLR expression (**B**), and LRP1 expression (**C**) in pure astrocytic populations using flow cytometry (n=8~11 from 2-3 independent differentiations); * = $p<0.05$, ** = $p<0.01$, *** = $p<0.001$, **** = $p<0.0001$.
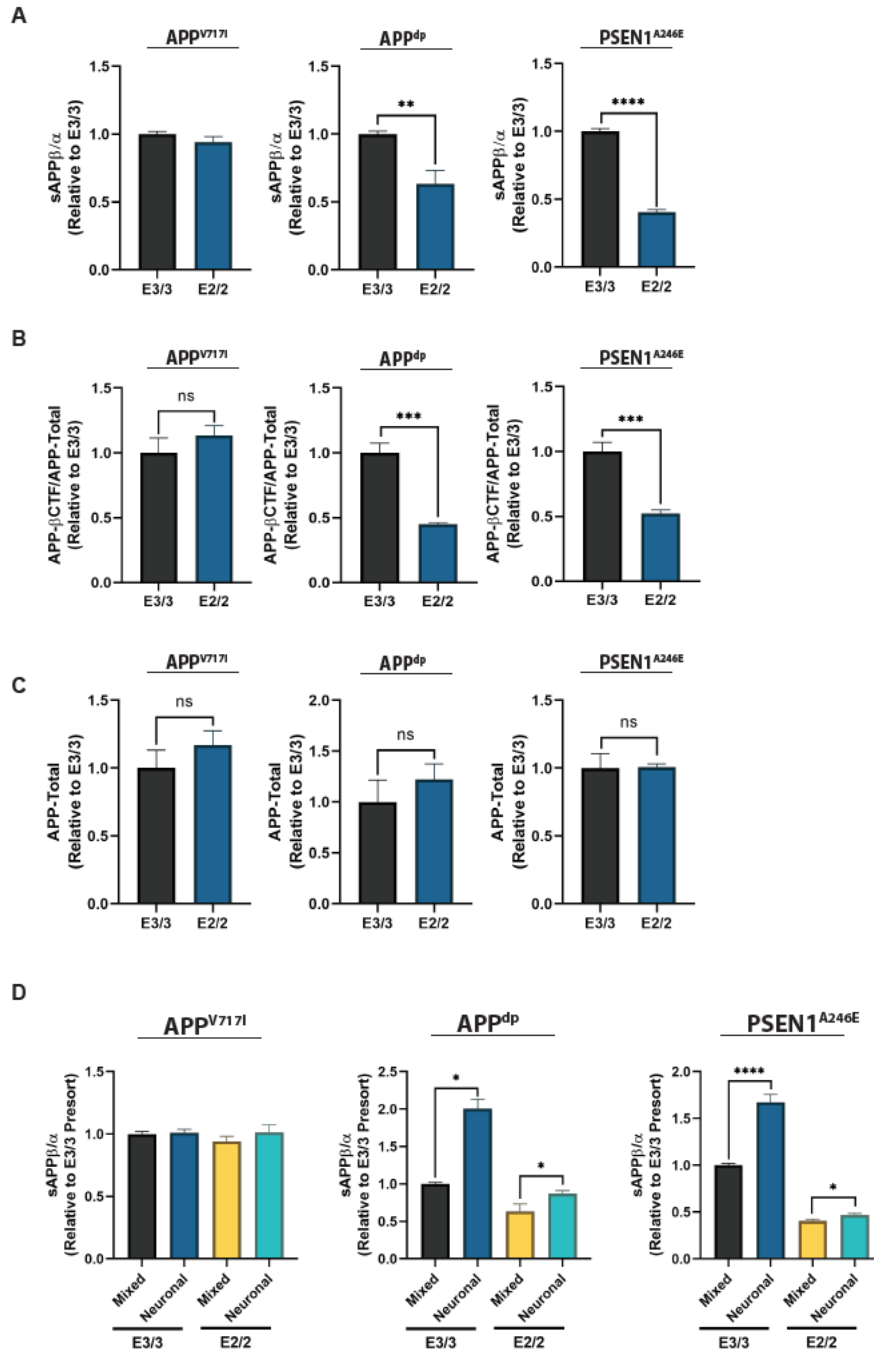
Figure 3.6. *APOE2* alters amyloidogenic processing of APP.
(**A**) Quantification of sAPPβ and sAPPα fragments in hiPSC-derived neural cultures (n=12~15 from 3 independent differentiations). **(B)** Quantification of the ratio of APP-βCTF to total protein in cell lysate (n=4). **(C)** Quantification of total APP protein normalized to total protein in lysate (n=4~8). (**D**) Comparison of sAPPβ and sAPPα levels in mixed and pure neuronal cultures (n=3~15). * = p<0.05, ** = p<0.01, *** = p<0.001, **** = p<0.0001.

CHAPTER 4

INVESTIGATING THE MOLECULAR MECHANISMS UNDERLYING THE DIFFERENTIAL

AMYLOIDOGENIC PROCESSING OF APP IN *APOE* ISOGENIC NEURONS

4.1   Introduction

The elevated amyloid burden in AD patient brains manifests from amyloid precursor

protein (APP) processivity defects. Four anti-amyloid therapeutics, that have been shown to

reduce levels of insoluble oligomers and amyloid deposits to varying degrees in patients are

currently vying for clinical approval (Tolar et al., 2020). However, inconsistencies in their late

stage clinical outcomes have raised doubts of their efficacy (Knopman et al., 2020). These

therapeutics address the long-debated amyloid hypothesis, which has implicated the Aβ peptide

and its extracellular deposition to be the primary cause of neurodegeneration and dementia in AD

brains. Other studies implicate amyloidogenic pathway precursors, such as the APP-βCTF

accumulation within endosomes, to cause endolysosomal network defects that lead to

neurodegeneration (s). Although anti-amyloid drugs might induce a favorable response in a

subset of AD patients when administered at an early disease stage, there is a need to address

the needs of the remainder of the affected population by studying the effects of the multitude of

genetic risk factors, such as APOE, on upstream amyloidogenic pathway intermediates. As

described in the chapter 3, we observed that *APP^{dp}* and *PSEN1^{A246E} APOE2* neurons have lower

levels of APP-βCTF (relative to total APP), compared to *APOE3* neurons. As the intraneuronal

accumulation of the cytotoxic βCTF has been reported in the background of fAD mutations by

others, it is remarkable to observe a decrease of this fragment in *APOE2* neurons (Kim et al.,

2016; Kwart et al., 2019; McPhie et al., 1997; Pera et al., 2013). In this chapter, the molecular

basis of the differences in APP processing in *APOE2* and *APOE3* fAD neural cultures is further

investigated. Additionally, APOE isogenic non-demented control neurons were excluded from this

downstream analysis as differences in AD phenotype were not observed based on *APOE*

genotype and was unlikely to contribute to the investigation of molecular mechanism.

4.2 Experimental Methods

4.2.1 Neural differentiation of fAD-hiPSCs.

HiPSCs were differentiated to neurons as previously described with some modifications, detailed in chapter 3 of this manuscript (Cutts et al., 2016).

4.2.2 Dissociation and isolation of pure neuronal populations from microcarrier cultures.

Pure neuronal populations derived from fAD-hiPSCs, depleted of CD44-positive astrocytes, were generated as previously described in chapter 3 of this manuscript.

4.2.3 Measurement of APP phosphorylated at Thr-668.

Neurons seeded in a 24-well plate at a density of 1-2 x 10^6 cells per well for six days were lysed in TBS buffer containing 1% Triton-X100 (Sigma) [TBS-T] and protease inhibitors (ThermoFisher). Total protein in these lysates were quantified using a detergent compatible Bradford assay (ThermoFisher). APP phosphorylated at Threonine-668, as well as total APP,was measured using a commercially available semi-quantitative ELISA(Ray Biotech) in equal amounts of total protein across each isogenic pair.

4.2.4 Measurement of total GSK3β and GSK3β phosphorylated at Ser-9.

Neurons were lysed in TBS-T buffer with protease inhibitors as described above. Equal protein lysate was assayed using a semi-quantitative ELISA (Ray Biotech) to measure relative amounts of total and phosphor-Ser-9 GSK3β between isogenic pairs. Additionally, a human GSK3β quantitative ELISA (Aviva Systems Bio) was used to measure the total GSK3β in cell lysates.

4.2.5   Measurement of ADAM10 and BACE1 protein

ADAM10 levels in TBS-T neuronal lysates were measured using the human ADAM10 quantitative ELISA (Aviva Systems Bio) and normalized to total protein levels. BACE1 levels in neuronal lysates in RIPA buffer were measured using the human BACE1 ELISA (IBL).

4.2.6   RNA-seq analysis

RNA-sequencing samples were analyzed as discussed in chapter 3. Briefly, single end sequenced reads were mapped to the human hg19 reference genome using HISAT2 and differentially expressed genes were identified using the DESeq2 algorithm (Kim et al., 2015; Love et al., 2014).

4.2.7   Statistical analysis

Two-sided t-tests were used to identify statistically significant (p-value less than 0.05) differences between two groups, with Welch's correction for unequal sample sizes. All data is denoted as mean ± s.e.m using GraphPad Prism (v9) unless otherwise noted.

4.3   Results

4.3.1   *APP^{dp} APOE2* neurons express a distinct profile of APP processing enzymes

The primary enzyme responsible for α-site cleavage of APP in human neurons is a disintegrin and metalloproteinase 10 (ADAM10) (Kuhn et al., 2010). The aspartyl protease β-site APP cleaving enzyme I (BACE1) predominantly expressed in neurons, is responsible for the first cleavage APP in the amyloidogenic pathway (Vassar et al., 1999). Previous studies have shown that neurons derived from BACE1 knockout mice do not secrete detectable levels of Aβ, whereas their BACE2 knockout counterparts displayed no difference in Aβ level compared to wildtype mice, identifying BACE1 as the primary β-secretase enzyme in neurons (Dominguez et al., 2005). Moreover, BACE2 has been reported to preclude the formation of Aβ by cleaving near the α-secretase site (Sun et al., 2005; Yan et al., 2001).

The reduced sAPPβ/sAPPα ratio, coupled with lower levels of APP-βCTF relative to total APP in APP^{dp} *APOE2* neurons (**Figure 3.6**) point to preferential non-amyloidogenic processing of APP by α-secretase in *APOE2* neurons, and elevated amyloidogenic APP processing by β-secretase in *APOE3* cultures. We hypothesized that this difference stems from the differential expression of enzymes responsible for the first cleavage of APP. To investigate this hypothesis, we first looked at the transcriptional profile of the cleavage enzymes in mixed neuronal cultures, and subsequently measured their concentration in neuronal cell lysates. At the transcriptional level, we observed elevated levels of the non-amyloidogenic pathway enzymes ADAM10, ADAM9 and BACE2 only in the APP^{dp} *APOE2* neurons **(Figure 4.1a)**. Surprisingly, we observed elevated levels of ADAM9 mRNA in the PSEN1^{A246E} *APOE3* cultures. Additionally, there was no significant difference in BACE1 mRNA expression across the fAD mutant pairs. This observation parallels other studies that did not observe a difference in BACE1 expression at the mRNA level between AD and control brains (Gatta et al., 2002; Holsinger et al., 2002; Preece et al., 2003; Yasojima et al., 2001).

We proceeded to quantify the amount of ADAM10 protein in *APOE* isogenic mixed neuronal culture lysate. We found that the level of ADAM10 protein was significantly higher in the APP^{dp} *APOE2* neurons, but no significant difference was observed in the APP^{V717I} and PSEN1^{A246E} pairs **(Figure 4.1b)**. Although the elevated level of ADAM10 would suggest that more APP was processed by the non-amyloidogenic pathway reducing the amount of APP processed by BACE1, others have reported that the secretases do not always compete for APP (Kuhn et al., 2010; Skovronsky et al., 2000). It was later reported that the 'inverse coupling' of ADAM10 and BACE1 was only partial in primary cortical neurons, with the inhibition of BACE1 activity resulting in increased ADAM10 cleavage, but not vice versa (Colombo et al., 2013). Therefore, we subsequently examined the BACE1 protein levels in our *APOE* isogenic mixed neuronal culture lysates. As expected, we observed that higher levels of BACE1 protein were present in the APP^{dp} and PSEN1^{A246E} *APOE3* neurons **(Figure 4.1c)**, corroborating the elevated levels of APP-βCTF in these *APOE3* cultures.

4.3.2   *APP^{dp} APOE2* neurons have altered APP phosphorylation profile

APP undergoes a number of post-translational modifications, including N- and O-glycosylation and phosphorylation at different ectodomain and cytoplasmic sites, that affect its trafficking, processing and function (Haass et al., 2012). In human neurons, the APP695 isoform is N-glycosylated to generate immature APP (imAPP) within the endoplasmic reticulum and Golgi, followed by further O-glycosylation within the Golgi network, to generate mature APP (mAPP) in preparation for subsequent α- or β-secretase cleavage (Thinakaran and Koo, 2008). Deficiencies in APP glycosylation could affect its trafficking and enzymatic cleavage. The potential for phosphorylation of serine, threonine and tyrosine of APP695 has been reported at least eight residues in the cytoplasmic domain and two residues in the ectodomain in the AD brain (Oliveira et al., 2017). Further, others reported that APP-CTFs in the AD brain can be phosphorylated at seven different cytoplasmic sites, including at Threonine 668 (T668) (Lee et al., 2003; Shin et al., 2007). Remarkably, Lee et al. not only revealed that the levels of APP-CTF fragments phosphorylated at T668(pT668) was elevated in the hippocampal lysates of AD patients relative to control subjects, but also that this phosphorylation leads to preferential BACE1 cleavage and subsequent Aβ generation. To investigate the extent to which APOE2 affects the phosphorylation of APP, we compared the proportion of pT668 to total APP in mixed neuronal cultures. Interestingly, we found that the APP^{dp} *APOE3* neurons have a higher proportion of pT668 relative to *APOE2* neurons (**Figure 4.2a**). However, the levels of pT668 were not significantly different between the *APOE* isogenic pairs in the context of the PSEN1^{A246E} and APP^{V717I} mutations. A large number of kinases and signaling pathways are involved in APP695 phosphorylation, each influencing different downstream effects (reviewed in Zhang et al., 2019) .

In vitro studies have shown that APP phosphorylation is mediated by distinct pathways modulated by cyclin-dependent kinase 5 (CDK5), glycogen synthase kinase 3β (GSK3β) and other key kinases depending on the cellular state of a neuron (Muresan and Muresan, 2007). We examined the transcriptomic profile of the isogenic *APOE* neurons across the fAD lines to ascertain the level of expression of these key kinases. Remarkably, we saw a significant upregulation of *CDK5* and *GSK3*β mRNA in the APP^{dp} *APOE3* neurons relative to their *APOE2*

counterparts (**Figure 4.2b**). Strikingly the *MAPT* gene encoding the tau protein, a key target of the GSK3β, was upregulated in both APP[dp] and PSEN1[A246E] *APOE3* neurons. We also observed that CDK5 regulatory subunit 1 (*CDK5R1*) expression was upregulated in both APP[dp] and PSEN1[A246E] *APOE3* neurons. The *CDK5R1* gene encodes the p35 activator protein which is essential for the enzymatic activity of CDK5 in neurons. Others have previously shown that the truncated form of the p35 protein, p25, is elevated in AD brains and associates with CDK5 to form a hyperactive CDK5/p25 complex that has prolonged activity (Patrick et al., 1999; Taniguchi et al., 2001). Notably, we observed that *CAPN2* expression, encoding calcium dependent protease calpain-2, was upregulated in PSEN1[A246E] *APOE3* neurons. This is consistent with a previous report of elevated calpain-2 protease levels in AD brains, that cleaved the p35 protein to p25 postmortem in human and rat brains (Taniguchi et al., 2001; Zhang et al., 2017). However, others have found no difference in p25 levels in AD brains postmortem, which suggests that AD pathology manifests via different pathways dependent on mutations and associated risk factors (Nguyen et al., 2002; Tandon et al., 2003).

The elevated expression of the GSK3β transcript in APP[dp] *APOE3* neurons prompted us to explore GSK3β protein and activity in our isogenic mixed cultures. As it relates to protein expression, we observed higher levels of total GSK3β in in both APP[dp] and APP[V717I] *APOE3* neurons, but this trend was reversed in the case of the PSEN[A246E] mutation **(Figure 4.3A)**. GSK3β is a constitutively active kinase, with phosphorylation at its Ser9 residue rendering the enzyme inactive (Fang et al., 2000). To measure the amount of active GSK3β in our cultures, we first quantified the proportion of inactive GSK3β phosphorylated at the S9 residue **(Figure 4.3B)** and then calculated the fraction of active GSK3β based on the total GSK3β in the culture. We observed that the amount of active GSK3β paralleled the trend previously reported for the total GSK3β in our cultures (**Figure 4.3C)**. As GSK3β is a key kinase involved in tau phosphorylation and taking into consideration our observation of elevated pTau levels in both APP[dp] and PSEN[A246E] *APOE3* neurons **(Figure 3.2A)**, it is possible that elevated tau phosphorylation occurs through other kinases in the PSEN1 *APOE3* mutant line. Indeed, we observed the elevated

84

mRNA expression of *MARK1* and *PRKACB* **(Figure 4.3D)**, two key kinases implicated in tau

phosphorylation PSEN[A246E] *APOE3* neurons (Johnson and Stoothoff, 2004; L. Wang et al., 2019).

4.4   Conclusion

With recent anti-amyloid drugs failing to satisfy their primary endpoints in late-stage

clinical trials, it is crucial to understand the mechanism of action and target pathway intermediates

upstream of Aβ. In this study we aimed to delve into the molecular mechanism driving the

'protective' effect of APOE2 in cortical fAD-iPSC derived neurons that lead to a lower level of Aβ

production relative to their isogenic *APOE3* neurons. Endosome enlargement is the earliest sign

of AD pathology, preceding the deposition of amyloid by decades in Down syndrome (DS)

patients (Cataldo et al., 2000). Kwart et al. have previously reported β-CTF levels to correlate

with observed endosomal abnormalities in iPSC derived neurons to a larger degree than the Aβ

load (Kwart et al., 2019). Indeed, the inhibition of BACE1 and subsequent reduction in β-CTF in

DS fibroblasts reverses endosome abnormalities, whereas the overexpression of in β-CTF

induces endosome dysfunction (Jiang et al., 2010). In a detailed investigation of both APP and

PSEN1 fAD iPSC derived neurons Hung et al. report the presence of endosomal defects in APP

mutants and endo-lysosomal defects in the PSEN1 mutation background (Hung and Livesey,

2018). Interestingly, BACE1 inhibition reduced APP-β-CTF levels and corrected lysosome-

autophagy defects observed in these neurons. We report here that the level of BACE1 protein

was lower in *APOE2* neurons derived from both APP[dp] and PSEN[A246E] mutants. In addition, the

level of non-amyloidogenic processing was significantly elevated in *APOE2* APP[dp] neurons. In

sum, the APOE2 protein is seemingly involved in the differential expression of the APP α- and β-

secretases and the mechanism underlying this effect remains to be explored.

Post-translational modifications of the APP protein, and its processing enzymes,

influence its trafficking and processing via either the amyloidogenic pathway in the

endolysosomal network, or the nonamyloidogenic pathway at the plasma membrane. The

cytoplasmic phosphorylation of APP at Thr668 is one such modification, that increases the

BACE1 cleavage of APP(Lee et al., 2003). Our transcriptomic analysis showed that various key

kinases involved in APP-T668 phosphorylation (reviewed in Zhang et al., 2019) were differentially expressed between the APP^{dp} and PSEN^{A246E} *APOE* isogenic neurons. However, we observed that the proportion of pAPP-T668 was elevated only in the APP^{dp} *APOE3* neurons, suggesting that elevated BACE1 processing of APP in the PSEN^{A246E} *APOE3* neurons is not directed by the increased phosphorylation of this residue. As the Cdk5 mediated phosphorylation of BACE1 at the Thr252 residue has been reported to increase its activity, further experimentation to explore this avenue in PSEN^{A246E} *APOE3* neurons might explain the elevated level of APP β-CTF relative to their *APOE2* counterparts (Song et al., 2015). Additionally, we observed significantly higher levels of active GSK3β, a key kinase involved in both APP-T668 and Tau phosphorylation, in *APOE3* neurons of both APP mutants, whereas the PSEN^{A246E} *APOE2* neurons had higher levels of active GSK3β. Strikingly, the PSEN^{A246E} *APOE3* neurons had significantly more *MARK1* and *PRKACB* mRNA that their *APOE2* variants, which might be involved in equalizing the level of pAPP-T668 in this isogenic pair.

In addition to affecting the processing of APP by BACE1 as described previously, phosphorylation at APP-T668 can modulate APP endocytosis. The phosphorylation of the T668 residue causes confirmational changes in the cytoplasmic domain of APP that interfere with the binding of adaptor proteins, such as FE65, to the proximal ^{682}YENPTY^{687} motif affecting its trafficking and processing (Ando et al., 2001). Studies have shown that FE65 increases the translocation of APP in the endoplasmic reticulum and Golgi to the plasma membrane, where it can be processed by α-secretase or trafficked to endosomes for β-secretase cleavage (Sabo et al., 1999). Interestingly our transcriptomic analysis revealed that the components of the late endosomal machinery, namely the endosomal sorting complexes required for transport (ESCRT-1) complex -*MVB12*, *VPS28* and *VPS37*, were significantly upregulated in APP^{dp} *APOE3* neurons (data not shown). This coupled with the fact that the accumulation of APP β-CTF correlates with the endosomal dysfunction in AD leads us to hypothesize that *APOE2* exerts its protective effect by modulating the endocytosis and intracellular trafficking of APP to encourage it toward non-amyloidogenic processing in neurons. Measuring the surface expression of APP and APOE

receptors such as LRP1 involved in APP trafficking might yield insight into the role of APOE2 in

the reduction of pathogenic β-CTF in these cells.
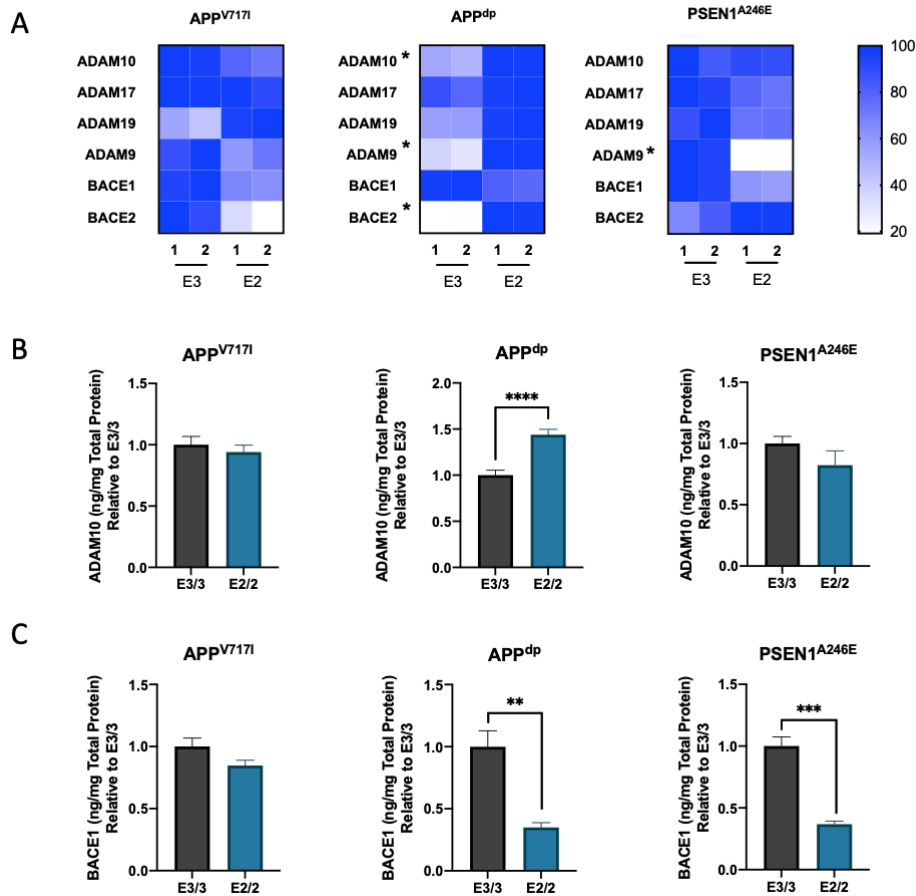
Figure 4.1. APP processing enzyme expression in *APOE* isogenic neurons.
(A) Comparison of the transcriptomic profile of α- and β-site cleavage enzymes implicated in APP processing with '*' indicating genes that were differentially expressed. Quantification of ADAM10 (**B**), and BACE1 **(C)** protein expression normalized to total protein in mixed neuronal cell lysates. n=4~17 from 1-2 independent differentiations; * = $p < 0.05$, ** = $p < 0.01$, *** = $p < 0.001$, **** = $p < 0.0001$.
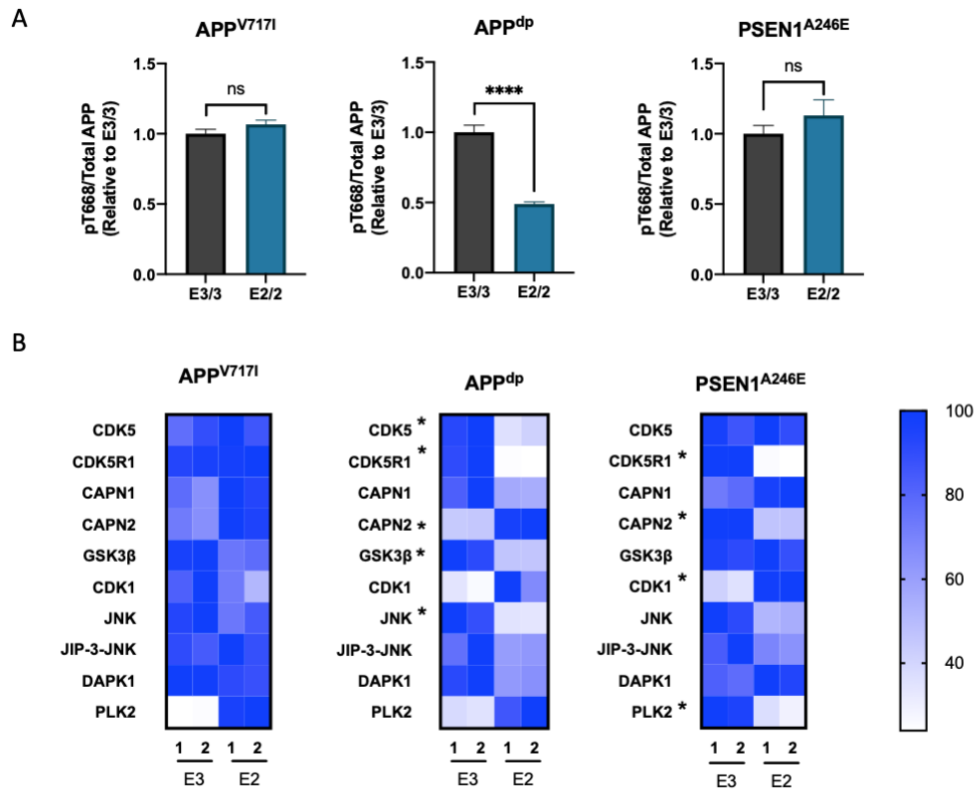
Figure 4.2. Isoform-specific effect of *APOE2* on APP phosphorylation.
(A) Quantification of pT668-APP in cell lysates normalized to total APP protein. n=5~6 **(B)** Comparison of the expression of key genes implicated in APP phosphorylation with '*' indicating genes that were significantly upregulated; * = p<0.05, ** = p<0.01, *** = p<0.001, **** = p<0.0001.
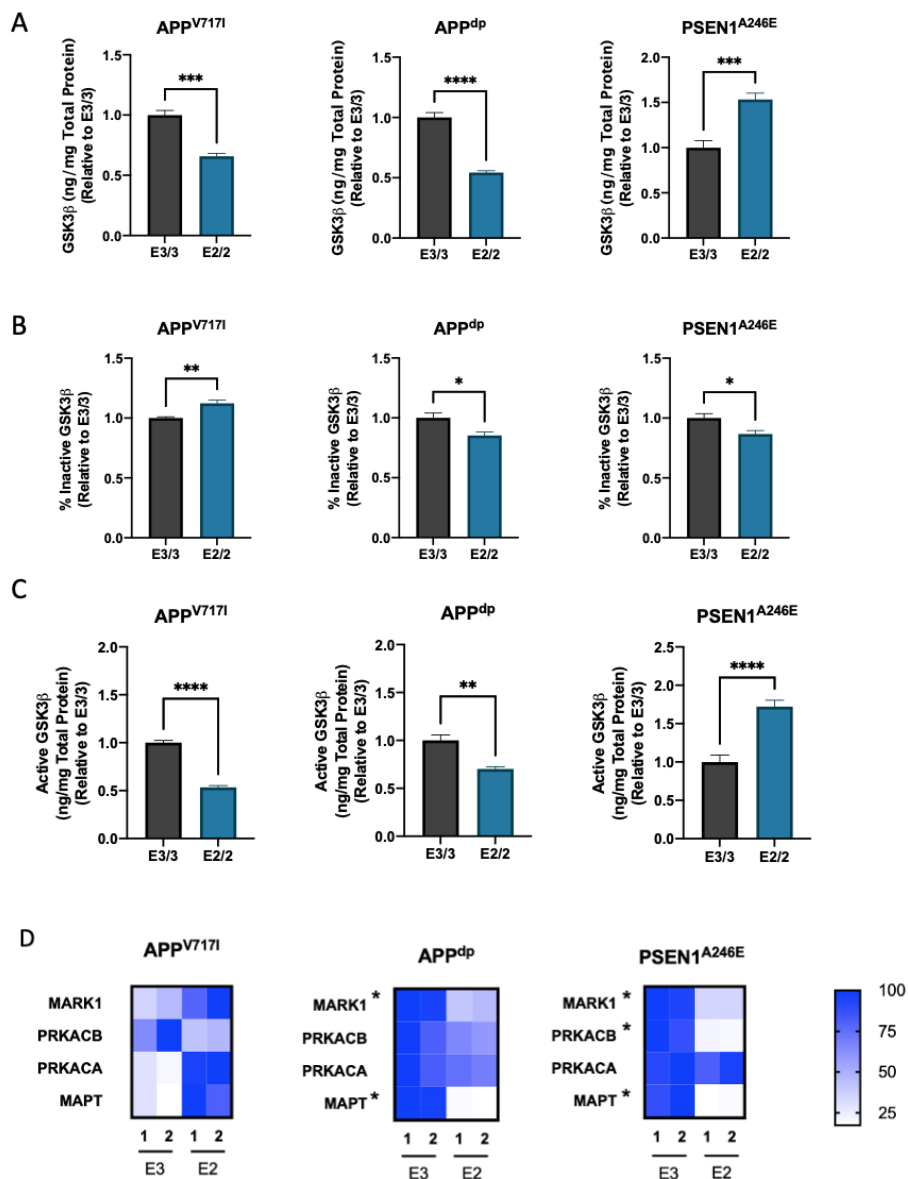
Figure 4.3. Isoform-specific effect of *APOE* on GSK3β activity.
(A) Quantification of total GSK3β in cell lysates normalized to total protein **(B)** Proportion of GSK3β phosphorylated at S9 (Inactive) to total GSK3β in lysate **(C)** Quantification of active GSK3β in cell lysate from proportion of inactive GSK3β in total GSK3β in sample. n=4~9 **(D)** Comparison of the expression of key genes implicated in Tau phosphorylation with '*' indicating genes that were significantly upregulated; * = $p<0.05$, ** = $p<0.01$, *** = $p<0.001$, **** = $p<0.0001$.

CHAPTER 5

SUMMARY AND FUTURE WORK

5.1 Project Summary

5.1.1   Specific Aim 1: Generate, characterize and evaluate the scalability and cryopreservation-potential of functional astrocytes derived from fAD-hiPSC lines so as to develop assays to measure AD phenotype across multiple cell lines.

As a part of our first specific aim to begin investigating the role of APOE2 in regulating AD phenotype, we proposed to develop a scalable system that allowed for the differentiation of a sufficient number of patient-iPSC derived astrocytes in chapter 2 of this manuscript. Following preliminary characterization using flow cytometry for CD44 expression, RT-qPCR for the canonical astrocyte markers *GFAP* and *VIM*, and immunofluorescence staining of GFAP and S100β, we proceeded to characterize our system further using RNA-seq and calcium imaging analysis. Not only did these astrocytes have a distinct transcriptomic profile compared to their parent NPCs and corresponding neurons, but they also secreted robust amounts of APOE protein and responded to inflammatory stimuli by secreting the cytokines MCP-1, IL-6 and IL-8. Additionally, as astrocytes are implicated in the uptake and degradation of Aβ, we used a flow cytometry-based assay to monitor the clearance of Aβ from the extracellular space. Finally, we confirmed the cryopreservation-potential of mature astrocytes by evaluating and comparing their functionality with that of astrocytes prior to cryopreservation.

5.1.2   Specific Aim 2: Develop and characterize a system to evaluate the cell-type specific contribution of both neurons and astrocytes to AD phenotype in *APOE2* and *APOE3* isogenic neural cultures derived from fAD and non-demented control patient iPSCs.

We explored the second specific aim in chapter 3 of this manuscript, where we developed a system to ascertain the role of *APOE-2* and *-3* isogenic neurons and astrocytes in

manifesting the AD phenotype. By measuring the level of Aβ42 secretion by neurons (source) and the level of Aβ42-FAM uptake by astrocytes (sink), we concluded that the elevated Aβ42 levels observed in our *APOE3* cultures was regulated by the preferential amyloidogenic processing of APP in these neurons, as opposed to the enhanced clearance of Aβ by *APOE2* astrocytes. This conclusion is corroborated by the observation that the amyloidogenic pathway intermediates sAPPβ and APP-βCTF were elevated in the APP^{dp} and PSEN1^{A246E} *APOE3* neurons, despite there being no significant difference in the level of APP protein between the isogenic pairs. This trend was absent in our third fAD mutant pair APP^{V717I} suggesting that the non-amyloidogenic protein processing prompted by APOE2 in the two other fAD lines was insufficient to overcome the enhanced BACE1 cleavage characteristic of this mutant.

5.1.3 Specific Aim 3: Elucidate differences in APP processing between *APOE2* and *APOE3* isogenic neural cultures by investigating pathway intermediates that may confer a protective effect to APOE2.

Our third specific aim to further explore the differences in APP processing between the *APOE* isogenic pairs is addressed in chapter 4 of this manuscript. As there was no significant difference in total APP levels between the fAD isogenic pairs, we hypothesized that ADAM10 (the primary α-secretase) and BACE1(the primary neuronal β-secretase) compete for APP as a substrate in an APOE dependent manner. Specifically, that in *APOE2* neurons, APP is processed preferentially by ADAM10 and therefore the levels of APP available for endosomal BACE1 processing are lower than in *APOE3* neurons. However, we only observed this inverse relationship between the secretases in the APP^{dp} isogenic neurons. Although ADAM10 expression was not elevated in the PSEN1^{A246E} APOE*2* neurons, the level of BACE1 protein was significantly lower, supporting the notion of a partial inverse coupling previously reported by others (Colombo et al., 2013) . These differences in APP processing are likely mediated by the enhanced phosphorylation of APP at the Thr668 residue in APP^{dp} APOE*3* neurons. Transcriptome analysis revealed that various key kinases involved in the phosphorylation of APP, Tau and BACE1, including *CDK5*, its regulator *CDK5R1* and *GSK3β* are differentially expressed

between the isogenic *APOE* neurons. The levels of active GSK3β protein were significantly higher in both APP fAD mutant *APOE3* neurons, but lower in the PSEN1 mutant. Therefore, further analysis of these kinases and their activity in these isogenic neurons are sure to yield insights into differential APP endocytosis, trafficking and processing.

5.2 Future Work

In this study we used patient iPSC derived neurons isogenic for *APOE* to explore the role of the rare, understudied and neuroprotective APOE2 in the manifestation of AD phenotype *in vitro*. Remarkably, the presence of the *APOE2* allele markedly reduced neuronal Aβ secretion and the level of intracellular APP-βCTF, even in the context of fully penetrant monogenic mutations in APP and PSEN1. A similar study in sAD cell lines, with well characterized AD pathology, and an isogenic conversion of the native *APOE-3* or *-4* allele to the *APOE2* variant is required to bolster the conclusions of this study. Although this study examined the role of astrocyte in the uptake of Aβ from the extracellular space, further study of the secreted Aβ degrading enzymes and co-culture with a physiological ratio of neurons will be beneficial to evaluate their contribution in the context of APOE2.

Others have reported that APP-βCTF accumulation leads to, and is a better predictor of, endosomal dysfunction - including upregulation of endocytic genes, endosome enlargement and increased endosomal count (Nixon, 2017). Interestingly, *APOE4* carriers present enlarged early endosomes compared to the *E2* and *E3* carriers in the preclinical stages of sAD (Cataldo et al., 2000). Experiments to measure alterations in the endosomal, lysosomal and autophagy machinery of *APOE* isogenic neurons will allow for the elucidation of the role of *APOE2* in APP trafficking and processing. He et al. have previously reported that exogenously added APOE4 protein increases APP-βCTF by triggering the endocytosis of APP, BACE1 and the APOE receptor ApoER2 in neuroblastoma cells (He et al., 2007). The generation of *APOE* knockout neurons in NDC and fAD backgrounds will allow us to measure the APOE2 isoform and dose-dependent effect on endocytosis, intracellular trafficking and processing of APP.

REFERENCES

2019 Alzheimer's disease facts and figures, 2019. . Alzheimer's & Dementia 15, 321–387. https://doi.org/10.1016/j.jalz.2019.01.010

Abraham, E., Ahmadian, B.B., Holderness, K., Levinson, Y., McAfee, E., 2017. Platforms for Manufacturing Allogeneic, Autologous and iPSC Cell Therapy Products: An Industry Perspective. Advances in biochemical engineering/biotechnology 165, 323–350. https://doi.org/10.1007/10_2017_14

Abud, E.M., Ramirez, R.N., Martinez, E.S., Healy, L.M., Nguyen, C.H.H., Newman, S.A., Yeromin, V.A., Scarfone, V.M., Marsh, S.E., Fimbres, C., Caraway, C.A., Fote, G.M., Madany, A.M., Agrawal, A., Kayed, R., Gylys, K.H., Cahalan, M.D., Cummings, B.J., Antel, J.P., Mortazavi, A., Carson, M.J., Poon, W.W., Blurton-Jones, M., 2017. iPSC-Derived Human Microglia-like Cells to Study Neurological Diseases. Neuron 94, 278-293.e9. https://doi.org/10.1016/j.neuron.2017.03.042

Aijaz, A., Li, M., Smith, D., Khong, D., LeBlon, C., Fenton, O.S., Olabisi, R.M., Libutti, S., Tischfield, J., Maus, M. V, Deans, R., Barcia, R.N., Anderson, D.G., Ritz, J., Preti, R., Parekkadan, B., 2018. Biomanufacturing for clinically advanced cell therapies. Nature biomedical engineering 2, 362–376. https://doi.org/10.1038/s41551-018-0246-6

Ando, K., Iijima, K.I., Elliott, J.I., Kirino, Y., Suzuki, T., 2001. Phosphorylation-dependent regulation of the interaction of amyloid precursor protein with Fe65 affects the production of beta-amyloid. J Biol Chem 276, 40353–40361. https://doi.org/10.1074/jbc.M104059200

Arber, C., Toombs, J., Lovejoy, C., Ryan, N.S., Paterson, R.W., Willumsen, N., Gkanatsiou, E., Portelius, E., Blennow, K., Heslegrave, A., Schott, J.M., Hardy, J., Lashley, T., Fox, N.C., Zetterberg, H., Wray, S., 2019. Familial Alzheimer's disease patient-derived neurons reveal distinct mutation-specific effects on amyloid beta. Molecular psychiatry. https://doi.org/10.1038/s41380-019-0410-8

Armijo, E., Gonzalez, C., Shahnawaz, M., Flores, A., Davis, B., Soto, C., 2017. Increased susceptibility to Aβ toxicity in neuronal cultures derived from familial Alzheimer's disease (PSEN1-A246E) induced pluripotent stem cells. Neuroscience letters 639, 74–81. https://doi.org/10.1016/j.neulet.2016.12.060

Aschenbrenner, A.J., Gordon, B.A., Benzinger, T.L.S., Morris, J.C., Hassenstab, J.J., 2018. Influence of tau PET, amyloid PET, and hippocampal volume on cognition in Alzheimer disease. Neurology 91, e859–e866. https://doi.org/10.1212/WNL.0000000000006075

Astashkina, A., Mann, B., Grainger, D.W., 2012. A critical evaluation of in vitro cell culture models for high-throughput drug screening and toxicity. Pharmacology & therapeutics 134, 82–106. https://doi.org/10.1016/j.pharmthera.2012.01.001

Badenes, S.M., Fernandes-Platzgummer, A., Rodrigues, C.A.V., Diogo, M.M., da Silva, C.L., Cabral, J.M.S., 2016. Microcarrier Culture Systems for Stem Cell Manufacturing. Stem Cell Manufacturing 77–104. https://doi.org/10.1016/B978-0-444-63265-4.00004-2

Bales, K.R., Liu, F., Wu, S., Lin, S., Koger, D., DeLong, C., Hansen, J.C., Sullivan, P.M., Paul, S.M., 2009. Human APOE isoform-dependent effects on brain beta-amyloid levels in PDAPP transgenic mice. The Journal of neuroscience : the official journal of the Society for Neuroscience 29, 6771–9. https://doi.org/10.1523/JNEUROSCI.0887-09.2009

Bardy, C., Van Den Hurk, M., Eames, T., Marchand, C., Hernandez, V.R., Kellogg, M., Gorris, M., Galet, B., Palomares, V., Brown, J., Bang, A.G., Mertens, J., Böhnke, L., Boyer, L., Simon, S., Gage, F.H., 2015. Neuronal medium that supports basic synaptic functions and activity of human neurons in vitro. Proceedings of the National Academy of Sciences of the United States of America 112, E2725–E2734. https://doi.org/10.1073/pnas.1504393112

Basak, J.M., Verghese, P.B., Yoon, H., Kim, J., Holtzman, D.M., 2012. Low-density lipoprotein receptor represents an apolipoprotein E-independent pathway of Aβ uptake and degradation by astrocytes. J Biol Chem 287, 13959–13971. https://doi.org/10.1074/jbc.M111.288746

Begum, A.N., Guoynes, C., Cho, J., Hao, J., Lutfy, K., Hong, Y., 2015. Rapid generation of sub-type, region-specific neurons and neural networks from human pluripotent stem cell-derived neurospheres. Stem cell research 15, 731–741. https://doi.org/10.1016/j.scr.2015.10.014

Bekris, L.M., Yu, C.-E., Bird, T.D., Tsuang, D.W., 2010. Review Article: Genetics of Alzheimer Disease. Journal of Geriatric Psychiatry and Neurology 23, 213–227. https://doi.org/10.1177/0891988710383571

Bell, R.D., Sagare, A.P., Friedman, A.E., Bedi, G.S., Holtzman, D.M., Deane, R., Zlokovic, V.B., 2007. Transport pathways for clearance of human Alzheimer's amyloid beta-peptide and apolipoproteins E and J in the mouse central nervous system. Journal of cerebral blood flow and metabolism : official journal of the International Society of Cerebral Blood Flow and Metabolism 27, 909–18. https://doi.org/10.1038/sj.jcbfm.9600419

Belloy, M.E., Napolioni, V., Greicius, M.D., 2019. A Quarter Century of APOE and Alzheimer's Disease: Progress to Date and the Path Forward. Neuron 101, 820–838. https://doi.org/10.1016/j.neuron.2019.01.056

Berlau, D.J., Corrada, M.M., Head, E., Kawas, C.H., 2009. APOE epsilon2 is associated with intact cognition but increased Alzheimer pathology in the oldest old. Neurology 72, 829–834. https://doi.org/10.1212/01.wnl.0000343853.00346.a4

Bertram, L., Tanzi, R.E., 2009. Genome-wide association studies in Alzheimer's disease. Hum. Mol. Genet. 18, R137-145. https://doi.org/10.1093/hmg/ddp406

Bertram, L., Tanzi, R.E., 2005. The genetic epidemiology of neurodegenerative disease. The Journal of clinical investigation 115, 1449–57. https://doi.org/10.1172/JCI24761

Bettens, K., Sleegers, K., Van Broeckhoven, C., 2010. Current status on Alzheimer disease molecular genetics: from past, to present, to future. Human Molecular Genetics 19, R4–R11. https://doi.org/10.1093/hmg/ddq142

Boyles, J.K., Pitas, R.E., Wilson, E., Mahley, R.W., Taylor, J.M., 1985. Apolipoprotein E associated with astrocytic glia of the central nervous system and with nonmyelinating glia of the peripheral nervous system. Journal of Clinical Investigation 76, 1501–1513. https://doi.org/10.1172/JCI112130

Brecht, W.J., Harris, F.M., Chang, S., Tesseur, I., Yu, G.-Q., Xu, Q., Dee Fish, J., Wyss-Coray, T., Buttini, M., Mucke, L., Mahley, R.W., Huang, Y., 2004. Neuron-specific apolipoprotein e4 proteolysis is associated with increased tau phosphorylation in brains of transgenic

mice. The Journal of neuroscience : the official journal of the Society for Neuroscience 24, 2527–34. https://doi.org/10.1523/JNEUROSCI.4315-03.2004

Brookhouser, N., Raman, S., Potts, C., Brafman, D.A., 2017a. May I Cut in? Gene Editing Approaches in Human Induced Pluripotent Stem Cells. Cells 6. https://doi.org/10.3390/cells6010005

Brookhouser, N., Tekel, S.J., Standage-Beier, K., Nguyen, T., Schwarz, G., Wang, X., Brafman, D.A., 2020. BIG-TREE: Base-Edited Isogenic hPSC Line Generation Using a Transient Reporter for Editing Enrichment. Stem Cell Reports 14, 184–191. https://doi.org/10.1016/j.stemcr.2019.12.013

Brookhouser, N., Zhang, P., Caselli, R., Kim, J.J., Brafman, D.A., 2018. Generation and characterization of two human induced pluripotent stem cell (hiPSC) lines homozygous for the Apolipoprotein e4 (APOE4) risk variant-Alzheimer's disease (ASUi005-A) and healthy non-demented control (ASUi006-A). Stem cell research 32, 145–149. https://doi.org/10.1016/j.scr.2018.09.007

Brookhouser, N., Zhang, P., Caselli, R., Kim, J.J., Brafman, D.A., 2017b. Generation and characterization of human induced pluripotent stem cell (hiPSC) lines from an Alzheimer's disease (ASUi003-A) and non-demented control (ASUi004-A) patient homozygous for the Apolipoprotein e4 (APOE4) risk variant. Stem cell research 25, 266–269. https://doi.org/10.1016/j.scr.2017.07.003

Brookhouser, N., Zhang, P., Caselli, R., Kim, J.J., Brafman, D.A., 2017c. Generation and characterization of human induced pluripotent stem cell (hiPSC) lines from an Alzheimer's disease (ASUi001-A) and non-demented control (ASUi002-A) patient homozygous for the Apolipoprotein e4 (APOE4) risk variant. Stem cell research 24, 160–163. https://doi.org/10.1016/j.scr.2017.06.003

Buttini, M., Yu, G.Q., Shockley, K., Huang, Y., Jones, B., Masliah, E., Mallory, M., Yeo, T., Longo, F.M., Mucke, L., 2002. Modulation of Alzheimer-like synaptic and cholinergic deficits in transgenic mice by human apolipoprotein E depends on isoform, aging, and overexpression of amyloid β peptides but not on plaque formation. Journal of Neuroscience 22, 10539–10548. https://doi.org/10.1523/jneurosci.22-24-10539.2002

Cai, X.D., Golde, T.E., Younkin, S.G., 1993. Release of excess amyloid beta protein from a mutant amyloid beta protein precursor. Science (New York, N.Y.) 259, 514–6. https://doi.org/10.1126/science.8424174

Campion, D., Pottier, C., Nicolas, G., Le Guennec, K., Rovelet-Lecrux, A., 2016. Alzheimer disease: modeling an Aβ-centered biological network. Mol Psychiatry 21, 861–871. https://doi.org/10.1038/mp.2016.38

Canning, D.R., McKeon, R.J., DeWitt, D.A., Perry, G., Wujek, J.R., Frederickson, R.C., Silver, J., 1993. beta-Amyloid of Alzheimer's disease induces reactive gliosis that inhibits axonal outgrowth. Experimental neurology 124, 289–98. https://doi.org/10.1006/exnr.1993.1199

Cataldo, A.M., Peterhoff, C.M., Troncoso, J.C., Gomez-Isla, T., Hyman, B.T., Nixon, R.A., 2000. Endocytic pathway abnormalities precede amyloid beta deposition in sporadic Alzheimer's disease and Down syndrome: differential effects of APOE genotype and presenilin mutations. Am J Pathol 157, 277–286. https://doi.org/10.1016/s0002-9440(10)64538-5

Chartier-Harlin, M.C., Crawford, F., Houlden, H., Warren, A., Hughes, D., Fidani, L., Goate, A., Rossor, M., Roques, P., Hardy, J., 1991. Early-onset Alzheimer's disease caused by mutations at codon 717 of the beta-amyloid precursor protein gene. Nature 353, 844–6. https://doi.org/10.1038/353844a0

Chen, H., Qian, K., Chen, W., Hu, B., Blackbourn, L.W., Du, Z., Ma, L., Liu, H., Knobel, K.M., Ayala, M., Zhang, S.-C., 2015. Human-derived neural progenitors functionally replace astrocytes in adult mice. The Journal of clinical investigation 125, 1033–42. https://doi.org/10.1172/JCI69097

Chen, Y., Durakoglugil, M.S., Xian, X., Herz, J., 2010. ApoE4 reduces glutamate receptor function and synaptic plasticity by selectively impairing ApoE receptor recycling. Proceedings of the National Academy of Sciences of the United States of America 107, 12011–6. https://doi.org/10.1073/pnas.0914984107

Chiang, G.C., Insel, P.S., Tosun, D., Schuff, N., Truran-Sacrey, D., Raptentsetsang, S.T., Jack, C.R., Aisen, P.S., Petersen, R.C., Weiner, M.W., Alzheimer's Disease Neuroimaging Initiative, 2010. Hippocampal atrophy rates and CSF biomarkers in elderly APOE2 normal subjects. Neurology 75, 1976–1981. https://doi.org/10.1212/WNL.0b013e3181ffe4d1

Cho, S., Muthukumar, A.K., Stork, T., Coutinho-Budd, J.C., Freeman, M.R., 2018. Focal adhesion molecules regulate astrocyte morphology and glutamate transporters to suppress seizure-like behavior. Proceedings of the National Academy of Sciences of the United States of America 115, 11316–11321. https://doi.org/10.1073/pnas.1800830115

Choi, S.S., Lee, H.J., Lim, I., Satoh, J., Kim, S.U., 2014. Human astrocytes: secretome profiles of cytokines and chemokines. PloS one 9, e92325. https://doi.org/10.1371/journal.pone.0092325

Chow, Vivian W, Mattson, M.P., Wong, P.C., Gleichmann, M., 2010. An overview of APP processing enzymes and products. Neuromolecular medicine 12, 1–12. https://doi.org/10.1007/s12017-009-8104-z

Chung, W.-S., Verghese, P.B., Chakraborty, C., Joung, J., Hyman, B.T., Ulrich, J.D., Holtzman, D.M., Barres, B.A., 2016. Novel allele-dependent role for APOE in controlling the rate of synapse pruning by astrocytes. Proceedings of the National Academy of Sciences of the United States of America 113, 10186–91. https://doi.org/10.1073/pnas.1609896113

Citron, M., Oltersdorf, T., Haass, C., McConlogue, L., Hung, A.Y., Seubert, P., Vigo-Pelfrey, C., Lieberburg, I., Selkoe, D.J., 1992. Mutation of the beta-amyloid precursor protein in familial Alzheimer's disease increases beta-protein production. Nature 360, 672–4. https://doi.org/10.1038/360672a0

Clarke, L.E., Liddelow, S.A., Chakraborty, C., Münch, A.E., Heiman, M., Barres, B.A., 2018. Normal aging induces A1-like astrocyte reactivity. Proc Natl Acad Sci U S A 115, E1896–E1905. https://doi.org/10.1073/pnas.1800165115

Colombo, A., Wang, H., Kuhn, P.-H., Page, R., Kremmer, E., Dempsey, P.J., Crawford, H.C., Lichtenthaler, S.F., 2013. Constitutive α- and β-secretase cleavages of the amyloid precursor protein are partially coupled in neurons, but not in frequently used cell lines. Neurobiol Dis 49, 137–147. https://doi.org/10.1016/j.nbd.2012.08.011

Colombo, E., Farina, C., 2016. Astrocytes: Key Regulators of Neuroinflammation. Trends in immunology 37, 608–620. https://doi.org/10.1016/j.it.2016.06.006

Cong, L., Ran, F.A., Cox, D., Lin, S., Barretto, R., Habib, N., Hsu, P.D., Wu, X., Jiang, W., Marraffini, L.A., Zhang, F., 2013. Multiplex genome engineering using CRISPR/Cas systems. Science 339, 819–823. https://doi.org/10.1126/science.1231143

Cooper, J.M., Lathuiliere, A., Migliorini, M., Arai, A.L., Wani, M.M., Dujardin, S., Muratoglu, S.C., Hyman, B.T., Strickland, D.K., 2020. LRP1 and SORL1 regulate tau internalization and degradation and enhance tau seeding. bioRxiv 2020.11.17.386581. https://doi.org/10.1101/2020.11.17.386581

Corder, E.H., Saunders, A.M., Risch, N.J., Strittmatter, W.J., Schmechel, D.E., Gaskell, P.C., Rimmler, J.B., Locke, P.A., Conneally, P.M., Schmader, K.E., 1994. Protective effect of apolipoprotein E type 2 allele for late onset Alzheimer disease. Nature Genetics 7, 180–184. https://doi.org/10.1038/ng0694-180

Corder, E.H., Saunders, A.M., Strittmatter, W.J., Schmechel, D.E., Gaskell, P.C., Small, G.W., Roses, A.D., Haines, J.L., Pericak-Vance, M.A., 1993. Gene dose of apolipoprotein E type 4 allele and the risk of Alzheimer's disease in late onset families. Science (New York, N.Y.) 261, 921–923. https://doi.org/10.1126/science.8346443

Corona, A.W., Kodoma, N., Casali, B.T., Landreth, G.E., 2016. ABCA1 is Necessary for Bexarotene-Mediated Clearance of Soluble Amyloid Beta from the Hippocampus of APP/PS1 Mice. Journal of neuroimmune pharmacology : the official journal of the Society on NeuroImmune Pharmacology 11, 61–72. https://doi.org/10.1007/s11481-015-9627-8

Crowley, L.C., Marfell, B.J., Scott, A.P., Waterhouse, N.J., 2016. Quantitation of Apoptosis and Necrosis by Annexin V Binding, Propidium Iodide Uptake, and Flow Cytometry. Cold Spring Harbor Protocols 2016, pdb.prot087288. https://doi.org/10.1101/pdb.prot087288

Cutts, J., Brookhouser, N., Brafman, D.A., 2016. Generation of Regionally Specific Neural Progenitor Cells (NPCs) and Neurons from Human Pluripotent Stem Cells (hPSCs). Methods Mol. Biol. 1516, 121–144. https://doi.org/10.1007/7651_2016_357

De Pittà, M., Brunel, N., Volterra, A., 2016. Astrocytes: Orchestrating synaptic plasticity? Neuroscience. https://doi.org/10.1016/j.neuroscience.2015.04.001

De Sousa, P.A., Downie, J.M., Tye, B.J., Bruce, K., Dand, P., Dhanjal, S., Serhal, P., Harper, J., Turner, M., Bateman, M., 2016. Development and production of good manufacturing practice grade human embryonic stem cell lines as source material for clinical application. Stem cell research 17, 379–390. https://doi.org/10.1016/j.scr.2016.08.011

De Strooper, B., Saftig, P., Craessaerts, K., Vanderstichele, H., Guhde, G., Annaert, W., Von Figura, K., Van Leuven, F., 1998. Deficiency of presenilin-1 inhibits the normal cleavage of amyloid precursor protein. Nature 391, 387–390. https://doi.org/10.1038/34910

Deane, R., Sagare, A., Hamm, K., Parisi, M., Lane, S., Finn, M.B., Holtzman, D.M., Zlokovic, B.V., 2008. apoE isoform–specific disruption of amyloid β peptide clearance from mouse brain. J Clin Invest 118, 4002–4013. https://doi.org/10.1172/JCI36663

DeMattos, R.B., Brendza, R.P., Heuser, J.E., Kierson, M., Cirrito, J.R., Fryer, J., Sullivan, P.M., Fagan, A.M., Han, X., Holtzman, D.M., 2001. Purification and characterization of astrocyte-secreted apolipoprotein E and J-containing lipoproteins from wild-type and

human apoE transgenic mice. Neurochemistry International 39, 415–425. https://doi.org/10.1016/S0197-0186(01)00049-3

DeMattos, R.B., Cirrito, J.R., Parsadanian, M., May, P.C., O'Dell, M.A., Taylor, J.W., Harmony, J.A.K., Aronow, B.J., Bales, K.R., Paul, S.M., Holtzman, D.M., 2004. ApoE and Clusterin Cooperatively Suppress Aβ Levels and Deposition: Evidence that ApoE Regulates Extracellular Aβ Metabolism In Vivo. Neuron 41, 193–202. https://doi.org/10.1016/S0896-6273(03)00850-X

Deng, Y., Zhang, X., Zhao, Y., Liang, S., Xu, A., Gao, X., Deng, F., Fang, J., Wei, S., 2014. Peptide-decorated polyvinyl alcohol/hyaluronan nanofibers for human induced pluripotent stem cell culture. Carbohydrate polymers 101, 36–9. https://doi.org/10.1016/j.carbpol.2013.09.030

Di Lullo, E., Kriegstein, A.R., 2017. The use of brain organoids to investigate neural development and disease. Nature reviews. Neuroscience 18, 573–584. https://doi.org/10.1038/nrn.2017.107

Dickerson, B.C., Bakkour, A., Salat, D.H., Feczko, E., Pacheco, J., Greve, D.N., Grodstein, F., Wright, C.I., Blacker, D., Rosas, H.D., Sperling, R.A., Atri, A., Growdon, J.H., Hyman, B.T., Morris, J.C., Fischl, B., Buckner, R.L., 2009. The Cortical Signature of Alzheimer's Disease: Regionally Specific Cortical Thinning Relates to Symptom Severity in Very Mild to Mild AD Dementia and is Detectable in Asymptomatic Amyloid-Positive Individuals. Cerebral Cortex 19, 497–510. https://doi.org/10.1093/cercor/bhn113

Dickerson, B.C., Stoub, T.R., Shah, R.C., Sperling, R.A., Killiany, R.J., Albert, M.S., Hyman, B.T., Blacker, D., Detoledo-Morrell, L., 2011. Alzheimer-signature MRI biomarker predicts AD dementia in cognitively normal adults. Neurology 76, 1395–1402. https://doi.org/10.1212/WNL.0b013e3182166e96

Dobin, A., Davis, C.A., Schlesinger, F., Drenkow, J., Zaleski, C., Jha, S., Batut, P., Chaisson, M., Gingeras, T.R., 2013. STAR: ultrafast universal RNA-seq aligner. Bioinformatics (Oxford, England) 29, 15–21. https://doi.org/10.1093/bioinformatics/bts635

Dodart, J.C., Bales, K.R., Johnstone, E.M., Little, S.P., Paul, S.M., 2002. Apolipoprotein E alters the processing of the β-amyloid precursor protein in APPV717F transgenic mice. Brain Research 955, 191–199. https://doi.org/10.1016/S0006-8993(02)03437-6

Dodart, J.-C., Marr, R.A., Koistinaho, M., Gregersen, B.M., Malkani, S., Verma, I.M., Paul, S.M., 2005. Gene delivery of human apolipoprotein E alters brain Abeta burden in a mouse model of Alzheimer's disease. Proceedings of the National Academy of Sciences of the United States of America 102, 1211–6. https://doi.org/10.1073/pnas.0409072102

Dolev, I., Michaelson, D.M., 2004. A nontransgenic mouse model shows inducible amyloid-β (Aβ) peptide deposition and elucidates the role of apolipoprotein E in the amyloid cascade. Proceedings of the National Academy of Sciences of the United States of America 101, 13909–13914. https://doi.org/10.1073/pnas.0404458101

Dominguez, D., Tournoy, J., Hartmann, D., Huth, T., Cryns, K., Deforce, S., Serneels, L., Camacho, I.E., Marjaux, E., Craessaerts, K., Roebroek, A.J.M., Schwake, M., D'Hooge, R., Bach, P., Kalinke, U., Moechars, D., Alzheimer, C., Reiss, K., Saftig, P., De Strooper, B., 2005. Phenotypic and biochemical analyses of BACE1- and BACE2-deficient mice. J Biol Chem 280, 30797–30806. https://doi.org/10.1074/jbc.M505249200

Dong, Y., Benveniste, E.N., 2001. Immune function of astrocytes. Glia 36, 180–90.

Dose, J., Huebbe, P., Nebel, A., Rimbach, G., 2016. APOE genotype and stress response - a mini review. Lipids in health and disease 15, 121. https://doi.org/10.1186/s12944-016-0288-2

Drenos, F., Kirkwood, T.B.L., 2010. Selection on alleles affecting human longevity and late-life disease: the example of apolipoprotein E. PLoS ONE 5, e10022. https://doi.org/10.1371/journal.pone.0010022

Drouet, B., Fifre, A., Pinçon-Raymond, M., Vandekerckhove, J., Rosseneu, M., Guéant, J.L., Chambaz, J., Pillot, T., 2001. ApoE protects cortical neurones against neurotoxicity induced by the non-fibrillar C-terminal domain of the amyloid-beta peptide. J. Neurochem. 76, 117–127. https://doi.org/10.1046/j.1471-4159.2001.00047.x

Drummond, E., Wisniewski, T., 2017. Alzheimer's disease: experimental models and reality. Acta Neuropathologica 133, 155–175. https://doi.org/10.1007/s00401-016-1662-x

D'Souza, G.X., Rose, S.E., Knupp, A., Nicholson, D.A., Keene, C.D., Young, J.E., 2020. The application of in vitro-derived human neurons in neurodegenerative disease modeling. Journal of neuroscience research. https://doi.org/10.1002/jnr.24615

Duan, L., Bhattacharyya, B.J., Belmadani, A., Pan, L., Miller, R.J., Kessler, J.A., 2014. Stem cell derived basal forebrain cholinergic neurons from Alzheimer's disease patients are more susceptible to cell death. Molecular neurodegeneration 9, 3. https://doi.org/10.1186/1750-1326-9-3

Duff, K., Suleman, F., 2004. Transgenic mouse models of Alzheimer's disease: how useful have they been for therapeutic development? Briefings in functional genomics & proteomics 3, 47–59. https://doi.org/10.1093/bfgp/3.1.47

Durakoglugil, M.S., Chen, Y., White, C.L., Kavalali, E.T., Herz, J., 2009. Reelin signaling antagonizes beta-amyloid at the synapse. Proceedings of the National Academy of Sciences of the United States of America 106, 15938–43. https://doi.org/10.1073/pnas.0908176106

Dzamba, D., Harantova, L., Butenko, O., Anderova, M., 2016. Glial Cells - The Key Elements of Alzheimers Disease. Current Alzheimer Research 13, 894–911. https://doi.org/10.2174/1567205013666160129095924

Esquerda-Canals, G., Montoliu-Gaya, L., Güell-Bosch, J., Villegas, S., 2017. Mouse Models of Alzheimer's Disease. Journal of Alzheimer's Disease 57, 1171–1183. https://doi.org/10.3233/JAD-170045

Evans, D.A., Funkenstein, H.H., Albert, M.S., Scherr, P.A., Cook, N.R., Chown, M.J., Hebert, L.E., Hennekens, C.H., Taylor, J.O., 1989. Prevalence of Alzheimer's Disease in a Community Population of Older Persons: Higher Than Previously Reported. JAMA: The Journal of the American Medical Association 262, 2551–2556. https://doi.org/10.1001/jama.1989.03430180093036

Fagan, A.M., Watson, M., Parsadanian, M., Bales, K.R., Paul, S.M., Holtzman, D.M., 2002. Human and murine ApoE markedly alters A beta metabolism before and after plaque formation in a mouse model of Alzheimer's disease. Neurobiology of disease 9, 305–18. https://doi.org/10.1006/nbdi.2002.0483

Fan, J., Zareyan, S., Zhao, W., Shimizu, Y., Pfeifer, T.A., Tak, J.-H., Isman, M.B., Van den Hoven, B., Duggan, M.E., Wood, M.W., Wellington, C.L., Kulic, I., 2016. Identification of a Chrysanthemic Ester as an Apolipoprotein E Inducer in Astrocytes. PloS one 11, e0162384. https://doi.org/10.1371/journal.pone.0162384

Fang, X., Yu, S.X., Lu, Y., Bast, R.C., Woodgett, J.R., Mills, G.B., 2000. Phosphorylation and inactivation of glycogen synthase kinase 3 by protein kinase A. Proc Natl Acad Sci U S A 97, 11960–11965. https://doi.org/10.1073/pnas.220413597

Farfel, J.M., Yu, L., De Jager, P.L., Schneider, J.A., Bennett, D.A., 2016. Association of APOE with tau-tangle pathology with and without β-amyloid. Neurobiol. Aging 37, 19–25. https://doi.org/10.1016/j.neurobiolaging.2015.09.011

Farrell, M.E., Kennedy, K.M., Rodrigue, K.M., Wig, G., Bischof, G.N., Rieck, J.R., Chen, X., Festini, S.B., Devous, M.D., Park, D.C., 2017. Association of Longitudinal Cognitive Decline With Amyloid Burden in Middle-aged and Older Adults: Evidence for a Dose-Response Relationship. JAMA neurology 74, 830–838. https://doi.org/10.1001/jamaneurol.2017.0892

Farrer, L.A., Cupples, L.A., Haines, J.L., Hyman, B., Kukull, W.A., Mayeux, R., Myers, R.H., Pericak-Vance, M.A., Risch, N., Van Duijn, C.M., 1997. Effects of age, sex, and ethnicity on the association between apolipoprotein E genotype and Alzheimer disease: A meta-analysis. Journal of the American Medical Association 278, 1349–1356. https://doi.org/10.1001/jama.278.16.1349

Farris, W., Mansourian, S., Chang, Y., Lindsley, L., Eckman, E.A., Frosch, M.P., Eckman, C.B., Tanzi, R.E., Selkoe, D.J., Guénette, S., 2003. Insulin-degrading enzyme regulates the levels of insulin, amyloid β-protein, and the β-amyloid precursor protein intracellular domain in vivo. Proceedings of the National Academy of Sciences of the United States of America 100, 4162–4167. https://doi.org/10.1073/pnas.0230450100

Farris, W., Schütz, S.G., Cirrito, J.R., Shankar, G.M., Sun, X., George, A., Leissring, M.A., Walsh, D.M., Qiu, W.Q., Holtzman, D.M., Selkoe, D.J., 2007. Loss of neprilysin function promotes amyloid plaque formation and causes cerebral amyloid angiopathy. The American journal of pathology 171, 241–51. https://doi.org/10.2353/ajpath.2007.070105

Finan, G.M., Realubit, R., Chung, S., Lütjohann, D., Wang, N., Cirrito, J.R., Karan, C., Kim, T.-W., 2016. Bioactive Compound Screen for Pharmacological Enhancers of Apolipoprotein E in Primary Human Astrocytes. Cell chemical biology 23, 1526–1538. https://doi.org/10.1016/j.chembiol.2016.10.015

Fitz, N.F., Cronican, A.A., Saleem, M., Fauq, A.H., Chapman, R., Lefterov, I., Koldamova, R., 2012. Abca1 deficiency affects Alzheimer's disease-like phenotype in human ApoE4 but not in ApoE3-targeted replacement mice. The Journal of neuroscience : the official journal of the Society for Neuroscience 32, 13125–36. https://doi.org/10.1523/JNEUROSCI.1937-12.2012

Fong, L.K., Yang, M.M., Dos Santos Chaves, R., Reyna, S.M., Langness, V.F., Woodruff, G., Roberts, E.A., Young, J.E., Goldstein, L.S.B., 2018. Full-length amyloid precursor protein regulates lipoprotein metabolism and amyloid-β clearance in human astrocytes. The Journal of Biological Chemistry 293, 11341–11357. https://doi.org/10.1074/jbc.RA117.000441

Fu, Y., Zhao, J., Atagi, Y., Nielsen, H.M., Liu, C.-C., Zheng, H., Shinohara, M., Kanekiyo, T., Bu, G., 2016. Apolipoprotein E lipoprotein particles inhibit amyloid-β uptake through cell surface heparan sulphate proteoglycan. Molecular Neurodegeneration 11, 37. https://doi.org/10.1186/s13024-016-0099-y

Fusaki, N., Ban, H., Nishiyama, A., Saeki, K., Hasegawa, M., 2009. Efficient induction of transgene-free human pluripotent stem cells using a vector based on Sendai virus, an RNA virus that does not integrate into the host genome. Proceedings of the Japan Academy Series B: Physical and Biological Sciences 85, 348–362. https://doi.org/10.2183/pjab.85.348

Garcia-Marin, V., Ahmed, T.H., Afzal, Y.C., Hawken, M.J., 2013. Distribution of vesicular glutamate transporter 2 (VGluT2) in the primary visual cortex of the macaque and human. J Comp Neurol 521, 130–151. https://doi.org/10.1002/cne.23165

Gatta, L.B., Albertini, A., Ravid, R., Finazzi, D., 2002. Levels of beta-secretase BACE and alpha-secretase ADAM10 mRNAs in Alzheimer hippocampus. Neuroreport 13, 2031–2033. https://doi.org/10.1097/00001756-200211150-00008

Giau, V.V., Bagyinszky, E., Yang, Y.S., Youn, Y.C., An, S.S.A., Kim, S.Y., 2019. Genetic analyses of early-onset Alzheimer's disease using next generation sequencing. Scientific reports 9, 8368. https://doi.org/10.1038/s41598-019-44848-2

Glenner, G.G., Wong, C.W., 1984a. Alzheimer's disease: Initial report of the purification and characterization of a novel cerebrovascular amyloid protein. Biochemical and Biophysical Research Communications 120, 885–890. https://doi.org/10.1016/S0006-291X(84)80190-4

Glenner, G.G., Wong, C.W., 1984b. Alzheimer's disease and Down's syndrome: Sharing of a unique cerebrovascular amyloid fibril protein. Biochemical and Biophysical Research Communications 122, 1131–1135. https://doi.org/10.1016/0006-291X(84)91209-9

Goate, A., Chartier-Harlin, M.C., Mullan, M., Brown, J., Crawford, F., Fidani, L., Giuffra, L., Haynes, A., Irving, N., James, L., Mant, R., Newton, P., Rooke, K., Roques, P., Talbot, C., Pericak-Vance, M., Roses, A., Williamson, R., Rossor, M., Owen, M., Hardy, J., 1991. Segregation of a missense mutation in the amyloid precursor protein gene with familial Alzheimer's disease. Nature 349, 704–706. https://doi.org/10.1038/349704a0

Goldgaber, D., Lerman, M.I., McBride, O.W., Saffiotti, U., Gajdusek, D.C., 1987. Characterization and chromosomal localization of a cDNA encoding brain amyloid of Alzheimer's disease. Science 235, 877–880. https://doi.org/10.1126/science.3810169

Goldman, J.S., Hahn, S.E., Catania, J.W., LaRusse-Eckert, S., Butson, M.B., Rumbaugh, M., Strecker, M.N., Roberts, J.S., Burke, W., Mayeux, R., Bird, T., Genetics, A.C. of M., Counselors, the N.S. of G., 2011. Genetic counseling and testing for Alzheimer disease: joint practice guidelines of the American College of Medical Genetics and the National Society of Genetic Counselors. Genetics in medicine : official journal of the American College of Medical Genetics 13, 597–605. https://doi.org/10.1097/GIM.0b013e31821d69b8

Goldstein, L.S.B., Reyna, S., Woodruff, G., 2015. Probing the secrets of Alzheimer's disease using human-induced pluripotent stem cell technology. Neurotherapeutics 12, 121–125. https://doi.org/10.1007/s13311-014-0326-6

Gomez-Nicola, D., Boche, D., 2015. Post-mortem analysis of neuroinflammatory changes in human Alzheimer's disease. Alzheimer's research & therapy 7, 42. https://doi.org/10.1186/s13195-015-0126-1

Gong, J.-S., Kobayashi, M., Hayashi, H., Zou, K., Sawamura, N., Fujita, S.C., Yanagisawa, K., Michikawa, M., 2002. Apolipoprotein E (ApoE) isoform-dependent lipid release from astrocytes prepared from human ApoE3 and ApoE4 knock-in mice. The Journal of biological chemistry 277, 29919–26. https://doi.org/10.1074/jbc.M203934200

Gonzalez, D.M., Gregory, J., Brennand, K.J., 2017. The Importance of Non-neuronal Cell Types in hiPSC-Based Disease Modeling and Drug Screening. Frontiers in cell and developmental biology 5, 117. https://doi.org/10.3389/fcell.2017.00117

Grehan, S., Tse, E., Taylor, J.M., 2001. Two distal downstream enhancers direct expression of the human apolipoprotein E gene to astrocytes in the brain. Journal of Neuroscience 21, 812–822. https://doi.org/10.1523/jneurosci.21-03-00812.2001

Guerriero, F., Sgarlata, C., Francis, M., Maurizi, N., Faragli, A., Perna, S., Rondanelli, M., Rollone, M., Ricevuti, G., 2017. Neuroinflammation, immune system and Alzheimer disease: searching for the missing link. Aging clinical and experimental research 29, 821–831. https://doi.org/10.1007/s40520-016-0637-z

Guo, L., LaDu, M.J., Van Eldik, L.J., 2004. A dual role for apolipoprotein e in neuroinflammation: anti- and pro-inflammatory activity. Journal of molecular neuroscience : MN 23, 205–12. https://doi.org/10.1385/JMN:23:3:205

Guo, T., Noble, W., Hanger, D.P., 2017. Roles of tau protein in health and disease. Acta neuropathologica 133, 665–704. https://doi.org/10.1007/s00401-017-1707-9

Haass, C., Kaether, C., Thinakaran, G., Sisodia, S., 2012. Trafficking and proteolytic processing of APP. Cold Spring Harb Perspect Med 2, a006270. https://doi.org/10.1101/cshperspect.a006270

Haidet-Phillips, Amanda M, Roybon, L., Gross, S.K., Tuteja, A., Donnelly, C.J., Richard, J.-P., Ko, M., Sherman, A., Eggan, K., Henderson, C.E., Maragakis, N.J., 2014. Gene profiling of human induced pluripotent stem cell-derived astrocyte progenitors following spinal cord engraftment. Stem cells translational medicine 3, 575–85. https://doi.org/10.5966/sctm.2013-0153

Hamby, M.E., Coppola, G., Ao, Y., Geschwind, D.H., Khakh, B.S., Sofroniew, M. V, 2012. Inflammatory mediators alter the astrocyte transcriptome and calcium signaling elicited by multiple G-protein-coupled receptors. The Journal of neuroscience : the official journal of the Society for Neuroscience 32, 14489–510. https://doi.org/10.1523/JNEUROSCI.1256-12.2012

Hardy, J., Duff, K., Hardy, K.G., Perez-Tur, J., Hutton, M., 1998. Genetic dissection of Alzheimer's disease and related dementias: amyloid and its relationship to tau. Nature neuroscience 1, 355–8. https://doi.org/10.1038/1565

Hardy, J., Selkoe, D.J., 2002. The amyloid hypothesis of Alzheimer's disease: Progress and problems on the road to therapeutics. Science 297, 353–356. https://doi.org/10.1126/science.1072994

Harris, F.M., Brecht, W.J., Xu, Q., Tesseur, I., Kekonius, L., Wyss-Coray, T., Fish, J.D., Masliah, E., Hopkins, P.C., Scearce-Levie, K., Weisgraber, K.H., Mucke, L., Mahley, R.W., Huang, Y., 2003. Carboxyl-terminal-truncated apolipoprotein E4 causes Alzheimer's disease-like neurodegeneration and behavioral deficits in transgenic mice. Proceedings of the National Academy of Sciences of the United States of America 100, 10966–71. https://doi.org/10.1073/pnas.1434398100

Harris, F.M., Tesseur, I., Brecht, W.J., Xu, Q., Mullendorff, K., Chang, S., Wyss-Coray, T., Mahley, R.W., Huang, Y., 2004. Astroglial regulation of apolipoprotein E expression in neuronal cells. Implications for Alzheimer's disease. The Journal of biological chemistry 279, 3862–8. https://doi.org/10.1074/jbc.M309475200

Hashimoto, T., Serrano-Pozo, A., Hori, Y., Adams, K.W., Takeda, S., Banerji, A.O., Mitani, A., Joyner, D., Thyssen, D.H., Bacskai, B.J., Frosch, M.P., Spires-Jones, T.L., Finn, M.B., Holtzman, D.M., Hyman, B.T., 2012. Apolipoprotein E, especially apolipoprotein E4, increases the oligomerization of amyloid β peptide. J. Neurosci. 32, 15181–15192. https://doi.org/10.1523/JNEUROSCI.1542-12.2012

Hass, S., Fresser, F., Köchl, S., Beyreuther, K., Utermann, G., Baier, G., 1998. Physical interaction of ApoE with amyloid precursor protein independent of the amyloid Abeta region in vitro. J. Biol. Chem. 273, 13892–13897.

Hatters, D.M., Zhong, N., Rutenber, E., Weisgraber, K.H., 2006. Amino-terminal domain stability mediates apolipoprotein E aggregation into neurotoxic fibrils. Journal of molecular biology 361, 932–44. https://doi.org/10.1016/j.jmb.2006.06.080

Hauser, P.S., Ryan, R.O., 2013. Impact of apolipoprotein E on Alzheimer's disease. Current Alzheimer research 10, 809–17.

He, X., Cooley, K., Chung, C.H.Y., Dashti, N., Tang, J., 2007. Apolipoprotein receptor 2 and X11 alpha/beta mediate apolipoprotein E-induced endocytosis of amyloid-beta precursor protein and beta-secretase, leading to amyloid-beta production. The Journal of neuroscience : the official journal of the Society for Neuroscience 27, 4052–60. https://doi.org/10.1523/JNEUROSCI.3993-06.2007

Hemming, M.L., Patterson, M., Reske-Nielsen, C., Lin, L., Isacson, O., Selkoe, D.J., 2007. Reducing amyloid plaque burden via ex vivo gene delivery of an Abeta-degrading protease: a novel therapeutic approach to Alzheimer disease. PLoS medicine 4, e262. https://doi.org/10.1371/journal.pmed.0040262

Heurtaux, T., Michelucci, A., Losciuto, S., Gallotti, C., Felten, P., Dorban, G., Grandbarbe, L., Morga, E., Heuschling, P., 2010. Microglial activation depends on beta-amyloid conformation: role of the formylpeptide receptor 2. Journal of neurochemistry 114, 576–86. https://doi.org/10.1111/j.1471-4159.2010.06783.x

Hillen, A.E.J., Burbach, J.P.H., Hol, E.M., 2018. Cell adhesion and matricellular support by astrocytes of the tripartite synapse. Progress in neurobiology 165–167, 66–86. https://doi.org/10.1016/j.pneurobio.2018.02.002

Hirbec, H., Déglon, N., Foo, L.C., Goshen, I., Grutzendler, J., Hangen, E., Kreisel, T., Linck, N., Muffat, J., Regio, S., Rion, S., Escartin, C., 2020. Emerging technologies to study glial cells. GLIA. https://doi.org/10.1002/glia.23780

Hirsch-Reinshagen, V., Zhou, S., Burgess, B.L., Bernier, L., McIsaac, S.A., Chan, J.Y., Tansley, G.H., Cohn, J.S., Hayden, M.R., Wellington, C.L., 2004. Deficiency of ABCA1 impairs apolipoprotein E metabolism in brain. The Journal of biological chemistry 279, 41197–207. https://doi.org/10.1074/jbc.M407962200

Hjelm, B.E., Rosenberg, J.B., Szelinger, S., Sue, L.I., Beach, T.G., Huentelman, M.J., Craig, D.W., 2011. Induction of pluripotent stem cells from autopsy donor-derived somatic cells. Neurosci Lett 502, 219–224. https://doi.org/10.1016/j.neulet.2011.07.048

Holmberg, K.H., Patterson, P.H., 2006. Leukemia inhibitory factor is a key regulator of astrocytic, microglial and neuronal responses in a low-dose pilocarpine injury model. Brain Res 1075, 26–35. https://doi.org/10.1016/j.brainres.2005.12.103

Holsinger, R.M.D., McLean, C.A., Beyreuther, K., Masters, C.L., Evin, G., 2002. Increased expression of the amyloid precursor beta-secretase in Alzheimer's disease. Ann Neurol 51, 783–786. https://doi.org/10.1002/ana.10208

Holtzman, D.M., Bales, K.R., Tenkova, T., Fagan, A.M., Parsadanian, M., Sartorius, L.J., Mackey, B., Olney, J., McKeel, D., Wozniak, D., Paul, S.M., 2000. Apolipoprotein E isoform-dependent amyloid deposition and neuritic degeneration in a mouse model of Alzheimer's disease. Proceedings of the National Academy of Sciences 97, 2892–2897. https://doi.org/10.1073/pnas.050004797

Holtzman, D.M., Herz, J., Bu, G., 2012. Apolipoprotein E and apolipoprotein E receptors: normal biology and roles in Alzheimer disease. Cold Spring Harb Perspect Med 2, a006312. https://doi.org/10.1101/cshperspect.a006312

Huang, D.W., Sherman, B.T., Lempicki, R.A., 2009. Systematic and integrative analysis of large gene lists using DAVID bioinformatics resources. Nature protocols 4, 44–57. https://doi.org/10.1038/nprot.2008.211

Huang, Y., Liu, X.Q., Wyss-Coray, T., Brecht, W.J., Sanan, D.A., Mahley, R.W., 2001. Apolipoprotein E fragments present in Alzheimer's disease brains induce neurofibrillary tangle-like intracellular inclusions in neurons. Proceedings of the National Academy of Sciences of the United States of America 98, 8838–8843. https://doi.org/10.1073/pnas.151254698

Huang, Y.-W.A., Zhou, B., Nabet, A.M., Wernig, M., Südhof, T.C., 2019. Differential Signaling Mediated by ApoE2, ApoE3, and ApoE4 in Human Neurons Parallels Alzheimer's Disease Risk. The Journal of Neuroscience 39, 7408–7427. https://doi.org/10.1523/jneurosci.2994-18.2019

Huang, Y.-W.A., Zhou, B., Wernig, M., Südhof, T.C., 2017. ApoE2, ApoE3, and ApoE4 Differentially Stimulate APP Transcription and Aβ Secretion. Cell 168, 427-441.e21. https://doi.org/10.1016/j.cell.2016.12.044

Huch, M., Koo, B.-K., 2015. Modeling mouse and human development using organoid cultures. Development (Cambridge, England) 142, 3113–25. https://doi.org/10.1242/dev.118570

Hughes, C.S., Postovit, L.M., Lajoie, G.A., 2010. Matrigel: a complex protein mixture required for optimal growth of cell culture. Proteomics 10, 1886–90. https://doi.org/10.1002/pmic.200900758

Hung, C.O.Y., Livesey, F.J., 2018. Altered γ-Secretase Processing of APP Disrupts Lysosome and Autophagosome Function in Monogenic Alzheimer's Disease. Cell Rep 25, 3647-3660.e2. https://doi.org/10.1016/j.celrep.2018.11.095

Hunsberger, J., Lundberg, M.S., Allickson, J., Simon, C.G., Zylberberg, C., Beachy, S.H., 2019. Examining Resources, Initiatives, and Regulatory Pathways to Advance Regenerative Medicine Manufacturing. Current Stem Cell Reports 5, 162–172. https://doi.org/10.1007/s40778-019-00163-0

Hunsberger, J.G., Shupe, T., Atala, A., 2018. An Industry-Driven Roadmap for Manufacturing in Regenerative Medicine. Stem cells translational medicine 7, 564–568. https://doi.org/10.1002/sctm.18-0060

Ikegaya, Y., Le Bon-Jego, M., Yuste, R., 2005. Large-scale imaging of cortical network activity with calcium indicators. Neurosci. Res. 52, 132–138. https://doi.org/10.1016/j.neures.2005.02.004

Israel, M.A., Yuan, S.H., Bardy, C., Reyna, S.M., Mu, Y., Herrera, C., Hefferan, M.P., Van Gorp, S., Nazor, K.L., Boscolo, F.S., Carson, C.T., Laurent, L.C., Marsala, M., Gage, F.H., Remes, A.M., Koo, E.H., Goldstein, L.S.B., 2012. Probing sporadic and familial Alzheimer's disease using induced pluripotent stem cells. Nature 482, 216–220. https://doi.org/10.1038/nature10821

Itagaki, S., McGeer, P.L., Akiyama, H., Zhu, S., Selkoe, D., 1989. Relationship of microglia and astrocytes to amyloid deposits of Alzheimer disease. Journal of Neuroimmunology 24, 173–182. https://doi.org/10.1016/0165-5728(89)90115-X

Ito, K., Sanosaka, T., Igarashi, K., Ideta-Otsuka, M., Aizawa, A., Uosaki, Y., Noguchi, A., Arakawa, H., Nakashima, K., Takizawa, T., 2016. Identification of genes associated with the astrocyte-specific gene Gfap during astrocyte differentiation. Sci Rep 6, 23903. https://doi.org/10.1038/srep23903

Iwata, N., Mizukami, H., Shirotani, K., Takaki, Y., Muramatsu, S., Lu, B., Gerard, N.P., Gerard, C., Ozawa, K., Saido, T.C., 2004. Presynaptic localization of neprilysin contributes to efficient clearance of amyloid-beta peptide in mouse brain. The Journal of neuroscience : the official journal of the Society for Neuroscience 24, 991–8. https://doi.org/10.1523/JNEUROSCI.4792-03.2004

Iwata, N., Tsubuki, S., Takaki, Y., Shirotani, K., Lu, B., Gerard, N.P., Gerard, C., Hama, E., Lee, H.J., Saido, T.C., 2001. Metabolic regulation of brain Aβ by neprilysin. Science 292, 1550–1552. https://doi.org/10.1126/science.1059946

Iwata, N., Tsubuki, S., Takaki, Y., Watanabe, K., Sekiguchi, M., Hosoki, E., Kawashima-Morishima, M., Lee, H.J., Hama, E., Sekine-Aizawa, Y., Saido, T.C., 2000. Identification of the major Abeta1-42-degrading catabolic pathway in brain parenchyma: suppression leads to biochemical and pathological deposition. Nature medicine 6, 143–50. https://doi.org/10.1038/72237

Izrael, M., Slutsky, S.G., Admoni, T., Cohen, L., Granit, A., Hasson, A., Itskovitz-Eldor, J., Krush Paker, L., Kuperstein, G., Lavon, N., Yehezkel Ionescu, S., Solmesky, L.J., Zaguri, R., Zhuravlev, A., Volman, E., Chebath, J., Revel, M., 2018. Safety and efficacy of human embryonic stem cell-derived astrocytes following intrathecal transplantation in SOD1G93A and NSG animal models. Stem cell research & therapy 9, 152. https://doi.org/10.1186/s13287-018-0890-5

Jansen, I.E., Savage, J.E., Watanabe, K., Bryois, J., Williams, D.M., Steinberg, S., Sealock, J., Karlsson, I.K., Hägg, S., Athanasiu, L., Voyle, N., Proitsi, P., Witoelar, A., Stringer, S., Aarsland, D., Almdahl, I.S., Andersen, F., Bergh, S., Bettella, F., Bjornsson, S., Brækhus, A., Bråthen, G., de Leeuw, C., Desikan, R.S., Djurovic, S., Dumitrescu, L., Fladby, T., Hohman, T.J., Jonsson, V.P., Kiddle, S.J., Rongve, A., Saltvedt, I., Sando, S.B., Selbæk, G., Shoai, M., Skene, N.G., Snaedal, J., Stordal, E., Ulstein, I.D., Wang, Y., White, L.R., Hardy, J., Hjerling-Leffler, J., Sullivan, P.F., van der Flier, W.M., Dobson, R., Davis, L.K., Stefansson, H., Stefansson, K., Pedersen, N.L., Ripke, S., Andreassen, O.A., Posthuma, D., 2019. Genome-wide meta-analysis identifies new loci and functional pathways influencing Alzheimer's disease risk. Nature Genetics 51, 404–413. https://doi.org/10.1038/s41588-018-0311-9

Janssen, J.C., Beck, J.A., Campbell, T.A., Dickinson, A., Fox, N.C., Harvey, R.J., Houlden, H., Rossor, M.N., Collinge, J., 2003. Early onset familial Alzheimer's disease: Mutation frequency in 31 families. Neurology 60, 235–239. https://doi.org/10.1212/01.WNL.0000042088.22694.E3

Jiang, Q., Lee, C.Y.D., Mandrekar, S., Wilkinson, B., Cramer, P., Zelcer, N., Mann, K., Lamb, B., Willson, T.M., Collins, J.L., Richardson, J.C., Smith, J.D., Comery, T.A., Riddell, D., Holtzman, D.M., Tontonoz, P., Landreth, G.E., 2008. ApoE promotes the proteolytic degradation of Abeta. Neuron 58, 681–93. https://doi.org/10.1016/j.neuron.2008.04.010

Jiang, Y., Mullaney, K.A., Peterhoff, C.M., Che, S., Schmidt, S.D., Boyer-Boiteau, A., Ginsberg, S.D., Cataldo, A.M., Mathews, P.M., Nixon, R.A., 2010. Alzheimer's-related endosome dysfunction in Down syndrome is Abeta-independent but requires APP and is reversed by BACE-1 inhibition. Proc Natl Acad Sci U S A 107, 1630–1635. https://doi.org/10.1073/pnas.0908953107

Jin, S., Schatter, B., Weichel, O., Walev, I., Ryu, S., Klein, J., 2002. Stability of phospholipase D in primary astrocytes. Biochem Biophys Res Commun 297, 545–551. https://doi.org/10.1016/s0006-291x(02)02231-3

Johnson, G.V.W., Stoothoff, W.H., 2004. Tau phosphorylation in neuronal cell function and dysfunction. Journal of Cell Science 117, 5721–5729. https://doi.org/10.1242/jcs.01558

Junying, Y., Kejin, H., Kim, S.O., Shulan, T., Stewart, R., Slukvin, I.I., Thomson, J.A., 2009. Human induced pluripotent stem cells free of vector and transgene sequences. Science 324, 797–801. https://doi.org/10.1126/science.1172482

Kalsi, G., Whiting, P., Bourdelles, B.L., Callen, D., Barnard, E.A., Gurling, H., 1998. Localization of the human NMDAR2D receptor subunit gene (GRIN2D) to 19q13.1-qter, the NMDAR2A subunit gene to 16p13.2 (GRIN2A), and the NMDAR2C subunit gene (GRIN2C) to 17q24-q25 using somatic cell hybrid and radiation hybrid mapping panels. Genomics 47, 423–425. https://doi.org/10.1006/geno.1997.5132

Kanekiyo, T., Bu, G., 2014. The low-density lipoprotein receptor-related protein 1 and amyloid-β clearance in Alzheimer's disease. Front Aging Neurosci 6, 93. https://doi.org/10.3389/fnagi.2014.00093

Kanekiyo, T., Zhang, J., Liu, Q., Liu, C.-C., Zhang, L., Bu, G., 2011. Heparan sulphate proteoglycan and the low-density lipoprotein receptor-related protein 1 constitute major pathways for neuronal amyloid-beta uptake. J. Neurosci. 31, 1644–1651. https://doi.org/10.1523/JNEUROSCI.5491-10.2011

Kara, E., Marks, J.D., Fan, Z., Klickstein, J.A., Roe, A.D., Krogh, K.A., Wegmann, S., Maesako, M., Luo, C.C., Mylvaganam, R., Berezovska, O., Hudry, E., Hyman, B.T., 2017. Isoform- and cell type-specific structure of apolipoprotein E lipoparticles as revealed by a novel Forster resonance energy transfer assay. The Journal of biological chemistry 292, 14720–14729. https://doi.org/10.1074/jbc.M117.784264

Kelava, I., Lancaster, M.A., 2016. Dishing out mini-brains: Current progress and future prospects in brain organoid research. Developmental biology 420, 199–209. https://doi.org/10.1016/j.ydbio.2016.06.037

Khakh, B.S., Sofroniew, M. V, 2015. Diversity of astrocyte functions and phenotypes in neural circuits. Nature neuroscience 18, 942–52. https://doi.org/10.1038/nn.4043

Kim, D., Langmead, B., Salzberg, S.L., 2015. HISAT: a fast spliced aligner with low memory requirements. Nature Methods 12, 357–360. https://doi.org/10.1038/nmeth.3317

Kim, J., Castellano, J.M., Jiang, H., Basak, J.M., Parsadanian, M., Pham, V., Mason, S.M., Paul, S.M., Holtzman, D.M., 2009. Overexpression of low-density lipoprotein receptor in the brain markedly inhibits amyloid deposition and increases extracellular A beta clearance. Neuron 64, 632–644. https://doi.org/10.1016/j.neuron.2009.11.013

Kim, S., Sato, Y., Mohan, P.S., Peterhoff, C., Pensalfini, A., Rigoglioso, A., Jiang, Y., Nixon, R.A., 2016. Evidence that the rab5 effector APPL1 mediates APP-βCTF-induced dysfunction of endosomes in Down syndrome and Alzheimer's disease. Mol Psychiatry 21, 707–716. https://doi.org/10.1038/mp.2015.97

Kinney, M.A., Sargent, C.Y., McDevitt, T.C., 2011. The Multiparametric Effects of Hydrodynamic Environments on Stem Cell Culture. Tissue Engineering Part B: Reviews 17, 249–262. https://doi.org/10.1089/ten.teb.2011.0040

Knopman, D.S., Jones, D.T., Greicius, M.D., 2020. Failure to demonstrate efficacy of aducanumab: An analysis of the EMERGE and ENGAGE trials as reported by Biogen, December 2019. Alzheimer's & Dementia n/a. https://doi.org/10.1002/alz.12213

Knowles, R.B., Wyart, C., Buldyrev, V.S., Cruz, L., Urbanc, B., Hasselmo, M.E., Stanley, H.E., Hyman, B.T., 1999. Plaque-induced neurite abnormalities: Implications for disruption of neural networks in Alzheimer's disease. Proceedings of the National Academy of Sciences of the United States of America 96, 5274–5279. https://doi.org/10.1073/pnas.96.9.5274

Koch, P., Tamboli, I.Y., Mertens, J., Wunderlich, P., Ladewig, J., Stüber, K., Esselmann, H., Wiltfang, J., Brüstle, O., Walter, J., 2012. Presenilin-1 L166P mutant human pluripotent stem cell-derived neurons exhibit partial loss of γ-secretase activity in endogenous amyloid-β generation. The American journal of pathology 180, 2404–16. https://doi.org/10.1016/j.ajpath.2012.02.012

Kokaia, Z., Llorente, I.L., Carmichael, S.T., 2018. Customized Brain Cells for Stroke Patients Using Pluripotent Stem Cells. Stroke 49, 1091–1098. https://doi.org/10.1161/STROKEAHA.117.018291

Koldamova, R., Staufenbiel, M., Lefterov, I., 2005. Lack of ABCA1 considerably decreases brain ApoE level and increases amyloid deposition in APP23 mice. The Journal of biological chemistry 280, 43224–35. https://doi.org/10.1074/jbc.M504513200

Kondo, T., Asai, M., Tsukita, K., Kutoku, Y., Ohsawa, Y., Sunada, Y., Imamura, K., Egawa, N., Yahata, N., Okita, K., Takahashi, K., Asaka, I., Aoi, T., Watanabe, A., Watanabe, K., Kadoya, C., Nakano, R., Watanabe, D., Maruyama, K., Hori, O., Hibino, S., Choshi, T., Nakahata, T., Hioki, H., Kaneko, T., Naitoh, M., Yoshikawa, K., Yamawaki, S., Suzuki, S., Hata, R., Ueno, S.-I., Seki, T., Kobayashi, K., Toda, T., Murakami, K., Irie, K., Klein, W.L., Mori, H., Asada, T., Takahashi, R., Iwata, N., Yamanaka, S., Inoue, H., 2013. Modeling Alzheimer's disease with iPSCs reveals stress phenotypes associated with intracellular Aβ and differential drug responsiveness. Cell Stem Cell 12, 487–496. https://doi.org/10.1016/j.stem.2013.01.009

Konttinen, H., Cabral-da-Silva, M.E.C., Ohtonen, S., Wojciechowski, S., Shakirzyanova, A., Caligola, S., Giugno, R., Ishchenko, Y., Hernández, D., Fazaludeen, M.F., Eamen, S., Budia, M.G., Fagerlund, I., Scoyni, F., Korhonen, P., Huber, N., Haapasalo, A., Hewitt, A.W., Vickers, J., Smith, G.C., Oksanen, M., Graff, C., Kanninen, K.M., Lehtonen, S., Propson, N., Schwartz, M.P., Pébay, A., Koistinaho, J., Ooi, L., Malm, T., 2019. PSEN1ΔE9, APPswe, and APOE4 Confer Disparate Phenotypes in Human iPSC-Derived Microglia. Stem Cell Reports 13, 669–683. https://doi.org/10.1016/j.stemcr.2019.08.004

Koriath, C., Lashley, T., Taylor, W., Druyeh, R., Dimitriadis, A., Denning, N., Williams, J., Warren, J.D., Fox, N.C., Schott, J.M., Rowe, J.B., Collinge, J., Rohrer, J.D., Mead, S., 2019. ApoE4 lowers age at onset in patients with frontotemporal dementia and tauopathy independent of amyloid-β copathology. Alzheimers Dement (Amst) 11, 277–280. https://doi.org/10.1016/j.dadm.2019.01.010

Kowal, R.C., Herz, J., Weisgraber, K.H., Mahley, R.W., Brown, M.S., Goldstein, J.L., 1990. Opposing effects of apolipoproteins E and C on lipoprotein binding to low density lipoprotein receptor-related protein. Journal of Biological Chemistry 265, 10771–10779.

Krencik, R., Weick, J.P., Liu, Y., Zhang, Z.-J., Zhang, S.-C., 2011. Specification of transplantable astroglial subtypes from human pluripotent stem cells. Nature biotechnology 29, 528–34. https://doi.org/10.1038/nbt.1877

Krencik, R., Zhang, S.-C., 2011. Directed differentiation of functional astroglial subtypes from human pluripotent stem cells. Nature protocols 6, 1710–7. https://doi.org/10.1038/nprot.2011.405

Kuhn, P.-H., Wang, H., Dislich, B., Colombo, A., Zeitschel, U., Ellwart, J.W., Kremmer, E., Roßner, S., Lichtenthaler, S.F., 2010. ADAM10 is the physiologically relevant, constitutive α-secretase of the amyloid precursor protein in primary neurons. EMBO J 29, 3020–3032. https://doi.org/10.1038/emboj.2010.167

Kunkle, B.W., Grenier-Boley, B., Sims, R., Bis, J.C., Damotte, V., Naj, A.C., Boland, A., Vronskaya, M., van der Lee, S.J., Amlie-Wolf, A., Bellenguez, C., Frizatti, A., Chouraki, V., Martin, E.R., Sleegers, K., Badarinarayan, N., Jakobsdottir, J., Hamilton-Nelson, K.L., Moreno-Grau, S., Olaso, R., Raybould, R., Chen, Y., Kuzma, A.B., Hiltunen, M., Morgan, T., Ahmad, S., Vardarajan, B.N., Epelbaum, J., Hoffmann, P., Boada, M., Beecham, G.W., Garnier, J.G., Harold, D., Fitzpatrick, A.L., Valladares, O., Moutet, M.L., Gerrish, A., Smith, V.A., Qu, L., Bacq, D., Denning, N., Jian, X., Zhao, Y., Del Zompo, M., Fox, N.C., Choi, S.H., Mateo, I., Hughes, J.T., Adams, H.H., Malamon, J., Sanchez-Garcia, F., Patel, Y., Brody, J.A., Dombroski, B.A., Naranjo, M.C.D., Daniilidou, M., Eiriksdottir, G., Mukherjee, S., Wallon, D., Uphill, J., Aspelund, T., Cantwell, L.B., Garzia, F., Galimberti, D., Hofer, E., Butkiewicz, M., Fin, B., Scarpini, E., Sarnowski, C., Bush, W.S., Meslage, S., Kornhuber, J., White, C.C., Song, Y., Barber, R.C., Engelborghs, S., Sordon, S., Voijnovic, D., Adams, P.M., Vandenberghe, R., Mayhaus, M., Cupples, L.A., Albert, M.S.,

De Deyn, P.P., Gu, W., Himali, J.J., Beekly, D., Squassina, A., Hartmann, A.M., Orellana, A., Blacker, D., Rodriguez-Rodriguez, E., Lovestone, S., Garcia, M.E., Doody, R.S., Munoz-Fernadez, C., Sussams, R., Lin, H., Fairchild, T.J., Benito, Y.A., Holmes, C., Karamujić-Čomić, H., Frosch, M.P., Thonberg, H., Maier, W., Roschupkin, G., Ghetti, B., Giedraitis, V., Kawalia, A., Li, S., Huebinger, R.M., Kilander, L., Moebus, S., Hernández, I., Kamboh, M.I., Brundin, R.M., Turton, J., Yang, Q., Katz, M.J., Concari, L., Lord, J., Beiser, A.S., Keene, C.D., Helisalmi, S., Kloszewska, I., Kukull, W.A., Koivisto, A.M., Lynch, A., Tarraga, L., Larson, E.B., Haapasalo, A., Lawlor, B., Mosley, T.H., Lipton, R.B., Solfrizzi, V., Gill, M., Longstreth, W.T., Montine, T.J., Frisardi, V., Diez-Fairen, M., Rivadeneira, F., Petersen, R.C., Deramecourt, V., Alvarez, I., Salani, F., Ciaramella, A., Boerwinkle, E., Reiman, E.M., Fievet, N., Rotter, J.I., Reisch, J.S., Hanon, O., Cupidi, C., Andre Uitterlinden, A.G., Royall, D.R., Dufouil, C., Maletta, R.G., de Rojas, I., Sano, M., Brice, A., Cecchetti, R., George-Hyslop, P.S., Ritchie, K., Tsolaki, M., Tsuang, D.W., Dubois, B., Craig, D., Wu, C.K., Soininen, H., Avramidou, D., Albin, R.L., Fratiglioni, L., Germanou, A., Apostolova, L.G., Keller, L., Koutroumani, M., Arnold, S.E., Panza, F., Gkatzima, O., Asthana, S., Hannequin, D., Whitehead, P., Atwood, C.S., Caffarra, P., Hampel, H., Quintela, I., Carracedo, Á., Lannfelt, L., Rubinsztein, D.C., Barnes, L.L., Pasquier, F., Frölich, L., Barral, S., McGuinness, B., Beach, T.G., Johnston, J.A., Becker, J.T., Passmore, P., Bigio, E.H., Schott, J.M., Bird, T.D., Warren, J.D., Boeve, B.F., Lupton, M.K., Bowen, J.D., Proitsi, P., Boxer, A., Powell, J.F., Burke, J.R., Kauwe, J.S.K., Burns, J.M., Mancuso, M., Buxbaum, J.D., Bonuccelli, U., Cairns, N.J., McQuillin, A., Cao, C., Livingston, G., Carlson, C.S., Bass, N.J., Carlsson, C.M., Hardy, J., Carney, R.M., Bras, J., Carrasquillo, M.M., Guerreiro, R., Allen, M., Chui, H.C., Fisher, E., Masullo, C., Crocco, E.A., DeCarli, C., Bisceglio, G., Dick, M., Ma, L., Duara, R., Graff-Radford, N.R., Evans, D.A., Hodges, A., Faber, K.M., Scherer, M., Fallon, K.B., Riemenschneider, M., Fardo, D.W., Heun, R., Farlow, M.R., Kölsch, H., Ferris, S., Leber, M., Foroud, T.M., Heuser, I., Galasko, D.R., Giegling, I., Gearing, M., Hüll, M., Geschwind, D.H., Gilbert, J.R., Morris, J., Green, R.C., Mayo, K., Growdon, J.H., Feulner, T., Hamilton, R.L., Harrell, L.E., Drichel, D., Honig, L.S., Cushion, T.D., Huentelman, M.J., Hollingworth, P., Hulette, C.M., Hyman, B.T., Marshall, R., Jarvik, G.P., Meggy, A., Abner, E., Menzies, G.E., Jin, L.W., Leonenko, G., Real, L.M., Jun, G.R., Baldwin, C.T., Grozeva, D., Karydas, A., Russo, G., Kaye, J.A., Kim, R., Jessen, F., Kowall, N.W., Vellas, B., Kramer, J.H., Vardy, E., LaFerla, F.M., Jöckel, K.H., Lah, J.J., Dichgans, M., Leverenz, J.B., Mann, D., Levey, A.I., Pickering-Brown, S., Lieberman, A.P., Klopp, N., Lunetta, K.L., Wichmann, H.E., Lyketsos, C.G., Morgan, K., Marson, D.C., Brown, K., Martiniuk, F., Medway, C., Mash, D.C., Nöthen, M.M., Masliah, E., Hooper, N.M., McCormick, W.C., Daniele, A., McCurry, S.M., Bayer, A., McDavid, A.N., Gallacher, J., McKee, A.C., van den Bussche, H., Mesulam, M., Brayne, C., Miller, B.L., Riedel-Heller, S., Miller, C.A., Miller, J.W., Al-Chalabi, A., Morris, J.C., Shaw, C.E., Myers, A.J., Wiltfang, J., O'Bryant, S., Olichney, J.M., Alvarez, V., Parisi, J.E., Singleton, A.B., Paulson, H.L., Collinge, J., Perry, W.R., Mead, S., Peskind, E., Cribbs, D.H., Rossor, M., Pierce, A., Ryan, N.S., Poon, W.W., Nacmias, B., Potter, H., Sorbi, S., Quinn, J.F., Sacchinelli, E., Raj, A., Spalletta, G., Raskind, M., Caltagirone, C., Bossù, P., Orfei, M.D., Reisberg, B., Clarke, R., Reitz, C., Smith, A.D., Ringman, J.M., Warden, D., Roberson, E.D., Wilcock, G., Rogaeva, E., Bruni, A.C., Rosen, H.J., Gallo, M., Rosenberg, R.N., Ben-Shlomo, Y., Sager, M.A., Mecocci, P., Saykin, A.J., Pastor, P., Cuccaro, M.L., Vance, J.M., Schneider, J.A., Schneider, L.S., Slifer, S., Seeley, W.W., Smith, A.G., Sonnen, J.A., Spina, S., Stern, R.A., Swerdlow, R.H., Tang, M., Tanzi, R.E., Trojanowski, J.Q., Troncoso, J.C., Van Deerlin, V.M., Van Eldik, L.J., Vinters, V.H., Vonsattel, J.P., Weintraub, S., Welsh-Bohmer, K.A., Wilhelmsen, K.C., Williamson, J., Wingo, T.S., Woltjer, R.L., Wright, C.B., Yu, C.E., Yu, L., Saba, Y., Pilotto, A., Bullido, M.J., Peters, O., Crane, P.K., Bennett, D., Bosco, P., Coto, E., Boccardi, V., De Jager, P.L., Lleo, A., Warner, N., Lopez, O.L., Ingelsson, M., Deloukas, P., Cruchaga, C., Graff, C., Gwilliam, R., Fornage, M., Goate, A.M., Sanchez-Juan, P., Kehoe, P.G., Amin, N., Ertekin-Taner, N., Berr, C., Debette, S., Love, S., Launer, L.J., Younkin, S.G., Dartigues, J.F., Corcoran,

110

C., Ikram, M.A., Dickson, D.W., Nicolas, G., Campion, D., Tschanz, J.A., Schmidt, H., Hakonarson, H., Clarimon, J., Munger, R., Schmidt, R., Farrer, L.A., Van Broeckhoven, C., C. O'Donovan, M., DeStefano, A.L., Jones, L., Haines, J.L., Deleuze, J.F., Owen, M.J., Gudnason, V., Mayeux, R., Escott-Price, V., Psaty, B.M., Ramirez, A., Wang, L.S., Ruiz, A., van Duijn, C.M., Holmans, P.A., Seshadri, S., Williams, J., Amouyel, P., Schellenberg, G.D., Lambert, J.C., Pericak-Vance, M.A., 2019. Genetic meta-analysis of diagnosed Alzheimer's disease identifies new risk loci and implicates Aβ, tau, immunity and lipid processing. Nature Genetics 51, 414–430. https://doi.org/10.1038/s41588-019-0358-2

Kwak, S.S., Washicosky, K.J., Brand, E., von Maydell, D., Aronson, J., Kim, S., Capen, D.E., Cetinbas, M., Sadreyev, R., Ning, S., Bylykbashi, E., Xia, W., Wagner, S.L., Choi, S.H., Tanzi, R.E., Kim, D.Y., 2020. Amyloid-β42/40 ratio drives tau pathology in 3D human neural cell culture models of Alzheimer's disease. Nat Commun 11, 1377. https://doi.org/10.1038/s41467-020-15120-3

Kwart, D., Gregg, A., Scheckel, C., Murphy, E.A., Paquet, D., Duffield, M., Fak, J., Olsen, O., Darnell, R.B., Tessier-Lavigne, M., 2019. A Large Panel of Isogenic APP and PSEN1 Mutant Human iPSC Neurons Reveals Shared Endosomal Abnormalities Mediated by APP β-CTFs, Not Aβ. Neuron 104, 1022. https://doi.org/10.1016/j.neuron.2019.11.010

LaDu, M.J., Pederson, T.M., Frail, D.E., Reardon, C.A., Getz, G.S., Falduto, M.T., 1995. Purification of apolipoprotein E attenuates isoform-specific binding to beta-amyloid. The Journal of biological chemistry 270, 9039–42. https://doi.org/10.1074/jbc.270.16.9039

Laird, F.M., Cai, H., Savonenko, A.V., Farah, M.H., He, K., Melnikova, T., Wen, H., Chiang, H.-C., Xu, G., Koliatsos, V.E., Borchelt, D.R., Price, D.L., Lee, H.-K., Wong, P.C., 2005. BACE1, a major determinant of selective vulnerability of the brain to amyloid-beta amyloidogenesis, is essential for cognitive, emotional, and synaptic functions. J. Neurosci. 25, 11693–11709. https://doi.org/10.1523/JNEUROSCI.2766-05.2005

Lancaster, M.A., Renner, M., Martin, C.-A., Wenzel, D., Bicknell, L.S., Hurles, M.E., Homfray, T., Penninger, J.M., Jackson, A.P., Knoblich, J.A., 2013. Cerebral organoids model human brain development and microcephaly. Nature 501, 373–9. https://doi.org/10.1038/nature12517

Lane-Donovan, C., Herz, J., 2017. ApoE, ApoE Receptors, and the Synapse in Alzheimer's Disease. Trends in endocrinology and metabolism: TEM 28, 273–284. https://doi.org/10.1016/j.tem.2016.12.001

Lanz, T.A., Carter, D.B., Merchant, K.M., 2003. Dendritic spine loss in the hippocampus of young PDAPP and Tg2576 mice and its prevention by the ApoE2 genotype. Neurobiol. Dis. 13, 246–253. https://doi.org/10.1016/s0969-9961(03)00079-2

LeBlanc, A.C., Papadopoulos, M., Bélair, C., Chu, W., Crosato, M., Powell, J., Goodyer, C.G., 1997. Processing of amyloid precursor protein in human primary neuron and astrocyte cultures. J Neurochem 68, 1183–1190. https://doi.org/10.1046/j.1471-4159.1997.68031183.x

LeBlanc, A.C., Xue, R., Gambetti, P., 1996. Amyloid precursor protein metabolism in primary cell cultures of neurons, astrocytes, and microglia. J Neurochem 66, 2300–2310. https://doi.org/10.1046/j.1471-4159.1996.66062300.x

Lee, M.-S., Kao, S.-C., Lemere, C.A., Xia, W., Tseng, H.-C., Zhou, Y., Neve, R., Ahlijanian, M.K., Tsai, L.-H., 2003. APP processing is regulated by cytoplasmic phosphorylation. J Cell Biol 163, 83–95. https://doi.org/10.1083/jcb.200301115

Lee, Y., Aono, M., Laskowitz, D., Warner, D.S., Pearlstein, R.D., 2004. Apolipoprotein E protects against oxidative stress in mixed neuronal-glial cell cultures by reducing glutamate toxicity. Neurochemistry International 44, 107–118. https://doi.org/10.1016/S0197-0186(03)00112-8

Leissring, M.A., Farris, W., Chang, A.Y., Walsh, D.M., Wu, X., Sun, X., Frosch, M.P., Selkoe, D.J., 2003. Enhanced proteolysis of β-amyloid in APP transgenic mice prevents plaque formation, secondary pathology, and premature death. Neuron 40, 1087–1093. https://doi.org/10.1016/S0896-6273(03)00787-6

Levin, E.D., McGurk, S.R., Rose, J.E., Butcher, L.L., 1989. Reversal of a mecamylamine-induced cognitive deficit with the D2 agonist, LY 171555. Pharmacology, biochemistry, and behavior 33, 919–22. https://doi.org/10.1016/0091-3057(89)90494-2

Levy-Lahad, E., Wasco, W., Poorkaj, P., Romano, D.M., Oshima, J., Pettingell, W.H., Yu, C.E., Jondro, P.D., Schmidt, S.D., Wang, K., Crowley, A.C., Fu, Y.H., Guenette, S.Y., Galas, D., Nemens, E., Wijsman, E.M., Bird, T.D., Schellenberg, G.D., Tanzi, R.E., 1995. Candidate gene for the chromosome 1 familial Alzheimer's disease locus. Science 269, 973–977. https://doi.org/10.1126/science.7638622

Li, M.-Z., Zheng, L.-J., Shen, J., Li, X.-Y., Zhang, Q., Bai, X., Wang, Q.-S., Ji, J.-G., 2018. SIRT1 facilitates amyloid beta peptide degradation by upregulating lysosome number in primary astrocytes. Neural regeneration research 13, 2005–2013. https://doi.org/10.4103/1673-5374.239449

Li, S., Hong, S., Shepardson, N.E., Walsh, D.M., Shankar, G.M., Selkoe, D., 2009. Soluble oligomers of amyloid Beta protein facilitate hippocampal long-term depression by disrupting neuronal glutamate uptake. Neuron 62, 788–801. https://doi.org/10.1016/j.neuron.2009.05.012

Liao, Y., Smyth, G.K., Shi, W., 2014. featureCounts: an efficient general purpose program for assigning sequence reads to genomic features. Bioinformatics (Oxford, England) 30, 923–30. https://doi.org/10.1093/bioinformatics/btt656

Liddelow, S., Hoyer, D., 2016. Astrocytes: Adhesion Molecules and Immunomodulation. Current drug targets 17, 1871–1881.

Liddelow, S.A., Barres, B.A., 2017. Reactive Astrocytes: Production, Function, and Therapeutic Potential. Immunity 46, 957–967. https://doi.org/10.1016/j.immuni.2017.06.006

Lin, H., Li, Q., Lei, Y., 2017. An Integrated Miniature Bioprocessing for Personalized Human Induced Pluripotent Stem Cell Expansion and Differentiation into Neural Stem Cells. Scientific reports 7, 40191. https://doi.org/10.1038/srep40191

Lin, Y.-T., Seo, J., Gao, F., Feldman, H.M., Wen, H.-L., Penney, J., Cam, H.P., Gjoneska, E., Raja, W.K., Cheng, J., Rueda, R., Kritskiy, O., Abdurrob, F., Peng, Z., Milo, B., Yu, C.J., Elmsaouri, S., Dey, D., Ko, T., Yankner, B.A., Tsai, L.-H., 2018. APOE4 Causes Widespread Molecular and Cellular Alterations Associated with Alzheimer's Disease Phenotypes in Human iPSC-Derived Brain Cell Types. Neuron 98, 1141-1154.e7. https://doi.org/10.1016/j.neuron.2018.05.008

Liu, C.-C., Hu, J., Zhao, N., Wang, J., Wang, N., Cirrito, J.R., Kanekiyo, T., Holtzman, D.M., Bu, G., 2017a. Astrocytic LRP1 Mediates Brain Aβ Clearance and Impacts Amyloid Deposition. J Neurosci 37, 4023–4031. https://doi.org/10.1523/JNEUROSCI.3442-16.2017

Liu, C.-C., Zhao, N., Fu, Y., Wang, N., Linares, C., Tsai, C.-W., Bu, G., 2017b. ApoE4 Accelerates Early Seeding of Amyloid Pathology. Neuron 96, 1024-1032.e3. https://doi.org/10.1016/j.neuron.2017.11.013

Liu, Chia-Chen, Liu, Chia-Chan, Kanekiyo, T., Xu, H., Bu, G., 2013a. Apolipoprotein E and Alzheimer disease: risk, mechanisms and therapy. Nature Reviews. Neurology 9, 106–118. https://doi.org/10.1038/nrneurol.2012.263

Liu, Q., Waltz, S., Woodruff, G., Ouyang, J., Israel, M.A., Herrera, C., Sarsoza, F., Tanzi, R.E., Koo, E.H., Ringman, J.M., Goldstein, L.S.B., Wagner, S.L., Yuan, S.H., 2014. Effect of potent γ-secretase modulator in human neurons derived from multiple presenilin 1-induced pluripotent stem cell mutant carriers. JAMA neurology 71, 1481–9. https://doi.org/10.1001/jamaneurol.2014.2482

Liu, Y., Han, S.S.W., Wu, Y., Tuohy, T.M.F., Xue, H., Cai, J., Back, S.A., Sherman, L.S., Fischer, I., Rao, M.S., 2004. CD44 expression identifies astrocyte-restricted precursor cells. Developmental biology 276, 31–46. https://doi.org/10.1016/j.ydbio.2004.08.018

Love, M.I., Huber, W., Anders, S., 2014. Moderated estimation of fold change and dispersion for RNA-seq data with DESeq2. Genome Biol 15, 550. https://doi.org/10.1186/s13059-014-0550-8

Lucin, K.M., Wyss-Coray, T., 2009. Immune activation in brain aging and neurodegeneration: too much or too little? Neuron 64, 110–22. https://doi.org/10.1016/j.neuron.2009.08.039

Ludwin, S.K., Kosek, J.C., Eng, L.F., 1976. The topographical distribution of S-100 and GFA proteins in the adult rat brain: an immunohistochemical study using horseradish peroxidase-labelled antibodies. The Journal of comparative neurology 165, 197–207. https://doi.org/10.1002/cne.901650206

Lundin, A., Delsing, L., Clausen, M., Ricchiuto, P., Sanchez, J., Sabirsh, A., Ding, M., Synnergren, J., Zetterberg, H., Brolén, G., Hicks, R., Herland, A., Falk, A., 2018. Human iPS-Derived Astroglia from a Stable Neural Precursor State Show Improved Functionality Compared with Conventional Astrocytic Models. Stem Cell Reports 10, 1030–1045. https://doi.org/10.1016/j.stemcr.2018.01.021

Maartens, J.H., De-Juan-Pardo, E., Wunner, F.M., Simula, A., Voelcker, N.H., Barry, S.C., Hutmacher, D.W., 2017. Challenges and opportunities in the manufacture and expansion of cells for therapy. Expert opinion on biological therapy 17, 1221–1233. https://doi.org/10.1080/14712598.2017.1360273

Maezawa, I., Maeda, N., Montine, T.J., Montine, K.S., 2006. Apolipoprotein E-specific innate immune response in astrocytes from targeted replacement mice. Journal of neuroinflammation 3, 10. https://doi.org/10.1186/1742-2094-3-10

Mahley, R.W., 1988. Apolipoprotein E: cholesterol transport protein with expanding role in cell biology. Science 240, 622–630. https://doi.org/10.1126/science.3283935

Mahley, R.W., Huang, Y., 2012. Apolipoprotein e sets the stage: response to injury triggers neuropathology. Neuron 76, 871–85. https://doi.org/10.1016/j.neuron.2012.11.020

Mahley, R.W., Huang, Y., Rall, S.C., 1999. Pathogenesis of type III hyperlipoproteinemia (dysbetalipoproteinemia): Questions, quandaries, and paradoxes. Journal of Lipid Research 40, 1933–1949.

Mahley, R.W., Rall, S.C., 2000. Apolipoprotein E: far more than a lipid transport protein. Annual review of genomics and human genetics 1, 507–37. https://doi.org/10.1146/annurev.genom.1.1.507

Malik, N., Wang, X., Shah, S., Efthymiou, A.G., Yan, B., Heman-Ackah, S., Zhan, M., Rao, M., 2014. Comparison of the gene expression profiles of human fetal cortical astrocytes with pluripotent stem cell derived neural stem cells identifies human astrocyte markers and signaling pathways and transcription factors active in human astrocytes. PloS one 9, e96139. https://doi.org/10.1371/journal.pone.0096139

Martinez, M., Modric, S., 2010. Patient variation in veterinary medicine: part I. Influence of altered physiological states. Journal of veterinary pharmacology and therapeutics 33, 213–26. https://doi.org/10.1111/j.1365-2885.2009.01139.x

Matos, M., Augusto, E., Oliveira, C.R., Agostinho, P., 2008. Amyloid-beta peptide decreases glutamate uptake in cultured astrocytes: involvement of oxidative stress and mitogen-activated protein kinase cascades. Neuroscience 156, 898–910. https://doi.org/10.1016/j.neuroscience.2008.08.022

Mayeux, R., Stern, Y., 2012. Epidemiology of Alzheimer Disease. Cold Spring Harbor Perspectives in Medicine 2, a006239–a006239. https://doi.org/10.1101/cshperspect.a006239

McPhie, D.L., Lee, R.K.K., Eckman, C.B., Olstein, D.H., Durham, S.P., Yager, D., Younkin, S.G., Wurtman, R.J., Neve, R.L., 1997. Neuronal Expression of β-Amyloid Precursor Protein Alzheimer Mutations Causes Intracellular Accumulation of a C-terminal Fragment Containing Both the Amyloid β and Cytoplasmic Domains*. Journal of Biological Chemistry 272, 24743–24746. https://doi.org/10.1074/jbc.272.40.24743

Medeiros, R., Baglietto-Vargas, D., LaFerla, F.M., 2011. The role of tau in Alzheimer's disease and related disorders. CNS neuroscience & therapeutics 17, 514–24. https://doi.org/10.1111/j.1755-5949.2010.00177.x

Melkoumian, Z., Weber, J.L., Weber, D.M., Fadeev, A.G., Zhou, Y., Dolley-Sonneville, P., Yang, J., Qiu, L., Priest, C.A., Shogbon, C., Martin, A.W., Nelson, J., West, P., Beltzer, J.P., Pal, S., Brandenberger, R., 2010. Synthetic peptide-acrylate surfaces for long-term self-renewal and cardiomyocyte differentiation of human embryonic stem cells. Nature biotechnology 28, 606–10. https://doi.org/10.1038/nbt.1629

Meyer, K., Feldman, H.M., Lu, T., Drake, D., Lim, E.T., Ling, K.-H., Bishop, N.A., Pan, Y., Seo, J., Lin, Y.-T., Su, S.C., Church, G.M., Tsai, L.-H., Yankner, B.A., 2019. REST and Neural Gene Network Dysregulation in iPSC Models of Alzheimer's Disease. Cell reports 26, 1112-1127.e9. https://doi.org/10.1016/j.celrep.2019.01.023

Mi, H., Ebert, D., Muruganujan, A., Mills, C., Albou, L.-P., Mushayamaha, T., Thomas, P.D., 2021. PANTHER version 16: a revised family classification, tree-based classification tool,

enhancer regions and extensive API. Nucleic Acids Res 49, D394–D403. https://doi.org/10.1093/nar/gkaa1106

Michaelson, D.M., 2014. APOE ε4: the most prevalent yet understudied risk factor for Alzheimer's disease. Alzheimers Dement 10, 861–868. https://doi.org/10.1016/j.jalz.2014.06.015

Miller, B.C., Eckman, E.A., Sambamurti, K., Dobbs, N., Chow, K.M., Eckman, C.B., Hersh, L.B., Thiele, D.L., 2003. Amyloid-beta peptide levels in brain are inversely correlated with insulysin activity levels in vivo. Proceedings of the National Academy of Sciences of the United States of America 100, 6221–6. https://doi.org/10.1073/pnas.1031520100

Miyata, M., Smith, J.D., 1996. Apolipoprotein E allele-specific antioxidant activity and effects on cytotoxicity by oxidative insults and beta-amyloid peptides. Nature genetics 14, 55–61. https://doi.org/10.1038/ng0996-55

Moeton, M., Stassen, O.M.J.A., Sluijs, J.A., van der Meer, V.W.N., Kluivers, L.J., van Hoorn, H., Schmidt, T., Reits, E.A.J., van Strien, M.E., Hol, E.M., 2016. GFAP isoforms control intermediate filament network dynamics, cell morphology, and focal adhesions. Cellular and molecular life sciences : CMLS 73, 4101–20. https://doi.org/10.1007/s00018-016-2239-5

Molofsky, A. V, Krencik, R., Krenick, R., Ullian, E.M., Ullian, E., Tsai, H., Deneen, B., Richardson, W.D., Barres, B.A., Rowitch, D.H., 2012. Astrocytes and disease: a neurodevelopmental perspective. Genes & development 26, 891–907. https://doi.org/10.1101/gad.188326.112

Monyer, H., Sprengel, R., Schoepfer, R., Herb, A., Higuchi, M., Lomeli, H., Burnashev, N., Sakmann, B., Seeburg, P.H., 1992. Heteromeric NMDA receptors: molecular and functional distinction of subtypes. Science 256, 1217–1221. https://doi.org/10.1126/science.256.5060.1217

Moore, S., Evans, L.D.B., Andersson, T., Portelius, E., Smith, J., Dias, T.B., Saurat, N., McGlade, A., Kirwan, P., Blennow, K., Hardy, J., Zetterberg, H., Livesey, F.J., 2015. APP metabolism regulates tau proteostasis in human cerebral cortex neurons. Cell reports 11, 689–96. https://doi.org/10.1016/j.celrep.2015.03.068

Morris, C.M., Benjamin, R., Leake, A., McArthur, F.K., Candy, J.M., Ince, P.G., Torvik, A., Bjertness, E., Edwardson, J.A., 1995. Effect of apolipoprotein E genotype on Alzheimer's disease neuropathology in a cohort of elderly Norwegians. Neurosci. Lett. 201, 45–47. https://doi.org/10.1016/0304-3940(94)12126-b

Mullen, R.J., Buck, C.R., Smith, A.M., 1992. NeuN, a neuronal specific nuclear protein in vertebrates. Development 116, 201–211.

Muratore, C.R., Rice, H.C., Srikanth, P., Callahan, D.G., Shin, T., Benjamin, L.N.P., Walsh, D.M., Selkoe, D.J., Young-Pearse, T.L., 2014. The familial Alzheimer's disease APPV717I mutation alters APP processing and Tau expression in iPSC-derived neurons. Human Molecular Genetics 23, 3523–3536. https://doi.org/10.1093/hmg/ddu064

Muratore, C.R., Zhou, C., Liao, M., Fernandez, M.A., Taylor, W.M., Lagomarsino, V.N., Pearse, R.V., Rice, H.C., Negri, J.M., He, A., Srikanth, P., Callahan, D.G., Shin, T., Zhou, M., Bennett, D.A., Noggle, S., Love, J.C., Selkoe, D.J., Young-Pearse, T.L., 2017. Cell-type Dependent Alzheimer's Disease Phenotypes: Probing the Biology of Selective Neuronal Vulnerability. Stem Cell Reports 9, 1868–1884. https://doi.org/10.1016/j.stemcr.2017.10.015

Muresan, Z., Muresan, V., 2007. The Amyloid-β Precursor Protein Is Phosphorylated via Distinct Pathways during Differentiation, Mitosis, Stress, and Degeneration. Mol Biol Cell 18, 3835–3844. https://doi.org/10.1091/mbc.E06-07-0625

Mutations | ALZFORUM, 2019. URL https://www.alzforum.org/mutations (accessed 11.12.19).

Nagy, Z., Esiri, M.M., Jobst, K.A., Johnston, C., Litchfield, S., Sim, E., Smith, A.D., 1995. Influence of the apolipoprotein E genotype on amyloid deposition and neurofibrillary tangle formation in Alzheimer's disease. Neuroscience 69, 757–761. https://doi.org/10.1016/0306-4522(95)00331-c

Nehme, R., Zuccaro, E., Ghosh, S.D., Li, C., Sherwood, J.L., Pietilainen, O., Barrett, L.E., Limone, F., Worringer, K.A., Kommineni, S., Zang, Y., Cacchiarelli, D., Meissner, A., Adolfsson, R., Haggarty, S., Madison, J., Muller, M., Arlotta, P., Fu, Z., Feng, G., Eggan, K., 2018. Combining NGN2 Programming with Developmental Patterning Generates Human Excitatory Neurons with NMDAR-Mediated Synaptic Transmission. Cell reports 23, 2509–2523. https://doi.org/10.1016/j.celrep.2018.04.066

Nemes, C., Varga, E., Táncos, Z., Bock, I., Francz, B., Kobolák, J., Dinnyés, A., 2016. Establishment of PSEN1 mutant induced pluripotent stem cell (iPSC) line from an Alzheimer's disease (AD) female patient. Stem Cell Res 17, 69–71. https://doi.org/10.1016/j.scr.2016.05.019

Nguyen, K.C., Rosales, J.L., Barboza, M., Lee, K.-Y., 2002. Controversies over p25 in Alzheimer's disease. J Alzheimers Dis 4, 123–126. https://doi.org/10.3233/jad-2002-4207

Nishizawa, M., Chonabayashi, K., Nomura, M., Tanaka, A., Nakamura, M., Inagaki, A., Nishikawa, M., Takei, I., Oishi, A., Tanabe, K., Ohnuki, M., Yokota, H., Koyanagi-Aoi, M., Okita, K., Watanabe, A., Takaori-Kondo, A., Yamanaka, S., Yoshida, Y., 2016. Epigenetic Variation between Human Induced Pluripotent Stem Cell Lines Is an Indicator of Differentiation Capacity. Cell stem cell 19, 341–54. https://doi.org/10.1016/j.stem.2016.06.019

Nixon, R.A., 2017. Amyloid precursor protein and endosomal-lysosomal dysfunction in Alzheimer's disease: inseparable partners in a multifactorial disease. FASEB J 31, 2729–2743. https://doi.org/10.1096/fj.201700359

Oberheim, N.A., Takano, T., Han, X., He, W., Lin, J.H.C., Wang, F., Xu, Q., Wyatt, J.D., Pilcher, W., Ojemann, J.G., Ransom, B.R., Goldman, S.A., Nedergaard, M., 2009. Uniquely hominid features of adult human astrocytes. The Journal of neuroscience : the official journal of the Society for Neuroscience 29, 3276–87. https://doi.org/10.1523/JNEUROSCI.4707-08.2009

Oberheim, N.A., Wang, X., Goldman, S., Nedergaard, M., 2006. Astrocytic complexity distinguishes the human brain. Trends in neurosciences 29, 547–53. https://doi.org/10.1016/j.tins.2006.08.004

O'Brien, R.J., Wong, P.C., 2011. Amyloid precursor protein processing and Alzheimer's disease. Annual review of neuroscience 34, 185–204. https://doi.org/10.1146/annurev-neuro-061010-113613

Ochalek, A., Mihalik, B., Avci, H.X., Chandrasekaran, A., Téglási, A., Bock, I., Giudice, L.M., Táncos, Z., Molnár, K., László, L., Nielsen, J.E., Holst, B., Freude, K., Hyttel, P., Kobolák, J., Dinnyés, A., 2017. Neurons derived from sporadic Alzheimer's disease iPSCs reveal

elevated TAU hyperphosphorylation, increased amyloid levels, and GSK3B activation. Alzheimer's research & therapy 9, 90. https://doi.org/10.1186/s13195-017-0317-z

Okita, K., Matsumura, Y., Sato, Y., Okada, A., Morizane, A., Okamoto, S., Hong, H., Nakagawa, M., Tanabe, K., Tezuka, K., Shibata, T., Kunisada, T., Takahashi, M., Takahashi, J., Saji, H., Yamanaka, S., 2011. A more efficient method to generate integration-free human iPS cells. Nature methods 8, 409–12. https://doi.org/10.1038/nmeth.1591

Oksanen, M., Lehtonen, S., Jaronen, M., Goldsteins, G., Hämäläinen, R.H., Koistinaho, J., 2019. Astrocyte alterations in neurodegenerative pathologies and their modeling in human induced pluripotent stem cell platforms. Cellular and molecular life sciences : CMLS 76, 2739–2760. https://doi.org/10.1007/s00018-019-03111-7

Oksanen, M., Petersen, A.J., Naumenko, N., Puttonen, K., Lehtonen, Š., Gubert Olivé, M., Shakirzyanova, A., Leskelä, S., Sarajärvi, T., Viitanen, M., Rinne, J.O., Hiltunen, M., Haapasalo, A., Giniatullin, R., Tavi, P., Zhang, S.-C., Kanninen, K.M., Hämäläinen, R.H., Koistinaho, J., 2017. PSEN1 Mutant iPSC-Derived Model Reveals Severe Astrocyte Pathology in Alzheimer's Disease. Stem cell reports 9, 1885–1897. https://doi.org/10.1016/j.stemcr.2017.10.016

Olarte, L., Schupf, N., Lee, J.H., Tang, M.-X., Santana, V., Williamson, J., Maramreddy, P., Tycko, B., Mayeux, R., 2006. Apolipoprotein E epsilon4 and age at onset of sporadic and familial Alzheimer disease in Caribbean Hispanics. Arch Neurol 63, 1586–1590. https://doi.org/10.1001/archneur.63.11.1586

Olgiati, P., Politis, A., Malitas, P., Albani, D., Dusi, S., Polito, L., De Mauro, S., Zisaki, A., Piperi, C., Stamouli, E., Mailis, A., Batelli, S., Forloni, G., De Ronchi, D., Kalofoutis, A., Liappas, I., Serretti, A., 2010. APOE epsilon-4 allele and cytokine production in Alzheimer's disease. International journal of geriatric psychiatry 25, 338–44. https://doi.org/10.1002/gps.2344

Oliveira, J., Costa, M., de Almeida, M.S.C., da Cruz E Silva, O.A.B., Henriques, A.G., 2017. Protein Phosphorylation is a Key Mechanism in Alzheimer's Disease. J Alzheimers Dis 58, 953–978. https://doi.org/10.3233/JAD-170176

Ortiz-Virumbrales, M., Moreno, C.L., Kruglikov, I., Marazuela, P., Sproul, A., Jacob, S., Zimmer, M., Paull, D., Zhang, B., Schadt, E.E., Ehrlich, M.E., Tanzi, R.E., Arancio, O., Noggle, S., Gandy, S., 2017. CRISPR/Cas9-Correctable mutation-related molecular and physiological phenotypes in iPSC-derived Alzheimer's PSEN2 N141I neurons. Acta neuropathologica communications 5, 77. https://doi.org/10.1186/s40478-017-0475-z

Ortmann, D., Vallier, L., 2017. Variability of human pluripotent stem cell lines. Current opinion in genetics & development 46, 179–185. https://doi.org/10.1016/j.gde.2017.07.004

Ossenkoppele, R., Smith, R., Ohlsson, T., Strandberg, O., Mattsson, N., Insel, P.S., Palmqvist, S., Hansson, O., 2019. Associations between tau, Aβ, and cortical thickness with cognition in Alzheimer disease. Neurology 92, e601–e612. https://doi.org/10.1212/WNL.0000000000006875

Ovchinnikov, D.A., Korn, O., Virshup, I., Wells, C.A., Wolvetang, E.J., 2018. The Impact of APP on Alzheimer-like Pathogenesis and Gene Expression in Down Syndrome iPSC-Derived Neurons. Stem cell reports 11, 32–42. https://doi.org/10.1016/j.stemcr.2018.05.004

Palop, J.J., Mucke, L., 2010. Amyloid-beta-induced neuronal dysfunction in Alzheimer's disease: from synapses toward neural networks. Nature neuroscience 13, 812–8. https://doi.org/10.1038/nn.2583

Paquet, D., Kwart, D., Chen, A., Sproul, A., Jacob, S., Teo, S., Olsen, K.M., Gregg, A., Noggle, S., Tessier-Lavigne, M., 2016. Efficient introduction of specific homozygous and heterozygous mutations using CRISPR/Cas9. Nature 533, 125–129. https://doi.org/10.1038/nature17664

Park, I.-H., Arora, N., Huo, H., Maherali, N., Ahfeldt, T., Shimamura, A., Lensch, M.W., Cowan, C., Hochedlinger, K., Daley, G.Q., 2008. Disease-specific induced pluripotent stem cells. Cell 134, 877–886. https://doi.org/10.1016/j.cell.2008.07.041

Paşca, Anca M, Sloan, S.A., Clarke, L.E., Tian, Y., Makinson, C.D., Huber, N., Kim, C.H., Park, J.-Y., O'Rourke, N.A., Nguyen, K.D., Smith, S.J., Huguenard, J.R., Geschwind, D.H., Barres, B.A., Paşca, S.P., 2015. Functional cortical neurons and astrocytes from human pluripotent stem cells in 3D culture. Nature methods 12, 671–8. https://doi.org/10.1038/nmeth.3415

Pastor, P., Roe, C.M., Villegas, A., Bedoya, G., Chakraverty, S., García, G., Tirado, V., Norton, J., Ríos, S., Martínez, M., Kosik, K.S., Lopera, F., Goate, A.M., 2003. Apolipoprotein Eepsilon4 modifies Alzheimer's disease onset in an E280A PS1 kindred. Ann Neurol 54, 163–169. https://doi.org/10.1002/ana.10636

Patrick, G.N., Zukerberg, L., Nikolic, M., de la Monte, S., Dikkes, P., Tsai, L.-H., 1999. Conversion of p35 to p25 deregulates Cdk5 activity and promotes neurodegeneration. Nature 402, 615–622. https://doi.org/10.1038/45159

Pei, Y., Peng, J., Behl, M., Sipes, N.S., Shockley, K.R., Rao, M.S., Tice, R.R., Zeng, X., 2016. Comparative neurotoxicity screening in human iPSC-derived neural stem cells, neurons and astrocytes. Brain research 1638, 57–73. https://doi.org/10.1016/j.brainres.2015.07.048

Peitz, M., Bechler, T., Thiele, C.C., Veltel, M., Bloschies, M., Fliessbach, K., Ramirez, A., Brüstle, O., 2018. Blood-derived integration-free iPS cell line UKBi011-A from a diagnosed male Alzheimer's disease patient with APOE ε4/ε4 genotype. Stem cell research 29, 250–253. https://doi.org/10.1016/j.scr.2018.04.011

Pera, M., Alcolea, D., Sánchez-Valle, R., Guardia-Laguarta, C., Colom-Cadena, M., Badiola, N., Suárez-Calvet, M., Lladó, A., Barrera-Ocampo, A.A., Sepulveda-Falla, D., Blesa, R., Molinuevo, J.L., Clarimón, J., Ferrer, I., Gelpi, E., Lleó, A., 2013. Distinct patterns of APP processing in the CNS in autosomal-dominant and sporadic Alzheimer disease. Acta Neuropathol 125, 201–213. https://doi.org/10.1007/s00401-012-1062-9

Perriot, S., Mathias, A., Perriard, G., Canales, M., Jonkmans, N., Merienne, N., Meunier, C., El Kassar, L., Perrier, A.L., Laplaud, D.-A., Schluep, M., Déglon, N., Du Pasquier, R., 2018. Human Induced Pluripotent Stem Cell-Derived Astrocytes Are Differentially Activated by Multiple Sclerosis-Associated Cytokines. Stem cell reports 11, 1199–1210. https://doi.org/10.1016/j.stemcr.2018.09.015

Pitas, Robert E., Boyles, J.K., Lee, S.H., Foss, D., Mahley, R.W., 1987. Astrocytes synthesize apolipoprotein E and metabolize apolipoprotein E-containing lipoproteins. Biochimica et Biophysica Acta (BBA)/Lipids and Lipid Metabolism 917, 148–161. https://doi.org/10.1016/0005-2760(87)90295-5

Pitas, R. E., Boyles, J.K., Lee, S.H., Hui, D., Weisgraber, K.H., 1987. Lipoproteins and their receptors in the central nervous system. Characterization of the lipoproteins in cerebrospinal fluid and identification of apolipoprotein B,E(LDL) receptors in the brain. Journal of Biological Chemistry 262, 14352–14360.

Prasad, H., Rao, R., 2018. Amyloid clearance defect in ApoE4 astrocytes is reversed by epigenetic correction of endosomal pH. Proceedings of the National Academy of Sciences of the United States of America 115, E6640–E6649. https://doi.org/10.1073/pnas.1801612115

Preece, P., Virley, D.J., Costandi, M., Coombes, R., Moss, S.J., Mudge, A.W., Jazin, E., Cairns, N.J., 2003. Beta-secretase (BACE) and GSK-3 mRNA levels in Alzheimer's disease. Brain Res Mol Brain Res 116, 155–158. https://doi.org/10.1016/s0169-328x(03)00233-x

Qosa, H., Volpe, D.A., 2018. The development of biological therapies for neurological diseases: moving on from previous failures. Expert Opinion on Drug Discovery 13, 283–293. https://doi.org/10.1080/17460441.2018.1437142

Raber, J., Huang, Y., Ashford, J.W., 2004. ApoE genotype accounts for the vast majority of AD risk and AD pathology. Neurobiology of Aging 25, 641–650. https://doi.org/10.1016/j.neurobiolaging.2003.12.023

Raman, S., Brookhouser, N., Brafman, D.A., 2020. Using human induced pluripotent stem cells (hiPSCs) to investigate the mechanisms by which Apolipoprotein E (APOE) contributes to Alzheimer's disease (AD) risk. Neurobiol. Dis. 138, 104788. https://doi.org/10.1016/j.nbd.2020.104788

Rauch, J.N., Luna, G., Guzman, E., Audouard, M., Challis, C., Sibih, Y.E., Leshuk, C., Hernandez, I., Wegmann, S., Hyman, B.T., Gradinaru, V., Kampmann, M., Kosik, K.S., 2020. LRP1 is a master regulator of tau uptake and spread. Nature 580, 381–385. https://doi.org/10.1038/s41586-020-2156-5

Reiman, E.M., Arboleda-Velasquez, J.F., Quiroz, Y.T., Huentelman, M.J., Beach, T.G., Caselli, R.J., Chen, Y., Su, Y., Myers, A.J., Hardy, J., Paul Vonsattel, J., Younkin, S.G., Bennett, D.A., De Jager, P.L., Larson, E.B., Crane, P.K., Keene, C.D., Kamboh, M.I., Kofler, J.K., Duque, L., Gilbert, J.R., Gwirtsman, H.E., Buxbaum, J.D., Dickson, D.W., Frosch, M.P., Ghetti, B.F., Lunetta, K.L., Wang, L.-S., Hyman, B.T., Kukull, W.A., Foroud, T., Haines, J.L., Mayeux, R.P., Pericak-Vance, M.A., Schneider, J.A., Trojanowski, J.Q., Farrer, L.A., Schellenberg, G.D., Beecham, G.W., Montine, T.J., Jun, G.R., Alzheimer's Disease Genetics Consortium, 2020. Exceptionally low likelihood of Alzheimer's dementia in APOE2 homozygotes from a 5,000-person neuropathological study. Nat Commun 11, 667. https://doi.org/10.1038/s41467-019-14279-8

Reitz, C., Brayne, C., Mayeux, R., 2011. Epidemiology of Alzheimer disease. Nature Reviews Neurology 7, 137–152. https://doi.org/10.1038/nrneurol.2011.2

Rieker, C., Migliavacca, E., Vaucher, A., Baud, G., Marquis, J., Charpagne, A., Hegde, N., Guignard, L., McLachlan, M., Pooler, A.M., 2019. Apolipoprotein E4 Expression Causes Gain of Toxic Function in Isogenic Human Induced Pluripotent Stem Cell-Derived Endothelial Cells. Arterioscler. Thromb. Vasc. Biol. 39, e195–e207. https://doi.org/10.1161/ATVBAHA.118.312261

Ries, M., Sastre, M., 2016. Mechanisms of Aβ Clearance and Degradation by Glial Cells. Frontiers in aging neuroscience 8, 160. https://doi.org/10.3389/fnagi.2016.00160

Robakis, N.K., Ramakrishna, N., Wolfe, G., Wisniewski, H.M., 1987. Molecular cloning and characterization of a cDNA encoding the cerebrovascular and the neuritic plaque amyloid peptides. Proceedings of the National Academy of Sciences of the United States of America 84, 4190–4194. https://doi.org/10.1073/pnas.84.12.4190

Robbins, J.P., Price, J., 2017. Human induced pluripotent stem cells as a research tool in Alzheimer's disease. Psychological Medicine 47, 2587–2592. https://doi.org/10.1017/S0033291717002124

Robinson, M.D., McCarthy, D.J., Smyth, G.K., 2010. edgeR: a Bioconductor package for differential expression analysis of digital gene expression data. Bioinformatics (Oxford, England) 26, 139–40. https://doi.org/10.1093/bioinformatics/btp616

Rodríguez-Arellano, J.J., Parpura, V., Zorec, R., Verkhratsky, A., 2016. Astrocytes in physiological aging and Alzheimer's disease. Neuroscience 323, 170–182. https://doi.org/10.1016/j.neuroscience.2015.01.007

Rohn, T.T., 2013. Proteolytic cleavage of apolipoprotein E4 as the keystone for the heightened risk associated with Alzheimer's disease. International journal of molecular sciences 14, 14908–22. https://doi.org/10.3390/ijms140714908

Rovelet-Lecrux, A., Hannequin, D., Raux, G., Le Meur, N., Laquerrière, A., Vital, A., Dumanchin, C., Feuillette, S., Brice, A., Vercelletto, M., Dubas, F., Frebourg, T., Campion, D., 2006. APP locus duplication causes autosomal dominant early-onset Alzheimer disease with cerebral amyloid angiopathy. Nature genetics 38, 24–6. https://doi.org/10.1038/ng1718

Roybon, L., Lamas, N.J., Garcia, A.D., Yang, E.J., Sattler, R., Lewis, V.J., Kim, Y.A., Kachel, C.A., Rothstein, J.D., Przedborski, S., Wichterle, H., Henderson, C.E., 2013. Human stem cell-derived spinal cord astrocytes with defined mature or reactive phenotypes. Cell reports 4, 1035–1048. https://doi.org/10.1016/j.celrep.2013.06.021

Sabo, S.L., Lanier, L.M., Ikin, A.F., Khorkova, O., Sahasrabudhe, S., Greengard, P., Buxbaum, J.D., 1999. Regulation of β-Amyloid Secretion by FE65, an Amyloid Protein Precursor-binding Protein *. Journal of Biological Chemistry 274, 7952–7957. https://doi.org/10.1074/jbc.274.12.7952

Saito, H., Dhanasekaran, P., Baldwin, F., Weisgraber, K.H., Lund-Katz, S., Phillips, M.C., 2001. Lipid binding-induced conformational change in human apolipoprotein E. Evidence for two lipid-bound states on spherical particles. The Journal of biological chemistry 276, 40949–54. https://doi.org/10.1074/jbc.M106337200

Santos, R., Vadodaria, K.C., Jaeger, B.N., Mei, A., Lefcochilos-Fogelquist, S., Mendes, A.P.D., Erikson, G., Shokhirev, M., Randolph-Moore, L., Fredlender, C., Dave, S., Oefner, R., Fitzpatrick, C., Pena, M., Barron, J.J., Ku, M., Denli, A.M., Kerman, B.E., Charnay, P., Kelsoe, J.R., Marchetto, M.C., Gage, F.H., 2017. Differentiation of Inflammation-Responsive Astrocytes from Glial Progenitors Generated from Human Induced Pluripotent Stem Cells. Stem Cell Reports 8, 1757–1769. https://doi.org/10.1016/j.stemcr.2017.05.011

Saunders, A.M., Strittmatter, W.J., Schmechel, D., St. George-Hyslop, P.H., Pericak-Vance, M.A., Joo, S.H., Rosi, B.L., Gusella, J.F., Crapper-Mac Lachlan, D.R., Alberts, M.J., Hulette, C., Crain, B., Goldgaber, D., Roses, A.D., 1993. Association of apolipoprotein E allele ε4 with late-onset familial and sporadic alzheimer's disease. Neurology 43, 1467–1472. https://doi.org/10.1212/wnl.43.8.1467

Sawmiller, D., Habib, A., Hou, H., Mori, T., Fan, A., Tian, J., Zeng, J., Giunta, B., Sanberg, P.R., Mattson, M.P., Tan, J., 2019. A Novel Apolipoprotein E Antagonist Functionally Blocks Apolipoprotein E Interaction With N-terminal Amyloid Precursor Protein, Reduces β-Amyloid-Associated Pathology, and Improves Cognition. Biol. Psychiatry 86, 208–220. https://doi.org/10.1016/j.biopsych.2019.04.026

Scheuner, D., Eckman, C., Jensen, M., Song, X., Citron, M., Suzuki, N., Bird, T.D., Hardy, J., Hutton, M., Kukull, W., Larson, E., Levy-Lahad, E., Viitanen, M., Peskind, E., Poorkaj, P., Schellenberg, G., Tanzi, R., Wasco, W., Lannfelt, L., Selkoe, D., Younkin, S., 1996. Secreted amyloid β-protein similar to that in the senile plaques of Alzheimer's disease is increased in vivo by the presenilin 1 and 2 and APP mutations linked to familial Alzheimer's disease. Nature Medicine 2, 864–870. https://doi.org/10.1038/nm0896-864

Schindelin, J., Arganda-Carreras, I., Frise, E., Kaynig, V., Longair, M., Pietzsch, T., Preibisch, S., Rueden, C., Saalfeld, S., Schmid, B., Tinevez, J.-Y., White, D.J., Hartenstein, V., Eliceiri, K., Tomancak, P., Cardona, A., 2012. Fiji: an open-source platform for biological-image analysis. Nat. Methods 9, 676–682. https://doi.org/10.1038/nmeth.2019

Schnitzer, J., Franke, W.W., Schachner, M., 1981. Immunocytochemical demonstration of vimentin in astrocytes and ependymal cells of developing and adult mouse nervous system. The Journal of cell biology 90, 435–47. https://doi.org/10.1083/jcb.90.2.435

Scuderi, C., Stecca, C., Iacomino, A., Steardo, L., 2013. Role of astrocytes in major neurological disorders: the evidence and implications. IUBMB life 65, 957–61. https://doi.org/10.1002/iub.1223

Selkoe, D.J., 2002. Alzheimer's disease is a synaptic failure. Science 298, 789–791. https://doi.org/10.1126/science.1074069

Selkoe, D.J., 1991. The Molecular of Pathology Disease. Neuron 6, 487–498. https://doi.org/10.1016/0896-6273(91)90052-2

Seok, J., Warren, H.S., Cuenca, A.G., Mindrinos, M.N., Baker, V.H., Xu, W., Richards, D.R., Mcdonald-Smith, G.P., Gao, H., Hennessy, L., Finnerty, C.C., López, C.M., Honari, S., Moore, E.E., Minei, J.P., Cuschieri, J., Bankey, P.E., Johnson, J.L., Sperry, J., Nathens, A.B., Billiar, T.R., West, M.A., Jeschke, M.G., Klein, M.B., Gamelli, R.L., Gibran, N.S., Brownstein, B.H., Miller-Graziano, C., Calvano, S.E., Mason, P.H., Cobb, J.P., Rahme, L.G., Lowry, S.F., Maier, V.R., Moldawer, L.L., Herndon, D.N., Davis, R.W., Xiao, W., Tompkins, R.G., 2013. Genomic responses in mouse models poorly mimic human inflammatory diseases , and the Inflammation and Host Response to Injury, Large Scale Collaborative Research Program 4. Proc Natl Acad Sci U S A 110, 3507–3512. https://doi.org/10.1073/pnas.1222878110

Serio, A., Bilican, B., Barmada, S.J., Ando, D.M., Zhao, C., Siller, R., Burr, K., Haghi, G., Story, D., Nishimura, A.L., Carrasco, M.A., Phatnani, H.P., Shum, C., Wilmut, I., Maniatis, T., Shaw, C.E., Finkbeiner, S., Chandran, S., 2013. Astrocyte pathology and the absence of non-cell autonomy in an induced pluripotent stem cell model of TDP-43 proteinopathy. Proceedings of the National Academy of Sciences of the United States of America 110, 4697–702. https://doi.org/10.1073/pnas.1300398110

Serrano-Pozo, A., Frosch, M.P., Masliah, E., Hyman, B.T., 2011. Neuropathological alterations in Alzheimer disease. Cold Spring Harbor Perspectives in Medicine 1. https://doi.org/10.1101/cshperspect.a006189

Serrano-Pozo, A., Qian, J., Monsell, S.E., Betensky, R.A., Hyman, B.T., 2015. APOEε2 is associated with milder clinical and pathological Alzheimer disease. Ann. Neurol. 77, 917–929. https://doi.org/10.1002/ana.24369

Shaltouki, A., Peng, J., Liu, Q., Rao, M.S., Zeng, X., 2013. Efficient generation of astrocytes from human pluripotent stem cells in defined conditions. Stem cells (Dayton, Ohio) 31, 941–52. https://doi.org/10.1002/stem.1334

Shariatzadeh, M., Chandra, A., Wilson, S.L., McCall, M.J., Morizur, L., Lesueur, L., Chose, O., Gepp, M.M., Schulz, A., Neubauer, J.C., Zimmermann, H., Abranches, E., Man, J., O'Shea, O., Stacey, G., Hewitt, Z., Williams, D.J., 2020. Distributed automated manufacturing of pluripotent stem cell products. The International journal, advanced manufacturing technology 106, 1085–1103. https://doi.org/10.1007/s00170-019-04516-1

Shea, T.B., Rogers, E., Ashline, D., Ortiz, D., Sheu, M.S., 2002. Apolipoprotein E deficiency promotes increased oxidative stress and compensatory increases in antioxidants in brain tissue. Free Radical Biology and Medicine 33, 1115–1120. https://doi.org/10.1016/S0891-5849(02)01001-8

Sherrington, R., Froelich, S., Sorbi, S., Campion, D., Chi, H., Rogaeva, E.A., Levesque, G., Rogaev, E.I., Lin, C., Liang, Y., Ikeda, M., Mar, L., Brice, A., Agid, Y., Percy, M.E., Clerget-Darpoux, F., Piacentini, S., Marcon, G., Nacmias, B., Amaducci, L., Frebourg, T., Lannfelt, L., Rommens, J.M., St George-Hyslop, P.H., 1996. Alzheimer's disease associated with mutations in presenilin 2 is rare and variably penetrant. Human molecular genetics 5, 985–8. https://doi.org/10.1093/hmg/5.7.985

Sherrington, R., Rogaev, E.I., Liang, Y., Rogaeva, E.A., Levesque, G., Ikeda, M., Chi, H., Lin, C., Li, G., Holman, K., Tsuda, T., Mar, L., Foncin, J.-F., Bruni, A.C., Montesi, M.P., Sorbi, S., Rainero, I., Pinessi, L., Nee, L., Chumakov, I., Pollen, D., Brookes, A., Sanseau, P., Polinsky, R.J., Wasco, W., Da Silva, H.A.R., Haines, J.L., Pericak-Vance, M.A., Tanzi, R.E., Roses, A.D., Fraser, P.E., Rommens, J.M., St George-Hyslop, P.H., 1995. Cloning of a gene bearing missense mutations in early-onset familial Alzheimer's disease. Nature 375, 754–760. https://doi.org/10.1038/375754a0

Shi, Y., Kirwan, P., Smith, J., MacLean, G., Orkin, S.H., Livesey, F.J., 2012. A human stem cell model of early Alzheimer's disease pathology in Down syndrome. Science translational medicine 4, 124ra29. https://doi.org/10.1126/scitranslmed.3003771

Shi, Y., Manis, M., Long, J., Wang, K., Sullivan, P.M., Remolina Serrano, J., Hoyle, R., Holtzman, D.M., 2019. Microglia drive APOE-dependent neurodegeneration in a tauopathy mouse model. J Exp Med 216, 2546–2561. https://doi.org/10.1084/jem.20190980

Shi, Y., Yamada, K., Liddelow, S.A., Smith, S.T., Zhao, L., Luo, W., Tsai, R.M., Spina, S., Grinberg, L.T., Rojas, J.C., Gallardo, G., Wang, K., Roh, J., Robinson, G., Finn, M.B., Jiang, H., Sullivan, P.M., Baufeld, C., Wood, M.W., Sutphen, C., McCue, L., Xiong, C., Del-Aguila, J.L., Morris, J.C., Cruchaga, C., Initiative, A.D.N., Fagan, A.M., Miller, B.L., Boxer, A.L., Seeley, W.W., Butovsky, O., Barres, B.A., Paul, S.M., Holtzman, D.M., 2017. ApoE4 markedly exacerbates tau-mediated neurodegeneration in a mouse model of tauopathy. Nature 549, 523–527. https://doi.org/10.1038/nature24016

Shigetomi, E., Patel, S., Khakh, B.S., 2016. Probing the Complexities of Astrocyte Calcium Signaling. Trends in cell biology 26, 300–312. https://doi.org/10.1016/j.tcb.2016.01.003

Shin, R.-W., Ogino, K., Shimabuku, A., Taki, T., Nakashima, H., Ishihara, T., Kitamoto, T., 2007. Amyloid precursor protein cytoplasmic domain with phospho-Thr668 accumulates in Alzheimer's disease and its transgenic models: a role to mediate interaction of Aβ and tau. Acta Neuropathol 113, 627–636. https://doi.org/10.1007/s00401-007-0211-z

Shinohara, M., Tachibana, M., Kanekiyo, T., Bu, G., 2017. Role of LRP1 in the pathogenesis of Alzheimer's disease: evidence from clinical and preclinical studies. J. Lipid Res. 58, 1267–1281. https://doi.org/10.1194/jlr.R075796

Shirotani, K., Matsuo, K., Ohtsuki, S., Masuda, T., Asai, M., Kutoku, Y., Ohsawa, Y., Sunada, Y., Kondo, T., Inoue, H., Iwata, N., 2017. A simplified and sensitive method to identify Alzheimer's disease biomarker candidates using patient-derived induced pluripotent stem cells (iPSCs). Journal of biochemistry 162, 391–394. https://doi.org/10.1093/jb/mvx058

Silva, M., Daheron, L., Hurley, H., Bure, K., Barker, R., Carr, A.J., Williams, D., Kim, H.-W., French, A., Coffey, P.J., Cooper-White, J.J., Reeve, B., Rao, M., Snyder, E.Y., Ng, K.S., Mead, B.E., Smith, J.A., Karp, J.M., Brindley, D.A., Wall, I., 2015. Generating iPSCs: translating cell reprogramming science into scalable and robust biomanufacturing strategies. Cell stem cell 16, 13–7. https://doi.org/10.1016/j.stem.2014.12.013

Silva, M.M., Rodrigues, A.F., Correia, C., Sousa, M.F.Q., Brito, C., Coroadinha, A.S., Serra, M., Alves, P.M., 2015. Robust Expansion of Human Pluripotent Stem Cells: Integration of Bioprocess Design With Transcriptomic and Metabolomic Characterization. Stem cells translational medicine 4, 731–42. https://doi.org/10.5966/sctm.2014-0270

Simaria, A.S., Hassan, S., Varadaraju, H., Rowley, J., Warren, K., Vanek, P., Farid, S.S., 2014. Allogeneic cell therapy bioprocess economics and optimization: single-use cell expansion technologies. Biotechnology and bioengineering 111, 69–83. https://doi.org/10.1002/bit.25008

Skovronsky, D.M., Moore, D.B., Milla, M.E., Doms, R.W., Lee, V.M.-Y., 2000. Protein Kinase C-dependent α-Secretase Competes with β-Secretase for Cleavage of Amyloid-β Precursor Protein in the Trans-Golgi Network *. Journal of Biological Chemistry 275, 2568–2575. https://doi.org/10.1074/jbc.275.4.2568

Sofroniew, M. V, 2014. Multiple roles for astrocytes as effectors of cytokines and inflammatory mediators. The Neuroscientist : a review journal bringing neurobiology, neurology and psychiatry 20, 160–72. https://doi.org/10.1177/1073858413504466

Sofroniew, M. V., Vinters, H. V., 2010. Astrocytes: Biology and pathology. Acta Neuropathologica. https://doi.org/10.1007/s00401-009-0619-8

Sofroniew, V.M., 2015. Astrocyte barriers to neurotoxic inflammation. Nature reviews. Neuroscience 16, 249–63. https://doi.org/10.1038/nrn3898

Song, W.-J., Son, M.-Y., Lee, H.-W., Seo, H., Kim, J.H., Chung, S.-H., 2015. Enhancement of BACE1 Activity by p25/Cdk5-Mediated Phosphorylation in Alzheimer's Disease. PLoS One 10. https://doi.org/10.1371/journal.pone.0136950

Sorbi, S., Nacmias, B., Forleo, P., Piacentini, S., Latorraca, S., Amaducci, L., 1995. Epistatic effect of APP717 mutation and apolipoprotein E genotype in familial Alzheimer's disease. Ann Neurol 38, 124–127. https://doi.org/10.1002/ana.410380120

Spencer, B., Marr, R.A., Rockenstein, E., Crews, L., Adame, A., Potkar, R., Patrick, C., Gage, F.H., Verma, I.M., Masliah, E., 2008. Long-term neprilysin gene transfer is associated with reduced levels of intracellular Abeta and behavioral improvement in APP transgenic mice. BMC neuroscience 9, 109. https://doi.org/10.1186/1471-2202-9-109

Srinivasan, G., Morgan, D., Varun, D., Brookhouser, N., Brafman, D.A., 2018. An integrated biomanufacturing platform for the large-scale expansion and neuronal differentiation of human pluripotent stem cell-derived neural progenitor cells. Acta biomaterialia 74, 168–179. https://doi.org/10.1016/j.actbio.2018.05.008

Stacey, G., Andrews, P., Asante, C., Barbaric, I., Barry, J., Bisset, L., Braybrook, J., Buckle, R., Chandra, A., Coffey, P., Crouch, S., Driver, P., Evans, A., Gardner, J., Ginty, P., Goldring, C., Hay, D.C., Healy, L., Hows, A., Hutchinson, C., Jesson, H., Kalber, T., Kimber, S., Leathers, R., Moyle, S., Murray, T., Neale, M., Pan, D., Park, B.K., Rebolledo, R.E., Rees, I., Rivolta, M.N., Ritchie, A., Roos, E.J., Saeb-Parsy, K., Schröder, B., Sebastien, S., Thomas, A., Thomas, R.J., Turner, M., Vallier, L., Vitillo, L., Webster, A., Williams, D., 2018. Science-based assessment of source materials for cell-based medicines: report of a stakeholders workshop. Regenerative medicine 13, 935–944. https://doi.org/10.2217/rme-2018-0120

Stacey, G.N., Andrews, P.W., Barbaric, I., Boiers, C., Chandra, A., Cossu, G., Csontos, L., Frith, T.J., Halliwell, J.A., Hewitt, Z., McCall, M., Moore, H.D., Parmar, M., Panico, M.B., Pisupati, V., Shichkin, V.P., Stacey, A.R., Tedesco, F.S., Thompson, O., Wagey, R., 2019. Stem cell culture conditions and stability: a joint workshop of the PluriMes Consortium and Pluripotent Stem Cell Platform. Regenerative medicine 14, 243–255. https://doi.org/10.2217/rme-2019-0001

Standage-Beier, K., Tekel, S.J., Brookhouser, N., Schwarz, G., Nguyen, T., Wang, X., Brafman, D.A., 2019. A transient reporter for editing enrichment (TREE) in human cells. Nucleic Acids Res. 47, e120. https://doi.org/10.1093/nar/gkz713

Steinerman, J.R., Irizarry, M., Scarmeas, N., Raju, S., Brandt, J., Albert, M., Blacker, D., Hyman, B., Stern, Y., 2008. Distinct pools of beta-amyloid in Alzheimer disease-affected brain: a clinicopathologic study. Archives of neurology 65, 906–12. https://doi.org/10.1001/archneur.65.7.906

Strittmatter, W.J., Weisgraber, K.H., Huang, D.Y., Dong, L.M., Salvesen, G.S., Pericak-Vance, M., Schmechel, D., Saunders, A.M., Goldgaber, D., Roses, A.D., 1993. Binding of human apolipoprotein E to synthetic amyloid β peptide: Isoform-specific effects and implications for late-onset Alzheimer disease. Proceedings of the National Academy of Sciences of the United States of America 90, 8098–8102. https://doi.org/10.1073/pnas.90.17.8098

Strokin, M., Sergeeva, M., Reiser, G., 2011. Proinflammatory treatment of astrocytes with lipopolysaccharide results in augmented Ca2+ signaling through increased expression of via phospholipase A2 (iPLA2). American journal of physiology. Cell physiology 300, C542-9. https://doi.org/10.1152/ajpcell.00428.2010

Sun, A.X., Yuan, Q., Tan, S., Xiao, Y., Wang, D., Khoo, A.T.T., Sani, L., Tran, H.-D., Kim, P., Chiew, Y.S., Lee, K.J., Yen, Y.-C., Ng, H.H., Lim, B., Je, H.S., 2016. Direct Induction and Functional Maturation of Forebrain GABAergic Neurons from Human Pluripotent Stem Cells. Cell reports 16, 1942–53. https://doi.org/10.1016/j.celrep.2016.07.035

Sun, X., Wang, Y., Qing, H., Christensen, M.A., Liu, Y., Zhou, W., Tong, Y., Xiao, C., Huang, Y., Zhang, S., Liu, X., Song, W., 2005. Distinct transcriptional regulation and function of the

human BACE2 and BACE1 genes. FASEB J 19, 739–749. https://doi.org/10.1096/fj.04-3426com

Suri, S., Heise, V., Trachtenberg, A.J., Mackay, C.E., 2013. The forgotten APOE allele: a review of the evidence and suggested mechanisms for the protective effect of APOE ε2. Neurosci Biobehav Rev 37, 2878–2886. https://doi.org/10.1016/j.neubiorev.2013.10.010

Tai, L.M., Bilousova, T., Jungbauer, L., Roeske, S.K., Youmans, K.L., Yu, C., Poon, W.W., Cornwell, L.B., Miller, C.A., Vinters, V.H., Van Eldik, L.J., Fardo, D.W., Estus, S., Bu, G., Gylys, K.H., Ladu, M.J., 2013. Levels of soluble apolipoprotein E/amyloid-β (Aβ) complex are reduced and oligomeric Aβ increased with APOE4 and Alzheimer disease in a transgenic mouse model and human samples. The Journal of biological chemistry 288, 5914–26. https://doi.org/10.1074/jbc.M112.442103

Tai, L.M., Mehra, S., Shete, V., Estus, S., Rebeck, G.W., Bu, G., LaDu, M.J., 2014. Soluble apoE/Aβ complex: mechanism and therapeutic target for APOE4-induced AD risk. Molecular neurodegeneration 9, 2. https://doi.org/10.1186/1750-1326-9-2

Takahashi, K., Tanabe, K., Ohnuki, M., Narita, M., Ichisaka, T., Tomoda, K., Yamanaka, S., 2007. Induction of Pluripotent Stem Cells from Adult Human Fibroblasts by Defined Factors. Cell 131, 861–872. https://doi.org/10.1016/j.cell.2007.11.019

Talantova, M., Sanz-Blasco, S., Zhang, X., Xia, P., Akhtar, M.W., Okamoto, S., Dziewczapolski, G., Nakamura, T., Cao, G., Pratt, A.E., Kang, Y.-J., Tu, S., Molokanova, E., McKercher, S.R., Hires, S.A., Sason, H., Stouffer, D.G., Buczynski, M.W., Solomon, J.P., Michael, S., Powers, E.T., Kelly, J.W., Roberts, A., Tong, G., Fang-Newmeyer, T., Parker, J., Holland, E.A., Zhang, D., Nakanishi, N., Chen, H.-S.V., Wolosker, H., Wang, Y., Parsons, L.H., Ambasudhan, R., Masliah, E., Heinemann, S.F., Piña-Crespo, J.C., Lipton, S.A., 2013. Aβ induces astrocytic glutamate release, extrasynaptic NMDA receptor activation, and synaptic loss. Proceedings of the National Academy of Sciences of the United States of America 110, E2518-27. https://doi.org/10.1073/pnas.1306832110

Tamboli, I.Y., Heo, D., Rebeck, G.W., 2014. Extracellular proteolysis of apolipoprotein e (apoE) by secreted serine neuronal protease. PLoS ONE 9. https://doi.org/10.1371/journal.pone.0093120

Tandon, A., Yu, H., Wang, L., Rogaeva, E., Sato, C., Chishti, M.A., Kawarai, T., Hasegawa, H., Chen, F., Davies, P., Fraser, P.E., Westaway, D., George-Hyslop, P.H.S., 2003. Brain levels of CDK5 activator p25 are not increased in Alzheimer's or other neurodegenerative diseases with neurofibrillary tangles. Journal of Neurochemistry 86, 572–581. https://doi.org/10.1046/j.1471-4159.2003.01865.x

Taniguchi, S., Fujita, Y., Hayashi, S., Kakita, A., Takahashi, H., Murayama, S., Saido, T.C., Hisanaga, S., Iwatsubo, T., Hasegawa, M., 2001. Calpain-mediated degradation of p35 to p25 in postmortem human and rat brains. FEBS Lett 489, 46–50. https://doi.org/10.1016/s0014-5793(00)02431-5

Tarassishin, L., Suh, H.-S., Lee, S.C., 2014. LPS and IL-1 differentially activate mouse and human astrocytes: role of CD14. Glia 62, 999–1013. https://doi.org/10.1002/glia.22657

TCW, J., Wang, M., Pimenova, A.A., Bowles, K.R., Hartley, B.J., Lacin, E., Machlovi, S.I., Abdelaal, R., Karch, C.M., Phatnani, H., Slesinger, P.A., Zhang, B., Goate, A.M., Brennand, K.J., 2017. An Efficient Platform for Astrocyte Differentiation from Human

Induced Pluripotent Stem Cells. Stem Cell Reports 9, 600–614.
https://doi.org/10.1016/j.stemcr.2017.06.018

Thinakaran, G., Koo, E.H., 2008. Amyloid precursor protein trafficking, processing, and function. J Biol Chem 283, 29615–29619. https://doi.org/10.1074/jbc.R800019200

Thorne, N., Malik, N., Shah, S., Zhao, J., Class, B., Aguisanda, F., Southall, N., Xia, M., McKew, J.C., Rao, M., Zheng, W., 2016. High-Throughput Phenotypic Screening of Human Astrocytes to Identify Compounds That Protect Against Oxidative Stress. Stem cells translational medicine 5, 613–27. https://doi.org/10.5966/sctm.2015-0170

Tokuda, T., Calero, M., Matsubara, E., Vidal, R., Kumar, A., Permanne, B., Zlokovic, B., Smith, J.D., Ladu, M.J., Rostagno, A., Frangione, B., Ghiso, J., 2000. Lipidation of apolipoprotein E influences its isoform-specific interaction with Alzheimer's amyloid β peptides. Biochemical Journal 348, 359–365. https://doi.org/10.1042/0264-6021:3480359

Tolar, M., Abushakra, S., Hey, J.A., Porsteinsson, A., Sabbagh, M., 2020. Aducanumab, gantenerumab, BAN2401, and ALZ-801—the first wave of amyloid-targeting drugs for Alzheimer's disease with potential for near term approval. Alzheimer's Research & Therapy 12, 95. https://doi.org/10.1186/s13195-020-00663-w

Trommer, B.L., Shah, C., Yun, S.H., Gamkrelidze, G., Pasternak, E.S., Stine, W.B., Manelli, A., Sullivan, P., Pasternak, J.F., LaDu, M.J., 2005. ApoE isoform-specific effects on LTP: blockade by oligomeric amyloid-beta1-42. Neurobiology of disease 18, 75–82. https://doi.org/10.1016/j.nbd.2004.08.011

Tsuang, D., Leverenz, J.B., Lopez, O.L., Hamilton, R.L., Bennett, D.A., Schneider, J.A., Buchman, A.S., Larson, E.B., Crane, P.K., Kaye, J.A., Kramer, P., Woltjer, R., Trojanowski, J.Q., Weintraub, D., Chen-Plotkin, A.S., Irwin, D.J., Rick, J., Schellenberg, G.D., Watson, G.S., Kukull, W., Nelson, P.T., Jicha, G.A., Neltner, J.H., Galasko, D., Masliah, E., Quinn, J.F., Chung, K.A., Yearout, D., Mata, I.F., Wan, J.Y., Edwards, K.L., Montine, T.J., Zabetian, C.P., 2013. APOE ε4 increases risk for dementia in pure synucleinopathies. JAMA Neurol 70, 223–228. https://doi.org/10.1001/jamaneurol.2013.600

Valenza, M., Leoni, V., Karasinska, J.M., Petricca, L., Fan, J., Carroll, J., Pouladi, M.A., Fossale, E., Nguyen, H.P., Riess, O., MacDonald, M., Wellington, C., DiDonato, S., Hayden, M., Cattaneo, E., 2010. Cholesterol defect is marked across multiple rodent models of Huntington's disease and is manifest in astrocytes. Journal of Neuroscience 30, 10844–10850. https://doi.org/10.1523/JNEUROSCI.0917-10.2010

Valenza, M., Marullo, M., Di Paolo, E., Cesana, E., Zuccato, C., Biella, G., Cattaneo, E., 2015. Disruption of astrocyte-neuron cholesterol cross talk affects neuronal function in Huntington's disease. Cell Death and Differentiation 22, 690–702. https://doi.org/10.1038/cdd.2014.162

Vallée, A., Lecarpentier, Y., 2016. Alzheimer Disease: Crosstalk between the Canonical Wnt/Beta-Catenin Pathway and PPARs Alpha and Gamma. Frontiers in neuroscience 10, 459. https://doi.org/10.3389/fnins.2016.00459

van der Flier, W.M., Scheltens, P., 2005. Epidemiology and risk factors of dementia. Journal of neurology, neurosurgery, and psychiatry 76 Suppl 5, v2-7. https://doi.org/10.1136/jnnp.2005.082867

van Neerven, S., Regen, T., Wolf, D., Nemes, A., Johann, S., Beyer, C., Hanisch, U.-K., Mey, J., 2010. Inflammatory chemokine release of astrocytes in vitro is reduced by all-trans retinoic acid. Journal of neurochemistry 114, 1511–26. https://doi.org/10.1111/j.1471-4159.2010.06867.x

Varun, D., Srinivasan, G.R., Tsai, Y.-H., Kim, H.-J., Cutts, J., Petty, F., Merkley, R., Stephanopoulos, N., Dolezalova, D., Marsala, M., Brafman, D.A., 2017. A robust vitronectin-derived peptide for the scalable long-term expansion and neuronal differentiation of human pluripotent stem cell (hPSC)-derived neural progenitor cells (hNPCs). Acta biomaterialia 48, 120–130. https://doi.org/10.1016/j.actbio.2016.10.037

Vassar, R., Bennett, B.D., Babu-Khan, S., Kahn, S., Mendiaz, E.A., Denis, P., Teplow, D.B., Ross, S., Amarante, P., Loeloff, R., Luo, Y., Fisher, S., Fuller, J., Edenson, S., Lile, J., Jarosinski, M.A., Biere, A.L., Curran, E., Burgess, T., Louis, J.-C., Collins, F., Treanor, J., Rogers, G., Citron, M., 1999. β-Secretase Cleavage of Alzheimer's Amyloid Precursor Protein by the Transmembrane Aspartic Protease BACE. Science 286, 735–741. https://doi.org/10.1126/science.286.5440.735

Vehmas, A.K., Kawas, C.H., Stewart, W.F., Troncoso, J.C., 2003. Immune reactive cells in senile plaques and cognitive decline in Alzheimer's disease. Neurobiology of Aging 24, 321–331. https://doi.org/10.1016/S0197-4580(02)00090-8

Vélez, J.I., Lopera, F., Sepulveda-Falla, D., Patel, H.R., Johar, A.S., Chuah, A., Tobón, C., Rivera, D., Villegas, A., Cai, Y., Peng, K., Arkell, R., Castellanos, F.X., Andrews, S.J., Silva Lara, M.F., Creagh, P.K., Easteal, S., de Leon, J., Wong, M.L., Licinio, J., Mastronardi, C.A., Arcos-Burgos, M., 2016. APOE*E2 allele delays age of onset in PSEN1 E280A Alzheimer's disease. Mol Psychiatry 21, 916–924. https://doi.org/10.1038/mp.2015.177

Verghese, P.B., Castellano, J.M., Garai, K., Wang, Y., Jiang, H., Shah, A., Bu, G., Frieden, C., Holtzman, D.M., 2013. ApoE influences amyloid-β (Aβ) clearance despite minimal apoE/Aβ association in physiological conditions. Proceedings of the National Academy of Sciences of the United States of America 110, E1807-1816. https://doi.org/10.1073/pnas.1220484110

Verkhratsky, A., Olabarria, M., Noristani, H.N., Yeh, C.-Y., Rodriguez, J.J., 2010. Astrocytes in Alzheimer's disease. Neurotherapeutics 7, 399–412. https://doi.org/10.1016/j.nurt.2010.05.017

Vincent, B., Smith, J.D., 2001. Astrocytes down-regulate neuronal beta-amyloid precursor protein expression and modify its processing in an apolipoprotein E isoform-specific manner. Eur J Neurosci 14, 256–266. https://doi.org/10.1046/j.0953-816x.2001.01643.x

Volterra, A., Liaudet, N., Savtchouk, I., 2014. Astrocyte Ca^{2+} signalling: an unexpected complexity. Nature reviews. Neuroscience 15, 327–35. https://doi.org/10.1038/nrn3725

Wahrle, S.E., Jiang, H., Parsadanian, M., Hartman, R.E., Bales, K.R., Paul, S.M., Holtzman, D.M., 2005. Deletion of Abca1 increases Abeta deposition in the PDAPP transgenic mouse model of Alzheimer disease. The Journal of biological chemistry 280, 43236–42. https://doi.org/10.1074/jbc.M508780200

Wahrle, S.E., Jiang, H., Parsadanian, M., Legleiter, J., Han, X., Fryer, J.D., Kowalewski, T., Holtzman, D.M., 2004. ABCA1 is required for normal central nervous system ApoE levels

and for lipidation of astrocyte-secreted apoE. The Journal of biological chemistry 279, 40987–93. https://doi.org/10.1074/jbc.M407963200

Wang, C., Najm, R., Xu, Q., Jeong, D.-E., Walker, D., Balestra, M.E., Yoon, S.Y., Yuan, H., Li, G., Miller, Z.A., Miller, B.L., Malloy, M.J., Huang, Y., 2018. Gain of toxic apolipoprotein E4 effects in human iPSC-derived neurons is ameliorated by a small-molecule structure corrector. Nat. Med. 24, 647–657. https://doi.org/10.1038/s41591-018-0004-z

Wang, L., Liu, J., Wang, Q., Jiang, H., Zeng, L., Li, Z., Liu, R., 2019. MicroRNA-200a-3p Mediates Neuroprotection in Alzheimer-Related Deficits and Attenuates Amyloid-Beta Overproduction and Tau Hyperphosphorylation via Coregulating BACE1 and PRKACB. Front Pharmacol 10. https://doi.org/10.3389/fphar.2019.00806

Wang, S., Bates, J., Li, X., Schanz, S., Chandler-Militello, D., Levine, C., Maherali, N., Studer, L., Hochedlinger, K., Windrem, M., Goldman, S.A., 2013. Human iPSC-derived oligodendrocyte progenitor cells can myelinate and rescue a mouse model of congenital hypomyelination. Cell Stem Cell 12, 252–264. https://doi.org/10.1016/j.stem.2012.12.002

Wang, S.-M., Lee, C.-U., Lim, H.K., 2019. Stem cell therapies for Alzheimer's disease: is it time? Current opinion in psychiatry 32, 105–116. https://doi.org/10.1097/YCO.0000000000000478

Wang, Y., Cheng, J., Xie, D., Ding, X., Hou, H., Chen, X., Er, P., Zhang, F., Zhao, L., Yuan, Z., Pang, Q., Wang, P., Qian, D., 2018. NS1-binding protein radiosensitizes esophageal squamous cell carcinoma by transcriptionally suppressing c-Myc. Cancer communications (London, England) 38, 33. https://doi.org/10.1186/s40880-018-0307-y

Warren, H.S., Tompkins, R.G., Moldawer, L.L., Seok, J., Xu, W., Mindrinos, M.N., Maier, V.R., Xiao, W., Davis, R.W., 2015. Mice are not men. Proceedings of the National Academy of Sciences of the United States of America 112, E345. https://doi.org/10.1073/pnas.1414857111

Warren, L., Manos, P.D., Ahfeldt, T., Loh, Y.H., Li, H., Lau, F., Ebina, W., Mandal, P.K., Smith, Z.D., Meissner, A., Daley, G.Q., Brack, A.S., Collins, J.J., Cowan, C., Schlaeger, T.M., Rossi, D.J., 2010. Highly efficient reprogramming to pluripotency and directed differentiation of human cells with synthetic modified mRNA. Cell Stem Cell 7, 618–630. https://doi.org/10.1016/j.stem.2010.08.012

Wasser, C.R., Herz, J., 2017. Reelin: Neurodevelopmental Architect and Homeostatic Regulator of Excitatory Synapses. The Journal of biological chemistry 292, 1330–1338. https://doi.org/10.1074/jbc.R116.766782

Weisgraber, K.H., 1994. Apolipoprotein E: Structure-function relationships. Advances in Protein Chemistry 45, 249–302. https://doi.org/10.1016/s0065-3233(08)60642-7

Weisgraber, K.H., Innerarity, T.L., Mahley, R.W., 1982. Abnormal lipoprotein receptor-binding activity of the human E apoprotein due to cysteine-arginine interchange at a single site. The Journal of biological chemistry 257, 2518–21.

Wiese, S., Karus, M., Faissner, A., 2012. Astrocytes as a source for extracellular matrix molecules and cytokines. Frontiers in pharmacology 3, 120. https://doi.org/10.3389/fphar.2012.00120

Wijsman, E.M., Daw, E.W., Yu, X., Steinbart, E.J., Nochlin, D., Bird, T.D., Schellenberg, G.D., 2005. APOE and other loci affect age-at-onset in Alzheimer's disease families with PS2 mutation. Am J Med Genet B Neuropsychiatr Genet 132B, 14–20. https://doi.org/10.1002/ajmg.b.30087

Woodruff, G., Reyna, S.M., Dunlap, M., Van Der Kant, R., Callender, J.A., Young, J.E., Roberts, E.A., Goldstein, L.S.B., 2016. Defective Transcytosis of APP and Lipoproteins in Human iPSC-Derived Neurons with Familial Alzheimer's Disease Mutations. Cell reports 17, 759–773. https://doi.org/10.1016/j.celrep.2016.09.034

Woodruff, G., Young, J.E., Martinez, F.J., Buen, F., Gore, A., Kinaga, J., Li, Z., Yuan, S.H., Zhang, K., Goldstein, L.S.B., 2013. The presenilin-1 ΔE9 mutation results in reduced γ-secretase activity, but not total loss of PS1 function, in isogenic human stem cells. Cell reports 5, 974–85. https://doi.org/10.1016/j.celrep.2013.10.018

Xu, Q., Bernardo, A., Walker, D., Kanegawa, T., Mahley, R.W., Huang, Y., 2006. Profile and regulation of apolipoprotein E (ApoE) expression in the CNS in mice with targeting of green fluorescent protein gene to the ApoE locus. The Journal of neuroscience : the official journal of the Society for Neuroscience 26, 4985–94. https://doi.org/10.1523/JNEUROSCI.5476-05.2006

Xu, Q., Walker, D., Bernardo, A., Brodbeck, J., Balestra, M.E., Huang, Y., 2008. Intron-3 retention/splicing controls neuronal expression of apolipoprotein E in the CNS. The Journal of neuroscience : the official journal of the Society for Neuroscience 28, 1452–9. https://doi.org/10.1523/JNEUROSCI.3253-07.2008

Yagi, T., Ito, D., Okada, Y., Akamatsu, W., Nihei, Y., Yoshizaki, T., Yamanaka, S., Okano, H., Suzuki, N., 2011. Modeling familial Alzheimer's disease with induced pluripotent stem cells. Human molecular genetics 20, 4530–9. https://doi.org/10.1093/hmg/ddr394

Yan, R., Munzner, J.B., Shuck, M.E., Bienkowski, M.J., 2001. BACE2 functions as an alternative alpha-secretase in cells. J Biol Chem 276, 34019–34027. https://doi.org/10.1074/jbc.M105583200

Yang, J., Zhao, H., Ma, Y., Shi, G., Song, J., Tang, Y., Li, S., Li, T., Liu, N., Tang, F., Gu, J., Zhang, L., Zhang, Z., Zhang, X., Jin, Y., Le, W., 2017. Early pathogenic event of Alzheimer's disease documented in iPSCs from patients with PSEN1 mutations. Oncotarget 8, 7900–7913. https://doi.org/10.18632/oncotarget.13776

Yasojima, K., McGeer, E.G., McGeer, P.L., 2001. Relationship between beta amyloid peptide generating molecules and neprilysin in Alzheimer disease and normal brain. Brain Res 919, 115–121. https://doi.org/10.1016/s0006-8993(01)03008-6

Ye, S., Huang, Y., Müllendorff, K., Dong, L., Giedt, G., Meng, E.C., Cohen, F.E., Kuntz, I.D., Weisgraber, K.H., Mahley, R.W., 2005. Apolipoprotein (apo) E4 enhances amyloid beta peptide production in cultured neuronal cells: apoE structure as a potential therapeutic target. Proceedings of the National Academy of Sciences of the United States of America 102, 18700–5. https://doi.org/10.1073/pnas.0508693102

Yu, C.E., Marchani, E., Nikisch, G., Müller, U., Nolte, D., Hertel, A., Wijsman, E.M., Bird, T.D., 2010. The N141I mutation in PSEN2: Implications for the quintessential case of Alzheimer disease. Archives of Neurology 67, 631–633. https://doi.org/10.1001/archneurol.2010.87

Yu, W., Bozza, P.T., Tzizik, D.M., Gray, J.P., Cassara, J., Dvorak, A.M., Weller, P.F., 1998. Co-compartmentalization of MAP kinases and cytosolic phospholipase A2 at cytoplasmic arachidonate-rich lipid bodies. Am J Pathol 152, 759–769.

Yuksel, M., Tacal, O., 2019. Trafficking and proteolytic processing of amyloid precursor protein and secretases in Alzheimer's disease development: An up-to-date review. Eur J Pharmacol 856, 172415. https://doi.org/10.1016/j.ejphar.2019.172415

Zamanian, J.L., Xu, L., Foo, L.C., Nouri, N., Zhou, L., Giffard, R.G., Barres, B.A., 2012. Genomic analysis of reactive astrogliosis. The Journal of neuroscience : the official journal of the Society for Neuroscience 32, 6391–410. https://doi.org/10.1523/JNEUROSCI.6221-11.2012

Zhang, Hongmei, Chang, L., Zhang, Huajun, Nie, J., Zhang, Z., Yang, X., Vuong, A.M., Wang, Z., Chen, A., Niu, Q., 2017. Calpain-2/p35-p25/Cdk5 pathway is involved in the neuronal apoptosis induced by polybrominated diphenyl ether-153. Toxicol Lett 277, 41–53. https://doi.org/10.1016/j.toxlet.2017.05.027

Zhang, J., Liu, Q., 2015. Cholesterol metabolism and homeostasis in the brain. Protein and Cell 6, 254–264. https://doi.org/10.1007/s13238-014-0131-3

Zhang, T., Chen, D., Lee, T.H., 2019. Phosphorylation Signaling in APP Processing in Alzheimer's Disease. Int J Mol Sci 21. https://doi.org/10.3390/ijms21010209

Zhang, Y., Barres, B.A., 2010. Astrocyte heterogeneity: an underappreciated topic in neurobiology. Current opinion in neurobiology 20, 588–94. https://doi.org/10.1016/j.conb.2010.06.005

Zhang, Y., Chen, K., Sloan, S.A., Bennett, M.L., Scholze, A.R., O'Keeffe, S., Phatnani, H.P., Guarnieri, P., Caneda, C., Ruderisch, N., Deng, S., Liddelow, S.A., Zhang, C., Daneman, R., Maniatis, T., Barres, B.A., Wu, J.Q., 2014. An RNA-sequencing transcriptome and splicing database of glia, neurons, and vascular cells of the cerebral cortex. J Neurosci 34, 11929–11947. https://doi.org/10.1523/JNEUROSCI.1860-14.2014

Zhang, Y., Pak, C.H., Han, Y., Ahlenius, H., Zhang, Z., Chanda, S., Marro, S., Patzke, C., Acuna, C., Covy, J., Xu, W., Yang, N., Danko, T., Chen, L., Wernig, M., Südhof, T.C., 2013. Rapid single-step induction of functional neurons from human pluripotent stem cells. Neuron 78, 785–798. https://doi.org/10.1016/j.neuron.2013.05.029

Zhang, Y., Sloan, S.A., Clarke, L.E., Caneda, C., Plaza, C.A., Blumenthal, P.D., Vogel, H., Steinberg, G.K., Edwards, M.S.B., Li, G., Duncan, J.A., Cheshier, S.H., Shuer, L.M., Chang, E.F., Grant, G.A., Gephart, M.G.H., Barres, B.A., 2016. Purification and Characterization of Progenitor and Mature Human Astrocytes Reveals Transcriptional and Functional Differences with Mouse. Neuron 89, 37–53. https://doi.org/10.1016/j.neuron.2015.11.013

Zhang, Y., Thompson, R., Zhang, H., Xu, H., 2011. APP processing in Alzheimer's disease. Molecular brain 4, 3. https://doi.org/10.1186/1756-6606-4-3

Zhao, J., Davis, M.D., Martens, Y.A., Shinohara, M., Graff-Radford, N.R., Younkin, S.G., Wszolek, Z.K., Kanekiyo, T., Bu, G., 2017. APOE ε4/ε4 diminishes neurotrophic function of human iPSC-derived astrocytes. Human molecular genetics 26, 2690–2700. https://doi.org/10.1093/hmg/ddx155

Zhao, J., Paganini, L., Mucke, L., Gordon, M., Refolo, L., Carman, M., Sinha, S., Oltersdorf, T., Lieberburg, I., McConlogue, L., 1996. Beta-secretase processing of the beta-amyloid precursor protein in transgenic mice is efficient in neurons but inefficient in astrocytes. J. Biol. Chem. 271, 31407–31411. https://doi.org/10.1074/jbc.271.49.31407

Zhao, L., Gottesdiener, A.J., Parmar, M., Li, M., Kaminsky, S.M., Chiuchiolo, M.J., Sondhi, D., Sullivan, P.M., Holtzman, D.M., Crystal, R.G., Paul, S.M., 2016. Intracerebral adeno-associated virus gene delivery of apolipoprotein E2 markedly reduces brain amyloid pathology in Alzheimer's disease mouse models. Neurobiol. Aging 44, 159–172. https://doi.org/10.1016/j.neurobiolaging.2016.04.020

Zhou, S., Wu, H., Zeng, C., Xiong, X., Tang, S., Tang, Z., Sun, X., 2013. Apolipoprotein E protects astrocytes from hypoxia and glutamate-induced apoptosis. FEBS letters 587, 254–8. https://doi.org/10.1016/j.febslet.2012.12.003

Zhu, Y., Nwabuisi-Heath, E., Dumanis, S.B., Tai, L.M., Yu, C., Rebeck, G.W., Ladu, M.J., 2012. APOE genotype alters glial activation and loss of synaptic markers in mice. GLIA 60, 559–569. https://doi.org/10.1002/glia.22289

Zollo, A., Allen, Z., Rasmussen, H.F., Iannuzzi, F., Shi, Y., Larsen, A., Maier, T.J., Matrone, C., 2017. Sortilin-Related Receptor Expression in Human Neural Stem Cells Derived from Alzheimer's Disease Patients Carrying the APOE Epsilon 4 Allele. Neural plasticity 2017, 1892612. https://doi.org/10.1155/2017/1892612

Zulfiqar, S., Fritz, B., Nieweg, K., 2016a. Episomal plasmid-based generation of an iPSC line from a 79-year-old individual carrying the APOE4/4 genotype: i11001. Stem cell research 17, 544–546. https://doi.org/10.1016/j.scr.2016.09.023

Zulfiqar, S., Fritz, B., Nieweg, K., 2016b. Episomal plasmid-based generation of an iPSC line from an 83-year-old individual carrying the APOE4/4 genotype: i10984. Stem cell research 17, 523–525. https://doi.org/10.1016/j.scr.2016.09.017

APPENDIX A

SUPPLEMENTARY FIGURES FOR CHAPTER 1

Table A-1. Summary of studies using hiPSC-derived brain cells to model effects of fAD and sAD mutations and risk factors.

| fAD Models			
Mutation	Cell Type Analyzed	Phenotype	Reference
PSEN1[A246E]	Neurons	Increased Aβ42 levels; Decreased by γ-secretase inhibitors	Yagi et al. 2011
PSEN1[A246E]	Neurons	Increased susceptibility to Aβ toxicity	Armijo et al. 2017
PSEN1[A246E]	Neurons	Increased Aβ42 levels; Increased Aβ42/40; Robust response to γ-secretase modulators	Liu et al. 2014
PSEN1[ΔE9]	Neurons	Increased Aβ42/40 through reduction of Aβ40; Altered γ-secretase activity; Increased APP CTFs; No difference in Tau phosphorylation	Woodruff et al. 2013
PSEN1[ΔE9]	Neurons	Altered sub-cellular distribution of APP; Accumulation of APP CTFs in the soma; Reduced endocytosis and transcytosis of APP and LDL; Impaired Recycling of LRP1	Woodruff et al. 2016
PSEN1[ΔE9]	Astrocytes	Increased Aβ production, altered cytokine release, dysregulated Ca^{2+} homeostasis	Oksanen et al. 2017
PSEN1[ΔE9]	Microglia	Decrease in cytokine release, increase in chemokinesis	Konttinen et al. 2019
PSEN1[ΔS169]	Neurons	Increased Aβ42 levels; Increased Aβ42/40; Increased levels of Tau phosphorylation; Premature neural differentiation from hNPCs	Yang et al. 2017
PSEN1[V89L]	Neurons	Increased Aβ42 levels; Increased Aβ42/40; Increased levels of Tau phosphorylation	Ochalek et al. 2017
PSEN1[M146L]	Neurons	Increased Aβ42 levels; Increased Aβ42/40; Robust response to γ-secretase modulators	Liu et al. 2014
PSEN1[M146V]	Neurons	Three-fold increase in secreted Aβ42/40 ratio in homozygous and two-fold increase in heterozygous	Paquet et al. 2016

Mutation	Cell Type Analyzed	Phenotype	Reference
		PSEN1^{M146V} mutant knock in lines compared to isogenic controls	
PSEN1^{L150P}	Neurons	Increased Aβ42 levels; Increased Aβ42/40; Increased levels of Tau phosphorylation	Ochalek et al. 2017
PSEN1^{H163R}	Neurons	Increased Aβ42 levels; Increased Aβ42/40; Robust response to γ-secretase modulators	Liu et al. 2014
PSEN1^{L166P}	Neurons	Partial loss of γ-secretase function; Decreased production of endogenous Aβ40 and an increased Aβ42/40	Koch et al. 2012
PSEN1^{D385N}	Neurons	Catalytically inactive PSEN1; Accumulation of unprocessed full-length protein; Strong decrease in both Aβ42 and Aβ40	Koch et al. 2012
PSEN1 (various mutations)	Neurons, matched patient CSF, post-mortem brain tissue	Reduced γ-secretase carboxypeptidase-like activity; Mechanisms include decreased γ-secretase activity, decreased protein stability, and reduced PSEN1 maturation	Arber et al. 2019
PSEN2^{N141I}	Neurons	Increased Aβ42 levels; Decreased by γ-secretase inhibitors	Yagi et al. 2011
PSEN2^{N141I}	Basal forebrain cholinergic neurons (BFCN)	Increased Aβ42/40; Electrophysiological deficits; Phenotypes abolished by CRISPR/Cas9 gene correction	Ortiz-Virumbrales et al. 2017
APP^{dp}	Neurons	Increased Aβ40; Increased levels of Tau phosphorylation and active GSK3β levels; Accumulation of RAB5-positive endosomes	Israel et al. 2012
APP^{TP}	Neurons	Neuron-specific Aβ peptide production; Increased Aβ42 aggregate formation; Altered Tau phosphorylation and localization; Increased cell death	Shi et al. 2014
APP^{TP}	Neurons	Inactivating one copy of the	Ovchinnikov et al.

|		APP gene in a trisomy 21 background normalized APP, secreted levels of Aβ42, and Aβ42/Aβ40; Alteration did not decrease Tau phosphorylation	2018
Mutation	Cell Type Analyzed	Phenotype	Reference
APP^{V717I}	Forebrain neurons	Increased Aβ42 levels; Increased levels of Tau phosphorylation; Altered APP subcellular localization; Altered APP processing	Muratore et al. 2014
APP^{V717L}	Cortical neurons	Increased Aβ42 levels; Increased Aβ42/40	Kondo et al. 2013
APP^{V717F}	Neurons	Defective transcytosis of APP and lipoproteins	Woodruff et al. 2016
APP^{swe}	Neurons	Defective transcytosis of APP and lipoproteins	Woodruff et al. 2016
APP^{swe}	Microglia	Decrease in cytokine release, increase in chemokinesis	Konttinen et al. 2019
sAD Models			
Risk factor	Cell Type Analyzed	Phenotype	Reference
N/A	Neurons	Increased Aβ40 levels; Increased Tau phosphorylation; Increased active GSK3β	Israel et al. 2012
N/A	Neurons	Elevated Tau hyperphosphorylation; Increased amyloid levels; increased GSK3β activation	Ochalek et al. 2017
APOE4	Neurons, astrocytes, microglia	Neurons: increased Aβ42, increased synapse number Astrocytes: impaired Aβ uptake, cholesterol accumulation Microglia: reduced Aβ phagocytosis	Lin et al. 2018
APOE4	Neurons	Increased APP transcription and Aβ synthesis mediated by non-canonical MAP kinase pathway in the rank order ApoE4>ApoE3>ApoE2	Huang et al. 2017
APOE4	Neurons	Increased synaptogenesis mediated by CREB activation in the rank order ApoE4>ApoE3>ApoE2	Huang et al. 2019

Risk factor	Cell Type Analyzed	Phenotype	Reference
APOE4	Neurons	Calcium dysregulation and associated neurodegeneration; higher levels of cellular and secreted hyperphosphorylated Tau	Wadhwani et al. 2019
APOE4	Neurons	Increased Aβ levels; Increased Tau phosphorylation; GABAergic neuron degeneration	Wang et al. 2018
APOE4	Microglia	Decreased Metabolism, phagocytosis, and migration in APOE4 microglia-like cells	Konttinen et al. 2019
APOE4	Astrocytes	Decreased neurotrophic function	Zhao et al. 2017
TREM2, APOE	Microglia	Phenotypic switch from homeostatic to neurodegenerative phenotype via TREM2-APOE pathway	Krasemann et al. 2017

APPENDIX B

SUPPLEMENTARY FIGURES FOR CHAPTER 2
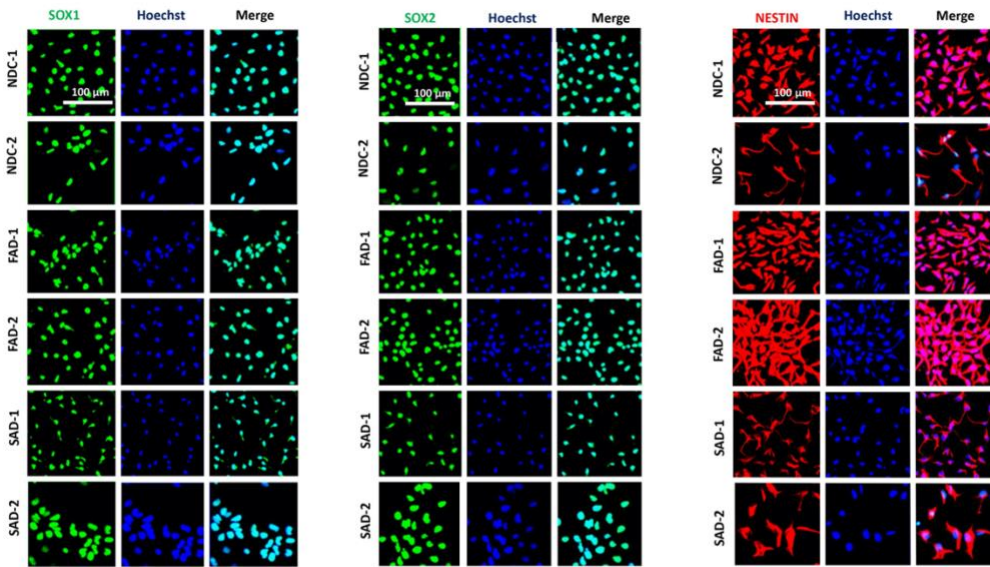
Supplementary Figure B.1. Characterization of hNPCs used in this study.
Immunofluorescence of hNPC markers SOX1, SOX2, and NESTIN.
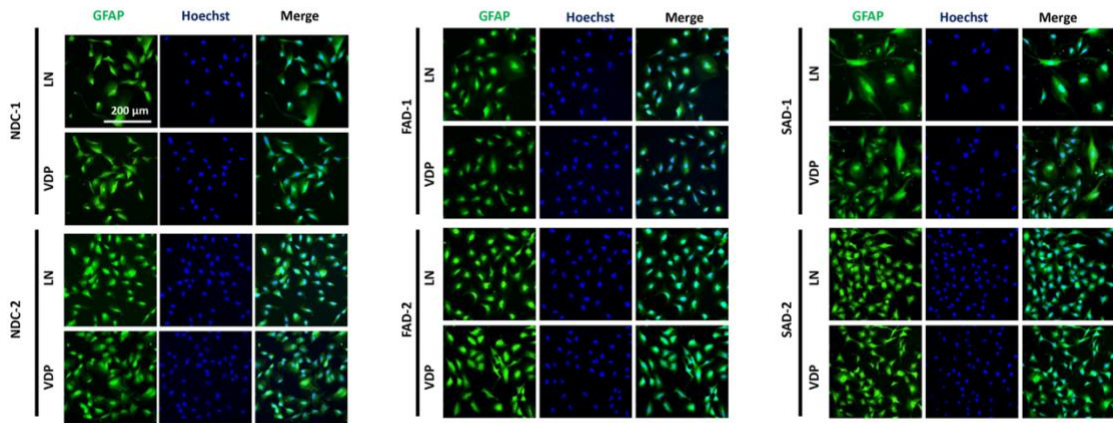
Supplementary Figure B.2. Immunofluorescence analysis for expression of GFAP in D50+ cultures.

Single channel images for immunofluorescent analysis for expression of GFAP presented in Figure 2.1 **(D)**.
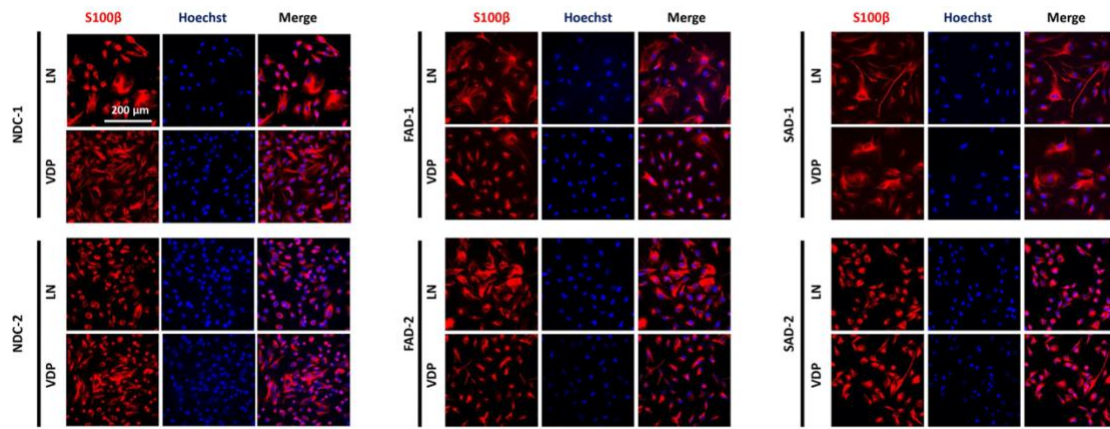
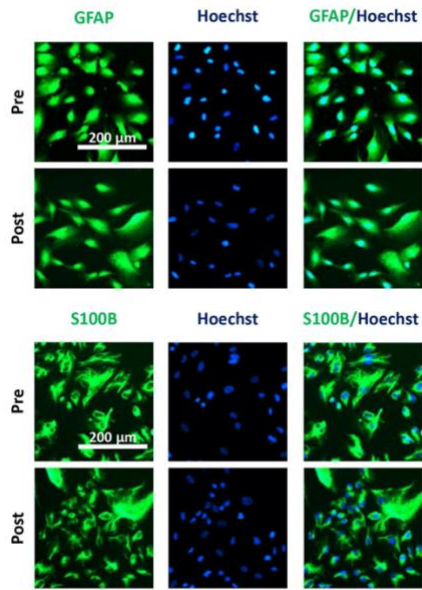**Supplementary Figure B.3. Immunofluorescence analysis for expression of S100β in D50+ cultures.**

Single channel images for immunofluorescent analysis for expression of S100β presented in Figure 2.1 **(D)**.
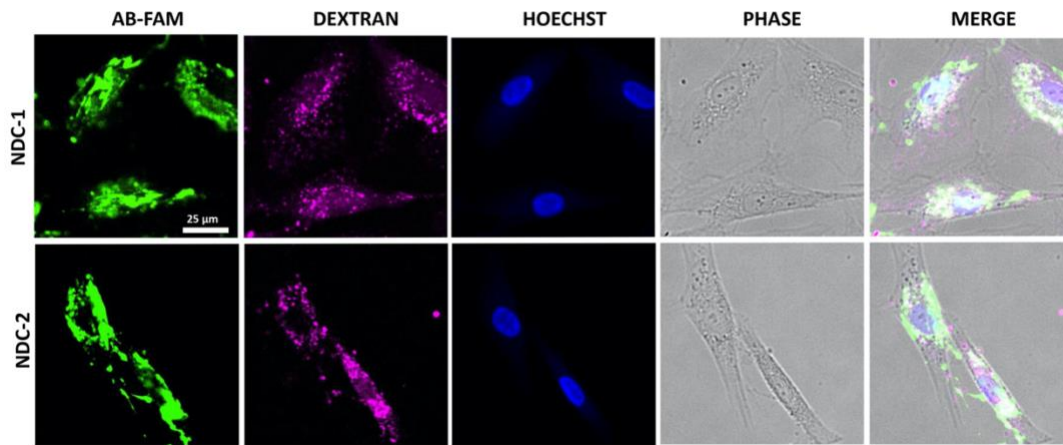
Supplementary Figure B.4. Confocal imaging analysis of β-amyloid (Aβ) uptake in astrocytes.

Fluorescent imaging analysis of FITC-Aβ and Alexa 647-dextran uptake in NDC-1 and NDC-2 astrocytes on VDP.

Supplementary Figure B.5. Analysis of calcium transients in single astrocytic cells derived on VDP- and LN-coated substrates.

Calcium transients were measured in single astrocyte cells using the fluorescent calcium indicator (Fluo-4). The maximum change ($\Delta F/F$) in fluorescent intensity is shown for the transients of individual cells (rows).

Supplementary Figure B.6. Immunofluorescent images of GFAP and S100β in pre- and post-cryopreserved astrocytes.

Single channel images for immunofluorescent analysis for expression of GFAP and S100β presented in Figure 2.7**(B)**.

Supplemental Table B.1 List of antibodies used in Chapter 2.

Antibody	Vendor	Catalog #	Concentration Used
Mouse PE anti-CD44	BD Biosciences	550989	20uL per test (1 × 10^6 cells)
Rabbit anti-GFAP	Abcam	AB7260	1:200
Mouse anti-S100β	Sigma	S2532	1:500
Goat anti-SOX2	Santa Cruz	SC-17320	1:50
Mouse anti-NESTIN	BD	560341	1:50 (IF), 1:10 (FC)
Mouse anti-SOX1	BD	560749	1:50
Mouse PE IgG1 isotype control	BD Biosciences	555749	20uL per test (1 × 10^6 cells)
Alexa 647 Donkey anti-Goat	Life Technologies	A-21447	1:200
Alexa 647 Donkey anti-Mouse	Life Technologies	A-31571	1:200
Alexa 647 donkey anti-Rabbit	Life Technologies	A-31573	1:200
Alexa 488 Donkey anti-Goat	Life Technologies	A-11055	1:200
Alexa 488 Donkey anti-Mouse	Life Technologies	A-21202	1:200
Alexa 488 Donkey anti-Rabbit	Life Technologies	A-21206	1:200

Supplemental Table B.2 List of qPCR primers used in Chapter 2.

Gene	Forward (5' --> 3')	Reverse (5' --> 3')	Product (bp)
18S	GTAACCCGTTGAACCCCATT	CCATCCAATCGGTAGTAGCG	151
GFAP	GGCCCGCCACTTGCAGGAGTACC AGG	CTTCTGCTCGGGCCCCTCATGAG ACG	328
VIM	GAGAACTTTGCCGTTGAAGC	TCCAGCAGCTTCCTGTAGGT	170

Supplemental Table B.3 Description of hPSC lines used in Chapter 2.

Cell Line	Disease Status	Reference
NDC-1	Non-demented control	Neuroscience Lett. 2011 Sep 20; 502(3): 219–224.
NDC-2	Non-demented control	Stem Cell Res. 2017 Dec;25:266-269
FAD-1	Familial AD	Nature. 2012 Jan 25;482(7384):216-20
FAD-2	Familial AD	https://biomanufacturing.cedars-sinai.org/product/cs40ifad-nxx/
SAD-1	Sporadic AD	Stem Cell Res. 2017 Dec;25:266-269
SAD-2	Sporadic AD	Stem Cell Res. 2017 Oct;24:160-163.

This table can be downloaded on the ACS publications website.

Supplemental Table B.4. Complete RNA-seq data set for hNPCs, neurons, and astrocytes generated on VDP- and LN-coated surfaces.

This table can be downloaded on the ACS publications website.

Supplemental Table B.5. List of genes that are expressed at statistically (FDR <0.05, Fold change > 1.5) different levels in RNA-seq dataset used in Chapter 2.

Supplemental Table B.6. Comparison of phenotypic characterization of astrocytes in Chapter 2 with astrocytes generated in previous studies using undefined, xenogeneic substrates.

	This Study	Zhao et al. Hum Mol Genet. 2017 Jul 15;26(14):2690-2700	Tcw et al. Stem Cell Reports. 2017 Aug 8;9(2):600-614	Santos et al. Stem Cell Reports. 2017 Jun 6;8(6) 1757-1769	Lundin et al. Stem Cell Reports. 2018 Mar 13;10(3):1030-1045
Morphology	Flat, star shaped (Figure 2.1A, Figure 2.7A)	Not assayed	Flat, star shaped	Flat, star shaped	Flat, star shaped
CD44	Positive (Flow Cytometry;Figure 2.1B)	Not assayed	Not assayed	Positive (Immunofluorescence)	Positive (Immunofluorescence, qPCR)
S100β/GFAP Expression	Positive (Immunofluorescence, Flow cytometry, qPCR; Figures 2.1C-E, 2.6C-D, 2.7B-C)	Positive (Immunofluorescence)	Positive (Flow Cytometry)	Positive (Immunofluorescence)	Positive (Immunofluorescence, qPCR)
RNA-Seq	Upregulation of genes and GO terms associated with astrocyte maturation , immune system process, cytokine-mediated signalling pathway, response to stress, regulation of immune system processes ; Downregulation of genes and GO-terms related to neuronal maturation and functionality (Figure 2.2)	Not assayed	Upregulation of genes related to signals promoting extracellular cell adhesion and interactions; Downregilation of genes regulating neuronal maturation such as synapse or ion channel formation	Upregulation of genes and GO terms related to inflammatory response, immune response and chemoking and cytokine activity.	Upregulation of canonical genes related to mature astrocytes
APOE Secretion	25-200 ng/mg Total Protein (Figure 2.3A, 2.7D)	50-100 ng/mg Total Protein	Not assayed	Not assayed	5-15 ng APOE /1000 cells
Inflammatory Response	Elevated IL-6, MCP-1, IL-8 in response to inflammatory stimuli (Figure 2.3B-C, 2.7E-F)	Not assayed	Elevated IL-6 in response to inflammatory stimuli	Elevated IL-6, IL-8 expression in response to inflammatory stimuli	Elevated IL-8 expression in response to inflammatory stimuli
Aβ Uptake	Robust uptake of Aβ (Figure 2.4)	Not assayed	Not assayed	Not assayed	Not assayed
Spontaneous Calcium Transient Activity	Spontaneous waves of calcium transients (Figure 2.5, 2.6E, 2.7G)	Not assayed	Spontaneous waves of calcium transients	Spontaneous waves of calcium transients	Spontaneous waves of calcium transients

The following videos can be downloaded on the ACS publications website.

**Supplementary Movie B.1. Representative recording of fluorescent calcium transients in NDC-1 astrocytes derived on VDP-coated substrates.**

Supplementary Movie B.2. Representative recording of fluorescent calcium transients in NDC-1 astrocytes derived on LN-coated substrates.

Supplementary Movie B.3. Representative recording of fluorescent calcium transients in FAD-1 astrocytes derived on VDP-coated substrates.

Supplementary Movie B.4. Representative recording of fluorescent calcium transients in FAD-1 astrocytes derived on LN-coated substrates.

Supplementary Movie B.5. Representative recording of fluorescent calcium transients in SAD-1 astrocytes derived on VDP-coated substrates.

Supplementary Movie B.6. Representative recording of fluorescent calcium transients in SAD-1 astrocytes derived on LN-coated substrates.

Supplementary Movie B.7. Representative recording of fluorescent calcium transients in NDC-1 astrocytes derived on VDP-coated MCs.

Supplementary Movie B.8. Representative recording of fluorescent calcium transients in NDC-2 astrocytes derived on VDP-coated MCs.

Supplementary Movie B.9. Representative recording of fluorescent calcium transients in NDC-1 astrocytes pre-cryopreservation.

Supplementary Movie B.10. Representative recording of fluorescent calcium transients in NDC-1 astrocytes post-cryopreservation.

APPENDIX C

SUPPLEMENTARY FIGURES FOR CHAPTER 3
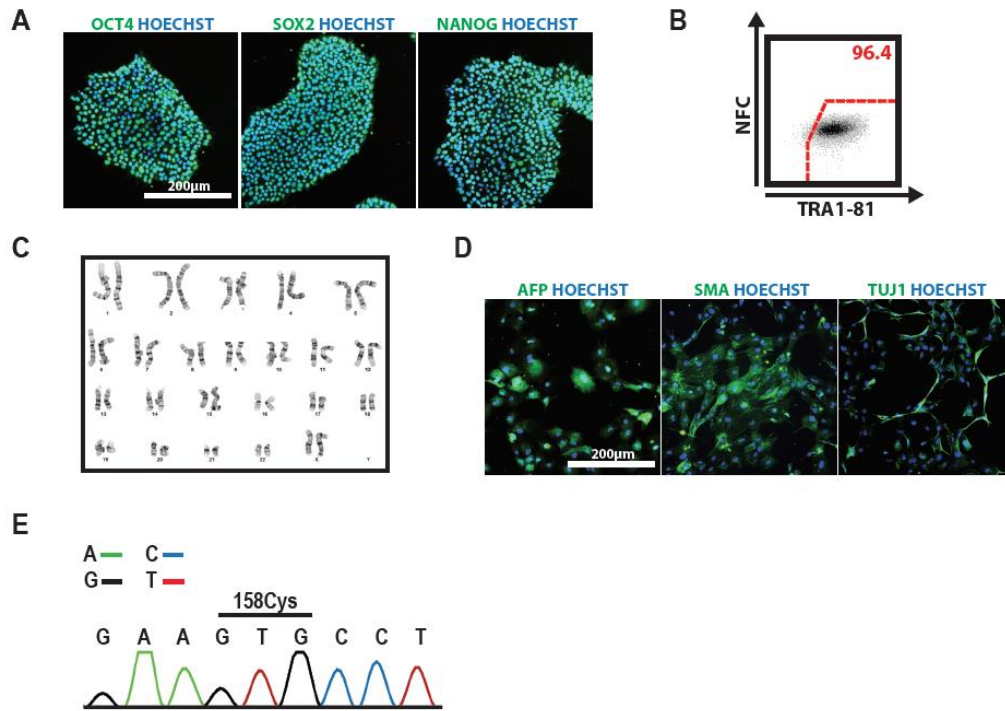
Supplemental Figure C.1. Characterization of isogenic *APOE2* fAD hiPSC line with APP^dp mutation.
(**A**) Immunofluorescence analysis of pluripotency markers OCT4, SOX2, NANOG. (**B**) Flow cytometry staining for pluripotency marker TRA1-81. An isotype control (Alexa Fluor 647 Mouse IgM, κ) was used for generating gates. (**C**) Karyotype analysis of edited hiPSCs. (**D**) Trilineage differentiation of *APOE2* hiPSCs and immunofluorescence staining of endoderm (AFP), mesoderm (SMA), and ectoderm (TUJ1) markers. (**E**) Sanger sequencing of the APOE locus confirming a cysteine at amino acid position 158.
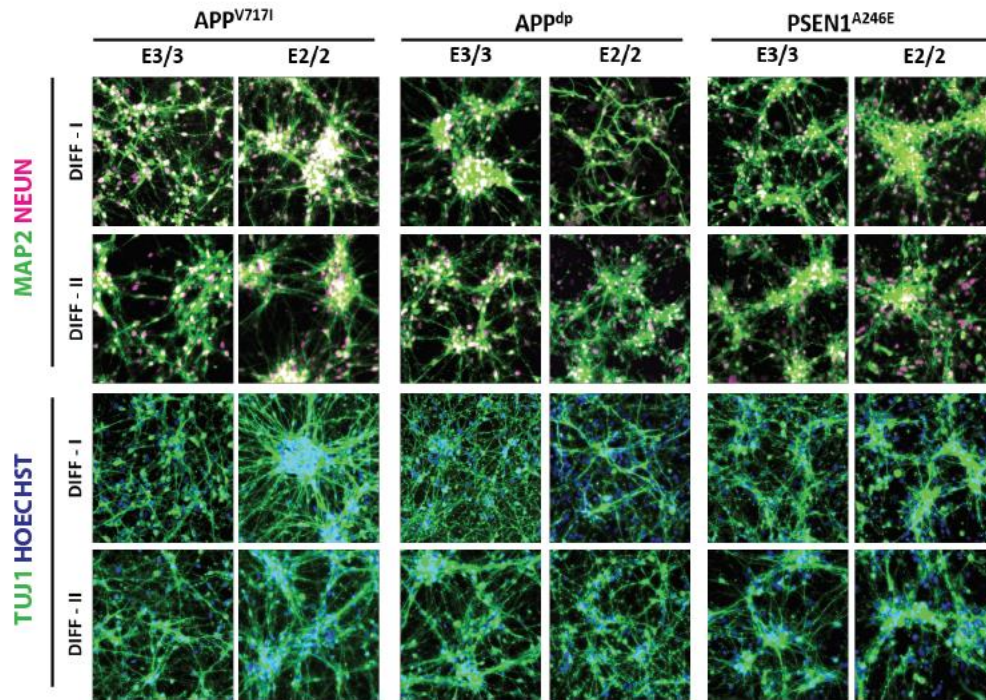
Supplemental Figure C.2. Comparison of neuronal marker expression across differentiations.
Representative immunofluorescence staining of mixed neuronal cultures from independent differentiations for neuronal marker TUJ1 and mature neuronal markers MAP2 and NEUN.
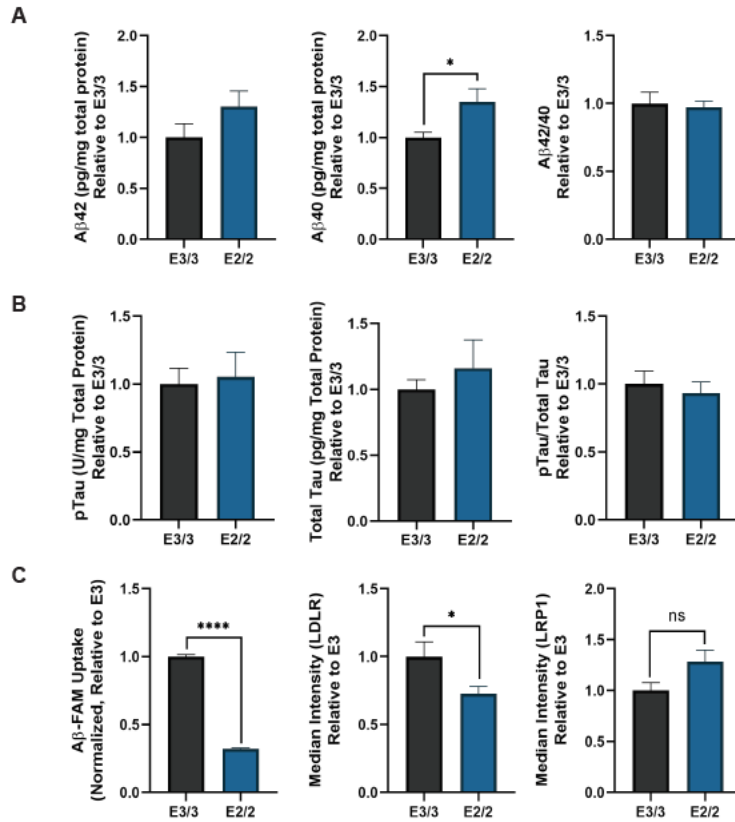
Supplemental Figure C.3. Amyloid and phosphorylated-tau (p-tau) levels in non-demented control (NDC) cultures.
(A) Quantification of secreted soluble Aβ levels and **(B)** Tau protein levels in NDC neuronal mixed cultures. (n=4); * = p<0.05
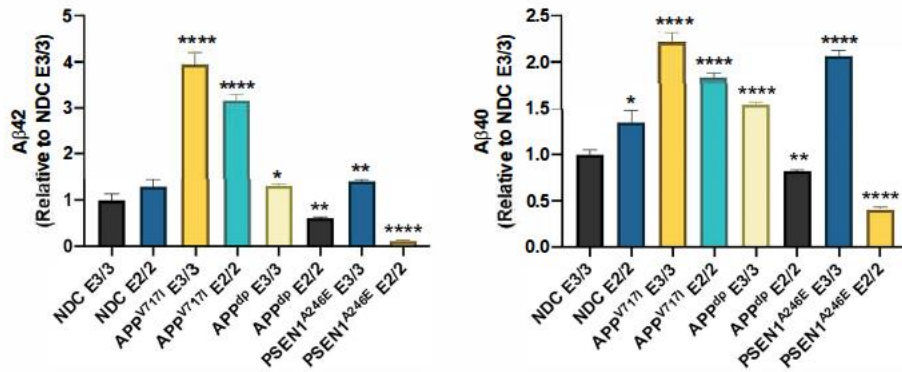
Supplemental Figure C.4. Comparison of Aβ release and phosphorylated tau (p-tau) levels between neural cultures derived from Alzheimer's disease (AD) and non-demented control (NDC) hiPSCs.

(**A**) Quantification of secreted soluble Aβ levels in AD neural cultures relative to those in NDC E3/3. n=4~15 from 1-3 independent differentiations; * = $p<0.05$, ** = $p<0.01$, *** = $p<0.001$, **** = $p<0.0001$.
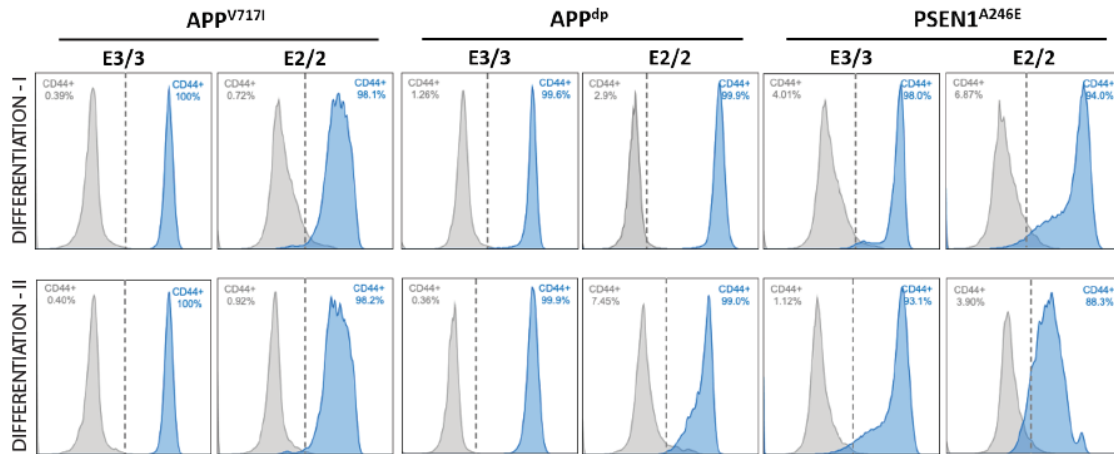
Supplemental Figure C.5. CD44 expression profile of purified fAD neurons and astrocytes across differentiations.
Flow cytometry plot overlay of purified neurons and astrocytes from two independent differentiations stained for CD44 surface protein, gated for corresponding isotype controls.
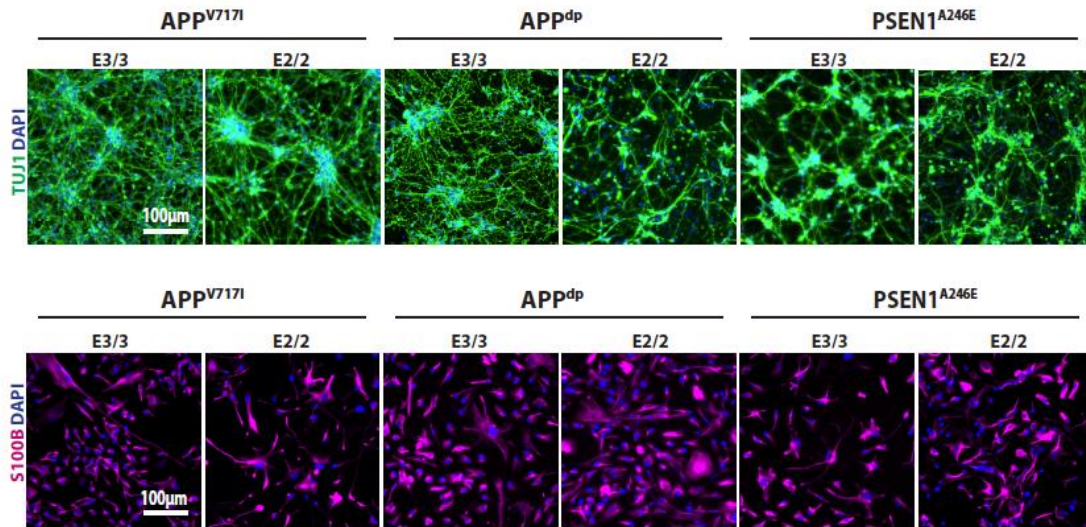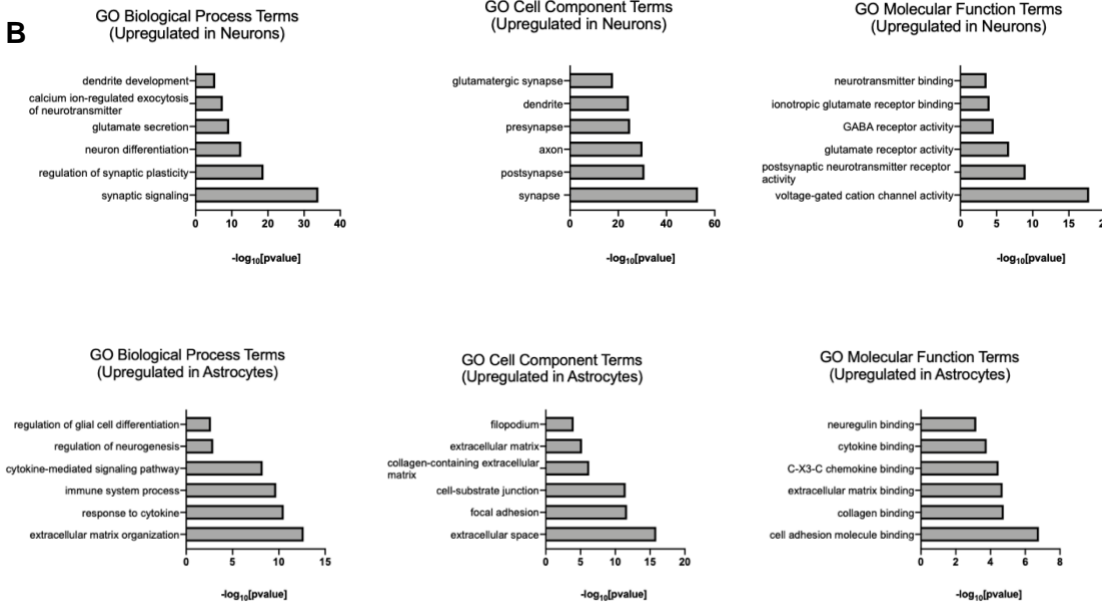
Supplemental Figure C.6. Additional characterization of purified neuronal and astrocytic populations.
(**A**) Representative immunofluorescence staining of purified neurons for neuronal marker TUJ1.
(**B**) Representative immunofluorescence staining of purified astrocytes for astrocytic maker S100β.
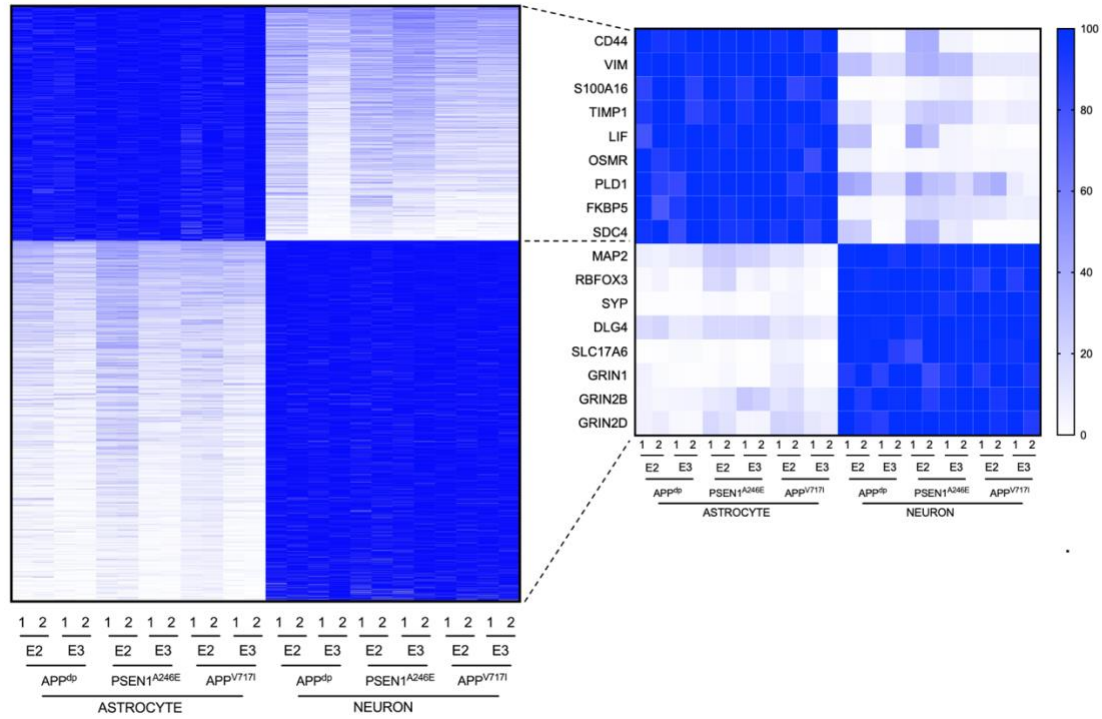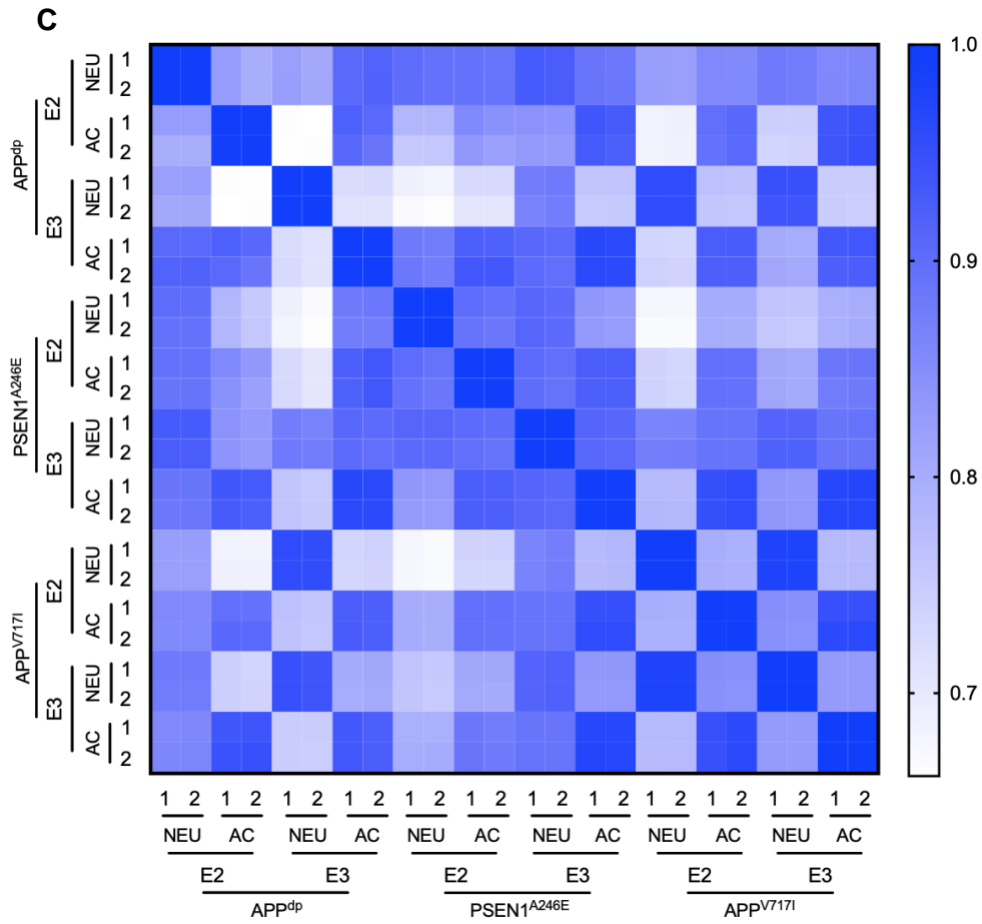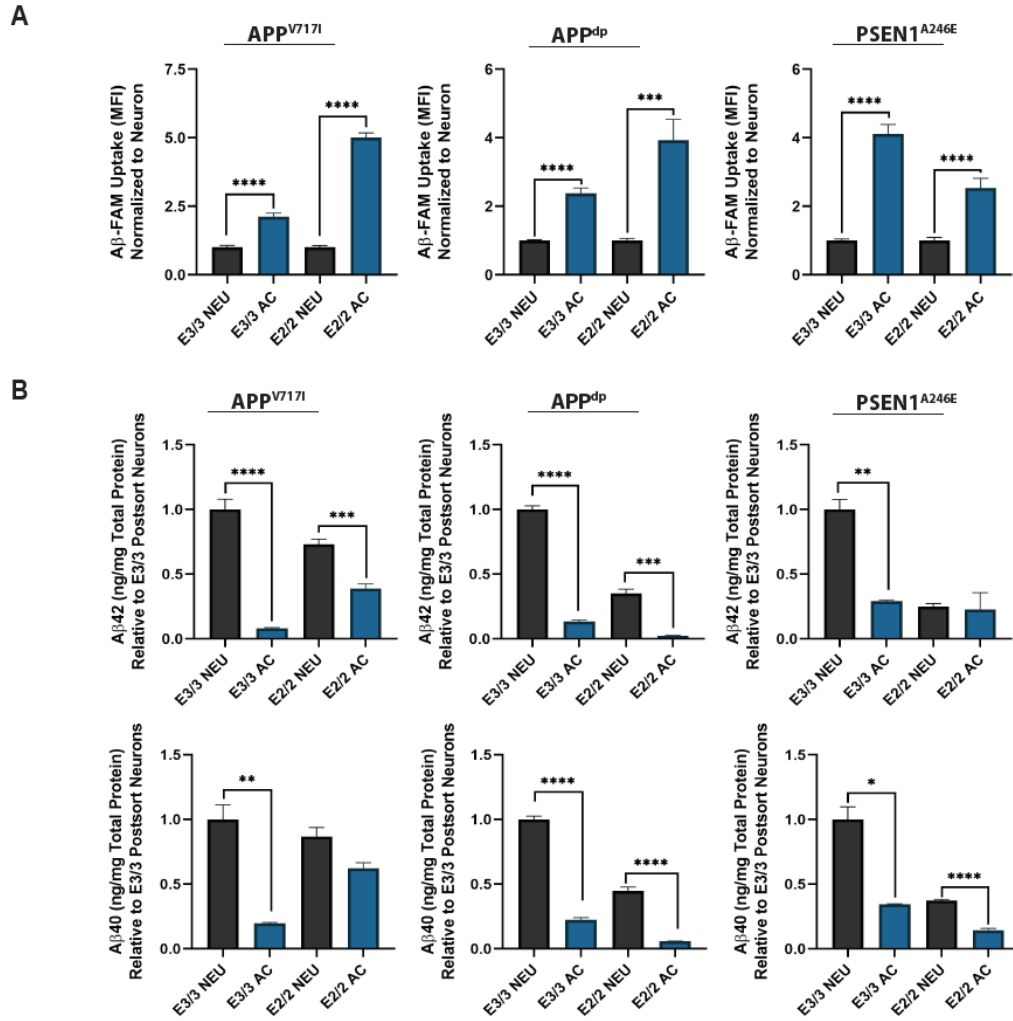
Supplemental Figure C.7

**Supplemental Figure C.7. Transcriptional profile of fAD isogenic neurons and astrocytes.**
(A) Comparison of the genes differentially expressed by neurons and astrocytes normalized to the maximum FPKM within each isoform, including several cell type specific markers in focus. **(B)** Gene ontology terms for biological process, cell component and molecular function upregulated in pure-neuron and -astrocyte cultures. **(C)** Heatmap depicting the Pearson correlation coefficients for gene expression levels between fAD neurons and astrocytes.

A

APP^V717I

APP^dp

PSEN1^A246E

B

APP^V717I

APP^dp

PSEN1^A246E

Supplemental Figure C.8. Aβ uptake and secretion levels in purified neuronal and astrocytic populations.
(A) Flow cytometry analysis of labeled FAM-Aβ42 peptide internalization in isogenic neurons and astrocyte (n=3 for neurons, n=14~20 for astrocytes). **(B)** Quantification of secreted Aβ in astrocytes compared to paired isogenic neurons (n=3 for astrocytes, n=11~15 for neurons). * = p<0.05, ** = p<0.01, *** = p<0.001, **** = p<0.0001.
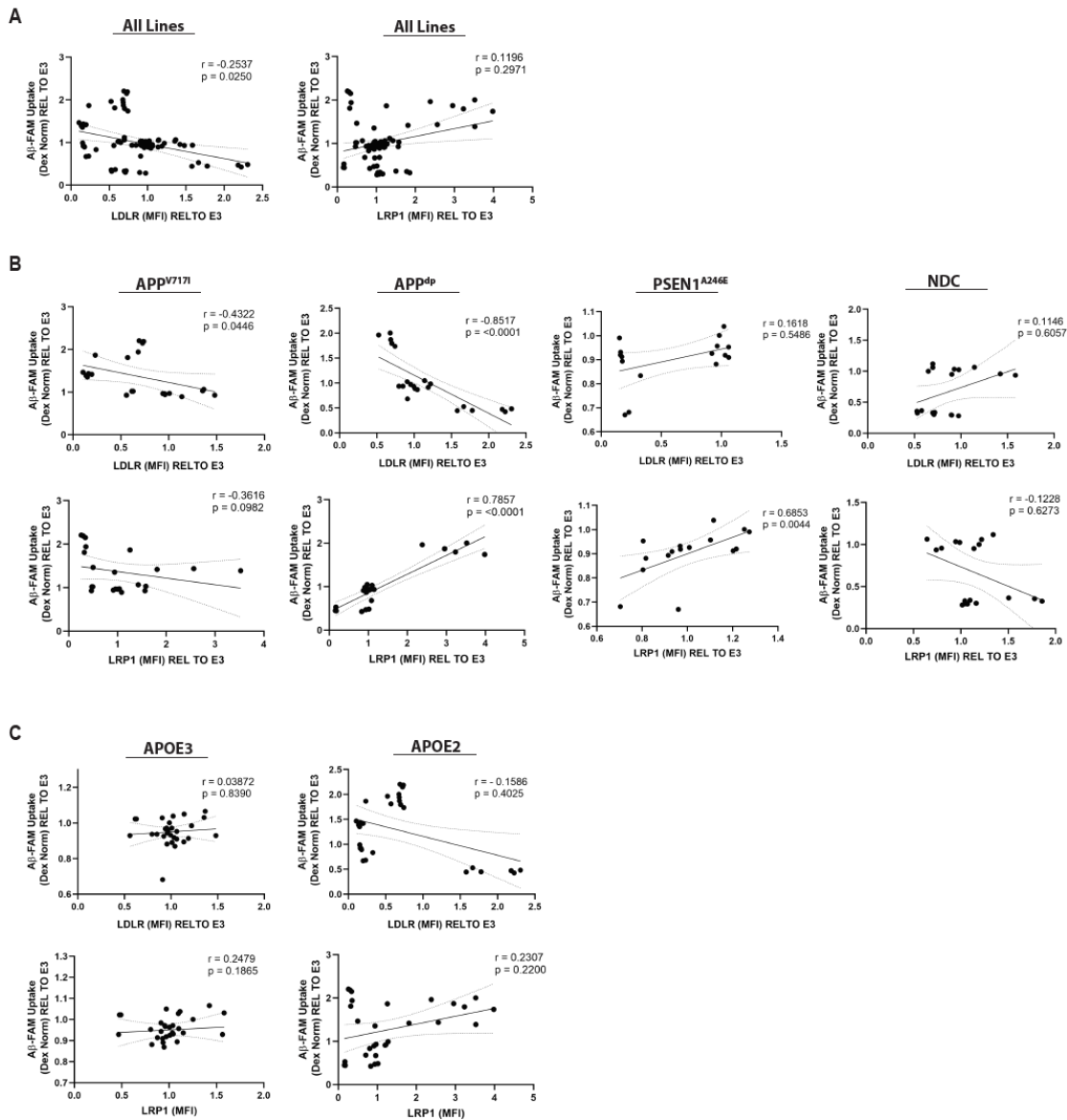
Supplemental Figure C.9. Relationship between Aβ uptake and LDL receptor expression in isogenic fAD and NDC astrocytes. (a) Flow cytometry based median intensity measurement of dextran normalized Aβ uptake (y axis) is plotted against surface expression of LDLR/LRP1 (x axis) receptors with a linear regression line (x-y pairs n=78). **(b)** Linear regression line of Aβ uptake (y axis) and LDLR/LRP1 expression (x axis – top/bottom) for each cell line (x-y pairs n= 22 [APP[V717I]] , 22 [APP[dp]], 16 [PSEN1[A246E]], 18 [NDC]). **(c)** ApoE isoform-specific linear regression line of Aβ uptake (y axis) and LDLR/LRP1 expression (x axis – top/bottom) for fAD astrocytes (x-y pairs n=30). Spearman correlation coefficient (r) and p values are reported on all plots.